

## Supporting Information

### Chemo-selective Formation of Cyclo-aliphatic and Cyclo-olefinic 1,3-Diols via Direct Hydrogenation of Potentially Biobased Platform Molecules using Knölker-type Catalysts.

Christian. A. M. R. van Slagmaat, Teresa Faber, Khi Chhay Chou, Alfonso Schwalb Freire, Darya Hadavi, Peiliang Han, Peter J. M. L. Quaedfleig, Gerard K. M. Verzijl, Paul L. Alsters, Stefaan M. A. De Wildeman\*

#### Contents:

S1.	Materials and Methods	S3
S1.1	<i>Chemicals</i>	S3
S1.2	<i>Synthesis and/or purification of substrates</i>	S4
S1.3	<i>Spectroscopic analysis of purchased substrates</i>	S9
S2.	Syntheses of Knölker-type catalysts	S11
S2.1	<i>Syntheses of dialkyne pre-ligands</i>	S11
S2.2	<i>General synthetic procedure for (cyclopentadienone)iron tricarbonyl complexes (<b>Fe-1</b> series)</i>	S15
S2.3	<i>General synthetic procedure for (cyclopentadienone)iron dicarbonyl mono-acetonitrile complexes (<b>Fe-2</b> series)</i>	S18
S3.	Representative gas chromatograms	S21
S3.1	<i>Piancatelli rearrangements of furfuryl alcohols towards 4-hydroxycyclopent-2-enone substrates</i>	S21
S3.2	<i>Hydrogenation reactions</i>	S25
S4.	<sup>1</sup> H-NMR and <sup>13</sup> C-NMR spectra	S26
S4.1	<i>Dialkyne pre-ligands</i>	S26
S4.2	<i>(cyclopentadienone)iron tricarbonyl complexes (<b>Fe-1</b> series)</i>	S31
S4.3	<i>(cyclopentadienone)iron dicarbonyl mono-acetonitrile complexes (<b>Fe-2</b> series)</i>	S38
S4.4	<i>Substrates</i>	S45
S4.5	<i>Hydrogenation products</i>	S64

S5.	FTIR spectra . . . . .	S82
	<i>S5.1 (cyclopentadienone)iron dicarbonyl mono-acetonitrile complexes (Fe-2 series)</i> . . . . .	S82
	<i>S5.2 Substrates</i> . . . . .	S85
	<i>S5.3 Hydrogenation products</i> . . . . .	S92
S6.	HR-MS spectra of some hydrogenation products . . . . .	S98
S7.	Miscellaneous . . . . .	S103
	<i>S7.1 Mechanism for the Knölker-catalyzed hydrogenation of ketones</i> . . . . .	S103
	<i>S7.2 DFT calculations for the diastereomers of 5g/5h</i> . . . . .	S104
	<i>S7.3 Schematic representations substrates aligning to Knölker's catalyst</i> . . . . .	S108
S8.	References . . . . .	S109

## S1. Materials and Methods

### S1.1 Chemicals:

NOTE: All chemicals were used as received from the supplier without purification, unless stated otherwise (see section S1.2).

Furfuryl alcohol (97%, Acros), 1-(furan-2-yl)ethanol ( $\geq 99.0\%$ , Sigma Aldrich), 3-(methylfuran-2-yl)methanol (95%, EnamineStore), 4-(methylfuran-2-yl)methanol (95%, EnamineStore), furan-2-yl(phenyl)methanol (95%, EnamineStore), Cyclopentane-1,3-dione (95%, Matrix Chemicals Inc.), 2-methylcyclopentane-1,3-dione (99%, Sigma Aldrich), 2-phenylcyclopentane-1,3-dione (95%, EnamineStore), 2-chlorocyclopentane-1,3-dione (95%, EnamineStore), 2-bromocyclopentane-1,3-dione (95%, EnamineStore), 2,2-dimethylcyclopentane-1,3-dione (95%, SageChem), 2-allyl-2-methylcyclopentane-1,3-dione (97%, Sigma Aldrich), Cyclopent-4-ene-1,3-dione (95%, Sigma Aldrich), Indan-1,3-dione (97%, Sigma Aldrich), 4,4-dimethylcyclopentane-1,3-dione (99%, EnamineStore), Cyclohexane-1,3-dione (97%, Sigma Aldrich), 5,5-dimethylcyclohexane-1,3-dione ( $\geq 99.5\%$ , Sigma Aldrich), 2,2,4,4-tetramethylcyclobutane-1,3-dione (99%, Sigma Aldrich), Pentane-2,4-dione (99%, Acros), 1,7-octadiyne (98%, Sigma Aldrich), 1,6-heptadiyne (97%, Sigma Aldrich), trimethylsilyl chloride ( $\geq 99.0\%$ , Sigma Aldrich), *tert*-butyldimethylsilyl chloride (97%, Sigma Aldrich), Tris-isopropylsilyl chloride (97%, Sigma Aldrich), Triphenylsilyl chloride (96%, Sigma Aldrich), *n*-Butyllithium (1.6M in hexanes, Sigma Aldrich), Phenylacetylene (98%, Sigma Aldrich), 1,4-diiodobutane ( $\geq 99.0\%$ , Sigma Aldrich), Phenyllithium (1.9M in dibutylether, Sigma Aldrich), Tetraphenylcyclopentadienone (98%, Sigma Aldrich), 2,5-dimethyl-3,4-diphenylcyclopentadienone dimer (97%, Sigma Aldrich), iron pentacarbonyl (99%, Sigma Aldrich), diiron nonacarbonyl (99%, Sigma Aldrich), trimethylamine-N-oxide (99%, Sigma Aldrich), Magnesium sulphate (anhydrous,  $\geq 99.5\%$ , Sigma Aldrich), Methanol (HPLC grade, Biosolve) Ethanol (96%, VWR), isopropanol (HPLC grade, Biosolve), *t*-butanol ( $\geq 99.0\%$ , Sigma Aldrich), Cyclopentanol (99%, Sigma Aldrich), Benzyl alcohol (99.8%, Sigma Aldrich), Ethyl acetate (HPLC grade, Biosolve),  $\gamma$ -Valerolactone (99%, Sigma Aldrich), Cyclopentyl methyl ether (99%, Sigma Aldrich), Methyl-*tert*-butyl ether (HPLC grade, Biosolve), Tetrahydrofuran (HPLC grade, Biosolve), 2-methyltetrahydrofuran ( $\geq 99.0\%$ , Sigma Aldrich), 1,4-Dioxane (99.8%, Acros), Dioxolane (99.8%, Sigma Aldrich), Heptane (99.5%, Sigma Aldrich), Toluene (HPLC grade, Biosolve), *m*-Xylene ( $\geq 99.0\%$ , Sigma Aldrich), Anisole (99%, Sigma Aldrich), Chlorobenzene ( $\geq 99.5\%$ , Sigma Aldrich), 1,2-Dichloroethane ( $\geq 99.8\%$ , Sigma Aldrich), Cyclopentane-1,3-diol (mixture of *cis* and *trans*, 95%, Sigma Aldrich), Cis-cyclopent-4-ene-1,3-diol ( $\geq 99.0\%$ , Sigma Aldrich), Naphthalene ( $\geq 99\%$ , Alfa Aesar), Acetonitrile (LCMS grade, Biosolve), Celite R566 (Acros), Silica (60 – 200  $\mu\text{m}$  mesh, Acros), Hexane (HPLC grade, Biosolve), Dichloromethane (HPLC grade, Biosolve), deuterium oxide (99.96%, Cambridge Isotope Laboratories), deuterated chloroform (99.96% Cambridge Isotope Laboratories), deuterated dimethyl sulfoxide (>99.7%, Fisher Scientific).

## S1.2 Synthesis and/or purification of substrates:

### Cyclopentane-1,3-dione (CPDO):<sup>[1]</sup>

In our case, purification of **4** was performed as follows. In a 5L round-bottomed flask, 500 g of a yellow-brown batch of CPDO was dissolved in 4L isopropanol under vigorous mechanical stirring for 1 hour, followed by filtration to remove undissolved solid impurities, and the filtrate was rotavaporized to retrieve CPDO. Subsequently, the resulting CPDO was suspended in 4.0 L THF, and dissolved by refluxing for 4 hours under vigorous stirring. Slow cooling allowed CPDO to crystallize overnight, which was collected via Buchner filtration over a glass frit. Drying *in vacuo* yielded 330 g (66%) of light-brown powder of CPDO with >99% purity by <sup>1</sup>H-NMR in d<sub>6</sub>-DMSO.

Appearance: white to beige solid.

<sup>1</sup>H-NMR (300 MHz), 25 °C, DMSO-d<sub>6</sub> (2.50 ppm): δ = 12.18 (br, 1H, OH), 5.07 (s, 1H, CH), 2.36 (s, 4H, CH<sub>2</sub>CH<sub>2</sub>) ppm.

<sup>13</sup>C-NMR (75 MHz), 25 °C, DMSO-d<sub>6</sub> (39.50 ppm): δ = 197.78, 105.02, 31.36 ppm.

FTIR: 2365, 1869, 1558, 1420, 1395, 1346, 1306, 1236, 1234, 1171, 999, 905, 843, 633 cm<sup>-1</sup>.

### General procedure for Piancatelli rearrangement reactions:

A dilute solution (1.2 – 2.5% v/v) of (a substituted) furfuryl alcohol in demineralized water was divided in portions of 20 mL in microwave vials with a nominal volume of 25 mL. The vials were sealed under aerobic conditions using dedicated aluminum crimp caps fitted with a PTFE septum. Each vial was irradiated using a Biotage Initiator+ microwave. The applied heating program contains a heating ramp to reach 200°C within 100 seconds, then remains at 200°C for 10 minutes (pressure builds up to 17 bar), and is finally cooled down to room temperature within 5 minutes by means of a pressurized air flow. The contents in the corresponding microwave vials were combined, and centrifuged for 15 minutes at 15 000 rpm, in order to trap all solids in a pellet. The liquid phase was then decanted carefully, while the solid pellets were discarded. The liquid phase was rotavaporized to afford the crude product.

#### **4-Hydroxycyclopent-2-enone (4-HCP):<sup>[2]</sup>**

A reaction solution was prepared by dissolving 11.0 g (112.1 mmol) freshly distilled furfuryl alcohol in demineralized water to a total of 500 mL. After microwave heating procedure, and work-up an orange oil (10.92 g) was obtained as crude product. Finally, this oil was vacuum-distilled at 83°C and 6·10<sup>-2</sup> mbar (oil bath at 115°C, vigreux = 8 cm long) to furnish 7.98 g (64.5%) of pure (99%) light-yellow product. A trace amount of levulinic acid impurity was observed in NMR.

Appearance: pale yellow viscous liquid.

<sup>1</sup>H-NMR (300 MHz), 25 °C, DMSO-d<sub>6</sub> (2.50 ppm): δ = 7.64 (dd, *J*<sub>1</sub> = 5.6; *J*<sub>2</sub> = 2.3 Hz, 1*H*, vinyl), 6.15 (dd, *J*<sub>1</sub> = 5.6; *J*<sub>2</sub> = 1.0 Hz, 1*H*, vinyl), 5.46 (d, *J* = 3.9 Hz, 1*H*, OH), 4.83 (s, 1*H*, methine), 2.63 (dd, *J*<sub>1</sub> = 18.2; *J*<sub>2</sub> = 6.0 Hz, 1*H*, CH<sub>2</sub>H), 2.03 (dd, *J*<sub>1</sub> = 18.2, *J*<sub>2</sub> = 2.1 Hz, 1*H*, CH<sub>2</sub>H) ppm.

<sup>13</sup>C-NMR (75 MHz), 25 °C, DMSO-d<sub>6</sub> (39.50 ppm): δ = 206.97, 165.95, 133.52, 69.07, 44.22 ppm.

FTIR: 3381, 2920, 1703, 1585, 1400, 1341, 1314, 1265, 1233, 1184, 1151, 1101, 1038, 945, 854, 831, 793, 731, 656 cm<sup>-1</sup>.

#### **2-Methyl-4-hydroxycyclopent-2-enone (1a):<sup>[3]</sup>**

A reaction solution was prepared by dissolving 6.728 g (60.0 mmol) of 1-(furan-2-yl)ethanol in demineralized water to a total of 250 mL. After microwave heating procedure, and work-up an orange oil (6.27 g, 93%) was obtained as crude product. Finally, this oil was vacuum-distilled at 83°C and 3·10<sup>-2</sup> mbar (oil bath at 120°C, vigreux = 8 cm long) to furnish 5.934 g (79.4%) of pure (99%) light-yellow product. <sup>1</sup>H-NMR and GC-FID analysis showed a *syn* / *anti* ratio of 77 : 23 with respect to the 2-methyl and 3-hydroxyl substituents.

Appearance: pale yellow viscous liquid.

FTIR: 3391, 2970, 2934, 2876, 2359, 2340, 1695, 1589, 1456, 1418, 1375, 1341, 1319, 1288, 1248, 1229, 1171, 1128, 1086, 1026, 988, 961, 883, 866, 826, 762, 729, 683, 529 cm<sup>-1</sup>.

*Cis (major)*: <sup>1</sup>H-NMR (300 MHz), 25 °C, DMSO-d<sub>6</sub> (2.50 ppm): δ = 7.58 (m, 1*H*, OC-CH=C), 6.16 (d, *J* = 5.8 Hz, 1*H*, OC-CH=CH), 5.59 (d, *J* = 6.1 Hz, 1*H*, OH), 4.37 (m, 1*H*, CH-OH), 2.07 (m, 1*H*, CH-Me), 1.08 (d, *J* = 7.4 Hz, 3*H*, Me) ppm.

<sup>13</sup>C-NMR (75 MHz), 25 °C, DMSO-d<sub>6</sub> (39.50 ppm): δ = 208.00, 164.21, 132.31, 76.88, 50.11, 12.31 ppm.

*Trans (minor)*: <sup>1</sup>H-NMR (300 MHz), 25 °C, DMSO-d<sub>6</sub> (2.50 ppm): δ = 7.61 (m, 1*H*, OC-CH=C), 6.15 (d, *J* = 5.8 Hz, 1*H*, OC-CH=CH), 5.23 (d, *J* = 6.7 Hz, 1*H*, OH), 4.80 (t, *J* = 5.8 Hz, 1*H*, CH-OH), 2.37 (m, 1*H*, CH-Me), 0.95 (d, *J* = 7.6 Hz, 3*H*, Me) ppm.

<sup>13</sup>C-NMR (75 MHz), 25 °C, DMSO-d<sub>6</sub> (39.50 ppm): δ = 200.63, 164.63, 132.31, 70.54, 44.13, 10.64 ppm.

**4-Methyl-4-hydroxycyclopent-2-enone (1b):**

A reaction solution was prepared by dissolving 860 mg (7.7 mmol) of 3-(methylfuran-2-yl)methanol in demineralized water to a total of 80 mL. After microwave heating procedure, and work-up an orange oil (628 mg, 73%) was obtained as crude product. This synthesized substrate was not purified further and used as is for its application in the hydrogenation reaction.

Appearance: light brown viscous liquid.

$^1\text{H-NMR}$  (300 MHz), 25 °C, DMSO-d<sub>6</sub> (2.50 ppm):  $\delta$  = 7.26 (s, 1*H*, OC-CH=C), 5.31 (d,  $J$  = 5.9 Hz, 1*H*, OH), 4.72 (m, 1*H*, CH-OH), 2.7 – 2.6 (dd,  $J_1$  = 18.3;  $J_2$  = 6.0 Hz, 1*H*, CHH), 2.1 – 2.0 (dd,  $J_1$  = 18.3;  $J_2$  = 1.9 Hz, 1*H*, CHH), 1.67 (s, 3*H*, Me) ppm.

$^{13}\text{C-NMR}$  (75 MHz), 25 °C, DMSO-d<sub>6</sub> (39.50 ppm):  $\delta$  = 206.64, 159.24, 141.05, 66.93, 44.30, 9.57 ppm.  
FTIR: 3385, 2922, 2357, 2332, 1694, 1637, 1435, 1400, 1381, 1325, 1252, 1200, 1153, 1080, 1045, 1030, 984, 949, 862, 760, 694, 610 cm<sup>-1</sup>.

**5-Methyl-4-hydroxycyclopent-2-enone (1c):** [3]

A reaction solution was prepared by dissolving 781 mg (7.0 mmol) of 4-(methylfuran-2-yl)methanol in demineralized water to a total of 80 mL. After microwave heating procedure, and work-up an orange oil (453 mg, 58%) was obtained as crude product. This synthesized substrate was not purified further and used as is for its application in the hydrogenation reaction.

Appearance: light brown viscous liquid.

$^1\text{H-NMR}$  (300 MHz), 25 °C, DMSO-d<sub>6</sub> (2.50 ppm):  $\delta$  = 5.89 (s, 1*H*, OC-CH=CH), 5.48 (d,  $J$  = 66 Hz, 1*H*, OH), 4.59 (t,  $J$  = 5.3 Hz, 1*H*, CH-OH), 2.6 – 2.5 (dd,  $J_1$  = 18.1;  $J_2$  = 6.2 Hz, 1*H*, CHH), 2.1 – 2.0 (dd,  $J_1$  = 18.0;  $J_2$  = 2.3 Hz, 1*H*, CHH), 2.07 (s, 3*H*, Me) ppm.

$^{13}\text{C-NMR}$  (75 MHz), 25 °C, DMSO-d<sub>6</sub> (39.50 ppm):  $\delta$  = 205.29, 178.95, 129.91, 71.03, 45.07, 15.65 ppm.

**2-Phenyl-4-hydroxycyclopent-2-enone (1d):** [2]

A reaction solution was prepared by dissolving 871 mg (5.0 mmol) furan-2-yl(phenyl)methanol in demineralized water to a total of 80 mL. After microwave heating procedure, and work-up an off-white solid (580 mg, 67%) was obtained as crude product. This synthesized substrate was not purified further and used as is for its application in the hydrogenation reaction. <sup>1</sup>H-NMR analysis showed a *syn* / *anti* ratio of 44 : 56 with respect to the 2-phenyl and 3-hydroxyl substituents.

Appearance: white fluffy solid.

FTIR: 3390, 3061, 3026, 1744, 1697, 1597, 1558, 1493, 1447, 1395, 1310, 1302, 1263, 1159, 1128, 1107, 1076, 1036, 1001, 953, 920, 916, 878, 766, 750, 696, 642, 640 cm<sup>-1</sup>.

*Cis (major):* <sup>1</sup>H-NMR (300 MHz), 25 °C, DMSO-d<sub>6</sub> (2.50 ppm): δ = 8.0 – 7.0 (m, 5H, Ph), 4.87 (m, 1H, OH), 3.35 (s, 1H, CH-OH), 2.89 (dd, *J*<sub>1</sub> = 18.3; *J*<sub>2</sub> = 6.1 Hz, 1H, Ph-CH) ppm.

<sup>13</sup>C-NMR (75 MHz), 25 °C, DMSO-d<sub>6</sub> (39.50 ppm): δ = 205.61, 165.02, 138.05, 132.52, 128.49, 127.74, 126.72, 77.63, 61.77 ppm.

*Trans (minor):* <sup>1</sup>H-NMR (300 MHz), 25 °C, DMSO-d<sub>6</sub> (2.50 ppm): δ = 8.0 – 7.0 (m, 5H, Ph), 6.30 (dd, *J*<sub>1</sub> = 5.7; *J*<sub>2</sub> = 1.0 Hz, 1H, OH), 4.87 (s, 1H, CH-OH), 2.31 (d, *J*<sub>1</sub> = 18.3; *J*<sub>2</sub> = 2.0 Hz, 1H, Ph-CH) ppm.

<sup>13</sup>C-NMR (75 MHz), 25 °C, DMSO-d<sub>6</sub> (39.50 ppm): δ = 204.68, 159.88, 141.44, 130.90, 128.64, 128.43, 128.40, 127.66, 66.31, 45.90 ppm.

### S1.3 Spectroscopic analysis of purchased substrates:

#### **2-Methylcyclopentane-1,3-dione (3e).**

Appearance: White crystalline solid.

<sup>1</sup>H-NMR (300 MHz), 25 °C, DMSO-d<sub>6</sub> (2.50 ppm): δ = 11.22 (br, 1H, OH), 2.33 (s, 4H, (CH<sub>2</sub>)<sub>2</sub>), 1.45 (s, 3H, CH<sub>3</sub>) ppm.

<sup>13</sup>C-NMR (75 MHz), 25 °C, DMSO-d<sub>6</sub> (39.50 ppm): δ = 194.20, 111.59, 30.13, 5.81 ppm.

FTIR: 2916, 2614, 2448, 2162, 2016, 1977, 1692, 1568, 1416, 1398, 1379, 1342, 1256, 1236, 1092, 1059, 997, 897, 818, 706, 660, 586 cm<sup>-1</sup>.

#### **2-Phenylcyclopentane-1,3-dione (3f).**

Appearance: Off-white solid.

<sup>1</sup>H-NMR (300 MHz), 25 °C, DMSO-d<sub>6</sub> (2.50 ppm): δ = 7.82 (d, 2H, Ph), 7.32 (t, 2H, Ph), 7.17 (t, 1H, Ph), 2.52 (s, 4H, CH<sub>2</sub>) ppm.

<sup>13</sup>C-NMR (75 MHz), 25 °C, DMSO-d<sub>6</sub> (39.50 ppm): δ = 194.22, 132.08, 127.67, 127.16, 125.86, 113.61, 30.46 ppm.

FTIR: 3067, 2930, 2448, 2162, 1869, 1653, 1603, 1547, 1497, 1447, 1427, 1348, 1304, 1288, 1252, 1229, 1173, 1074, 1013, 928, 827, 766, 752, 698, 667, 638, 611, 596, 561 cm<sup>-1</sup>.

#### **2-Chlorocyclopentane-1,3-dione (3g).**

Appearance: Brown solid.

<sup>1</sup>H-NMR (300 MHz), 25 °C, DMSO-d<sub>6</sub> (2.50 ppm): δ = 7.40 (br, 1H, OH), 2.50 (s, 4H, CH<sub>2</sub>) ppm.

<sup>13</sup>C-NMR (75 MHz), 25 °C, DMSO-d<sub>6</sub> (39.50 ppm): δ = 189.81, 105.22, 29.32 ppm.

FTIR: 2530, 1684, 1562, 1393, 1292, 1238, 1013, 1001, 966, 916, 822, 667, 642, 596, 569 cm<sup>-1</sup>.

#### **2-Bromocyclopentane-1,3-dione (3h).**

Appearance: Brown solid.

<sup>1</sup>H-NMR (300 MHz), 25 °C, DMSO-d<sub>6</sub> (2.50 ppm): δ = 7.82 (br 1H, OH), 2.53 (s, 4H, CH<sub>2</sub>) ppm.

<sup>13</sup>C-NMR (75 MHz), 25 °C, DMSO-d<sub>6</sub> (39.50 ppm): δ = 191.38, 94.79, 30.25 ppm.

FTIR: 2513, 1684, 1557, 1393, 1285, 1234, 1003, 922, 820, 660, 631, 592, 561 cm<sup>-1</sup>.

#### **2,2-Dimethylcyclopentane-1,3-dione (3i).**

Appearance: Yellow crystalline solid.

<sup>1</sup>H-NMR (300 MHz), 25 °C, DMSO-d<sub>6</sub> (2.50 ppm): δ = 2.73 (s, 4H, (CH<sub>2</sub>)<sub>2</sub>), 1.00 (s, 6H, CH<sub>3</sub>) ppm.

<sup>13</sup>C-NMR (75 MHz), 25 °C, DMSO-d<sub>6</sub> (39.50 ppm): δ = 216.66, 51.94, 34.35, 19.94 ppm.

FTIR: 2976, 2930, 2870, 2156, 2018, 1975, 1717, 1578, 1460, 1416, 1398, 1377, 1344, 1285, 1248, 1105, 1084, 1055, 993, 953, 908, 793, 664 cm<sup>-1</sup>.

**2-Allyl-2-methylcyclopentan-1,3-dione (3j).**

Appearance: Colorless liquid.

<sup>1</sup>H-NMR (300 MHz), 25 °C, DMSO-d<sub>6</sub> (2.50 ppm): δ = 5.53 (m, 1H, CH<sub>2</sub>=CH), 5.05 (s, 1H, CHH=CH) 5.00 (d, 1H, CHH=CH), 2.71 (s, 4H, CH<sub>2</sub>-CH<sub>2</sub>), 2.22 (d, 2H, CH<sub>2</sub>), 0.97 (s, 3H, CH<sub>3</sub>) ppm.

<sup>13</sup>C-NMR (75 MHz), 25 °C, DMSO-d<sub>6</sub> (39.50 ppm): δ = 215.92, 132.15, 119.06, 55.78, 39.03, 34.91, 17.23 ppm.

FTIR: 3078, 2978, 2926, 1763, 1717, 1653, 1639, 1558, 1452, 1418, 1371, 1319, 1206, 1161, 1103, 1067, 1028, 993, 924, 880, 829, 789, 696, 665, 623 cm<sup>-1</sup>.

**Cyclopent-4-ene-1,3-dione (3k).**

Appearance: White crystalline solid.

<sup>1</sup>H-NMR (300 MHz), 25 °C, DMSO-d<sub>6</sub> (2.50 ppm): δ = 7.46 (s, 4H, (CH<sub>2</sub>)<sub>2</sub>), 2.97 (s, 2H, CH<sub>2</sub>) ppm.

<sup>13</sup>C-NMR (75 MHz), 25 °C, DMSO-d<sub>6</sub> (39.50 ppm): δ = 202.32, 150.68, 41.64 ppm.

FTIR: 3078, 3071, 2158, 2023, 1965, 1744, 1694, 1670, 1558, 1360, 1329, 1288, 1254, 1223, 1136, 1070, 941, 816, 793, 704, 673, 583 cm<sup>-1</sup>.

**Indane-1,3-dione (3l).**

Appearance: Yellow crystalline solid (purple in solution).

<sup>1</sup>H-NMR (300 MHz), 25 °C, DMSO-d<sub>6</sub> (2.50 ppm): δ = 7.93 (s, 4H, Ar), 3.35 (s, 2H, CH<sub>2</sub>) ppm.

<sup>13</sup>C-NMR (75 MHz), 25 °C, DMSO-d<sub>6</sub> (39.50 ppm): δ = 198.17, 143.03, 135.62, 122.62, 45.15 ppm.

FTIR: 2160, 2016, 1985, 1744, 1701, 1585, 1350, 1254, 1225, 1184, 1159, 1092, 920, 920, 773, 729, 598 cm<sup>-1</sup>.

**4,4-dimethylcyclopentane-1,3-dione (3m).**

Appearance: Beige solid.

<sup>1</sup>H-NMR (300 MHz), 25 °C, DMSO-d<sub>6</sub> (2.50 ppm): δ = 12.11 (s, 1H, OH), 4.97 (s, 1H, CH), 2.30 (s, 2H, CH<sub>2</sub>), 1.05 (s, 6H, CH<sub>3</sub>) ppm.

<sup>13</sup>C-NMR (75 MHz), 25 °C, DMSO-d<sub>6</sub> (39.50 ppm): δ = 205.99, 192.21, 102.23, 46.00, 42.15, 25.33 ppm.

FTIR: 2965, 2926, 2868, 2673, 2465, 2245, 1927, 1634, 1578, 1558, 1456, 1429, 1422, 1379, 1315, 1256, 1219, 1134, 1007, 970, 903, 876, 839, 739, 644, 629, 552 cm<sup>-1</sup>.

**Cyclohexane-1,3-dione (3n).**

Appearance: White solid.

<sup>1</sup>H-NMR (300 MHz), 25 °C, DMSO-d<sub>6</sub> (2.50 ppm): δ = 10.98 (br, 1H, OH), 5.19 (s, 1H, CH<sub>2</sub>), 2.22 (t, J = 6.4 Hz, 4H, CH<sub>2</sub>), 1.83 (q, J = 6.3 Hz, 2H, CH<sub>2</sub>) ppm.

<sup>13</sup>C-NMR (75 MHz), 25 °C, DMSO-d<sub>6</sub> (39.50 ppm): δ = 188.10, 103.83, 32.19, 20.90 ppm.

FTIR: 2949, 2889, 2359, 1624, 1557, 1456, 1360, 1314, 1283, 1190, 1177, 1138, 1055, 964, 943, 912, 858, 826, 762, 654, 590, 550 cm<sup>-1</sup>.

**5,5-Dimethylcyclohexane-1,3-dione (3o).**

Appearance: White crystalline solid.

$^1\text{H-NMR}$  (300 MHz), 25 °C, DMSO-d<sub>6</sub> (2.50 ppm):  $\delta$  = 11.01 (br, 1H, OH), 5.19 (s, 1H, CH), 2.12 (s, 4H, (CH<sub>2</sub>)<sub>2</sub>), 0.98 (s, 6H, CH<sub>3</sub>) ppm.

$^{13}\text{C-NMR}$  (75 MHz), 25 °C, DMSO-d<sub>6</sub> (39.50 ppm):  $\delta$  = 186.84, 102.42, 46.08, 32.14, 27.96 ppm.

FTIR: 2953, 2866, 2501, 2359, 2158, 1965, 1717, 1586, 1576, 1516, 1464, 1410, 1346, 1304, 1248, 1225, 1144, 984, 964, 874, 827, 613, 592 cm<sup>-1</sup>.

**2,2,4,4-Tetramethylcyclobutane-1,3-dione (3p).**

Appearance: White crystalline solid.

$^1\text{H-NMR}$  (300 MHz), 25 °C, DMSO-d<sub>6</sub> (2.50 ppm):  $\delta$  = 1.24 (s, 12H, CH<sub>3</sub>) ppm.

$^{13}\text{C-NMR}$  (75 MHz), 25 °C, DMSO-d<sub>6</sub> (39.50 ppm):  $\delta$  = 215.37, 69.83, 18.38 ppm.

FTIR: 2968, 2963, 2870, 2158, 2018, 1975, 1744, 1717, 1456, 1375, 1362, 1265, 1177, 1045, 820, 766 cm<sup>-1</sup>.

**Pentane-2,4-dione (3q).**

Appearance: Colorless liquid.

$^1\text{H-NMR}$  (300 MHz), 25 °C, DMSO-d<sub>6</sub> (2.50 ppm):  $\delta$  = 5.68 (s, 2H, CH<sub>2</sub>, diketone), 3.68 (s, 2H, CH<sub>2</sub>, keto-enol), 2.13 (s, 6H, CH<sub>3</sub>, diketone), 2.02 (s, 6H, CH<sub>3</sub>, keto-enol) ppm.

$^{13}\text{C-NMR}$  (75 MHz), 25 °C, DMSO-d<sub>6</sub> (39.50 ppm):  $\delta$  = 203.46 (diketone), 191.29 (keto-enol), 100.51 (keto-enol), 57.77 (diketone), 30.68 (diketone), 24.50 (keto-enol) ppm.

FTIR: 2359, 2332, 1728, 1707, 1605, 1418, 1360, 1300, 1246, 1159, 1155, 999, 953, 912, 777, 638 cm<sup>-1</sup>.

## S2. Synthesis of Knölker-type catalysts

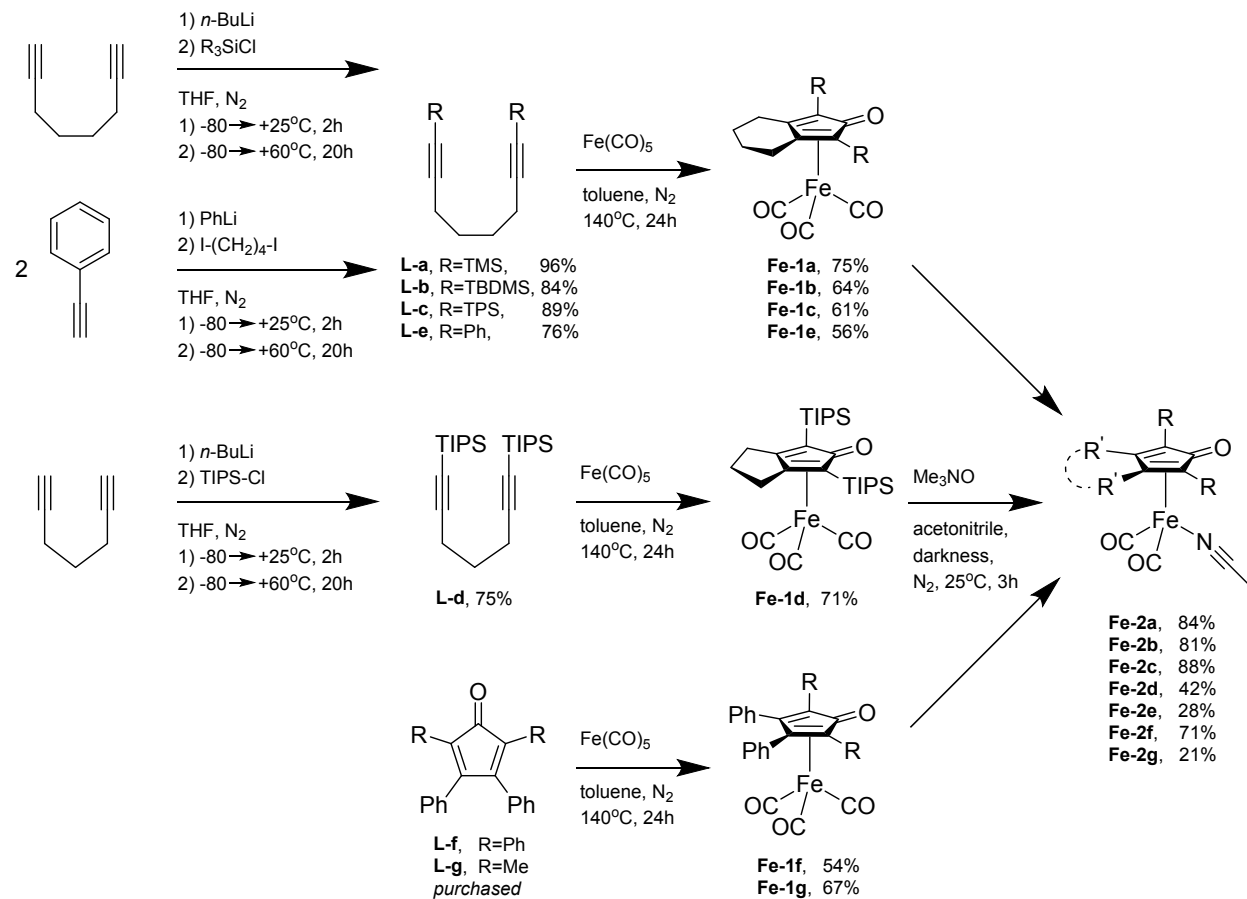


Figure S2.1: Ensemble of reaction schemes for the total syntheses of 'pre-activated' Knölker-type catalysts.

Note: **Fe-1d** was prepared from the 1,6-heptadiyne precursor ligand, because the synthesis of a 2,5-bis(TIPS) substituted  $\eta_4$ -cyclopentadiene iron<sup>0</sup> tricarbonyl complex from the 1,7-octadiyne precursor ligand failed several times in our hands. We suspect that the latter complex is unstable, due to excessive steric clashing of the TIPS groups with the fused cyclohexyl ring.

## *S2.1 Syntheses of dialkyne pre-ligands:*

### **General synthesis procedure for diyne pre-ligands L-a, L-b, L-c, and L-d:**

In an oven-dried 100 mL Schlenk flask fitted with an air-tight septum, purged under a nitrogen atmosphere, an  $\alpha,\omega$ -diyne (5.0 mmol) was dissolved in 20 mL dry and degassed THF. The mixture was cooled to -80°C using an isopropanol / liquid nitrogen bath. A solution of 1.6M *n*-BuLi in hexanes (6.9 mL, 11.0 mmol) was slowly added under vigorous stirring (1000 rpm), after which the reaction mixture was allowed warm up to room temperature. The reaction mixture was stirred for 2 hours at room temperature, during which it became bright yellow, indicating successful lithiation.

For the next step, a solution of silyl chloride (11.0 mmol) in 20 mL dry and degassed THF was prepared under a nitrogen atmosphere. The reaction mixture was cooled to -80°C again, and the silyl chloride solution was added slowly under vigorous stirring. The reaction mixture was allowed to warm up to room temperature over the course of 2 hours, and subsequently heated to 60°C using an oil bath for 18 hours. The resulting reaction mixture was cooled to room temperature, quenched with 25 mL water, and washed with 2x 25 mL water and 1x 25 mL brine solution. After phase separation, the organic fraction was dried over MgSO<sub>4</sub>, and was subjected to rotavaporization to afford a yellow to orange oil. This crude product was purified by silica gel column chromatography ( $\pm$ 120g silica,  $\pm$ 50cm path length) using a 0/100 to 10/90 gradient (slow increment) of ethyl acetate / *n*-hexane as eluent. The desired diyne pre-ligands were obtained as such in good to excellent yields and high purity according to NMR analysis.

**1,8-bis(trimethylsilyl)octa-1,7-diyne (L-a).**<sup>[4,5,6]</sup>

Appearance: Colorless viscous liquid.

<sup>1</sup>H-NMR (300 MHz), 25 °C, CDCl<sub>3</sub> (7.26 ppm): δ = 2.24 (m, 4H, C≡C-CH<sub>2</sub>), 1.61 (m, 4H, CH<sub>2</sub>), 0.14 (s, 18H, TMS) ppm.

<sup>13</sup>C-NMR (75 MHz), 25 °C, CDCl<sub>3</sub> (77.13 ppm): δ = 107.17, 84.81, 27.80, 19.53, 0.30 ppm.

**1,8-bis(tert-butyl dimethylsilyl)octa-1,7-diyne (L-b).**<sup>[5]</sup>

Appearance: white greasy solid.

<sup>1</sup>H-NMR (300 MHz), 25 °C, CDCl<sub>3</sub> (7.26 ppm): δ = 2.26 (t, J = 6.3 Hz, 4H, C≡C-CH<sub>2</sub>), 1.64 (p, J = 3.0 Hz, 4H, CH<sub>2</sub>), 0.92 (s, 18H, tBu), 0.08 (s, 12H, Me) ppm.

<sup>13</sup>C-NMR (75 MHz), 25 °C, CDCl<sub>3</sub> (77.13 ppm): δ = 107.62, 82.94, 27.76, 26.21, 19.44, 16.63, -4.32 ppm.

**1,8-bis(triphenylsilyl)octa-1,7-diyne (L-c).**<sup>[7]</sup>

Appearance: white solid.

<sup>1</sup>H-NMR (300 MHz), 25 °C, CDCl<sub>3</sub> (7.26 ppm): δ = 7.63 (m, 12H, Ph), 7.36 (m 18H, Ph), 2.43 (t, J = 5.9 Hz, 4H, C≡C-CH<sub>2</sub>), 1.82 (p, J = 2.9 Hz, 4H, CH<sub>2</sub>) ppm.

<sup>13</sup>C-NMR (75 MHz), 25 °C, CDCl<sub>3</sub> (77.13 ppm): δ = 135.61, 134.41, 129.86, 128.01, 112.01, 80.08, 27.72, 19.85 ppm.

**1,7-bis(triisopropylsilyl)hepta-1,6-diyne (L-d).**

Appearance: Colorless viscous liquid.

<sup>1</sup>H-NMR (300 MHz), 25 °C, CDCl<sub>3</sub> (7.26 ppm): δ = 2.41 (t, J = 6.9 Hz 4H, C≡C-CH<sub>2</sub>), 1.74 (p, J = 6.8 Hz, 2H, CH<sub>2</sub>), 1.07 (m, 6H, SiCHMe<sub>2</sub>), 1.05 (m, 12H, SiCHMe<sub>2</sub>) ppm.

<sup>13</sup>C-NMR (75 MHz), 25 °C, CDCl<sub>3</sub> (77.13 ppm): δ = 108.08, 81.02, 28.13, 18.92, 18.77, 11.43 ppm.

*Synthesis of 1,8-diphenylocta-1,7-diyne (L-e):*

In an oven-dried 100 mL Schlenk flask fitted with an air-tight septum, purged under a nitrogen atmosphere, phenylacetylene (22 mmol) was dissolved in 40 mL dry and degassed THF. The mixture was cooled to

-80°C using an isopropanol / liquid nitrogen bath. A solution of 1.9M PhLi in dibutyl ether (11.6 mL, 22.0 mmol) was slowly added under vigorous (1000 rpm) stirring, after which the resulting brown reaction mixture was allowed warm up to room temperature. The reaction mixture was stirred for 2 hours at room temperature.

For the next step, a solution of 1,4-diiodobutane (10.0 mmol) in 10 mL dry and degassed THF was prepared under a nitrogen atmosphere. The reaction mixture was cooled to -80°C again, and the 1,4-diiodobutane solution was added drop wise under vigorous stirring. The reaction mixture was allowed to warm up to room temperature over the course of 1 hour, and subsequently heated to 60°C using an oil bath for 19 hours. The resulting reaction mixture was cooled to room temperature, quenched with 25 mL water, and washed with 2x 25 mL water and 1x 25 mL brine solution. After phase separation, the organic fraction was dried over MgSO<sub>4</sub>, and was subjected to rotavaporation to afford a brown oil. This crude product was purified by silica gel column chromatography ( $\pm$ 120g silica,  $\pm$ 50cm path length) using a 0/100 to 5/95 gradient (slow increment) of ethyl acetate / *n*-hexane as eluent. **L-e** was obtained in 76% yield and with excellent purity according to NMR analysis.

*Analysis:* <sup>18</sup>

Appearance: Pale-yellow liquid.

<sup>1</sup>H-NMR (300 MHz), 25 °C, CDCl<sub>3</sub> (7.26 ppm):  $\delta$  = 7.43 (m, 12H, Ph), 7.31 (m, 18H, Ph), 2.51 (t, 4H, C≡C-CH<sub>2</sub>), 1.82 (p, *J* = 3.0 Hz, 4H, CH<sub>2</sub>) ppm.

<sup>13</sup>C-NMR (75 MHz), 25 °C, CDCl<sub>3</sub> (77.13 ppm):  $\delta$  = 131.71, 128.34, 127.69, 124.09, 89.96, 81.07, 28.04, 19.17 ppm.

## *S2.2 General synthesis procedure for (cyclopentadienone)iron tricarbonyl complexes (**Fe-1** series):*

CAUTION: This reaction builds up a significant pressure ( $\pm$  7 bar) of CO gas, and a very thorough consideration on how to handle and neutralize this pressurized lethal gas is essential to warrant safety! We used dedicated microwave equipment from Biotage, which firmly clamps the crimp-cap onto the vial, monitors the pressure in real-time, and has a steel-cage chamber equipped with a sponge to absorb any potential leakage or explosion. We neutralized the CO-pressurized vials via: 1) Ensuring that the reaction mixture was cooled to room temperature, 2) Applying a 10 mL syringe equipped with a Luer lock and a thin needle to release the CO pressure manually, while keeping all materials deep inside a well-ventilated fumehood. Hold the syringe firmly with your thumb on the plunger, pierce the septum carefully with the needle and collect the CO gas in the syringe in a controlled manner. Then, withdraw the needle and release the CO gas from the syringe deep and high inside the fumehood (the septum from Biotage will close and withstand the remaining pressure). Repeat the manual CO extractions with the syringe, until all pressure is released. 3) Purge the headspace of the microwave vial via needles using a balloon of nitrogen inside a well-ventilated fumehood. Then finally, the crimp-cap can be safely removed from the vial.

A 30 mL glass pressure vial from Biotage with a stirring magnet was mounted inside a large Schlenk flask, and the system was purged under a nitrogen atmosphere. Under an outflow of a nitrogen stream, a diyne pre-ligand or cyclopentadienone ligand (1.5 mmol) and 12 mL of dry toluene, and finally Fe(CO)<sub>5</sub> (3.0 mmol) were added into the pressure vial, and the vial was sealed using a dedicated crimp-cap septum. The mixture was reacted by microwave irradiation to a constant temperature of 140°C, while magnetically stirring at 600 rpm, for 24 hours, during which the formation of CO pressure was observed to build up to 10 bar over the course of 4 - 8 hours. After cooling down to room temperature, the vial was still pressurized with 7 bar CO gas, which was very carefully released as described above in the red ‘caution’ section. The neutralized reaction mixture was passed through a Celite column ( $\pm$ 30 cm x 1 cm) using 100 mL ethyl acetate to remove solid iron carbonyl particles, and the resulting solution was pushed through a Millipore filter subsequently, to remove paramagnetic iron nanoparticles. After removal of the ethyl acetate by rotary vaporization, the concentrated crude product was purified by silica gel column chromatography ( $\pm$ 120g silica,  $\pm$ 50 cm path length) using a 0/100 to 10/90 ethyl acetate / *n*-hexane gradient as eluent. Visualization of the product in TLC is possible under UV-light, but also by staining with KMnO<sub>4</sub>/alkaline solution. Rotary vaporization of the product fractions yielded the pure **Fe-1** series iron complexes in good yields and high purity according to NMR analysis.

**$\eta_4\{-1,3\text{-bis(trimethylsilyl)\text{-}4,5,6,7\text{-tetrahydro\text{-}2H\text{-}inden\text{-}2\text{-one}\text{\textgreater}iron}^0\text{ tricarbonyl (Fe-1a).}$** <sup>[4,5,6,9,10,11,12,13]</sup>

Appearance: Yellow crystalline solid.

<sup>1</sup>H-NMR (300 MHz), 25 °C, CDCl<sub>3</sub> (7.26 ppm): δ = 2.65 (m, 4H, Cp-CH<sub>2</sub>), 1.83 (m, 4H, CH<sub>2</sub>), 0.27 (s, 18H, TMS) ppm.

<sup>13</sup>C-NMR (75 MHz), 25 °C, CDCl<sub>3</sub> (77.13 ppm): δ = 209.20, 181.38, 111.14, 71.90, 24.92, 22.55, -0.14 ppm.

**$\eta_4\{-1,3\text{-bis(tert-butyl dimethylsilyl)\text{-}4,5,6,7\text{-tetrahydro\text{-}2H\text{-}inden\text{-}2\text{-one}\text{\textgreater}iron}^0\text{ tricarbonyl (Fe-1b).}$** <sup>[4,9,10,11]</sup>

Appearance: Yellow crystalline solid.

<sup>1</sup>H-NMR (300 MHz), 25 °C, CDCl<sub>3</sub> (7.26 ppm): δ = 2.60 (m, 4H, Cp-CH<sub>2</sub>), 1.80 (m, 4H, CH<sub>2</sub>), 0.96 (s, 18H, tBu), 0.36 (s, 6H, SiMe), 0.13 (s, 6H, SiMe) ppm.

<sup>13</sup>C-NMR (75 MHz), 25 °C, CDCl<sub>3</sub> (77.13 ppm): δ = 208.81, 179.82, 112.00, 72.78, 27.70, 25.32, 22.63, 19.17, -4.00 ppm.

**$\eta_4\{-1,3\text{-bis(triphenylsilyl)\text{-}4,5,6,7\text{-tetrahydro\text{-}2H\text{-}inden\text{-}2\text{-one}\text{\textgreater}iron}^0\text{ tricarbonyl (Fe-1c).}$** <sup>[7]</sup>

Appearance: Yellow crystalline solid.

<sup>1</sup>H-NMR (300 MHz), 25 °C, CDCl<sub>3</sub> (7.26 ppm): δ = 7.66 (d, J = 6.6 Hz, 12H, Ph), 7.42 – 7.31 (m, 18H, Ph), 2.1 – 1.9 (m, 2H, CH<sub>2</sub>), 1.7 – 1.3 (m, 6H, CH<sub>2</sub>) ppm.

<sup>13</sup>C-NMR (75 MHz), 25 °C, CDCl<sub>3</sub> (77.13 ppm): δ = 207.92, 180.36, 136.69, 133.71, 129.80, 127.88, 112.50, 70.19, 25.05, 22.40 ppm.

**$\eta_4\{-1,3\text{-bis(triisopropylsilyl)\text{-}5,6-dihydropentalen\text{-}2(4H\text{-}one)\text{\textgreater}iron}^0\text{ tricarbonyl (Fe-1d).}$**

Appearance: Yellow crystalline solid.

<sup>1</sup>H-NMR (300 MHz), 25 °C, CDCl<sub>3</sub> (7.26 ppm): δ = 2.92 (d, J = 21.8 Hz, 4H, Cp-CH<sub>2</sub>), 2.4 – 1.7 (dm, J = 156.8 Hz, 2H, CH<sub>2</sub>), 1.39 (m 6H, CHMe<sub>2</sub>), 1.15 (dd, J<sub>1</sub> = 7.5; J<sub>2</sub> = 13.3 Hz, 36H, Me) ppm.

<sup>13</sup>C-NMR (75 MHz), 25 °C, CDCl<sub>3</sub> (77.13 ppm): δ = 209.23, 183.83, 117.87, 71.60, 29.07, 26.23, 19.30, 19.23, 12.23 ppm.

**$\eta_4\{-1,3\text{-diphenyl\text{-}4,5,6,7\text{-tetrahydro\text{-}2H\text{-}inden\text{-}2\text{-one}\text{\textgreater}iron}^0\text{ tricarbonyl (Fe-1e).}$** <sup>[8,11,12,13]</sup>

Appearance: Yellow crystalline solid.

<sup>1</sup>H-NMR (300 MHz), 25 °C, CDCl<sub>3</sub> (7.26 ppm): δ = 7.74 (d, J = 7.0 Hz, 4H, Ph), 7.5 – 7.3 (m, 6H, Ph), 2.77 (dt, J<sub>1</sub> = 14.0; J<sub>2</sub> = 17.0 Hz, 4H, Cp-CH<sub>2</sub>), 1.94 (m, 4H, CH<sub>2</sub>) ppm.

<sup>13</sup>C-NMR (75 MHz), 25 °C, CDCl<sub>3</sub> (77.13 ppm): δ = 209.09, 169.59, 131.45, 129.79, 128.53, 128.04, 100.50, 82.03, 100.50, 82.03, 23.84, 22.41 ppm.

*$\eta$ -{2,3,4,5-tetraphenylcyclopentadienone}iron<sup>0</sup> tricarbonyl (Fe-1f).<sup>[4,12,13]</sup>*

Appearance: Yellow crystalline solid.

<sup>1</sup>H-NMR (300 MHz), 25 °C, CDCl<sub>3</sub> (7.26 ppm): δ = 7.6 – 7.1 (m, 20H, Ph) ppm.

<sup>13</sup>C-NMR (75 MHz), 25 °C, CDCl<sub>3</sub> (77.13 ppm): δ = 208.66, 169.93, 131.96, 130.96, 130.42, 130.06, 128.84, 128.20, 128.17, 128.03, 104.16, 82.63 ppm.

*$\eta$ -{3,4-diphenyl-2,5-dimethylcyclopentadienone}iron<sup>0</sup> tricarbonyl (Fe-1g).<sup>[13,13]</sup>*

Appearance: Yellow crystalline solid.

<sup>1</sup>H-NMR (300 MHz), 25 °C, CDCl<sub>3</sub> (7.26 ppm): δ = 7.4 – 7.2 (m, 10H, Ph), 1.90 (s, 6H, Me) ppm.

<sup>13</sup>C-NMR (75 MHz), 25 °C, CDCl<sub>3</sub> (77.13 ppm): δ = 209.62, 180.31, 131.31, 130.14, 128.92, 128.40, 104.50, 77.33, 10.52 ppm.

*S2.3 General synthesis procedure for (cyclopentadienone)iron tricarbonyl complexes  
(Fe-2 series):*

In an oven-dried 10 mL Schlenk flask fitted with an air-tight septum, purged under a nitrogen atmosphere, a (cyclopentadienone)iron tricarbonyl (**Fe-1** series) complex (0.50 mmol) was dissolved in 2.5 mL dry and degassed acetonitrile. When complete solvation was assured, the reaction mixture was protected against light by wrapping aluminum foil around the Schlenk flask. A solution of Me<sub>3</sub>NO (0.75 mmol) in 2.5 mL dry and degassed acetonitrile was prepared under a nitrogen atmosphere, and added to the reaction mixture. The resulting reaction mixture was stirred at 500 rpm for 3 hours at room temperature.

After this time, magnetic stirring was stopped, and an appreciable amount of ochre-yellow precipitate was observed for most complexes. For **Fe-2e** and **Fe-2g** further precipitation was promoted by storage of the reaction mixture at 4°C for 18 hours. Subsequently, the precipitates were vacuum-filtered over a glass frit, and washed with 2x 5 mL cold (stored at -20°C) acetonitrile. The filtered yellow powder was collected in a small Schlenk flask, and exposed to deep vacuum (<10<sup>-2</sup> bar) in order to remove residual acetonitrile.

**$\eta$ -{1,3-bis(trimethylsilyl)-4,5,6,7-tetrahydro-2H-inden-2-one}iron<sup>0</sup> dicarbonyl mono-acetonitrile (Fe-2a).<sup>[4,6,14,15]</sup>**

Appearance: Ochre yellow solid.

<sup>1</sup>H-NMR (300 MHz), 25 °C, CDCl<sub>3</sub> (7.26 ppm): δ = 2.30 (m, 4H, Cp-CH<sub>2</sub>), 2.01 (s, 3H, Fe-NCCH<sub>3</sub>), 1.56 (m, 4H, CH<sub>2</sub>), 0.23 (s, 18H, TMS) ppm.

<sup>13</sup>C-NMR (75 MHz), 25 °C, CDCl<sub>3</sub> (77.13 ppm): δ = 212.93, 180.24, 126.15, 106.70, 70.01, 24.94, 22.42, 4.53, -0.02 ppm.

FTIR: 2945, 2899, 2862, 2160, 1983, 1923, 1581, 1558, 1539, 1506, 1439, 1395, 1364, 1341, 1312, 1302, 1260, 1238, 1055, 1036, 964, 957, 891, 829, 768, 748, 692, 621 cm<sup>-1</sup>.

**$\eta$ -{1,3-bis(tert-butyl dimethylsilyl)-4,5,6,7-tetrahydro-2H-inden-2-one}iron<sup>0</sup> dicarbonyl mono-acetonitrile (Fe-2b).**

Appearance: Ochre yellow solid.

<sup>1</sup>H-NMR (300 MHz), 25 °C, CDCl<sub>3</sub> (7.26 ppm): δ = 2.34 (m, 4H, Cp-CH<sub>2</sub>), 2.21 (s, 3H, Fe-NCCH<sub>3</sub>), 1.57 (m, 4H, CH<sub>2</sub>), 0.97 (s, 18H, tBu), 0.18 (s, 12H, SiMe) ppm.

<sup>13</sup>C-NMR (75 MHz), 25 °C, CDCl<sub>3</sub> (77.13 ppm): δ = 212.85, 178.68, 127.71, 107.59, 70.47, 27.73, 25.37, 22.61, 19.27, 4.57, -3.74, -4.63 ppm.

FTIR: 2945, 2899, 2862, 2160, 1983, 1923, 1581, 1558, 1539, 1506, 1439, 1395, 1364, 1341, 1312, 1302, 1260, 1238, 1055, 1036, 964, 957, 891, 829, 768, 748, 692, 621 cm<sup>-1</sup>.

**$\eta$ -{1,3-bis(triphenylsilyl)-4,5,6,7-tetrahydro-2H-inden-2-one}iron<sup>0</sup> dicarbonyl mono-acetonitrile (Fe-2c).<sup>[7]</sup>**

Appearance: Yellow solid.

<sup>1</sup>H-NMR (300 MHz), 25 °C, CDCl<sub>3</sub> (7.26 ppm): δ = 7.76 (d, J = 5.9 Hz, 12H, Ph), 7.30 (m, 18H, Ph), 1.8 – 1.0 (m, 8H, CH<sub>2</sub>), 1.18 (s, 3H, Fe-NCCH<sub>3</sub>) ppm.

<sup>13</sup>C-NMR (75 MHz), 25 °C, CDCl<sub>3</sub> (77.13 ppm): δ = 212.21, 176.17, 137.08, 136.69, 136.42, 134.85, 134.60, 134.56, 129.21, 127.88, 127.85, 127.58, 108.08, 67.84, 25.05, 22.29, 5.02 ppm.

FTIR: 2945, 2899, 2862, 2160, 1983, 1923, 1898, 1582, 1558, 1438, 1394, 1364, 1259, 1238, 1055, 1036, 964, 891, 829, 768, 748, 692, 621, 581 cm<sup>-1</sup>.

**$\eta$ -{1,3-bis(triisopropylsilyl)-5,6-dihydropentalen-2(4H)-one}iron<sup>0</sup> dicarbonyl mono-acetonitrile (Fe-2d).**

Appearance: Yellow solid.

<sup>1</sup>H-NMR (300 MHz), 25 °C, CDCl<sub>3</sub> (7.26 ppm): δ = 2.61 (m, 2H, CH<sub>2</sub>), 2.3 – 2.1 (m, 4H, Cp-CH<sub>2</sub>), 2.01 (s, 3H, Fe-NCCH<sub>3</sub>), 1.41 (m, 6H, CHMe<sub>2</sub>), 1.3 – 0.8 (m, 36H, CHMe<sub>2</sub>) ppm.

<sup>13</sup>C-NMR (75 MHz), 25 °C, CDCl<sub>3</sub> (77.13 ppm): δ = 210.47, 186.10, 117.87, 107.20, 71.58, 29.06, 28.77, 19.23, 18.83, 12.23, 11.64, 4.94 ppm.

FTIR: 2941, 2864, 2160, 1992, 1942, 1582, 1558, 1506, 1456, 1387, 1352, 1225, 1016, 881, 760, 741, 708, 667, 633, 619 cm<sup>-1</sup>.

**$\eta_4\{-1,3\text{-diphenyl-4,5,6,7-tetrahydro-2H-inden-2-one}\}iron^0$  dicarbonyl mono-acetonitrile (Fe-2e).**

Appearance: Orange solid.

$^1\text{H-NMR}$  (300 MHz), 25 °C,  $\text{CDCl}_3$  (7.26 ppm):  $\delta = 7.82$  (d,  $J = 7.4$  Hz, 4H, Ph), 7.4 – 7.2 (m, 6H, Ph), 2.52 (dt,  $J_1 = 17.3$ ;  $J_2 = 23.4$  Hz, 4H, Cp- $\text{CH}_2$ ), 2.23 (s, 3H, Fe- $\text{NCCH}_3$ ), 1.69 (m, 4H,  $\text{CH}_2$ ) ppm.

$^{13}\text{C-NMR}$  (75 MHz), 25 °C,  $\text{CDCl}_3$  (77.13 ppm):  $\delta = 204.47, 168.63, 129.49, 129.36, 128.31, 128.13, 107.39, 101.44, 84.77, 23.80, 22.82, 5.04$  ppm.

FTIR: 2924, 2853, 2490, 2156, 1987, 1931, 1614, 1499, 1437, 1406, 1342, 1221, 1182, 1034, 895, 845, 793, 762, 708, 690, 615  $\text{cm}^{-1}$ .

**$\eta_4\{-2,3,4,5\text{-tetraphenylcyclopentadienone}\}iron^0$  dicarbonyl mono-acetonitrile (Fe-2f).**

Appearance: Yellow solid.

$^1\text{H-NMR}$  (300 MHz), 25 °C,  $\text{CDCl}_3$  (7.26 ppm):  $\delta = 7.7 – 6.9$  (m, 20H, Ph), 2.19 (s, 3H, Fe- $\text{NCCH}_3$ ) ppm.

$^{13}\text{C-NMR}$  (75 MHz), 25 °C,  $\text{CDCl}_3$  (77.13 ppm):  $\delta = 212.91, 177.85, 131.83, 130.96, 130.86, 130.42, 130.26, 129.44, 128.61, 128.14, 128.09, 127.85, 127.78, 127.69, 127.57, 126.73, 105.21, 80.88, 4.89$  ppm.

FTIR: 2160, 1996, 1946, 1614, 1558, 1506, 1496, 1442, 1395, 1339, 1314, 1217, 1155, 1074, 1026, 845, 806, 754, 711, 696, 640, 615, 575, 554  $\text{cm}^{-1}$ .

**$\eta_4\{-3,4\text{-diphenyl-2,5-dimethylcyclopentadienone}\}iron^0$  dicarbonyl mono-acetonitrile (Fe-2g).**

Appearance: Orange solid.

$^1\text{H-NMR}$  (300 MHz), 25 °C,  $\text{CDCl}_3$  (7.26 ppm):  $\delta = 7.3 – 7.1$  (m, 10H, Ph), 2.38 (s, 3H, Fe- $\text{NCCH}_3$ ), 1.77 (s, 6H, Me) ppm.

$^{13}\text{C-NMR}$  (75 MHz), 25 °C,  $\text{CDCl}_3$  (77.13 ppm):  $\delta = 213.23, 169.13, 132.00, 131.20, 128.37, 127.87, 127.84, 100.24, 77.87, 9.75, 4.90$  ppm.

FTIR: 2160, 1998, 1942, 1558, 1211, 972, 766, 698, 608, 584, 536  $\text{cm}^{-1}$ .

### S3. Representative chromatograms

S3.1 Piancatelli rearrangements of furfuryl alcohols towards 4-hydroxycyclopent-2-enone substrates:

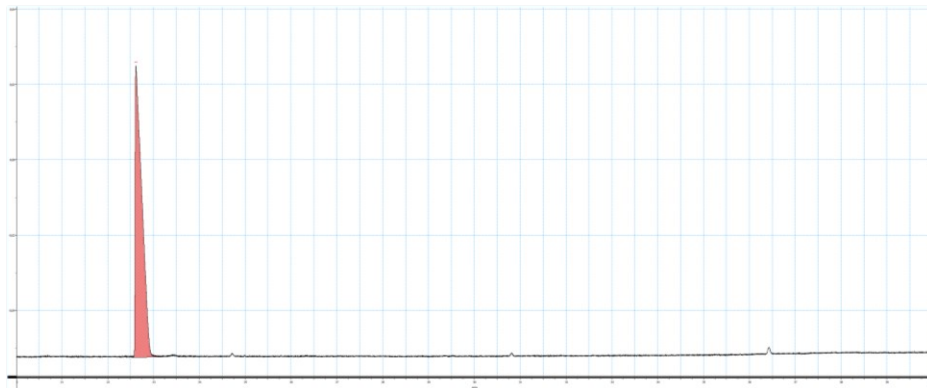
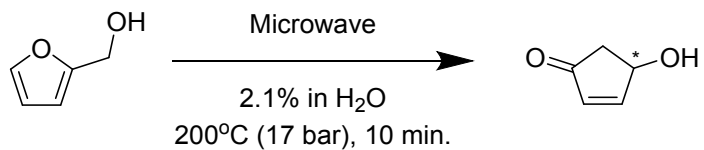


Figure S3.1.1: Gas chromatogram of furfuryl alcohol.

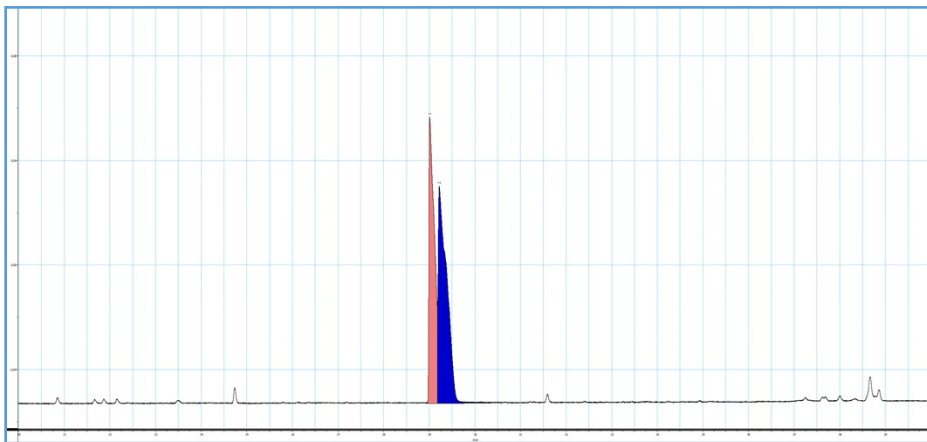


Figure S3.1.2: Gas chromatogram of 4-hydroxycyclopent-2-enone.

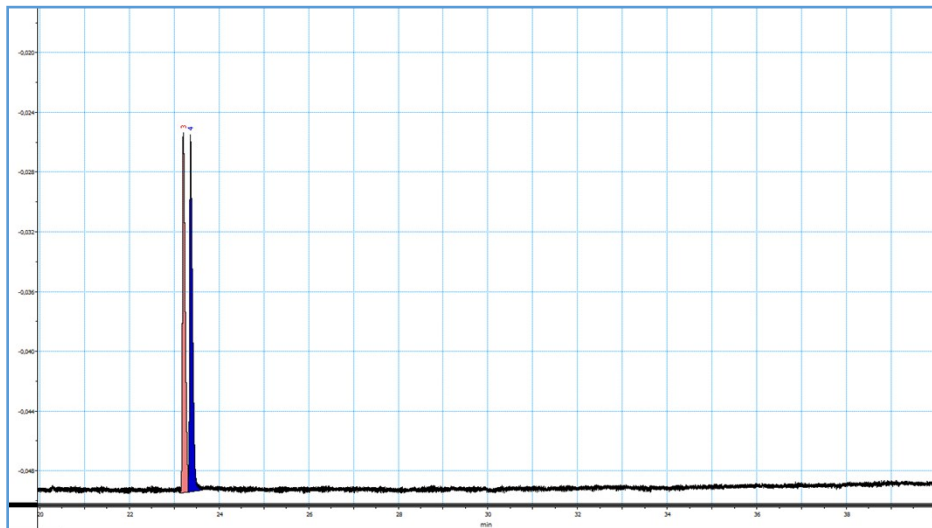
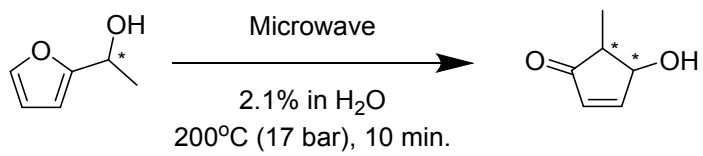


Figure S3.1.3: Gas chromatogram of (2-furyl)-1-yl-ethanol.

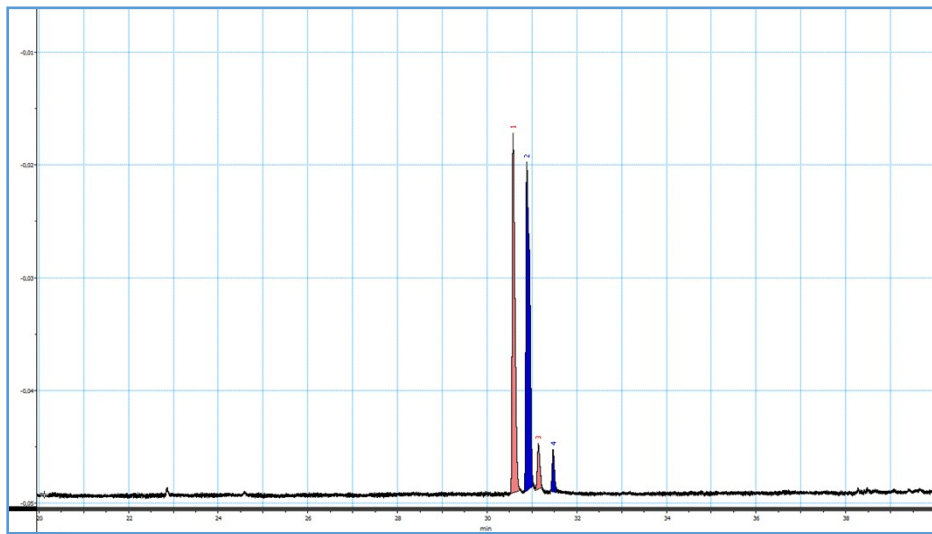


Figure S3.1.4: Gas chromatogram of 5-methyl-4-hydroxycyclopent-2-enone (**1a**).

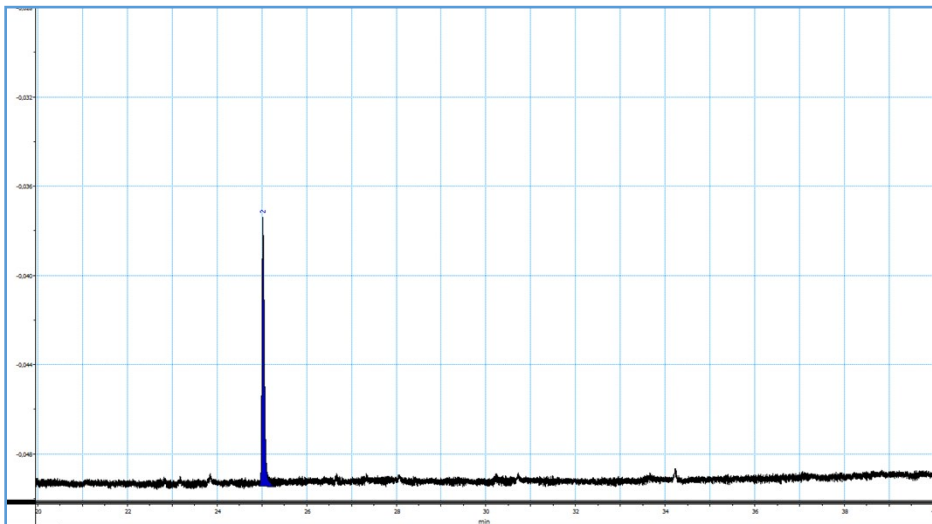
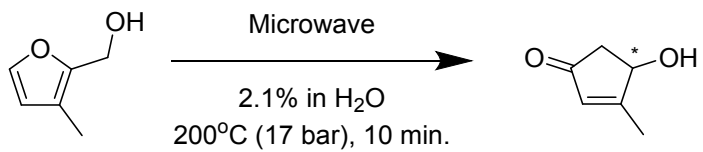


Figure S3.1.5: Gas chromatogram of 3-methyl-furfuryl alcohol.

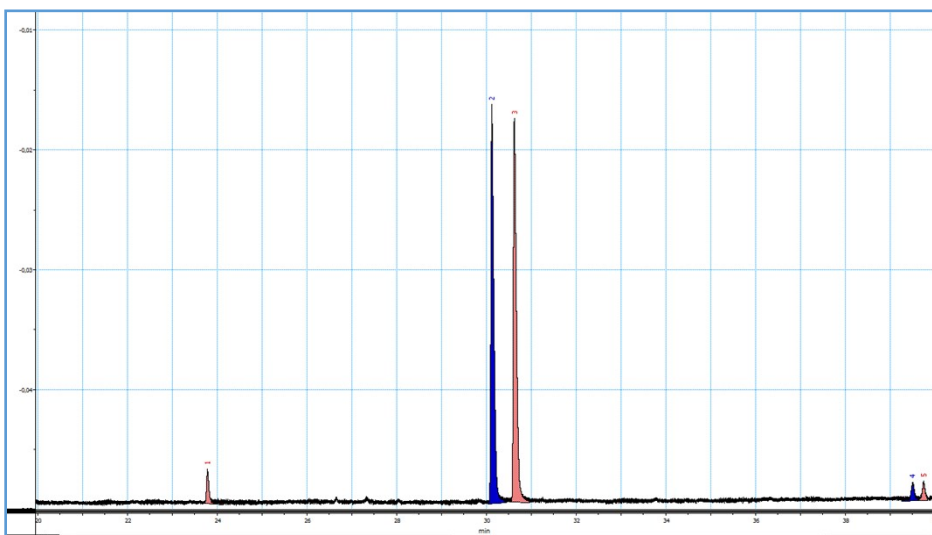


Figure S3.1.6: Gas chromatogram of 3-methyl 4-hydroxycyclopent-2-enone (**Ib**).

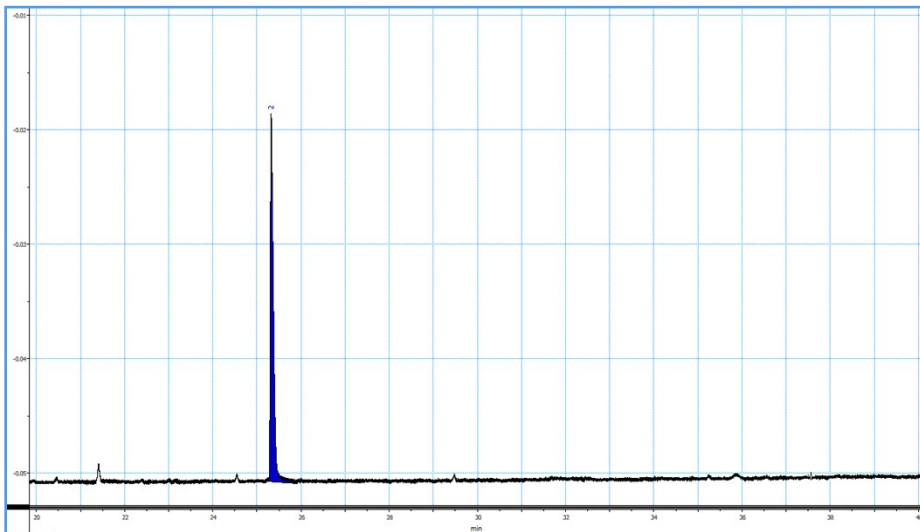
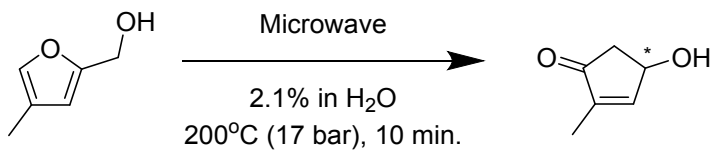


Figure S3.1.7: Gas chromatogram of 4-methylfurfuryl alcohol.

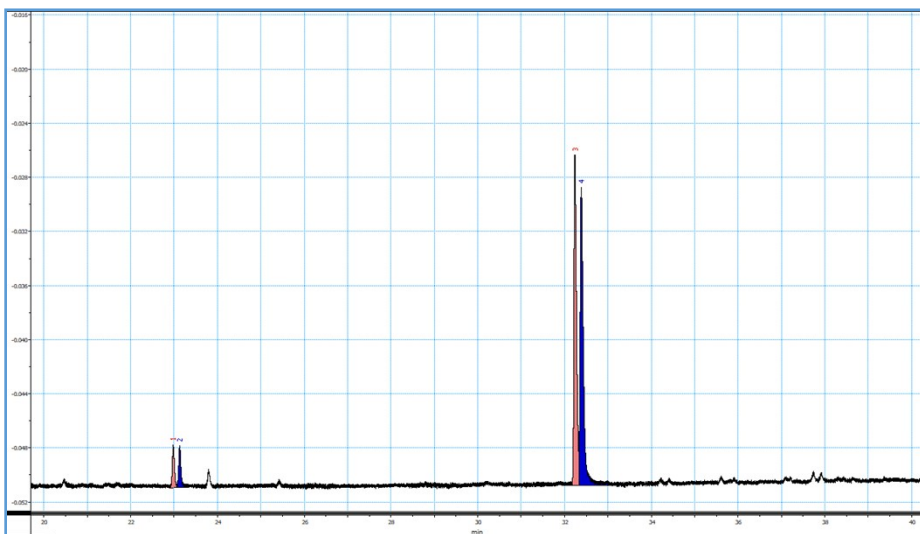


Figure S3.1.8: Gas chromatogram of 2-methyl-4-hydroxycyclopent-2-enone (**1c**).

### S3.2 Hydrogenation reactions

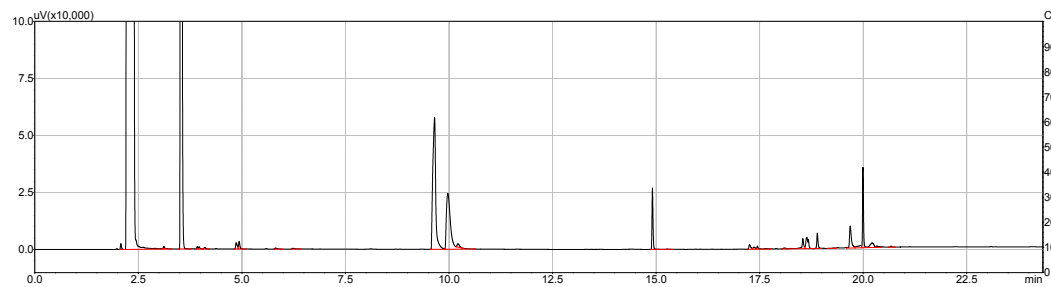


Figure S3.2.1: Representative chromatogram of a **Fe-2a** catalyzed hydrogenation of CPDO toward cpAdiols.

Retention times:    9.67 min                cis-cpAdiol  
                                10.07 min                trans-cpAdiol  
                                14.92 min                naphthalene (external standard)  
                                17 – 21 min            fragments of decomposed catalyst

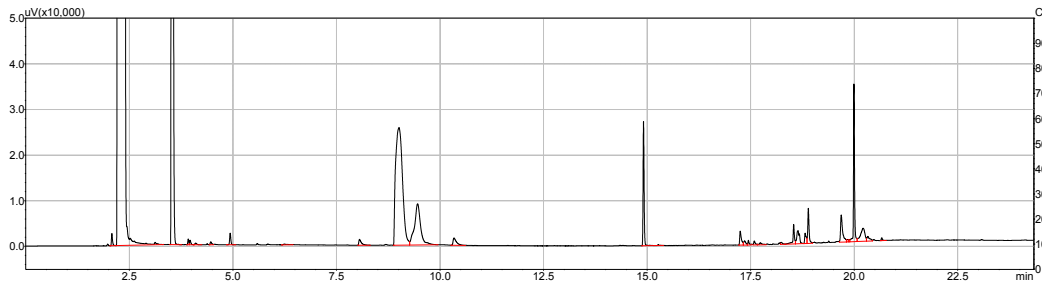


Figure S3.2.2: Representative chromatogram of a **Fe-2a** catalyzed hydrogenation of 4-HCP toward cpEdiols.

Retention times:    8.99 min                cis-cpEdiol  
                                9.42 min                trans-cpEdiol  
                                10.37 min              4-HCP  
                                14.92 min                naphthalene (external standard)  
                                17 – 21 min            fragments of decomposed catalyst

#### S4. $^1\text{H}$ -NMR and $^{13}\text{C}$ -NMR analysis

##### S4.1 Dialkyne pre-ligands

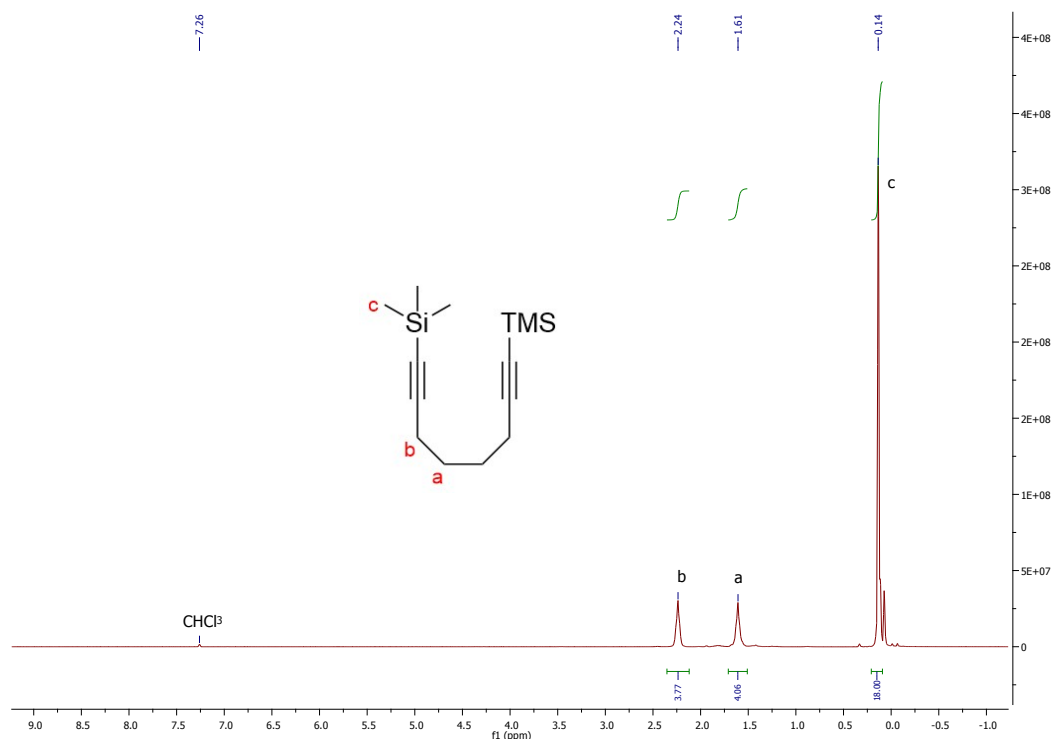


Figure S4.1.1:  $^1\text{H}$ -NMR spectrum of **L-I** in  $\text{CHCl}_3$ .

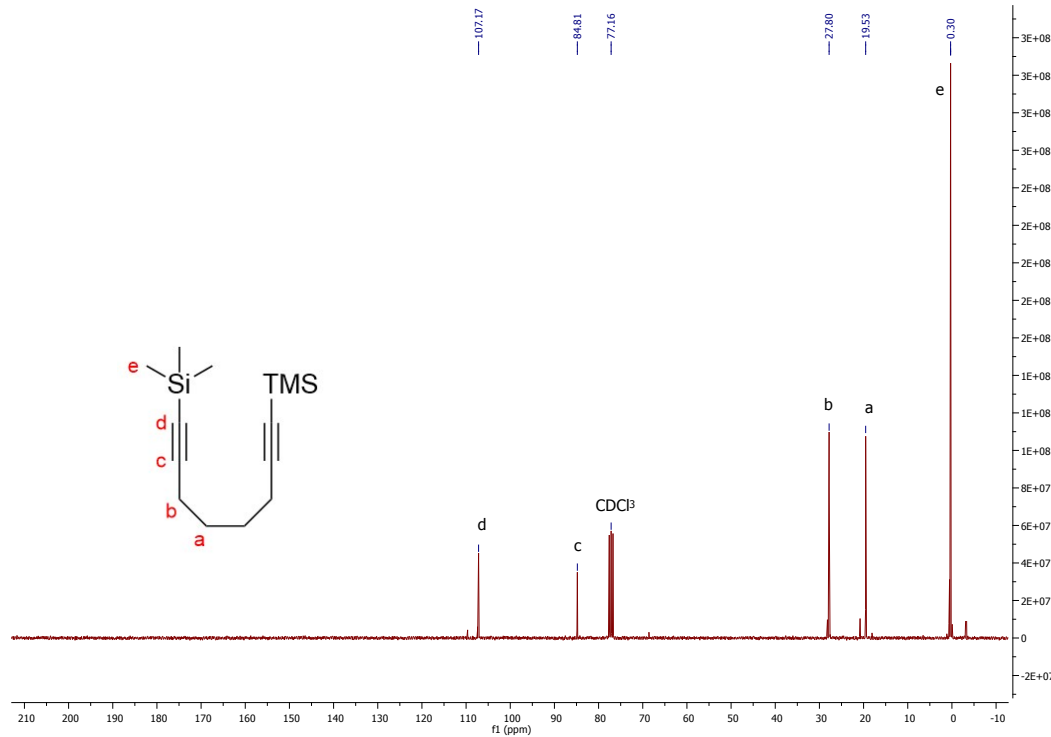


Figure S4.1.2:  $^{13}\text{C}$ -NMR spectrum of **L-I** in  $\text{CHCl}_3$ .

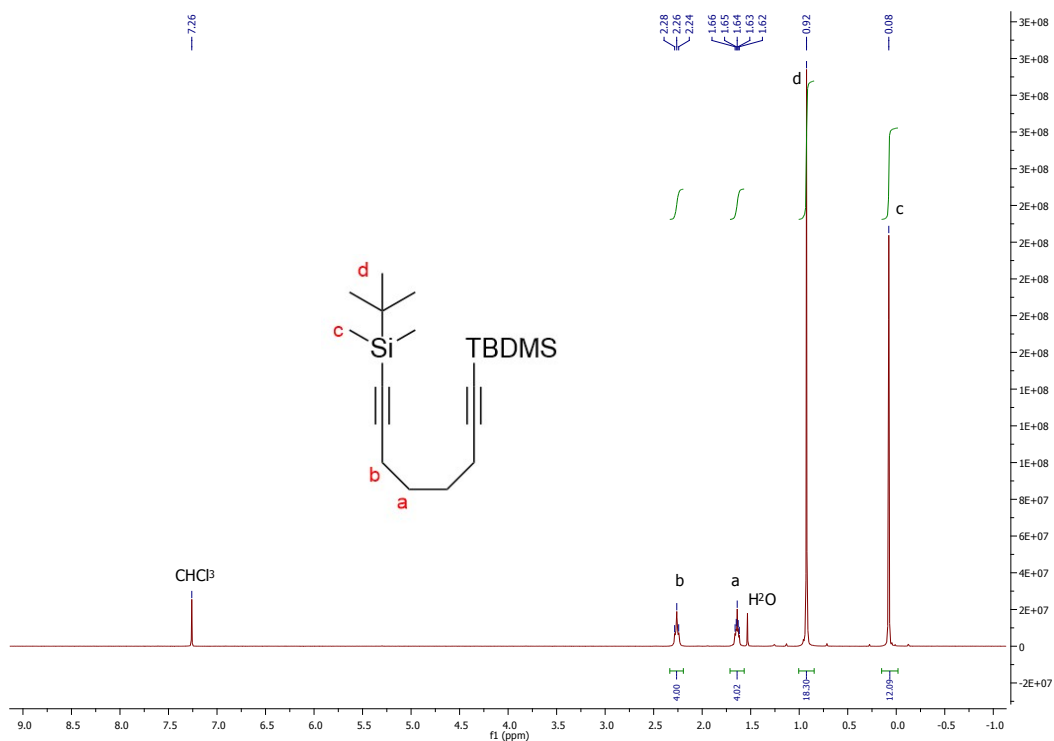


Figure S4.1.3: <sup>1</sup>H-NMR spectrum of **L-2** in  $\text{CHCl}_3$ .

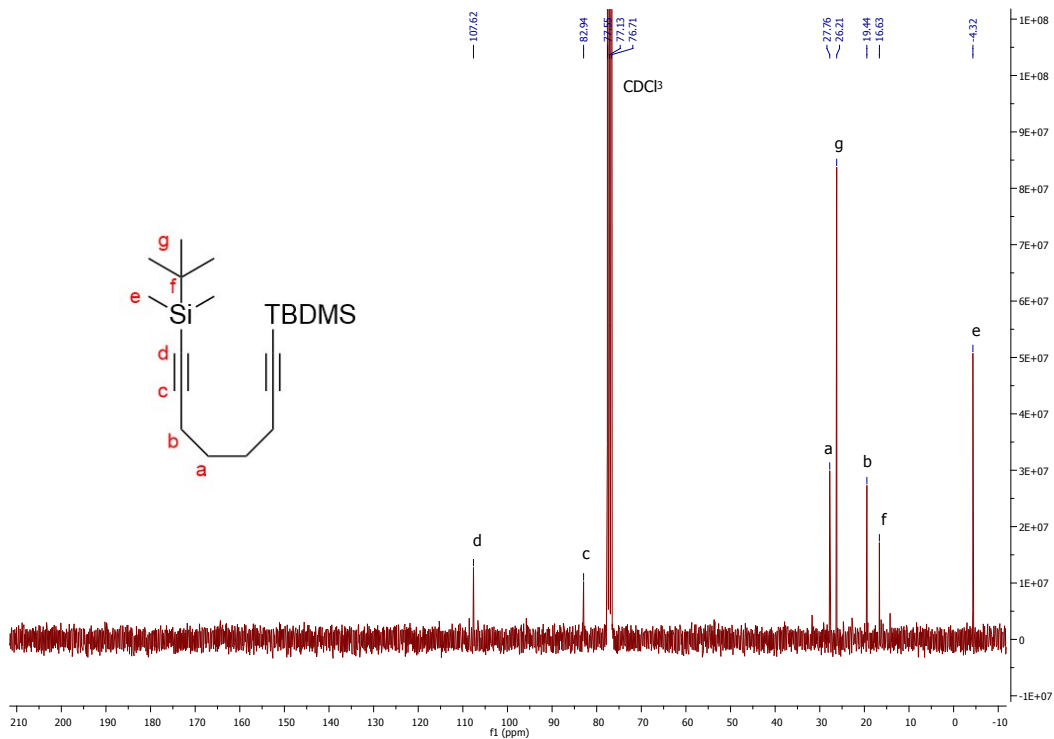


Figure S4.1.4: <sup>13</sup>C-NMR spectrum of **L-2** in  $\text{CHCl}_3$ .

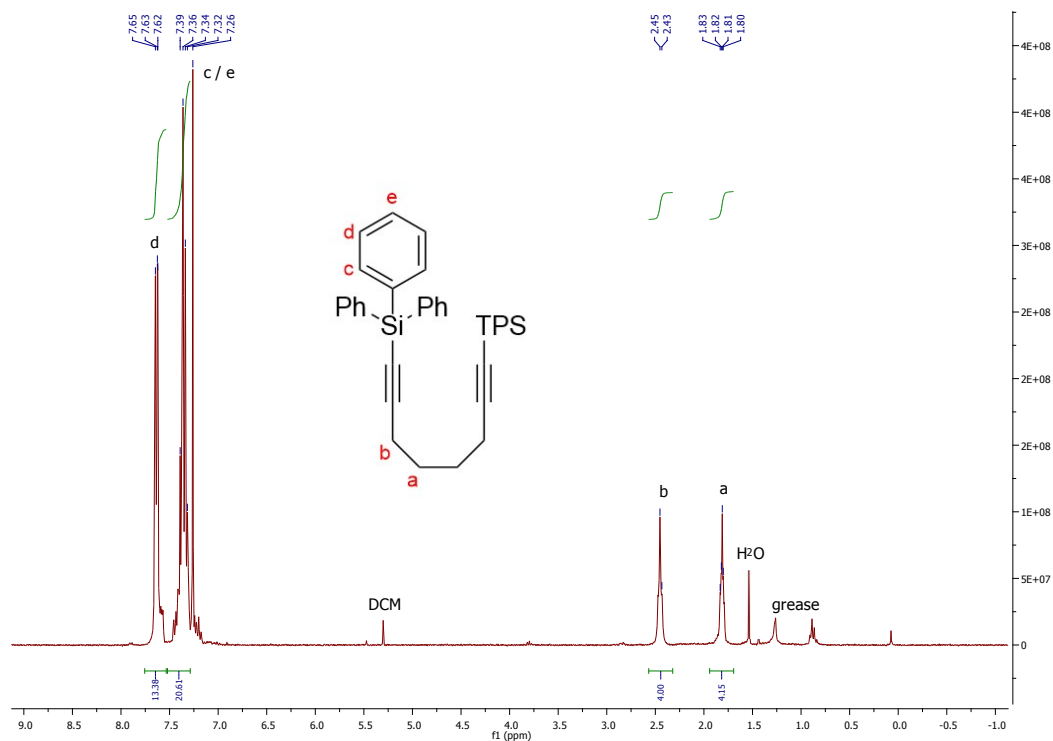


Figure S4.1.5:  $^1\text{H}$ -NMR spectrum of **L-3** in  $\text{CHCl}_3$ .

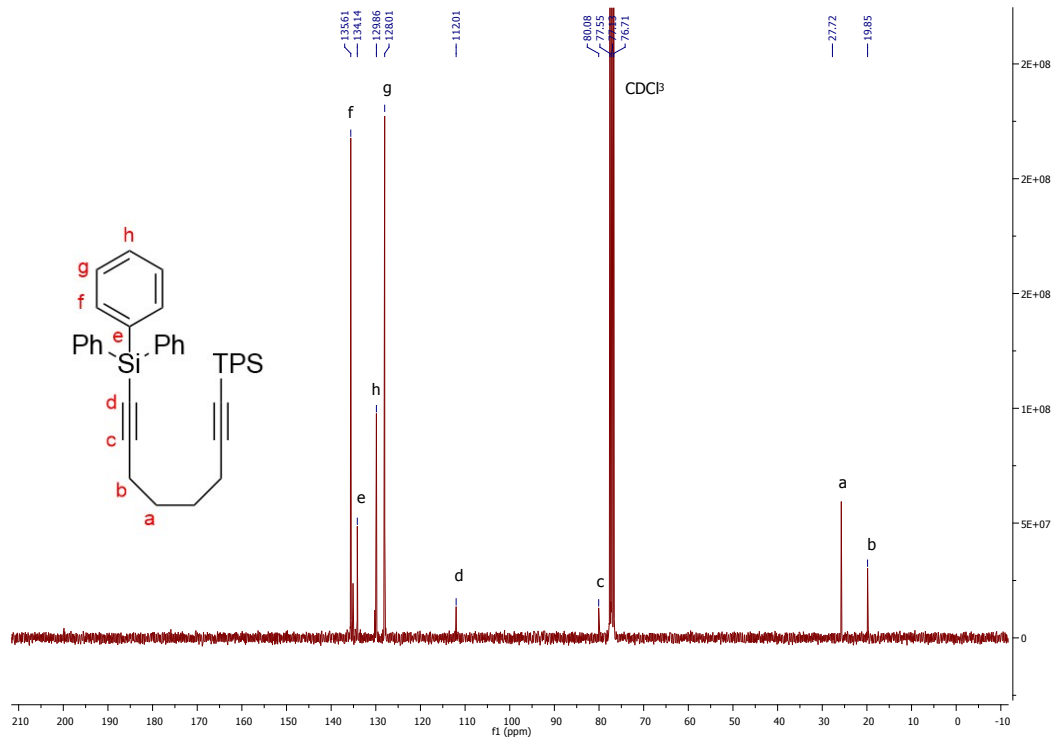


Figure S4.1.6:  $^1\text{H}$ -NMR spectrum of **L-3** in  $\text{CHCl}_3$ .

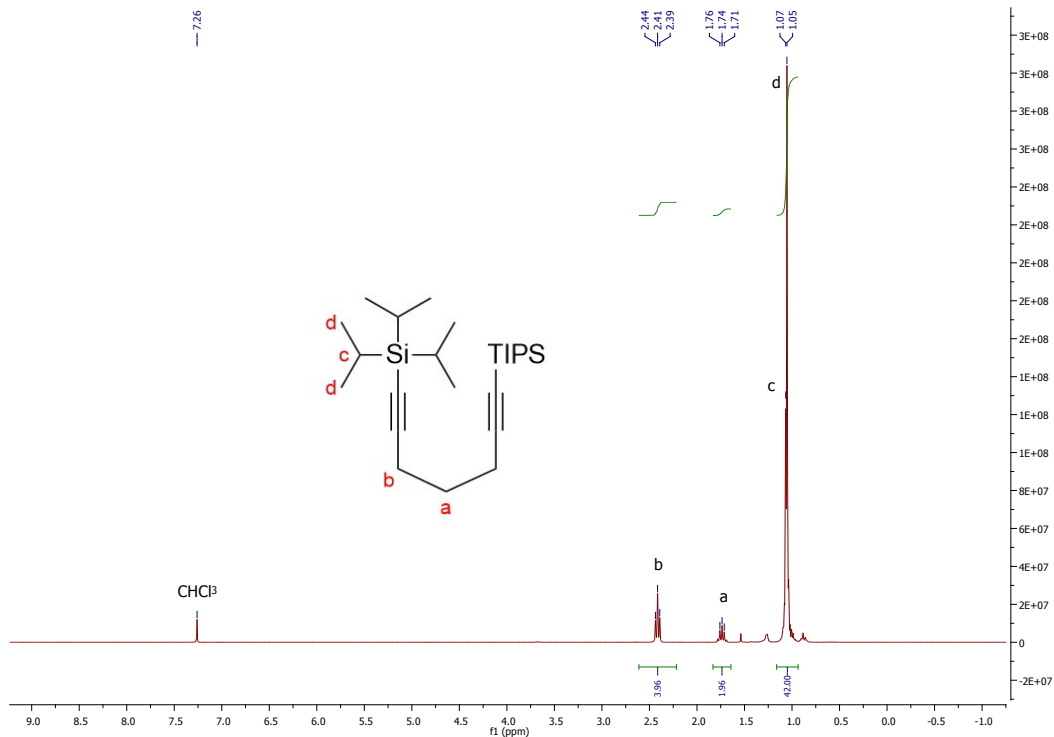


Figure S4.1.7: <sup>1</sup>H-NMR spectrum of **L-4** in  $\text{CHCl}_3$ .

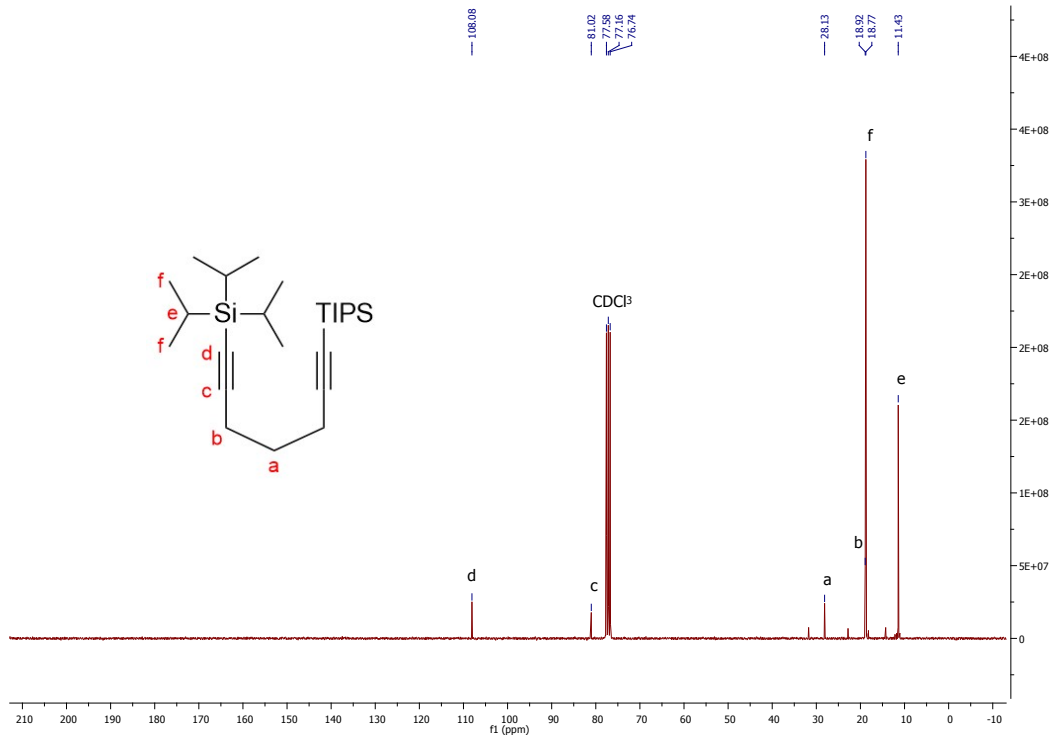


Figure S4.1.8: <sup>13</sup>C-NMR spectrum of **L-4** in  $\text{CHCl}_3$ .

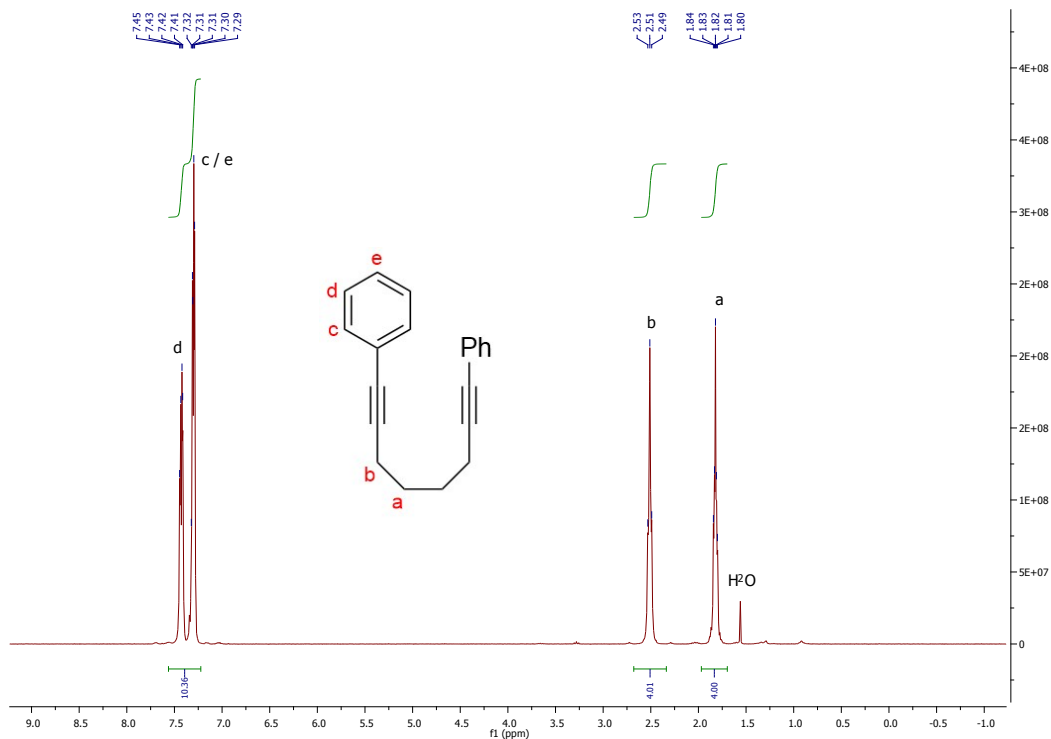


Figure S4.1.9: <sup>1</sup>H-NMR spectrum of **L-5** in  $\text{CHCl}_3$ .

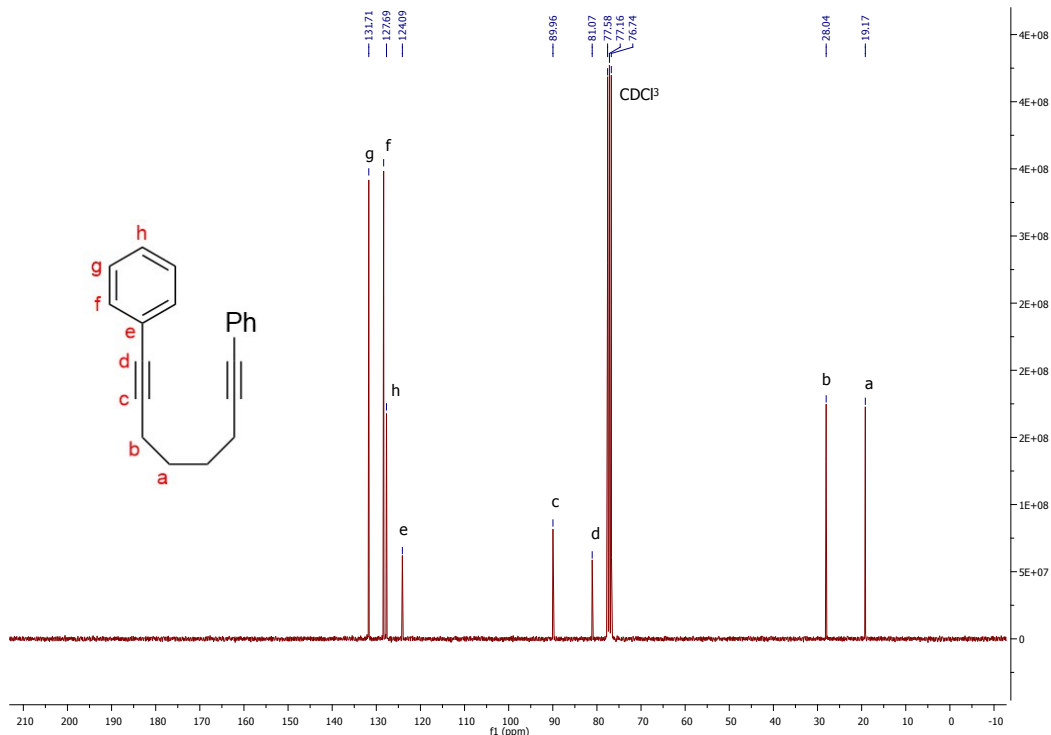


Figure S4.1.10: <sup>13</sup>C-NMR spectrum of **L-5** in  $\text{CHCl}_3$ .

S4.2 (*cyclopentadienone*)iron tricarbonyl complexes (**Fe-I** series)

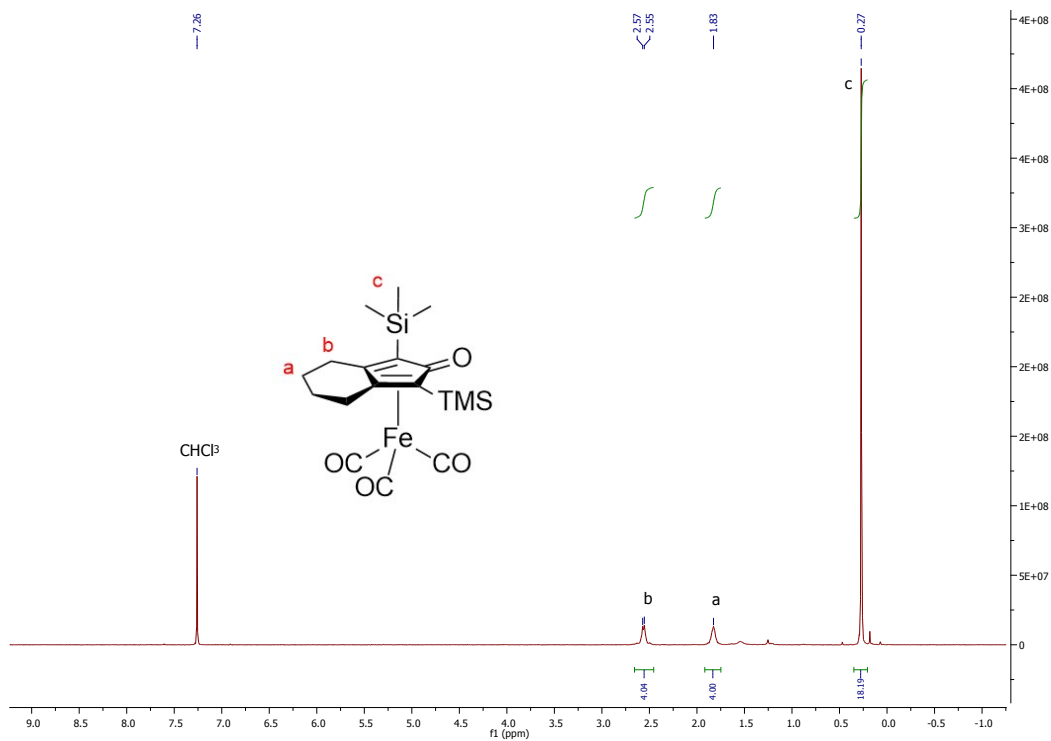


Figure S4.2.1: <sup>1</sup>H-NMR spectrum of **Fe-Ia** in  $\text{CHCl}_3$ .

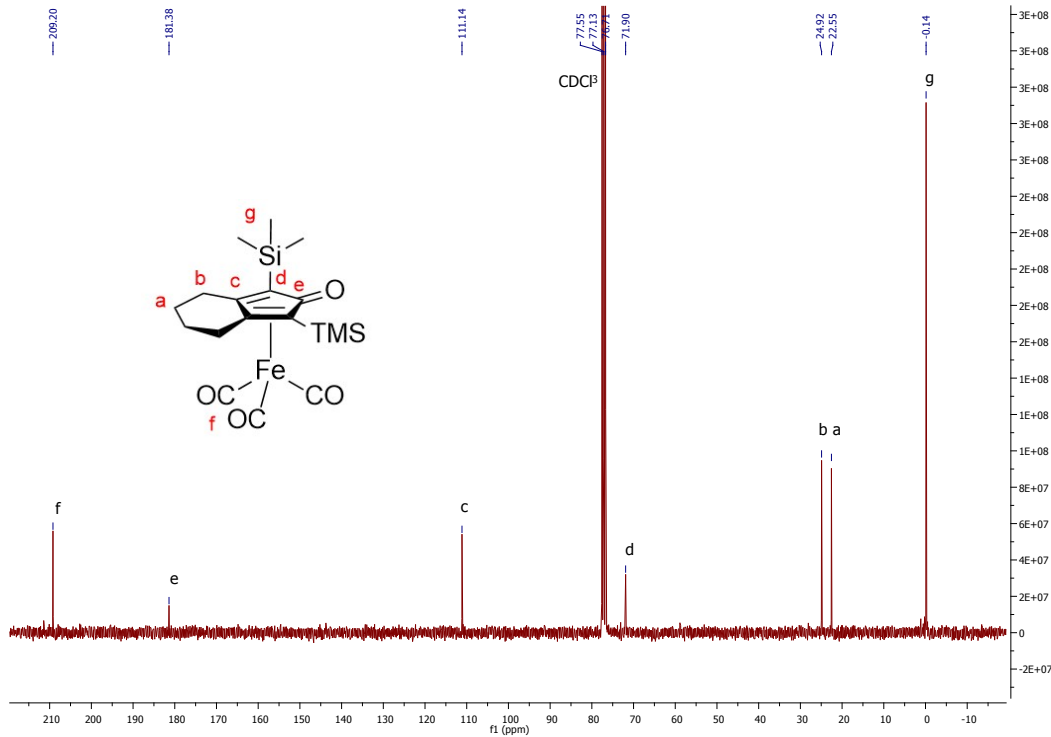


Figure S4.2.2: <sup>13</sup>C-NMR spectrum of **Fe-Ia** in  $\text{CHCl}_3$ .

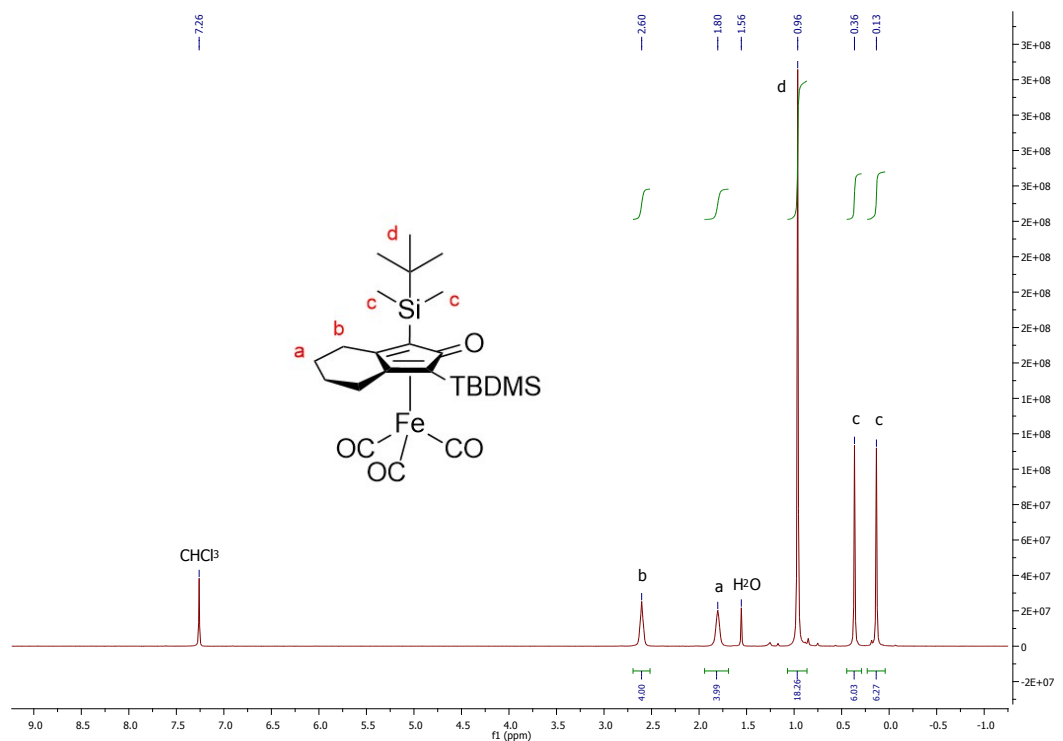


Figure S4.2.3: <sup>1</sup>H-NMR spectrum of **Fe-1b** in  $\text{CHCl}_3$ .

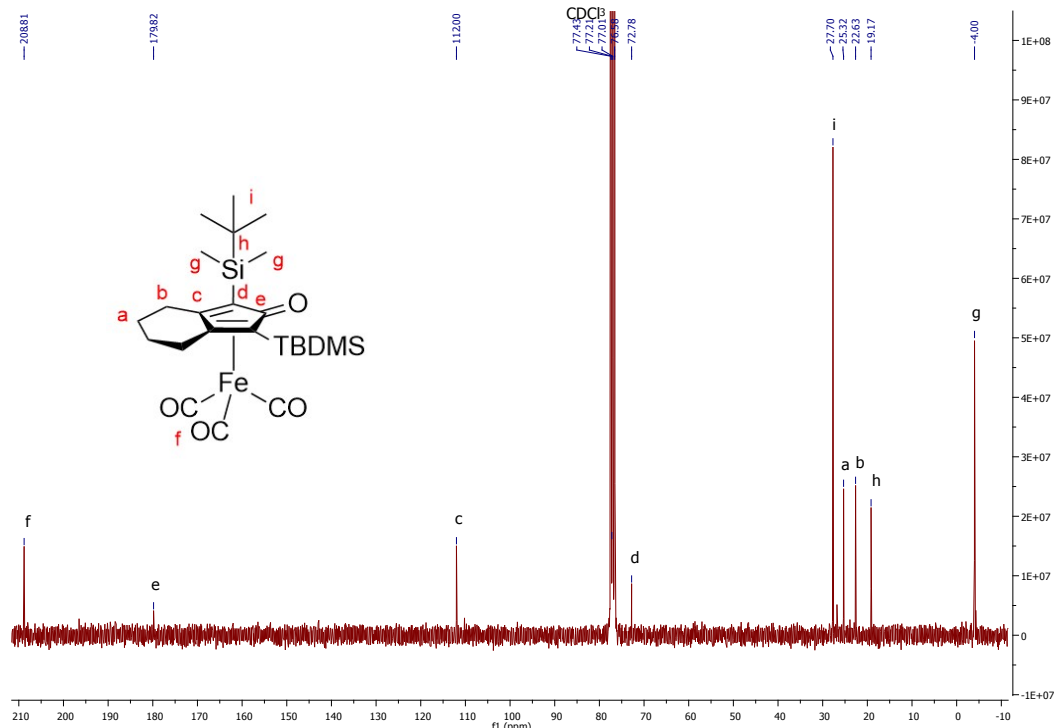


Figure S4.2.4: <sup>13</sup>C-NMR spectrum of **Fe-1b** in  $\text{CHCl}_3$ .

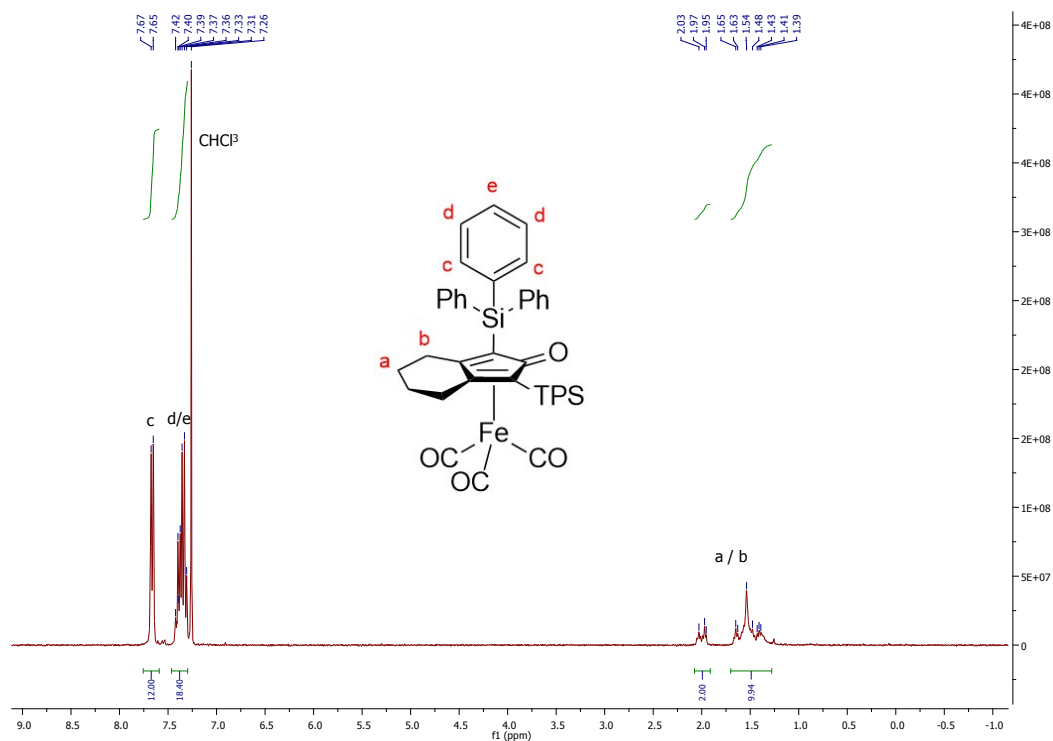


Figure S4.2. 5: <sup>1</sup>H-NMR spectrum of **Fe-1c** in  $\text{CHCl}_3$ .

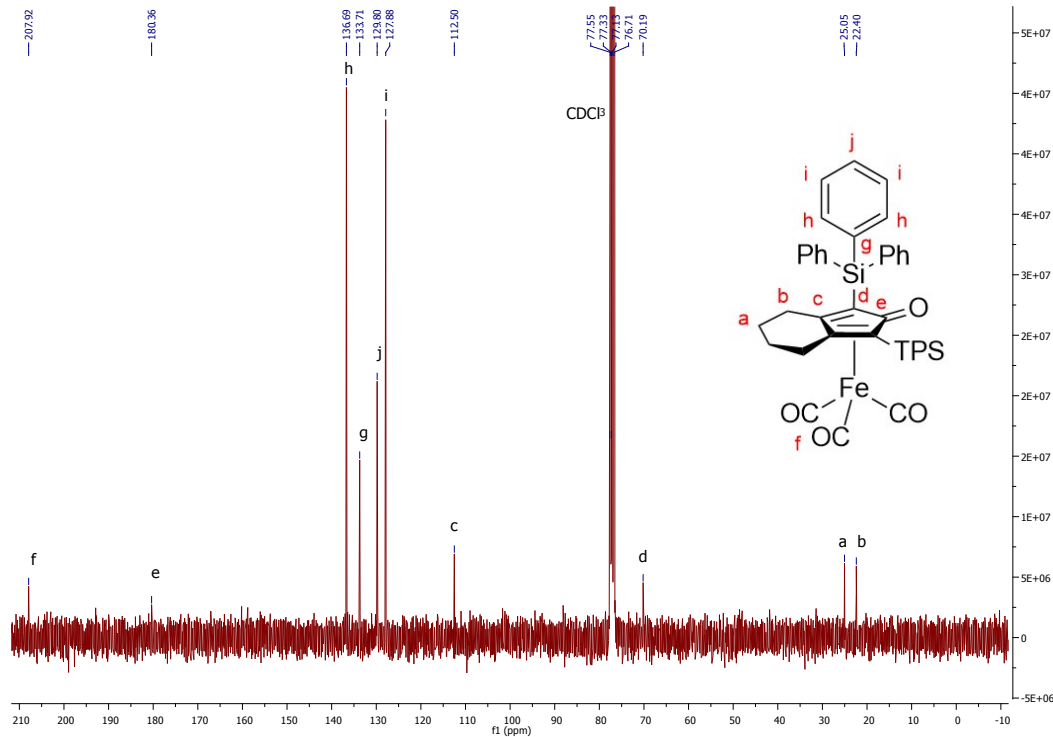


Figure S4.2.6: <sup>13</sup>C-NMR spectrum of **Fe-1c** in  $\text{CHCl}_3$ .

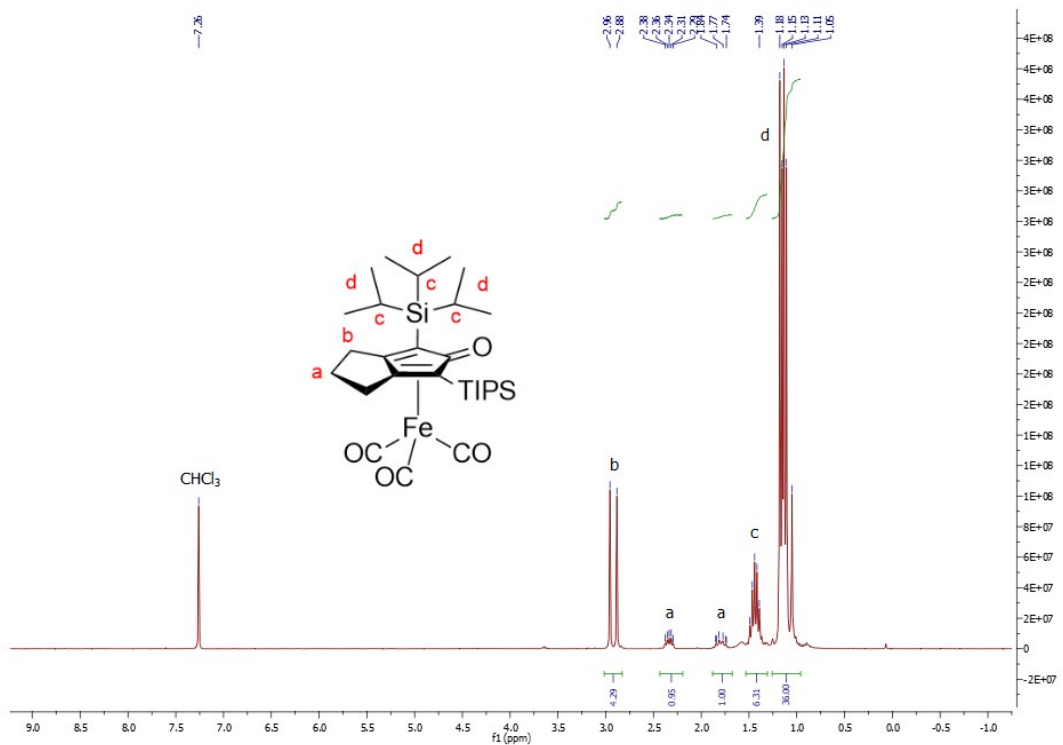


Figure S4.2.7:  $^1\text{H}$ -NMR spectrum of **Fe-1d** in  $\text{CHCl}_3$ .

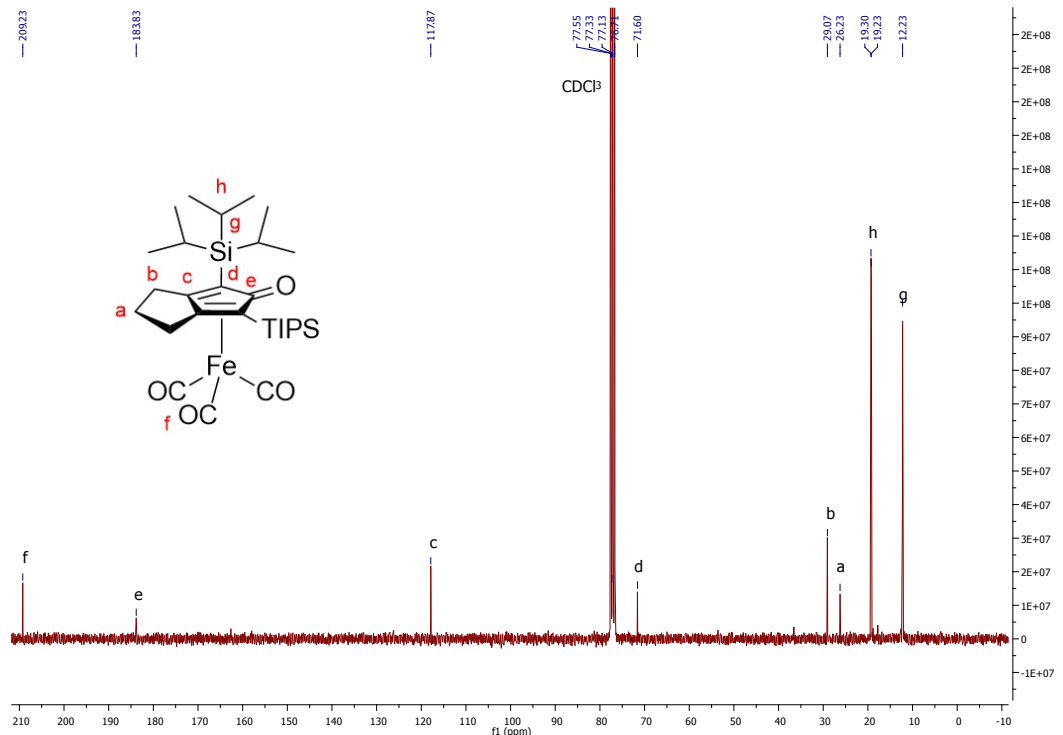


Figure S4.2.8:  $^{13}\text{C}$ -NMR spectrum of **Fe-1d** in  $\text{CHCl}_3$ .

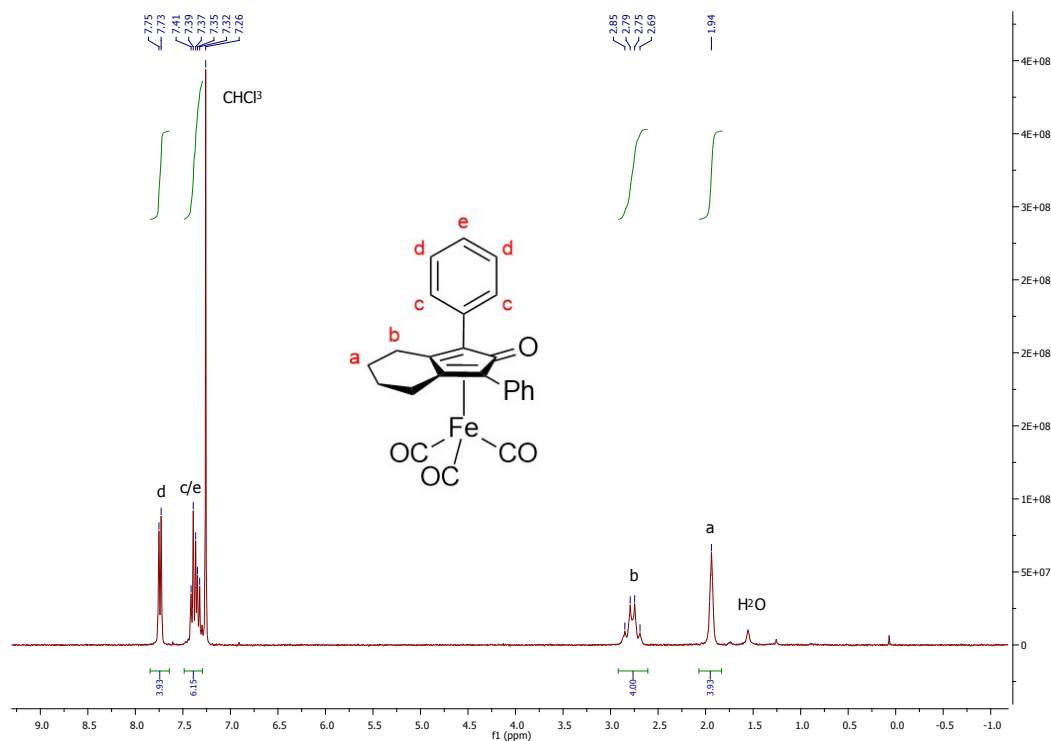


Figure S4.2. 9:  $^1\text{H}$ -NMR spectrum of **Fe-1e** in  $\text{CHCl}_3$ .

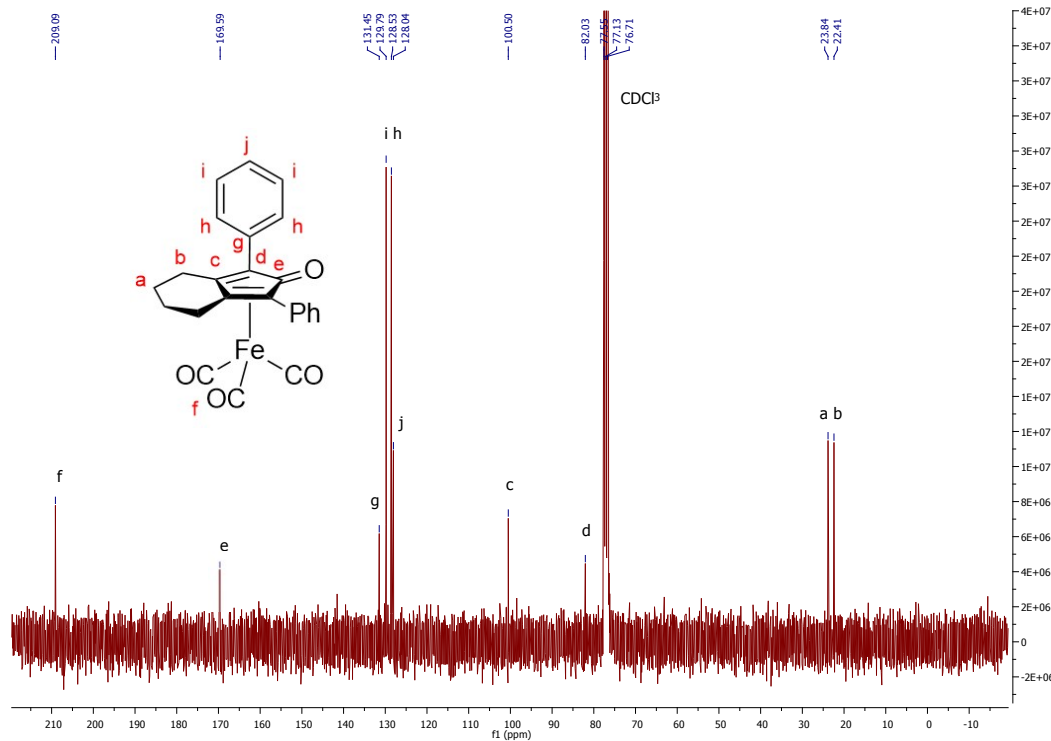


Figure S4.2.10:  $^{13}\text{C}$ -NMR spectrum of **Fe-1e** in  $\text{CHCl}_3$ .

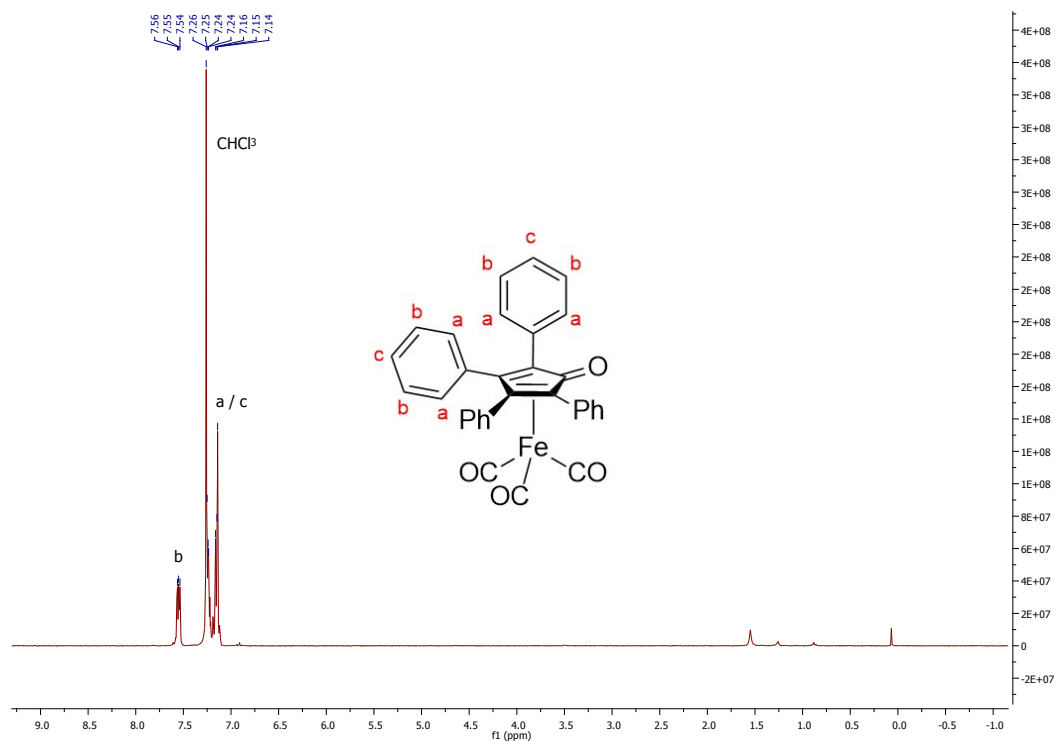


Figure S4.2.11: <sup>1</sup>H-NMR spectrum of **Fe-If** in  $\text{CHCl}_3$ .

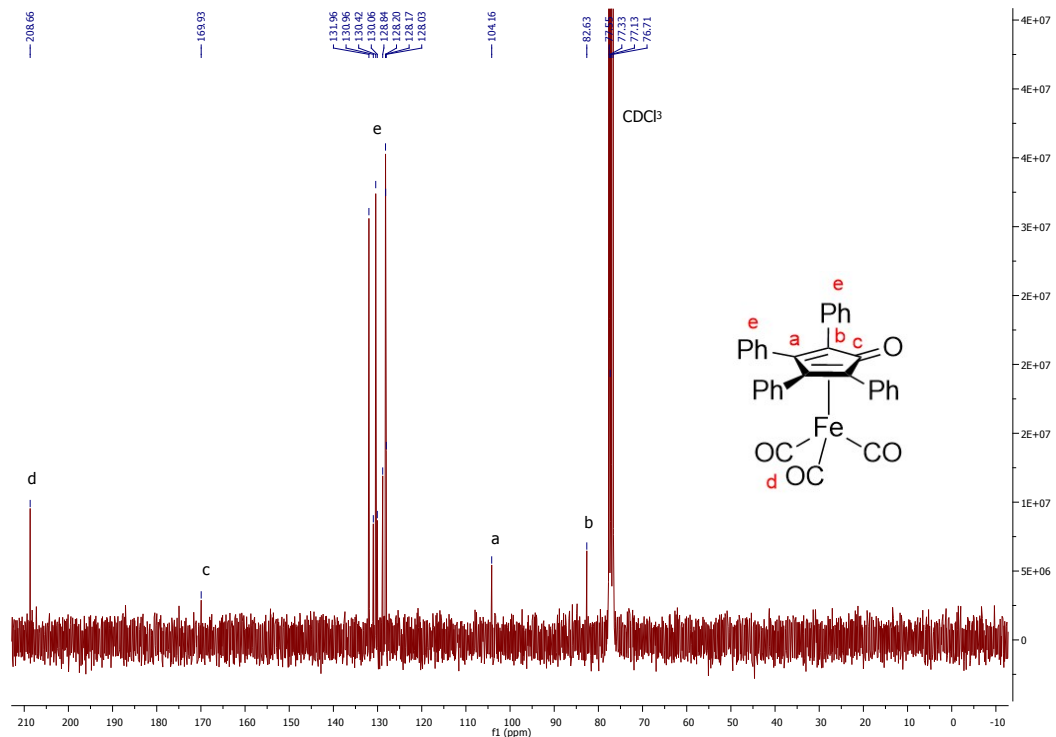


Figure S4.2.12: <sup>13</sup>C-NMR spectrum of **Fe-If** in  $\text{CHCl}_3$ .

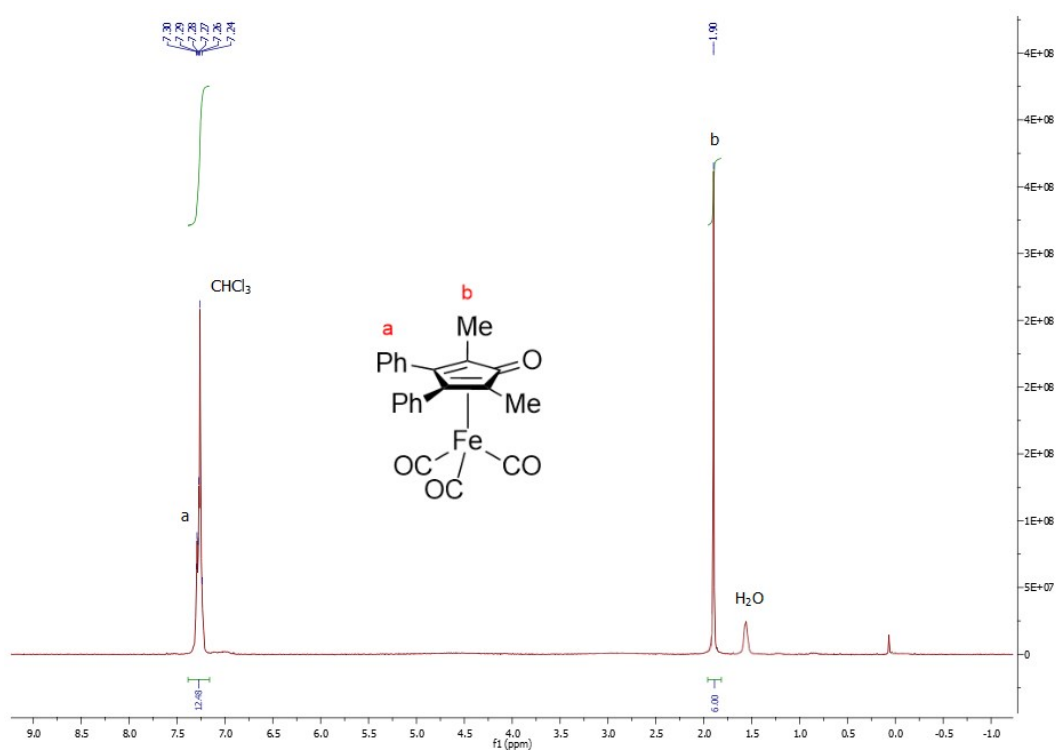


Figure S4.2.13: <sup>1</sup>H-NMR spectrum of **Fe-Ig** in  $\text{CHCl}_3$ .

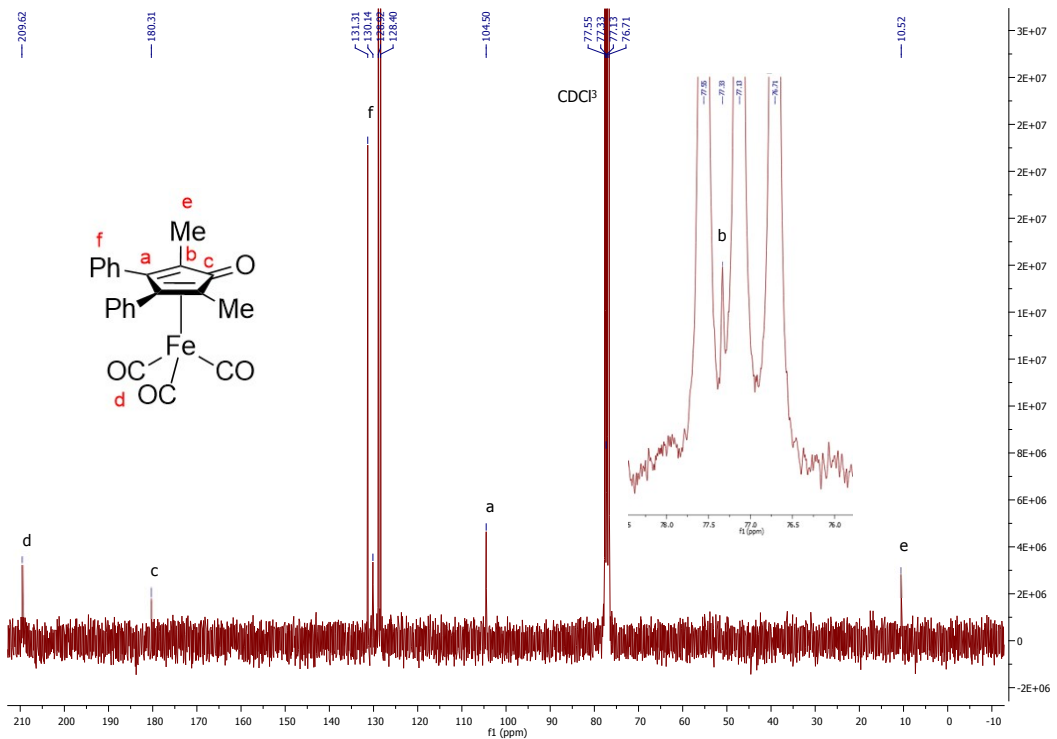


Figure S4.2.14: <sup>13</sup>C-NMR spectrum of **Fe-Ig** in  $\text{CHCl}_3$ .

S4.3 (*cyclopentadienone*)iron dicarbonyl mono-acetonitrile complexes (**Fe-2** series)

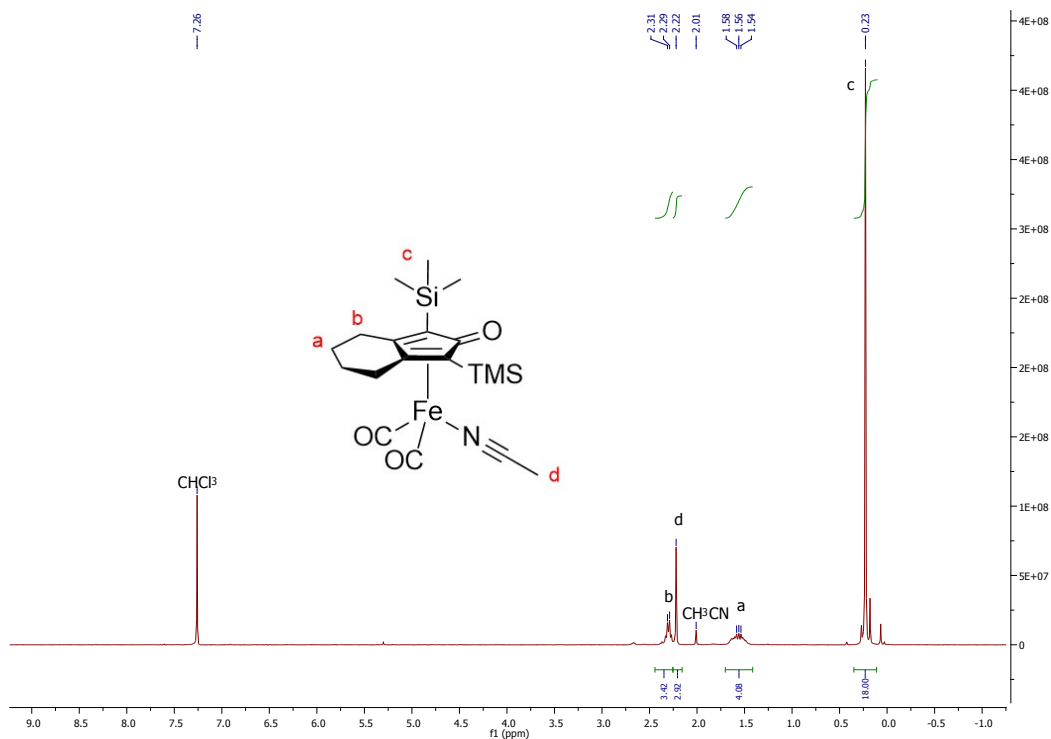


Figure S4.3.1:  $^1\text{H}$ -NMR spectrum of **Fe-2a** in  $\text{CHCl}_3$ .

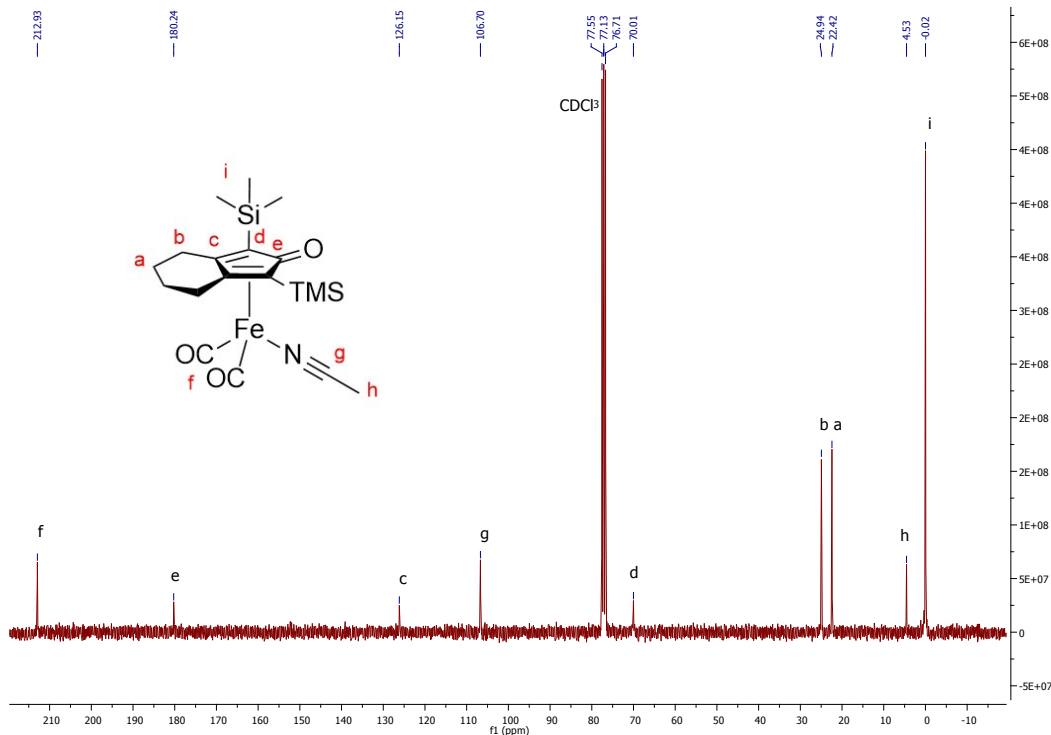


Figure S4.3.2:  $^{13}\text{C}$ -NMR spectrum of **Fe-2a** in  $\text{CHCl}_3$ .

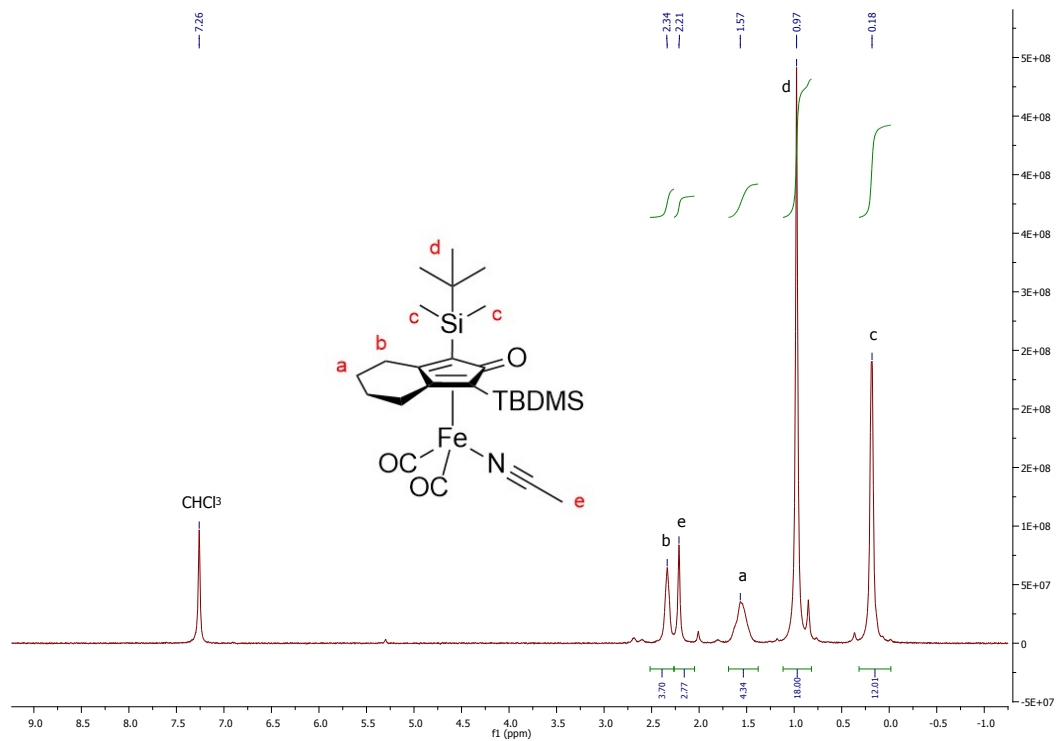


Figure S4.3.3:  $^1\text{H}$ -NMR spectrum of **Fe-2b** in  $\text{CHCl}_3$ .

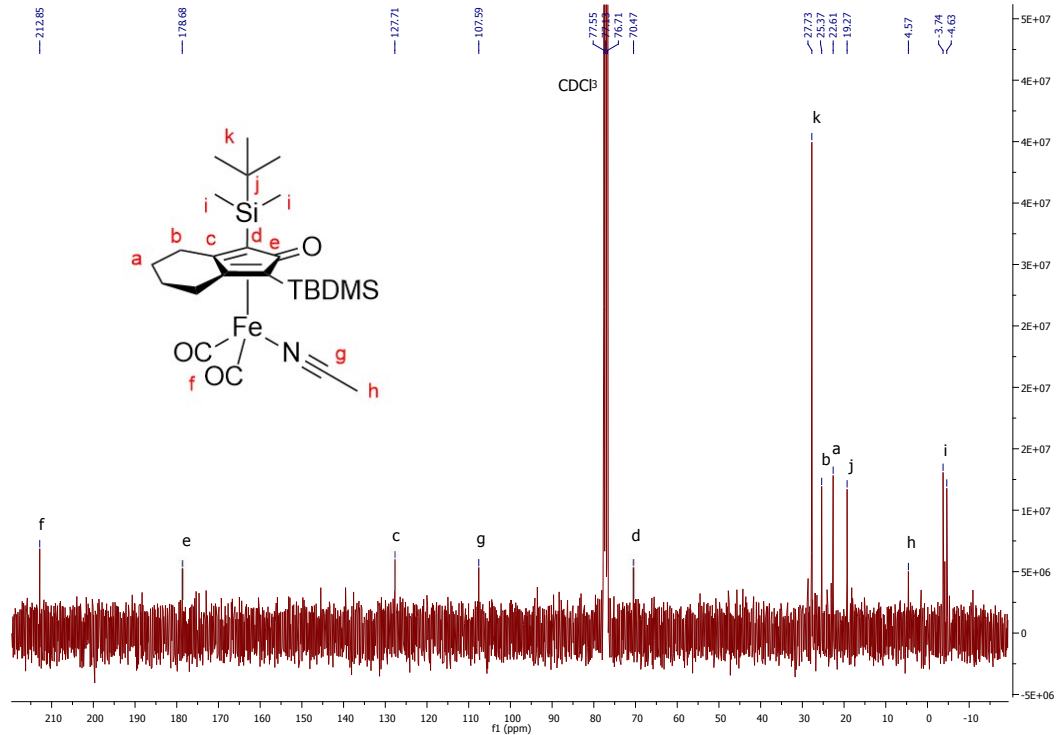


Figure S4.3.4:  $^{13}\text{C}$ -NMR spectrum of **Fe-2b** in  $\text{CHCl}_3$ .

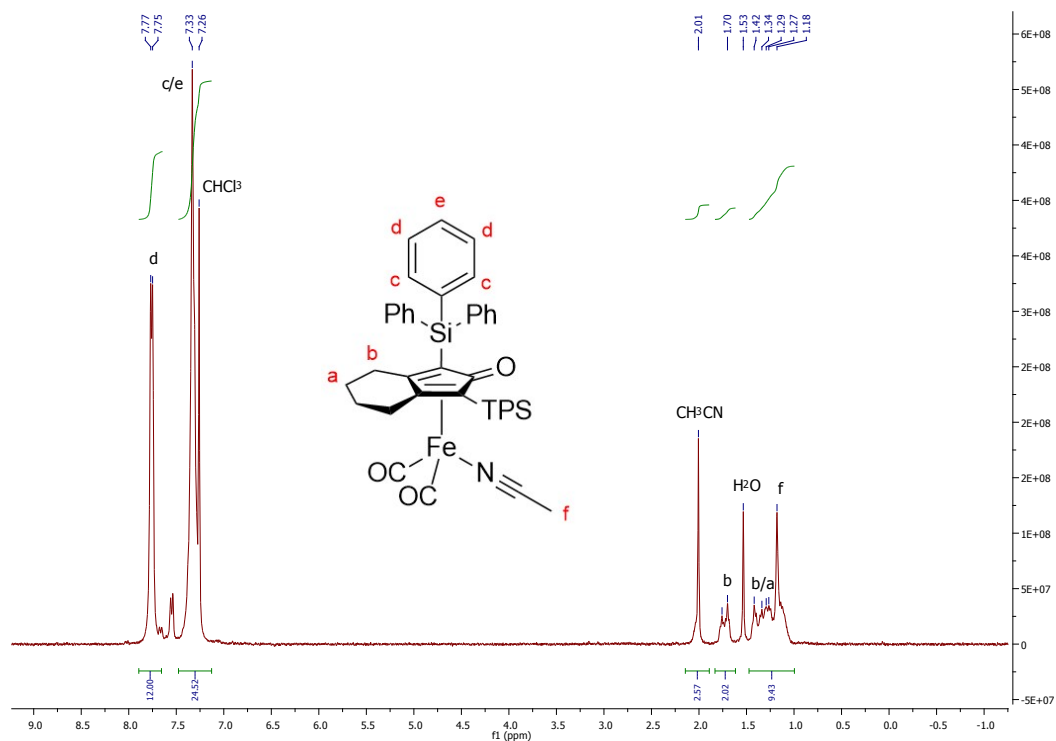


Figure S4.3.5: <sup>1</sup>H-NMR spectrum of **Fe-2c** in  $\text{CHCl}_3$ .

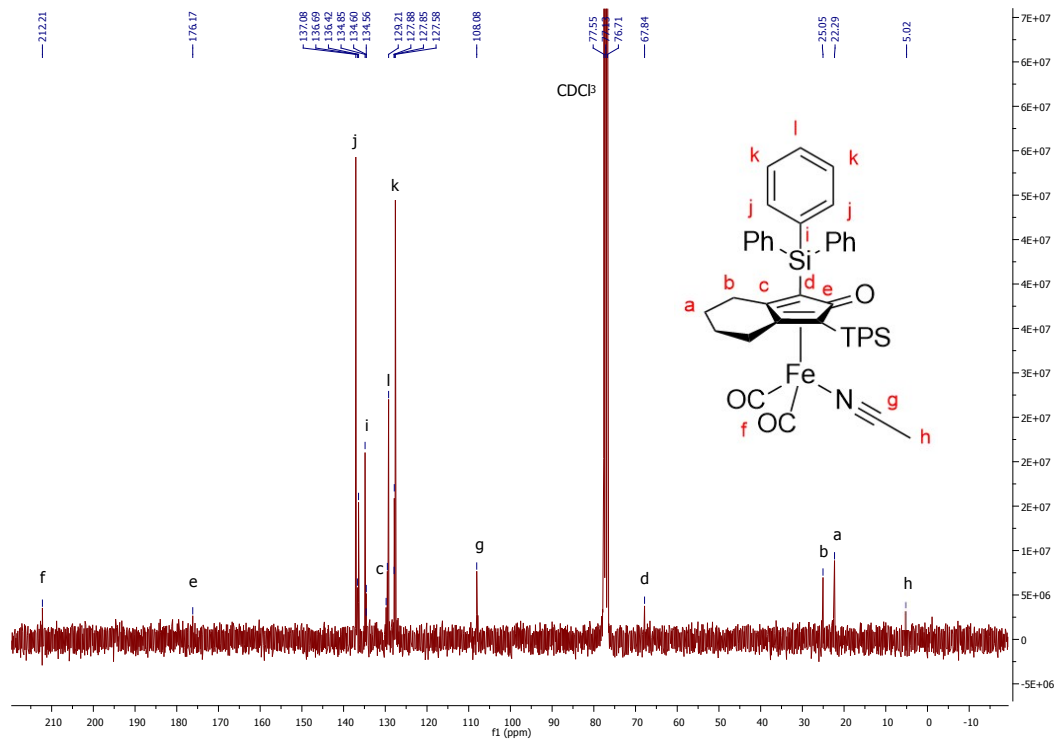


Figure S4.3.6: <sup>13</sup>C-NMR spectrum of **Fe-2c** in  $\text{CHCl}_3$ .

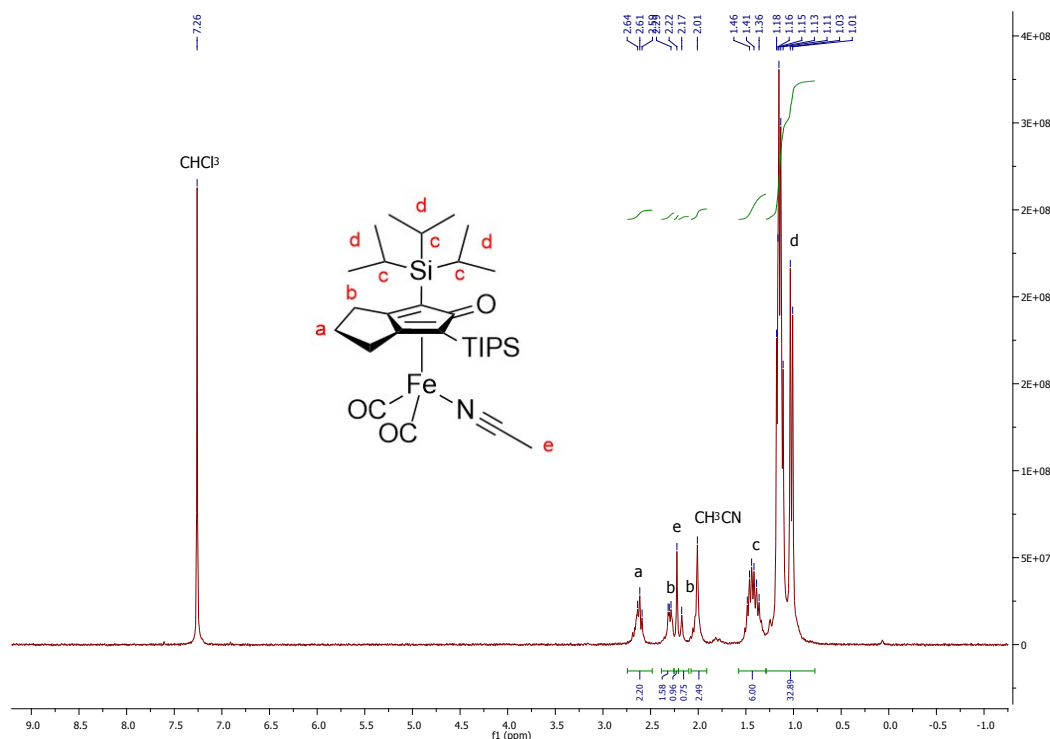


Figure S4.3.7: <sup>1</sup>H-NMR spectrum of Fe-2d in  $\text{CHCl}_3$ .

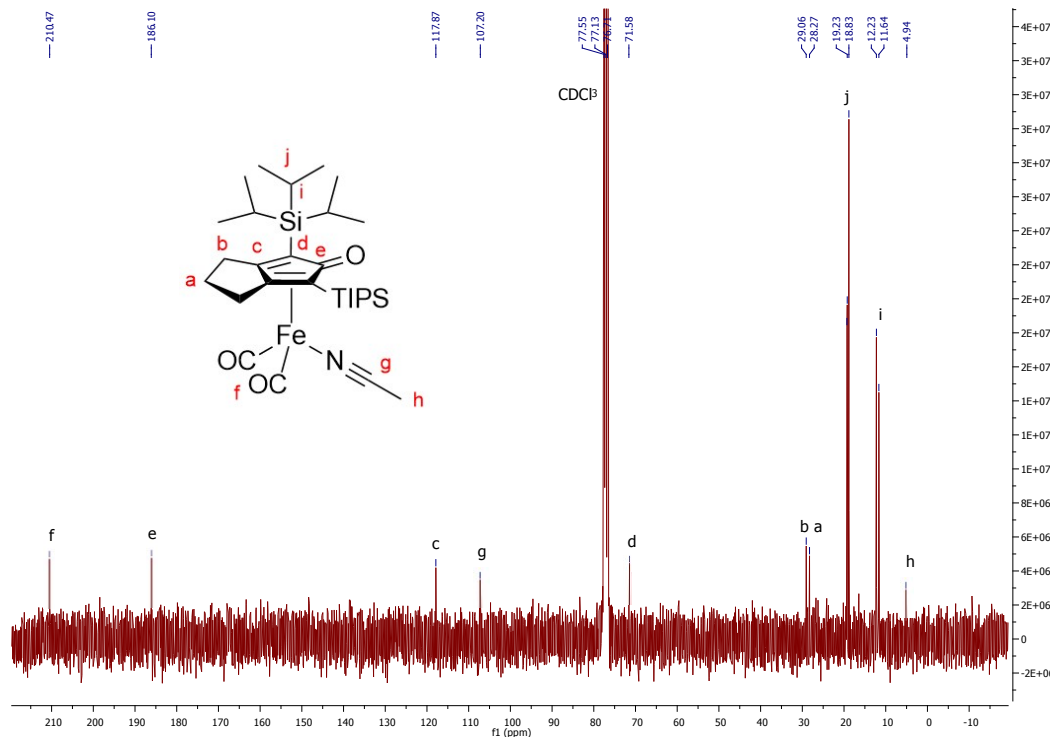


Figure S4.3.8: <sup>13</sup>C-NMR spectrum of Fe-2d in  $\text{CHCl}_3$ .

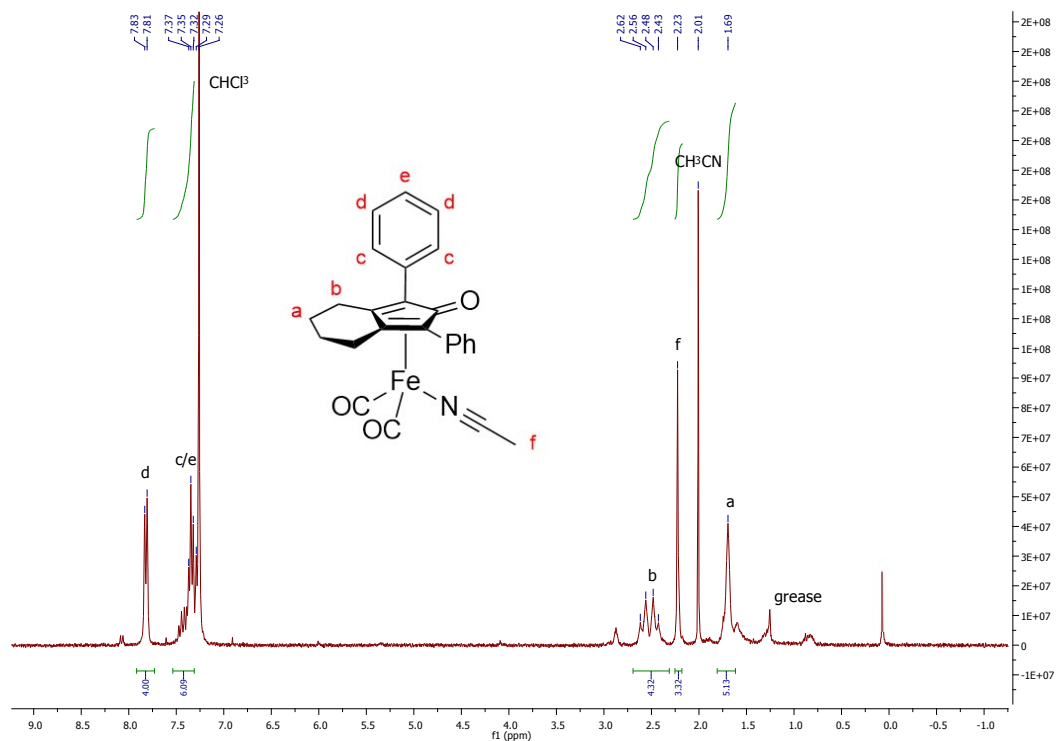


Figure S4.3.9: <sup>1</sup>H-NMR spectrum of Fe-2e in  $\text{CHCl}_3$ .

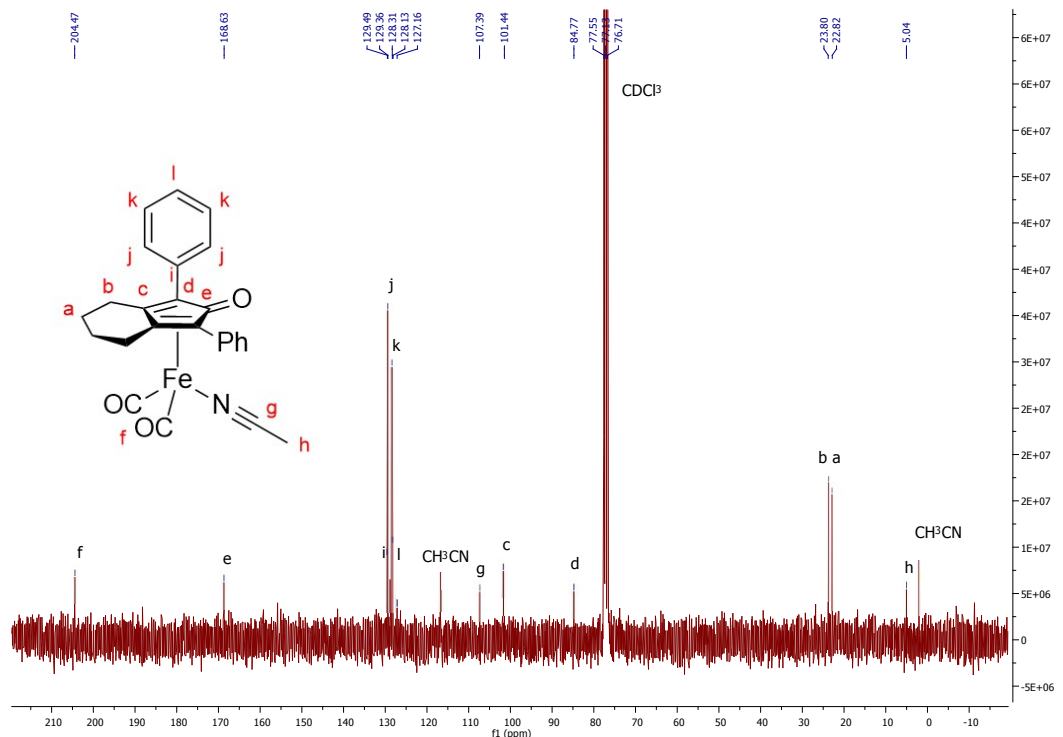


Figure S4.3.10: <sup>13</sup>C-NMR spectrum of Fe-2e in  $\text{CHCl}_3$ .

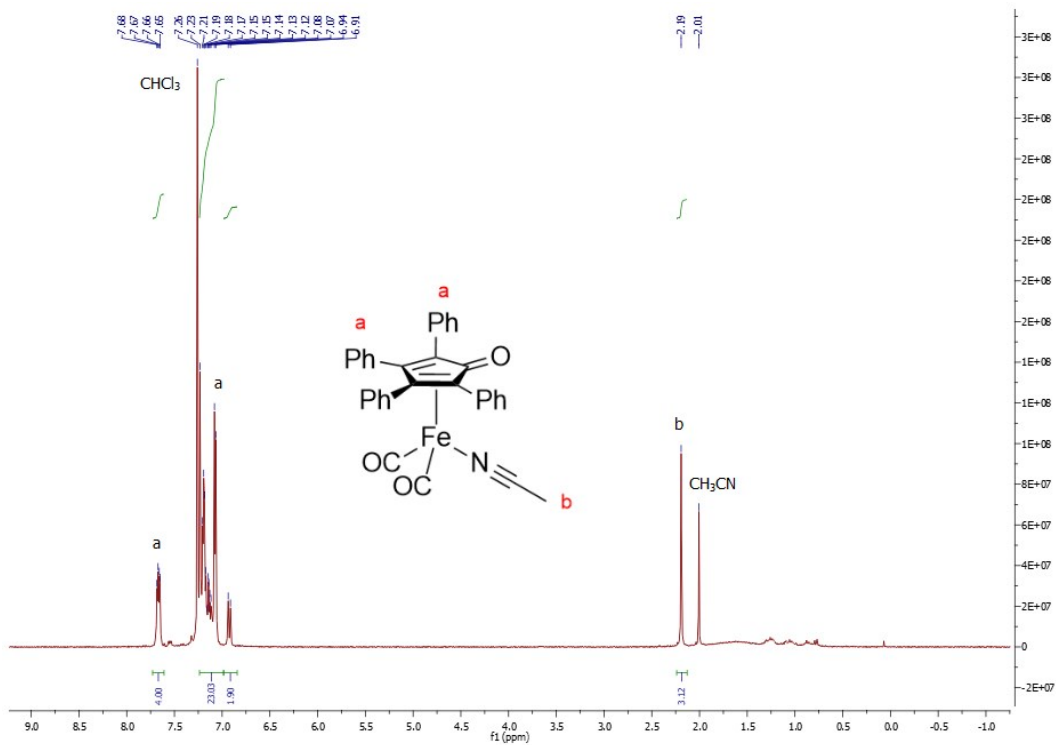


Figure S4.3.11: <sup>1</sup>H-NMR spectrum of **Fe-2f** in  $\text{CHCl}_3$ .

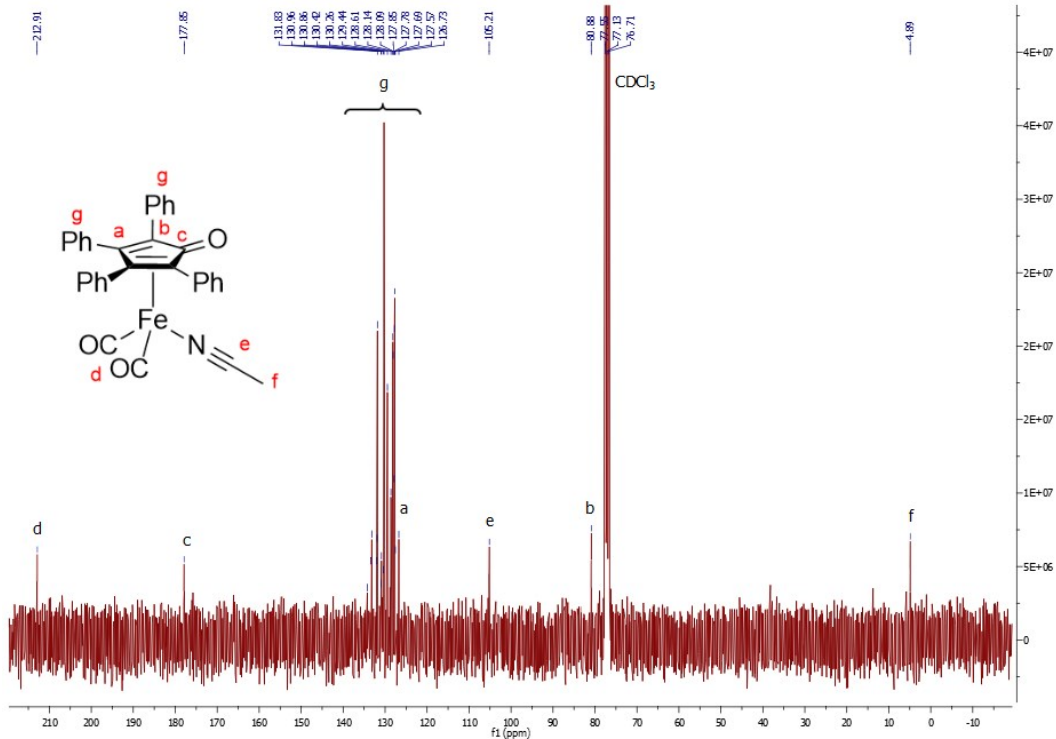


Figure S4.3.12: <sup>13</sup>C-NMR spectrum of **Fe-2f** in  $\text{CHCl}_3$ .

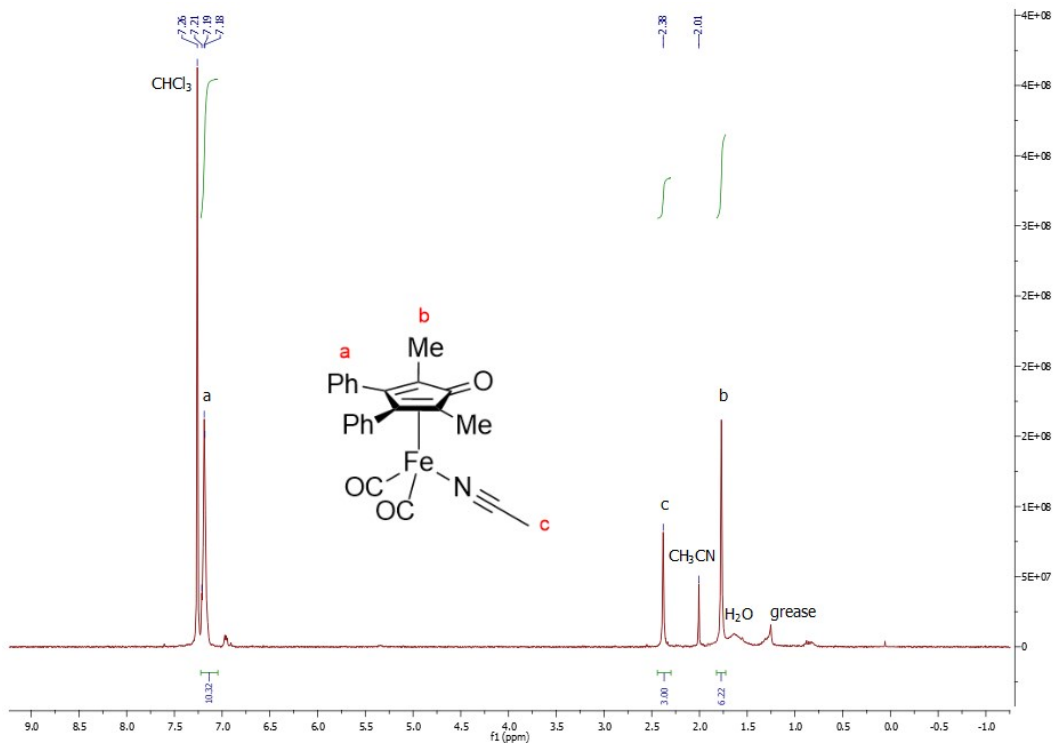


Figure S4.3.13:  $^1\text{H}$ -NMR spectrum of **Fe-2g** in  $\text{CHCl}_3$ .

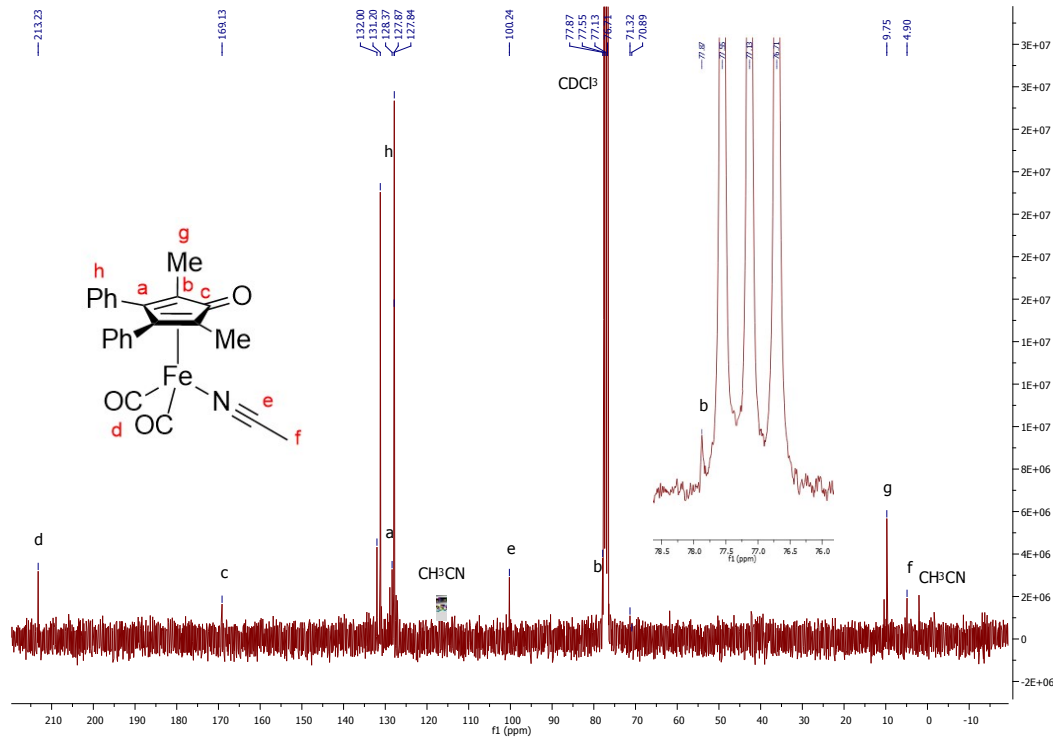


Figure S4.3.14:  $^1\text{H}$ -NMR spectrum of **Fe-2g** in  $\text{CHCl}_3$ .

S4.4 Substrates

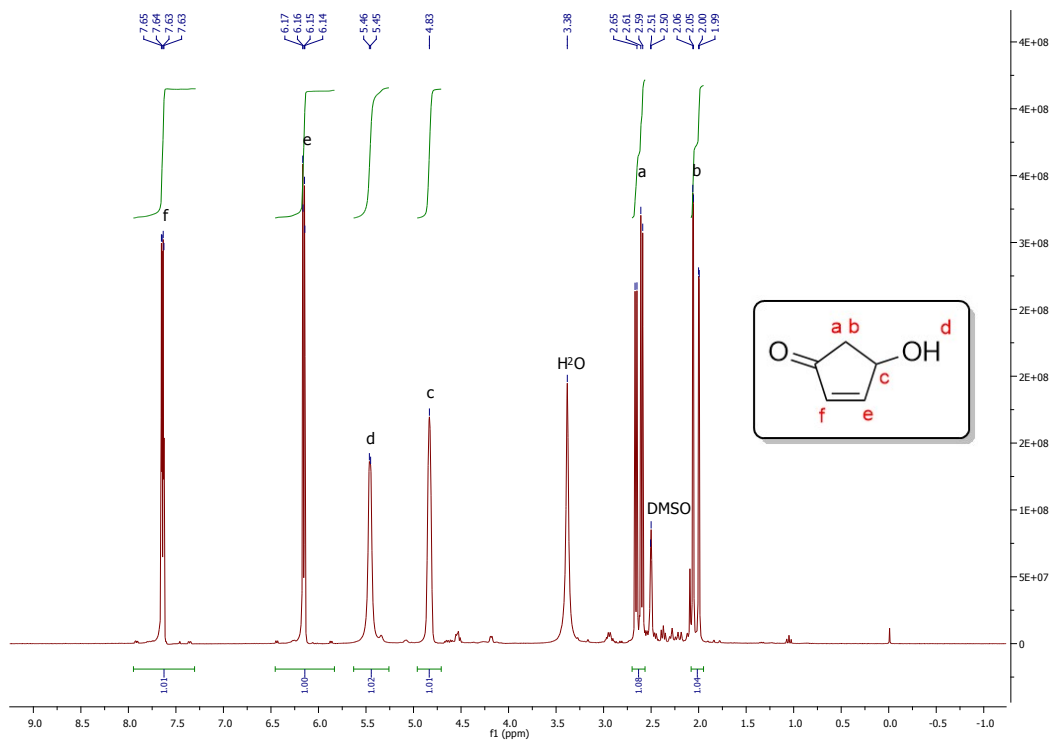


Figure S4.4.1:  $^1\text{H}$ -NMR spectrum of 4HCP in  $\text{DMSO}-d_6$ .

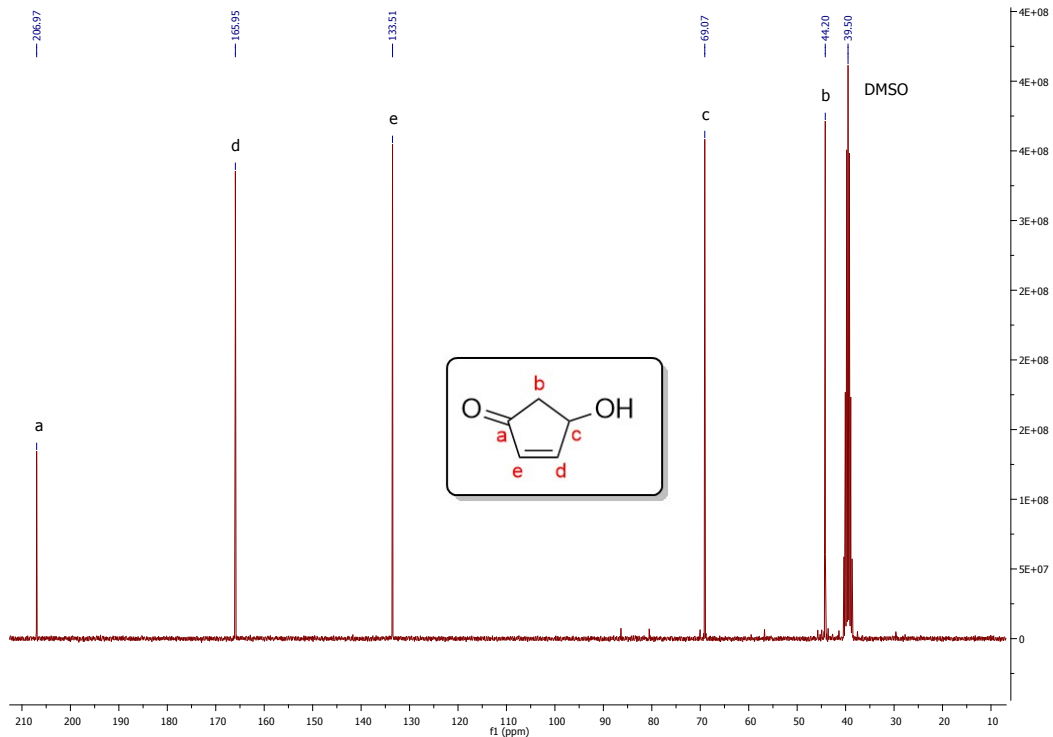
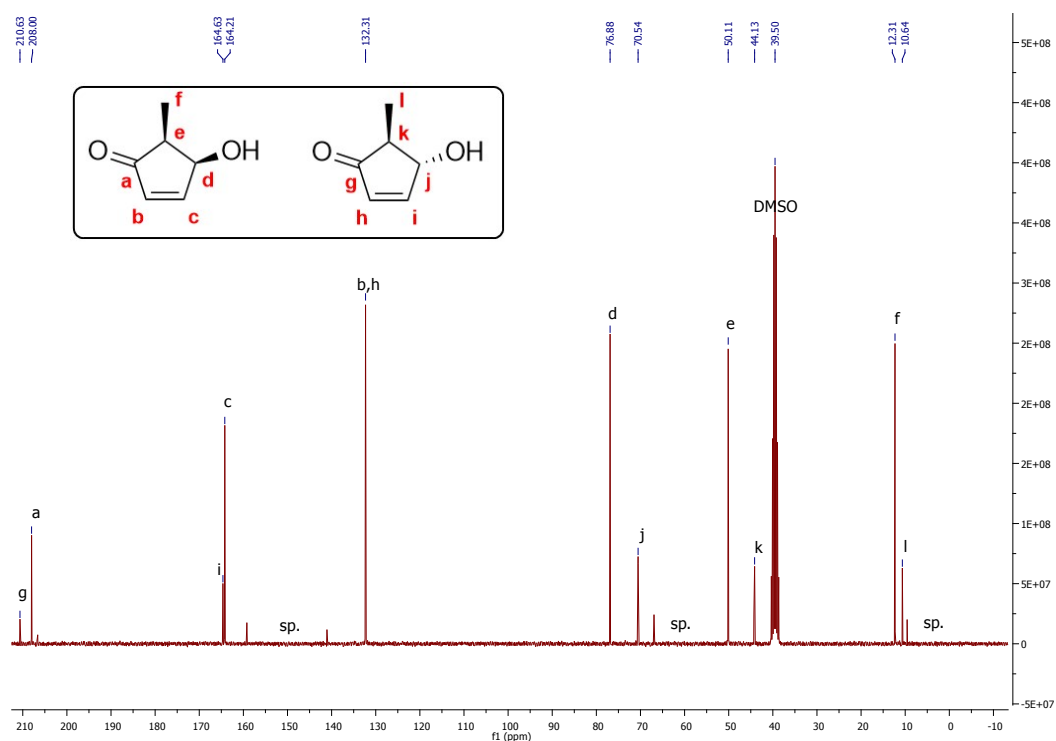
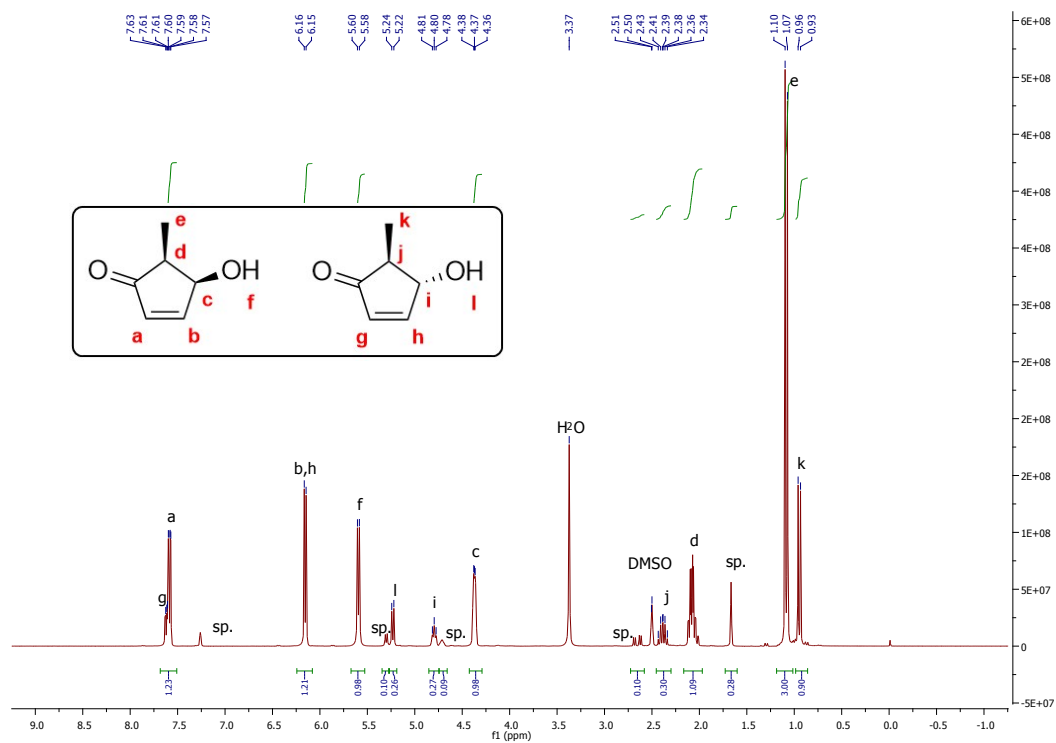


Figure S4.4.2:  $^{13}\text{C}$ -NMR spectrum of 4HCP in  $\text{DMSO}-d_6$ .



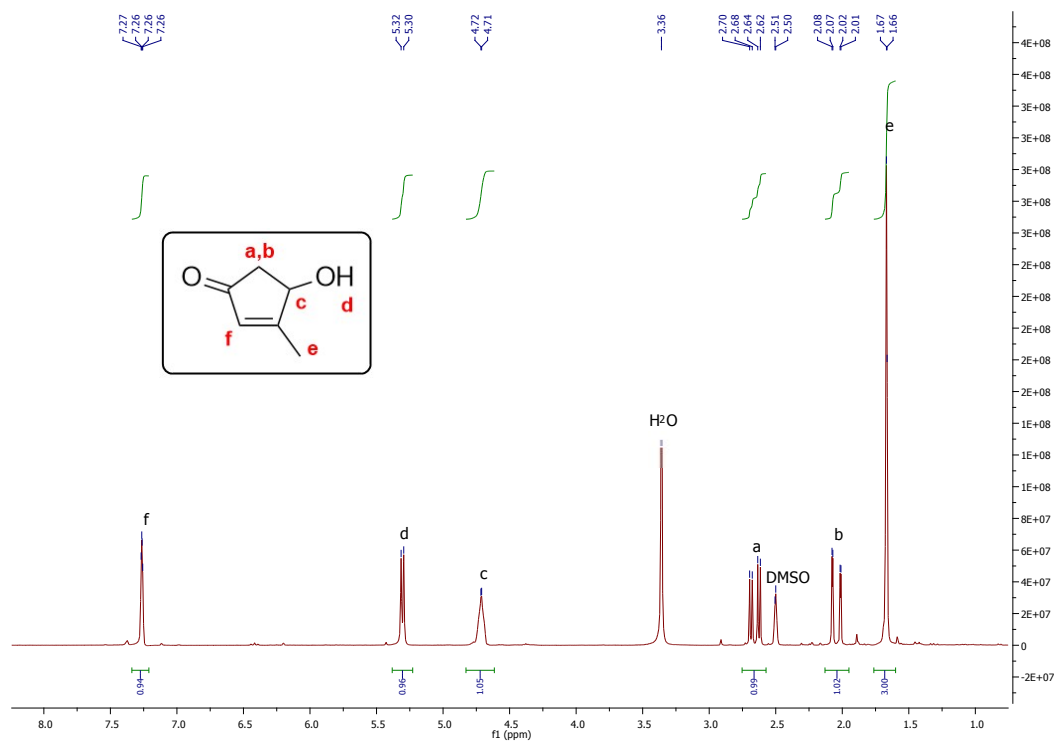


Figure S4.4.5: <sup>1</sup>H-NMR spectrum of **Ib** in  $\text{DMSO}-d_6$ .

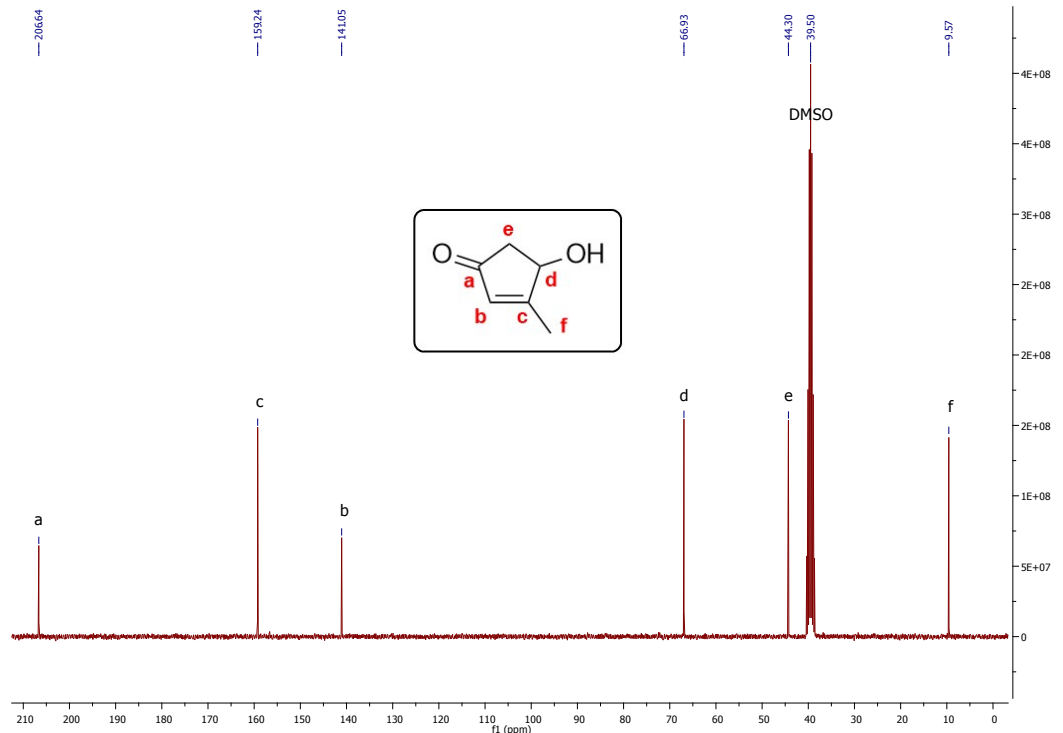
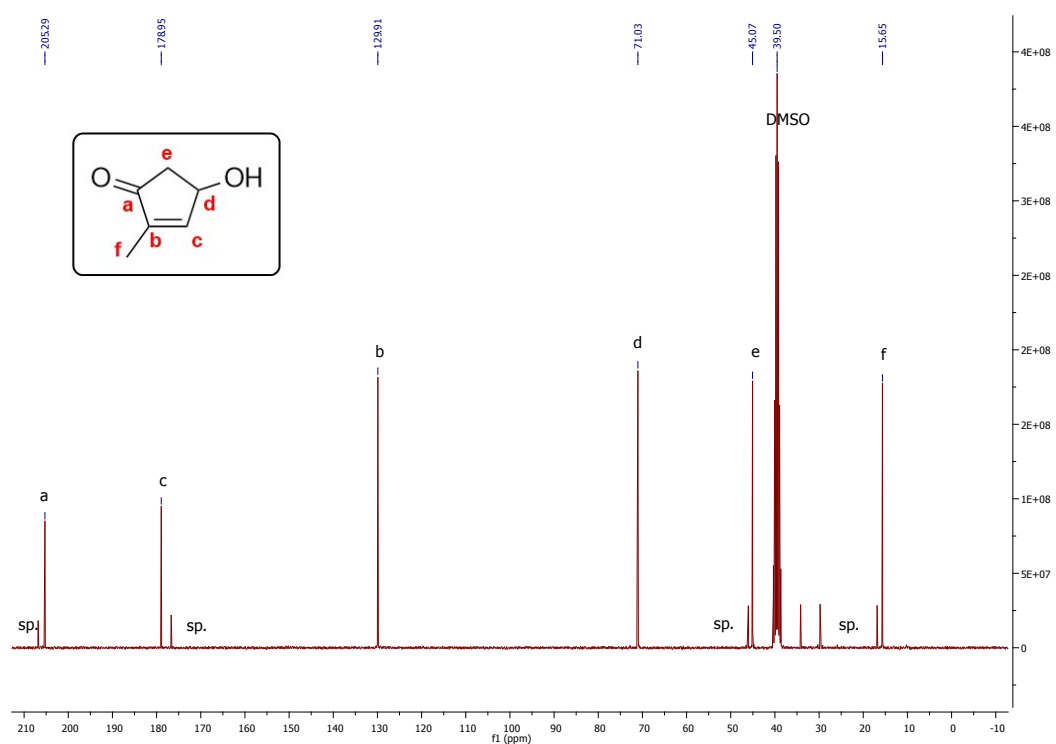
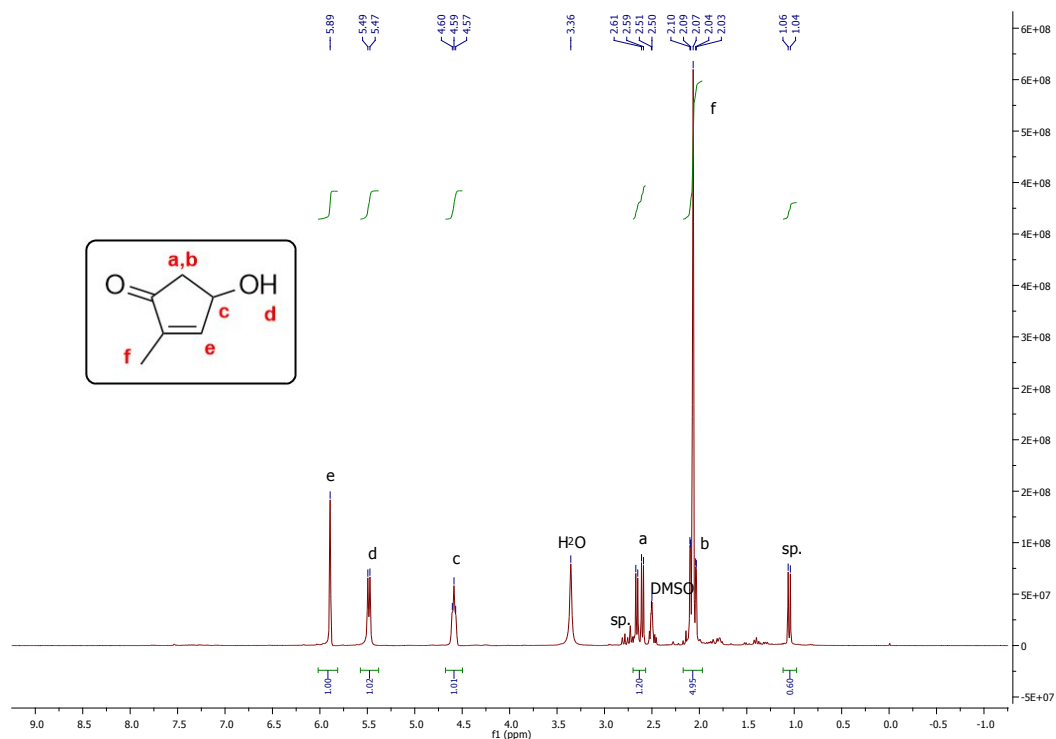


Figure S4.4.6: <sup>13</sup>C-NMR spectrum of **Ib** in  $\text{DMSO}-d_6$ .



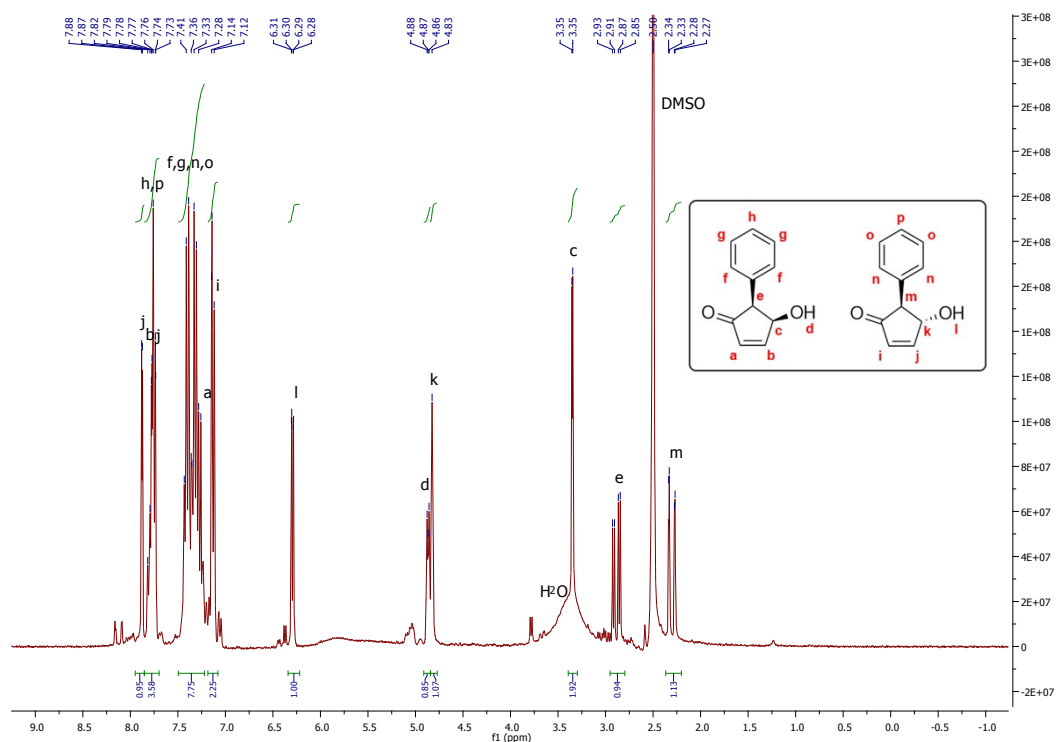


Figure S4.4.9:  $^1\text{H}$ -NMR spectrum of **1d** in  $\text{DMSO}-d_6$ .

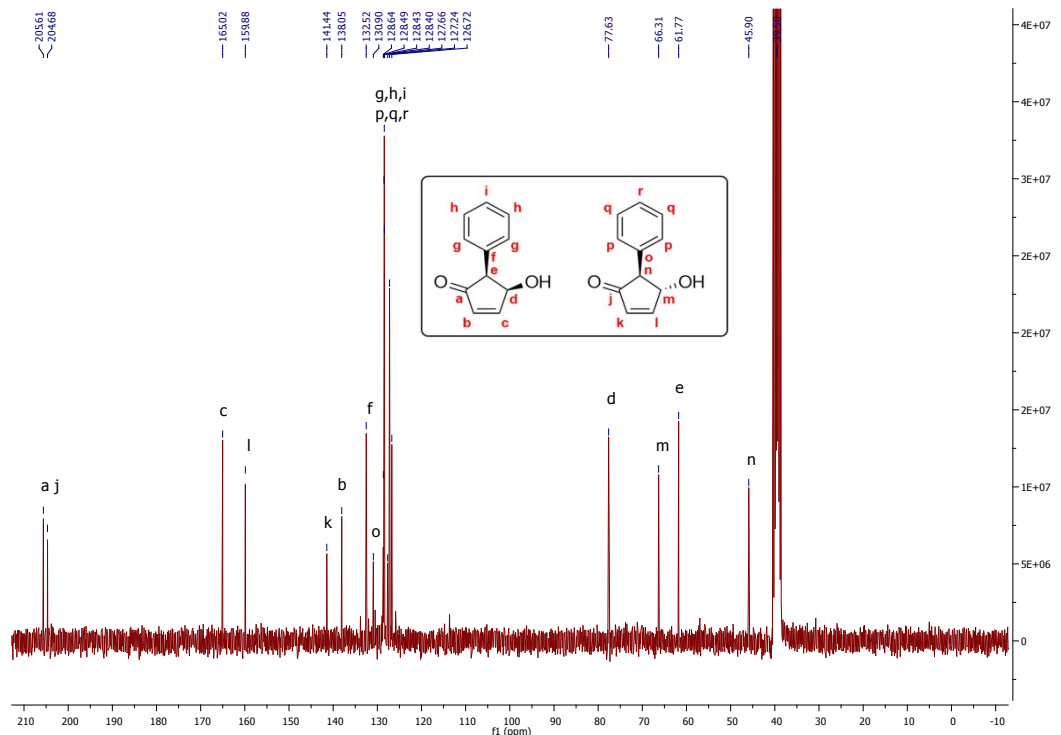


Figure S4.4.10:  $^{13}\text{C}$ -NMR spectrum of **1d** in  $\text{DMSO}-d_6$ .

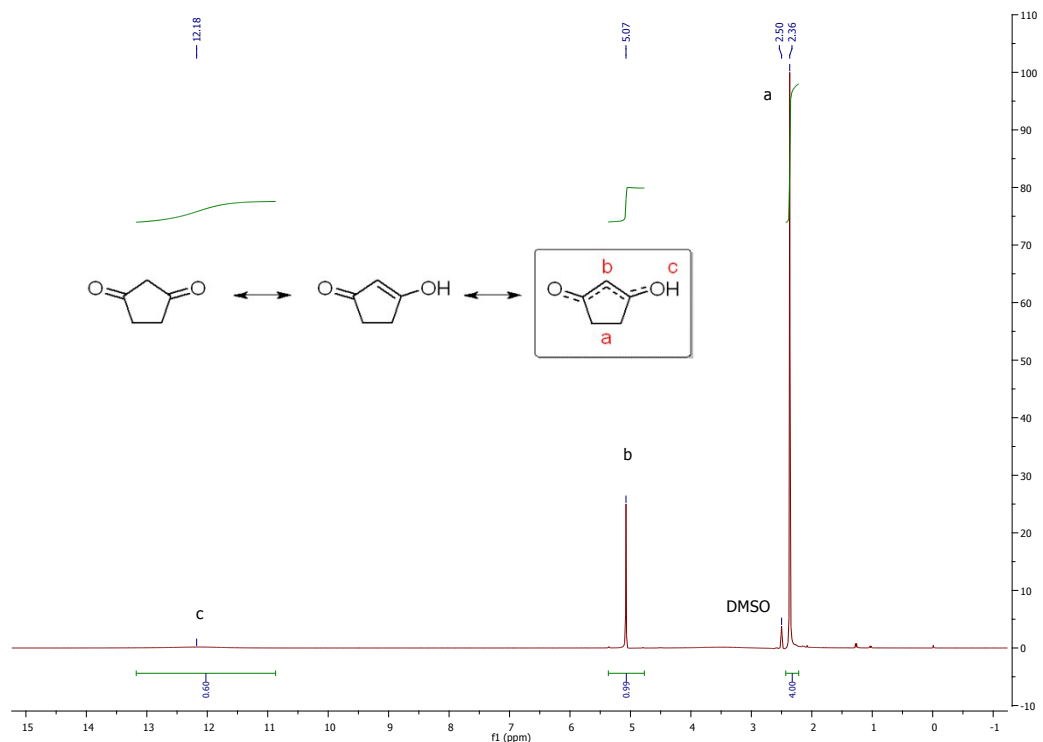


Figure S4.4.11:  $^1\text{H}$ -NMR spectrum of CPDO in  $\text{DMSO}-d_6$ .

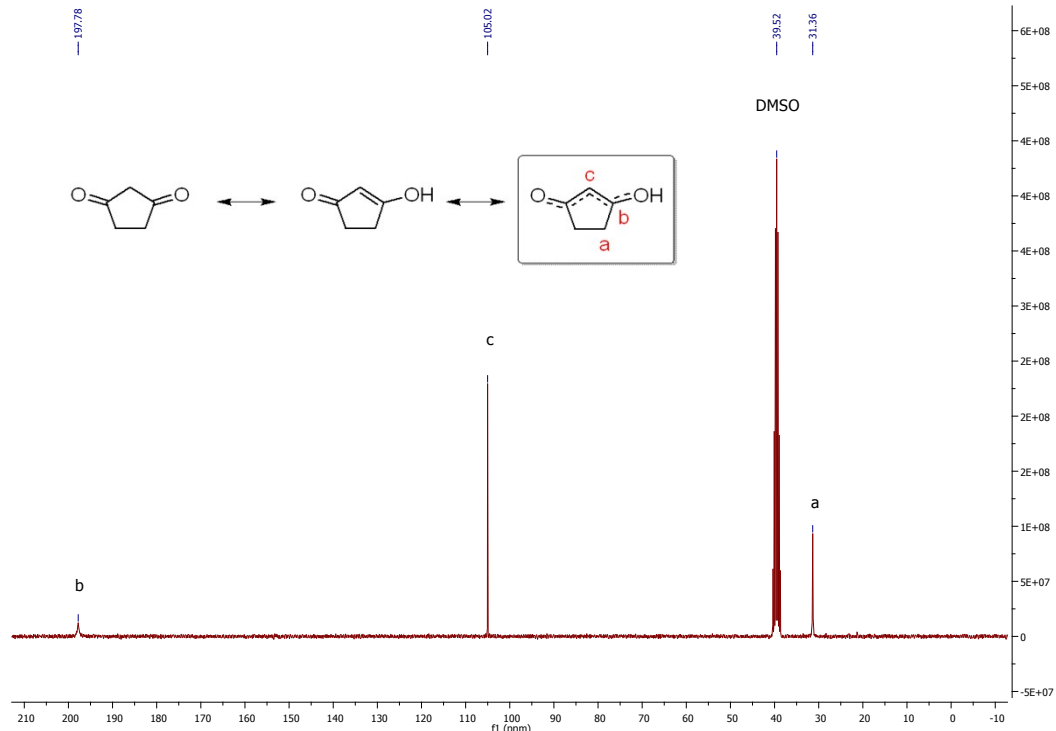


Figure S4.4.12:  $^{13}\text{C}$ -NMR spectrum of CPDO in  $\text{DMSO}-d_6$ .

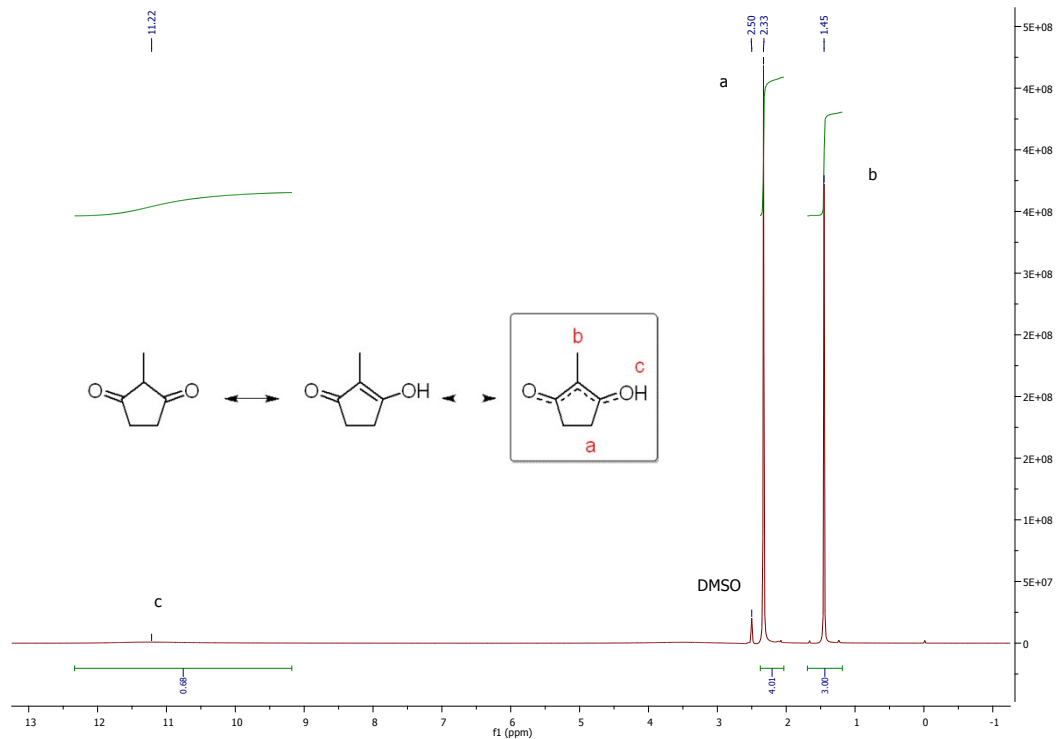


Figure S4.4.13:  $^1\text{H}$ -NMR spectrum of  $3e$  in  $\text{DMSO}-d_6$ .

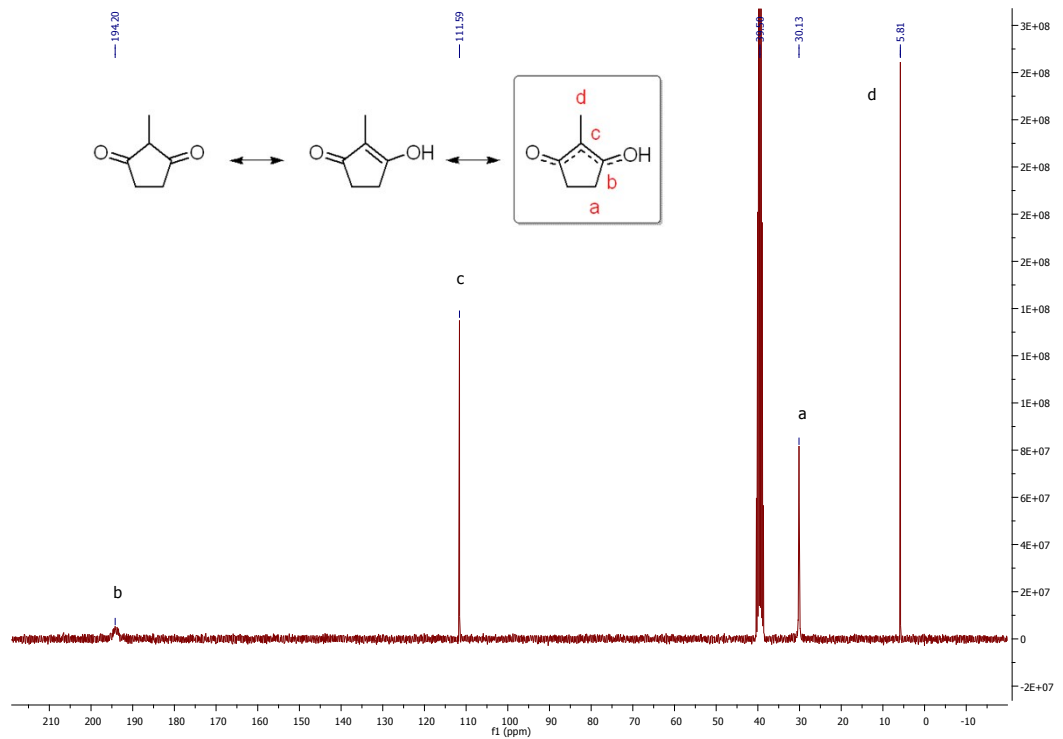


Figure S4.4.14:  $^{13}\text{C}$ -NMR spectrum of  $3e$  in  $\text{DMSO}-d_6$ .

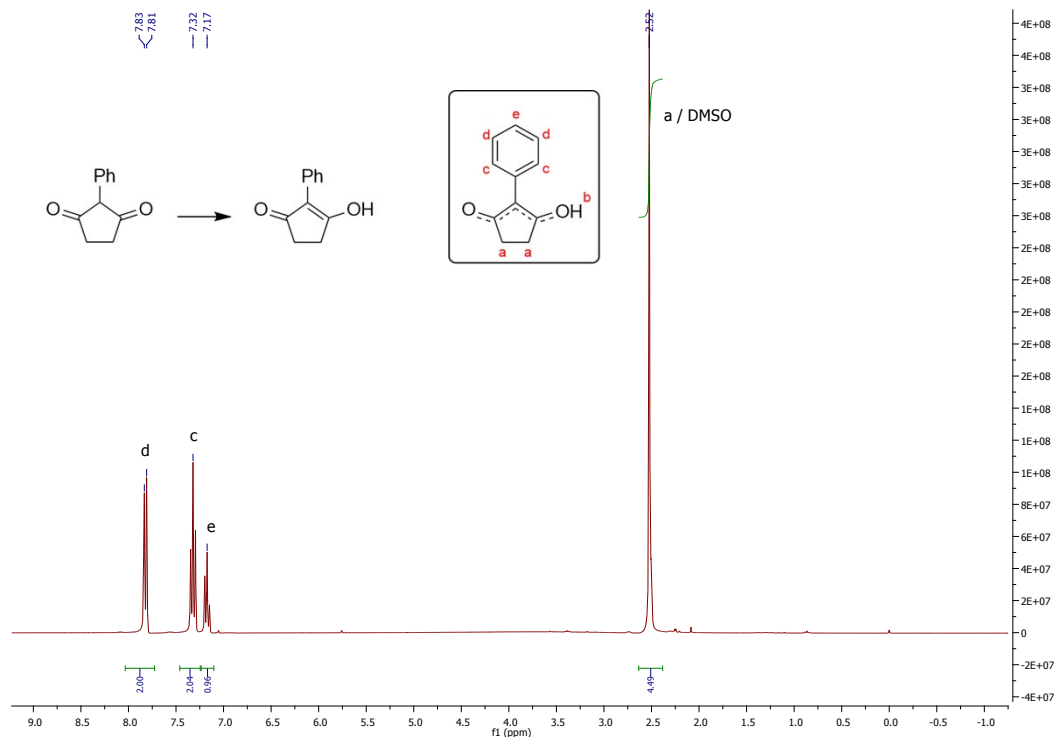


Figure S4.4.15: <sup>1</sup>H-NMR spectrum of 3f in  $\text{DMSO}-d_6$ .

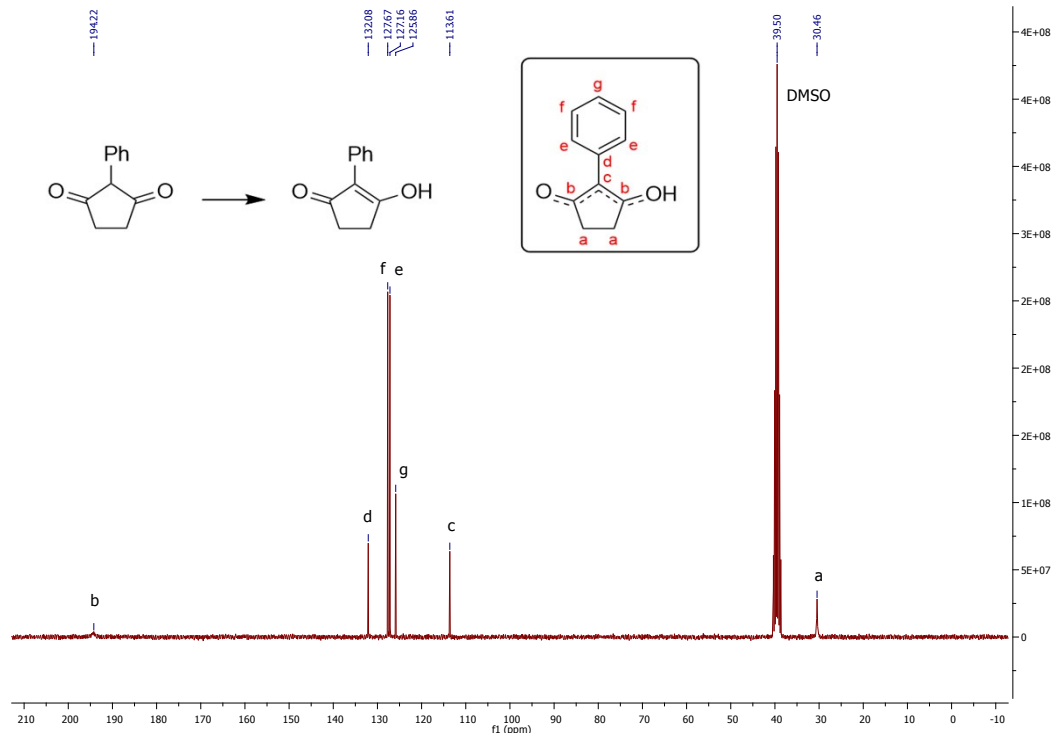


Figure S4.4.16: <sup>13</sup>C-NMR spectrum of 3f in  $\text{DMSO}-d_6$ .

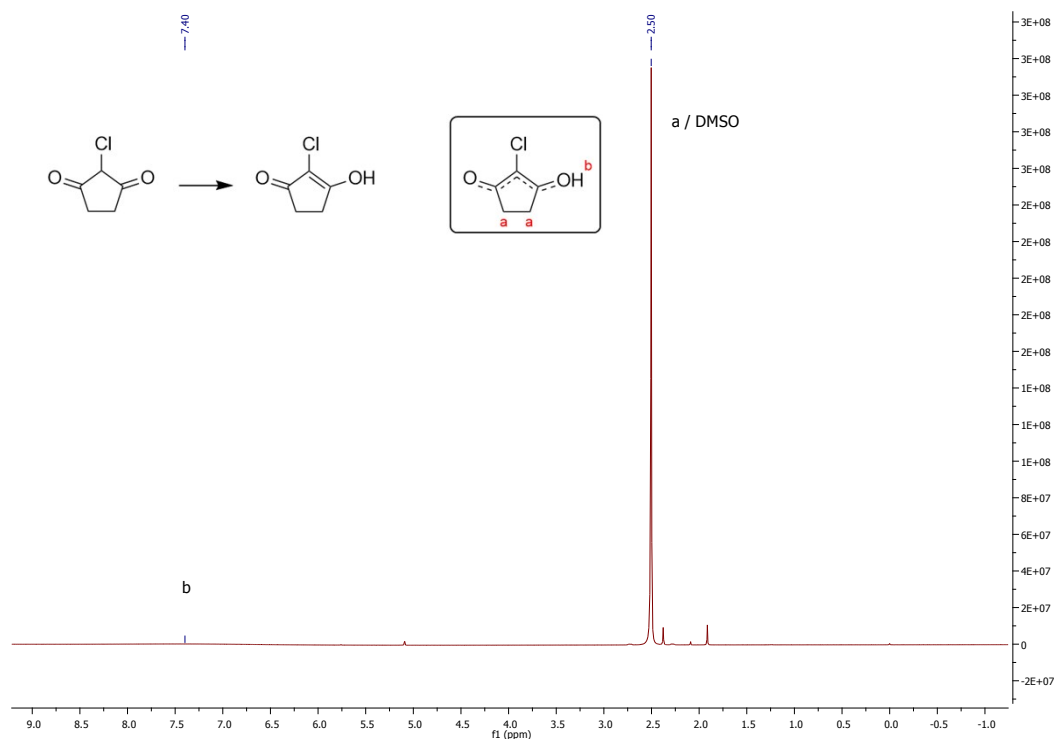


Figure S4.4.17:  $^1\text{H}$ -NMR spectrum of  $3\text{g}$  in  $\text{DMSO}-d_6$ .

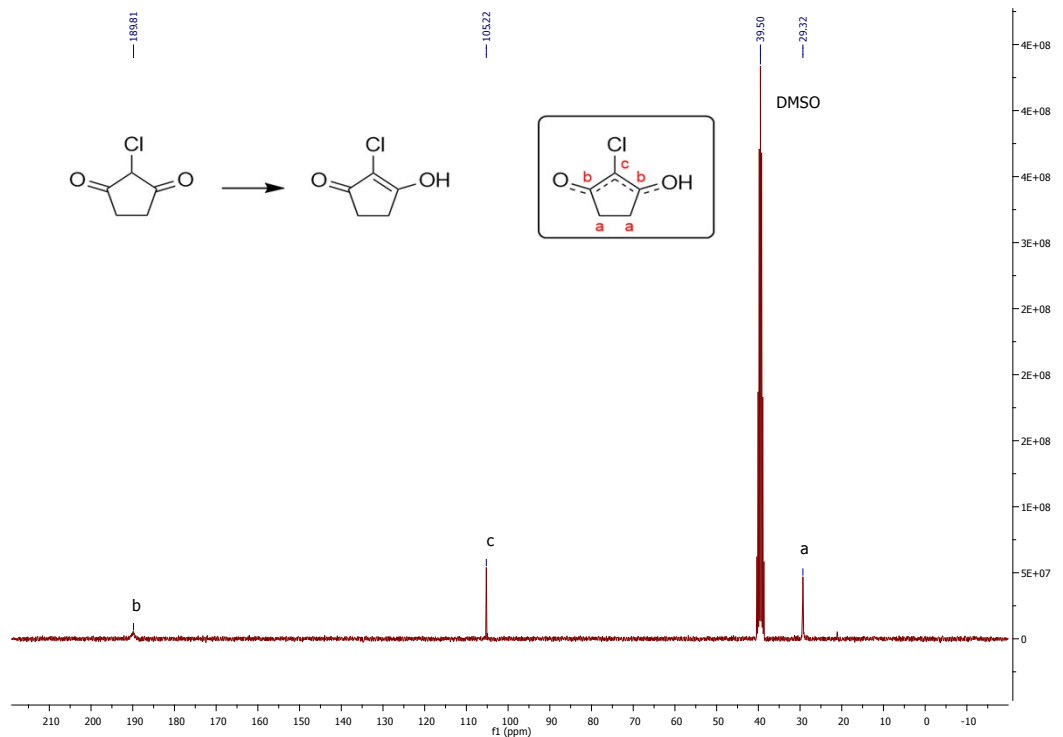


Figure S4.4.18:  $^{13}\text{C}$ -NMR spectrum of  $3\text{g}$  in  $\text{DMSO}-d_6$ .

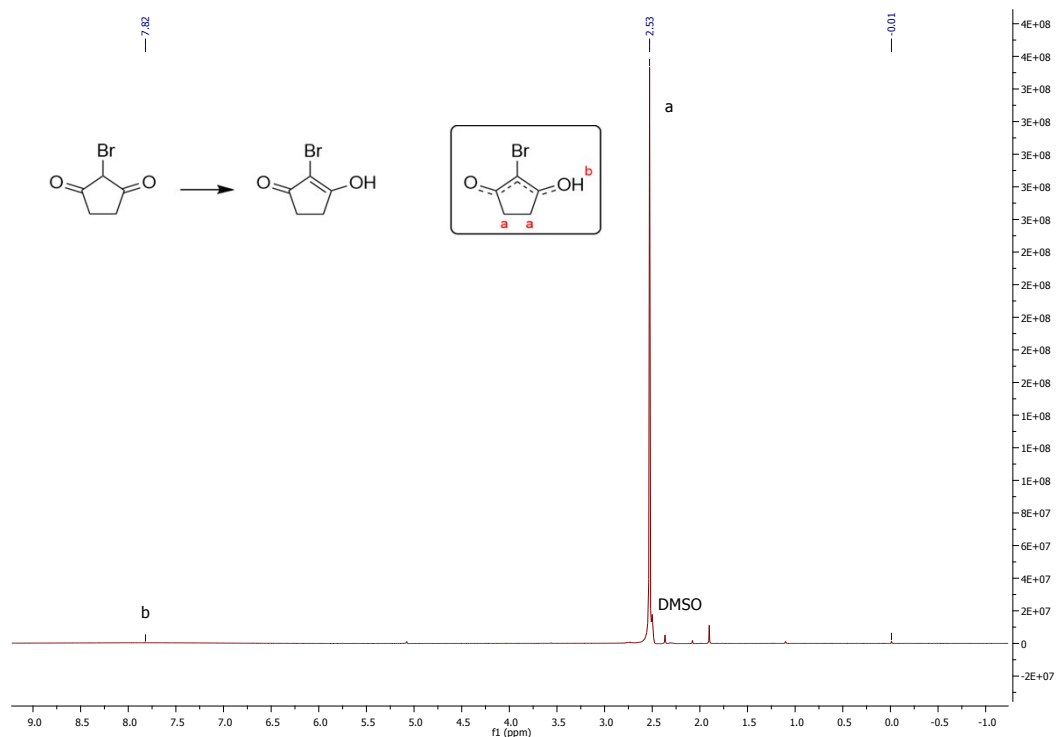


Figure S4.4.19:  $^1\text{H}$ -NMR spectrum of  $3\text{h}$  in  $\text{DMSO}-d_6$ .

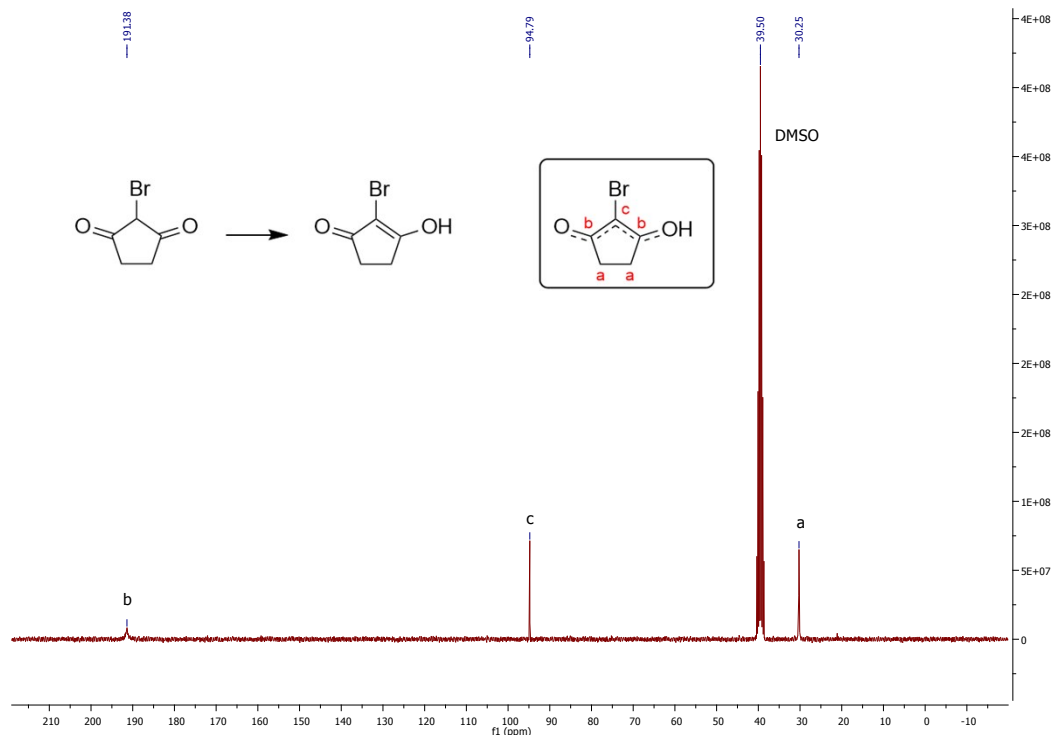


Figure S4.4.20:  $^{13}\text{C}$ -NMR spectrum of  $3\text{h}$  in  $\text{DMSO}-d_6$ .

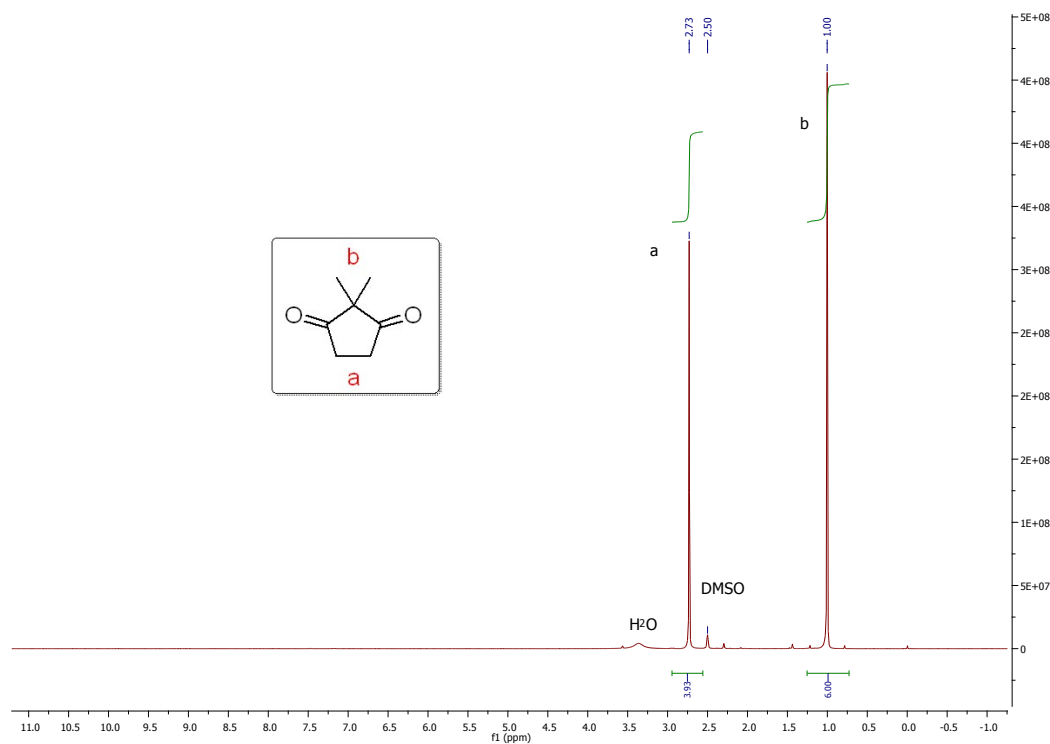


Figure S4.4.21:  $^1\text{H}$ -NMR spectrum of  $3\text{i}$  in  $\text{DMSO}-d_6$ .

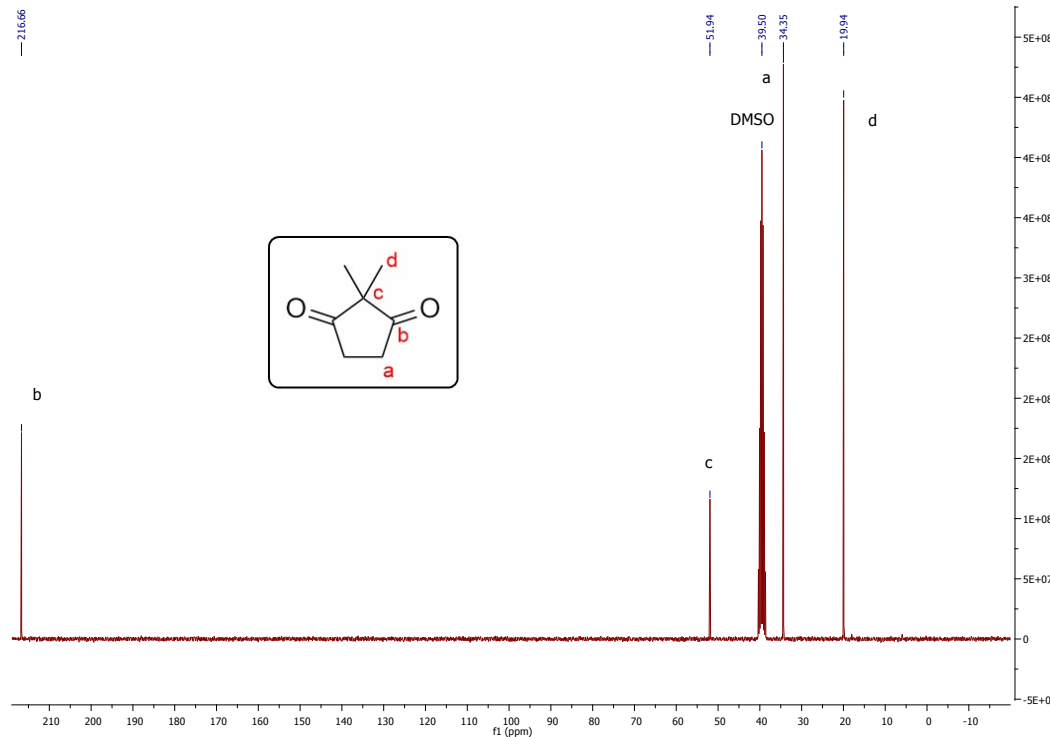


Figure S4.4.22:  $^{13}\text{C}$ -NMR spectrum of  $3\text{i}$  in  $\text{DMSO}-d_6$ .

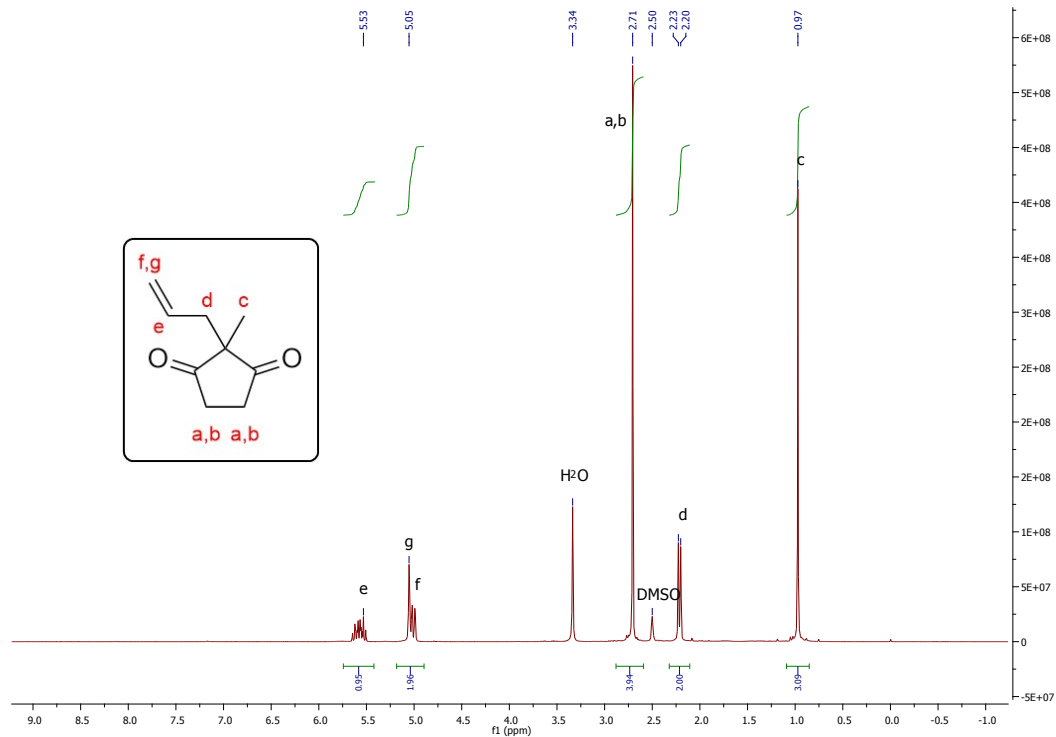


Figure S4.4.23:  $^1\text{H-NMR}$  spectrum of **3j** in  $\text{DMSO-}d_6$ .

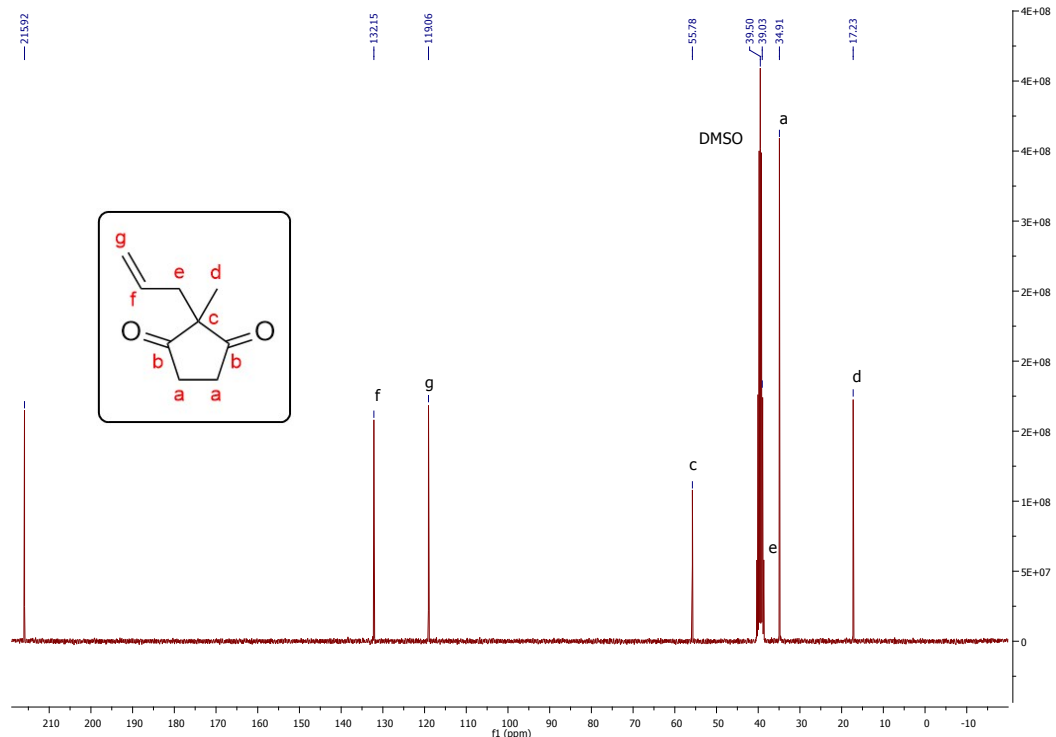


Figure S4.4.24:  $^{13}\text{C}$ -NMR spectrum of **3j** in  $\text{DMSO}-d_6$ .

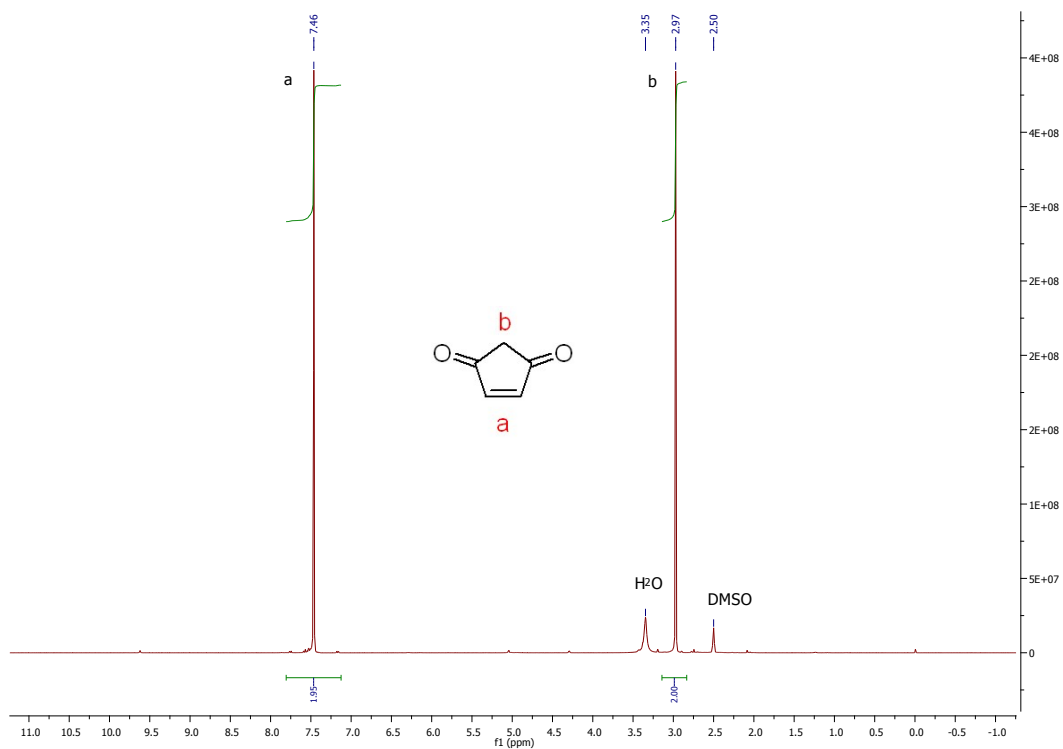


Figure S4.4.25: <sup>1</sup>H-NMR spectrum of **3k** in  $\text{DMSO}-d_6$ .

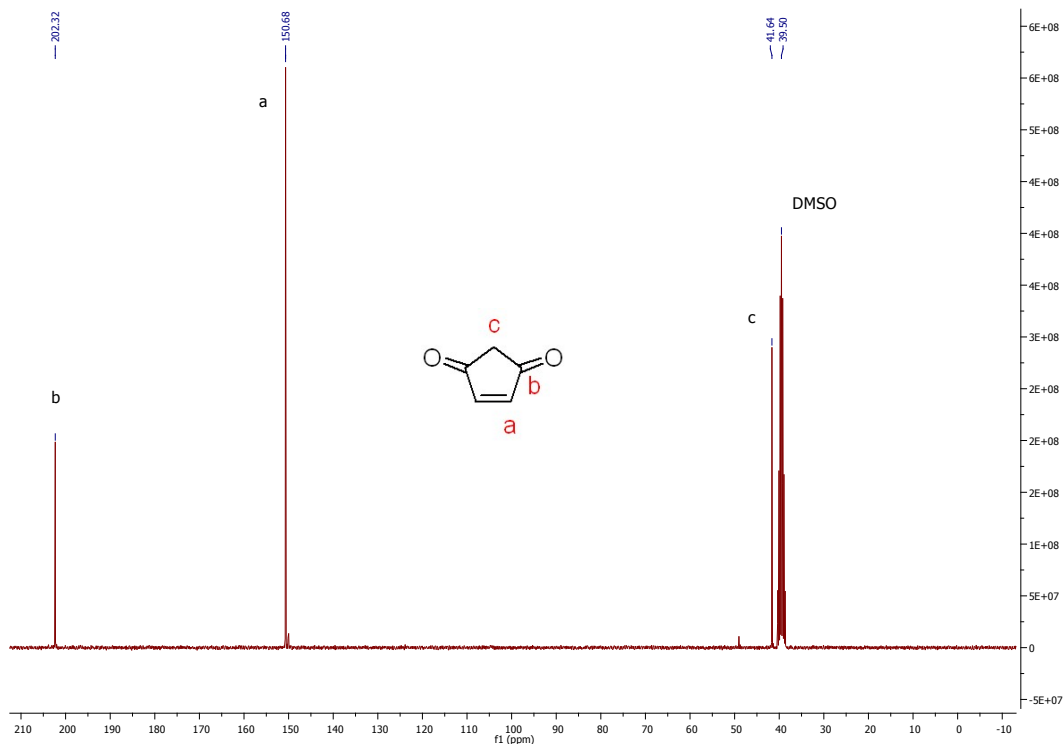


Figure S4.4.26: <sup>13</sup>C-NMR spectrum of **3k** in  $\text{DMSO}-d_6$ .

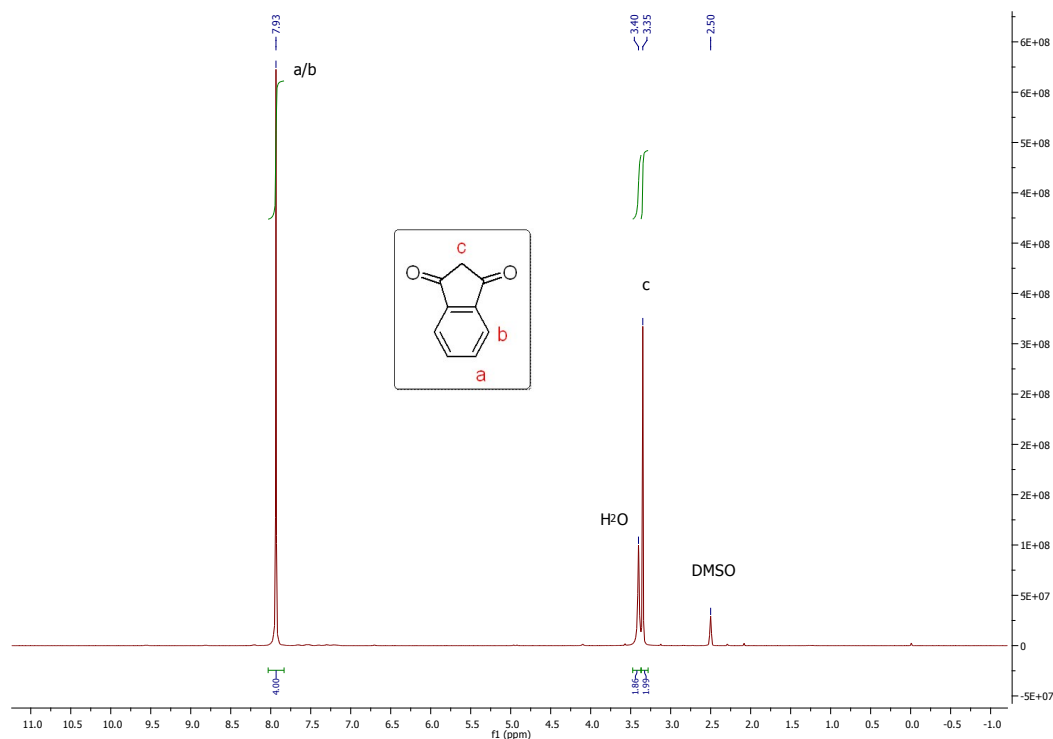


Figure S4.4.28: <sup>1</sup>H-NMR spectrum of **3I** in  $\text{DMSO}-d_6$ .

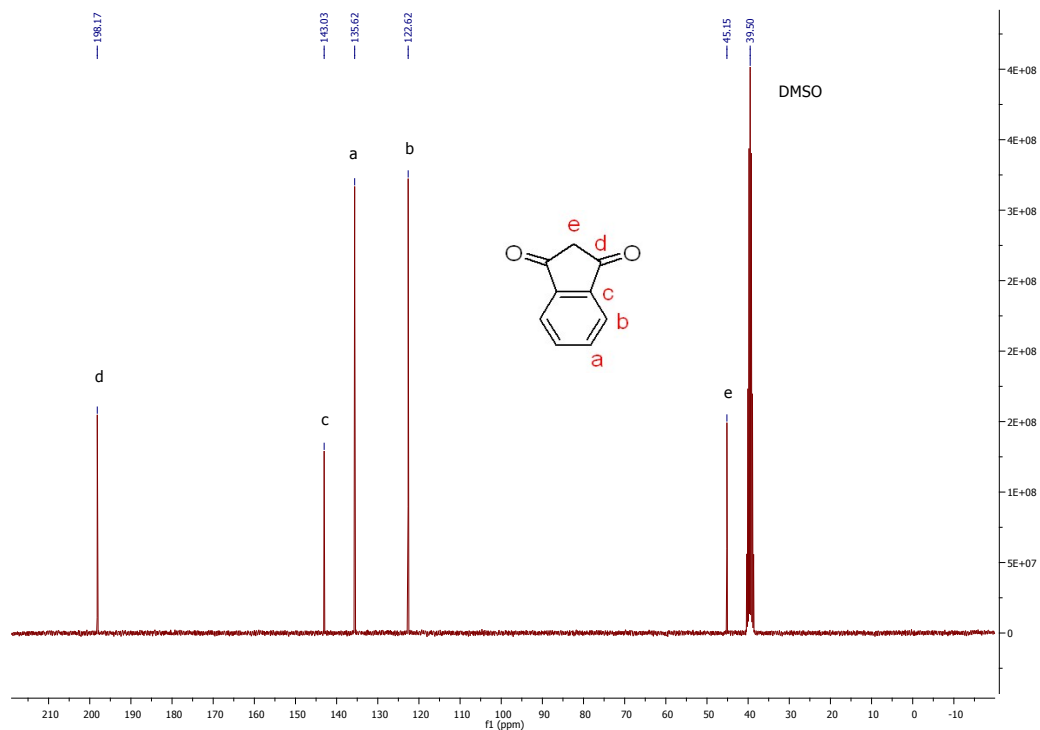


Figure S4.4.28: <sup>13</sup>C-NMR spectrum of **3I** in  $\text{DMSO}-d_6$ .

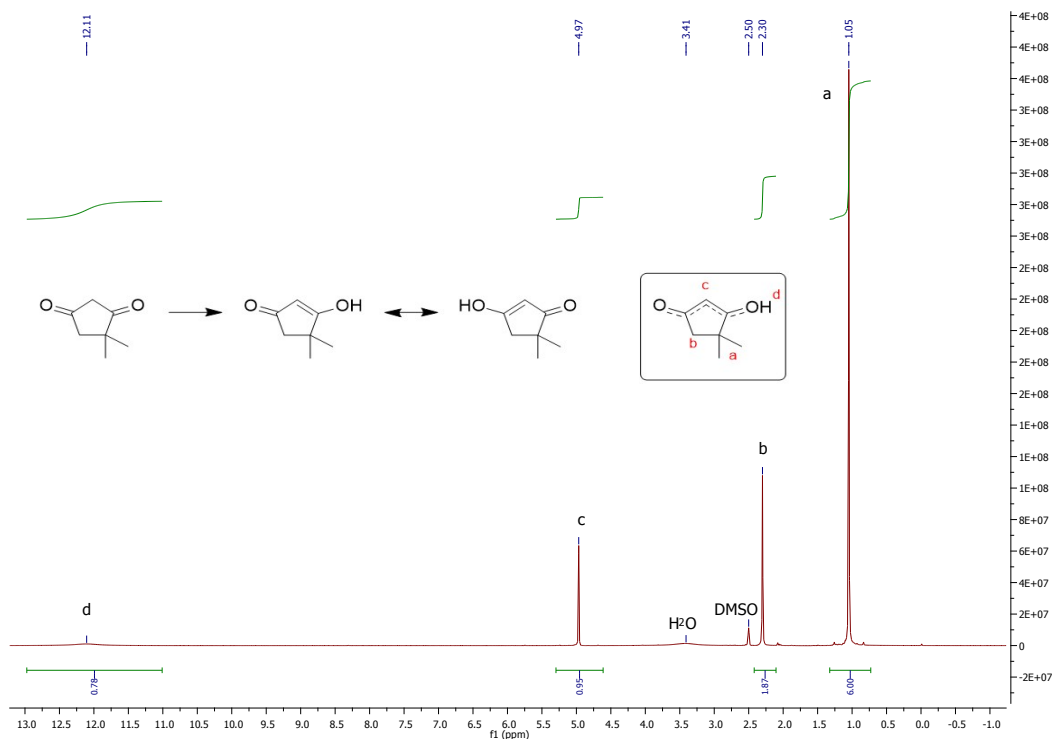


Figure S4.4.29:  $^1\text{H}$ -NMR spectrum of **3m** in  $\text{DMSO}-d_6$ .

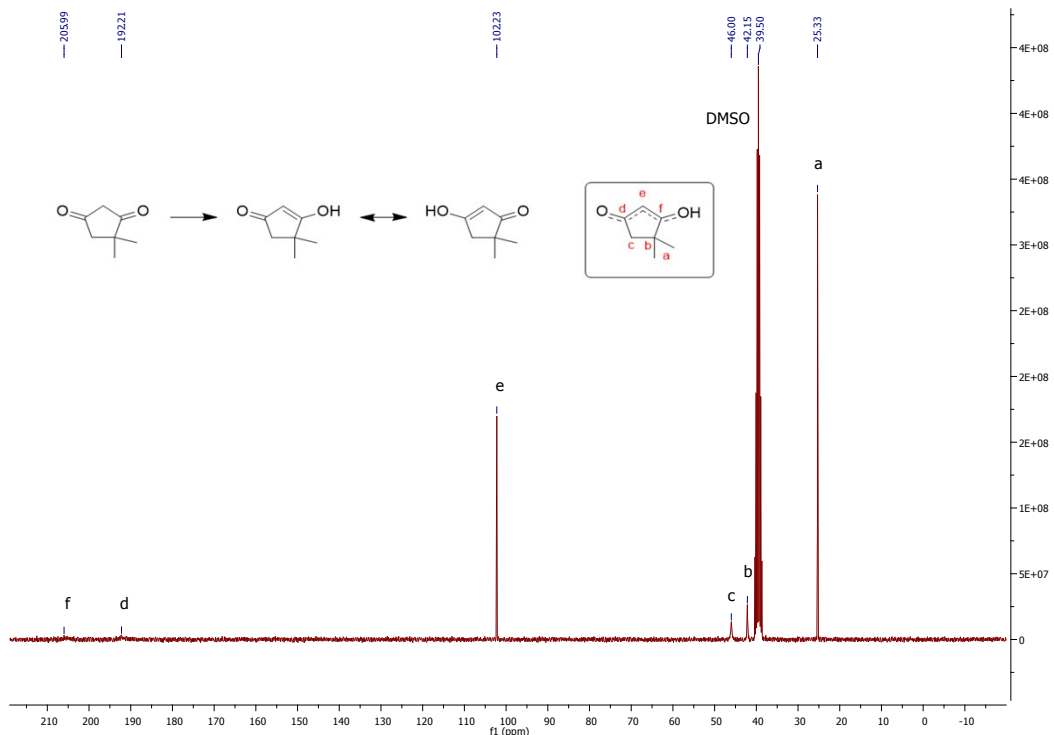


Figure S4.4.30:  $^{13}\text{C}$ -NMR spectrum of **3m** in  $\text{DMSO}-d_6$ .

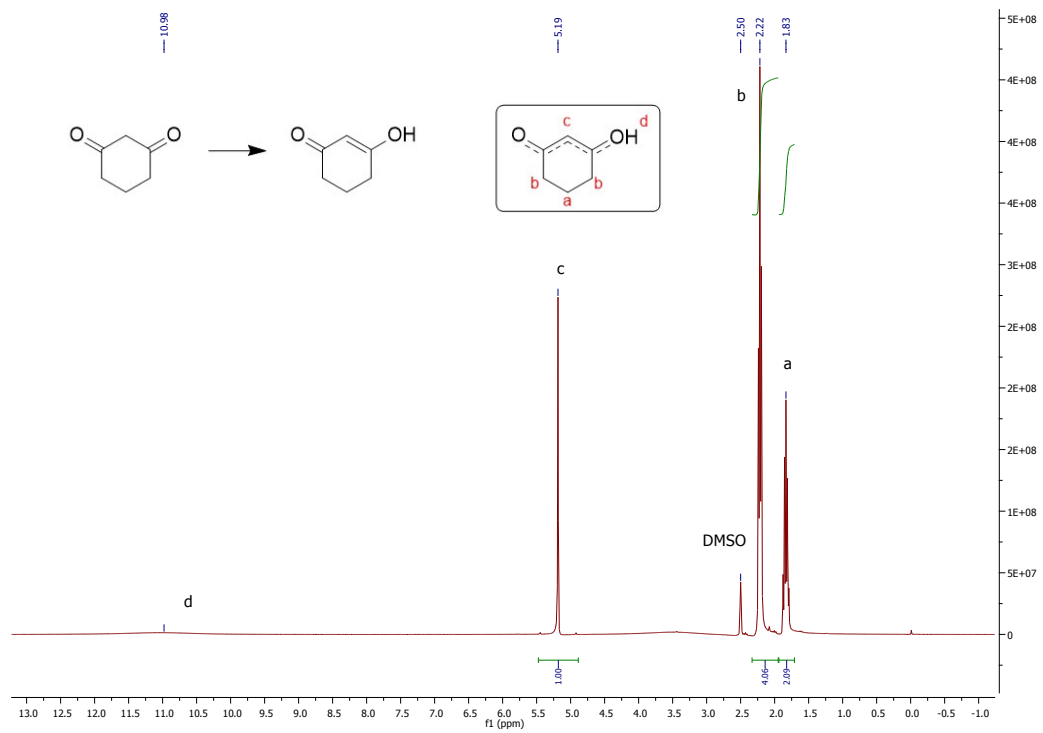


Figure S4.4.31:  $^1\text{H}$ -NMR spectrum of  $3\text{n}$  in  $\text{DMSO}-d_6$ .

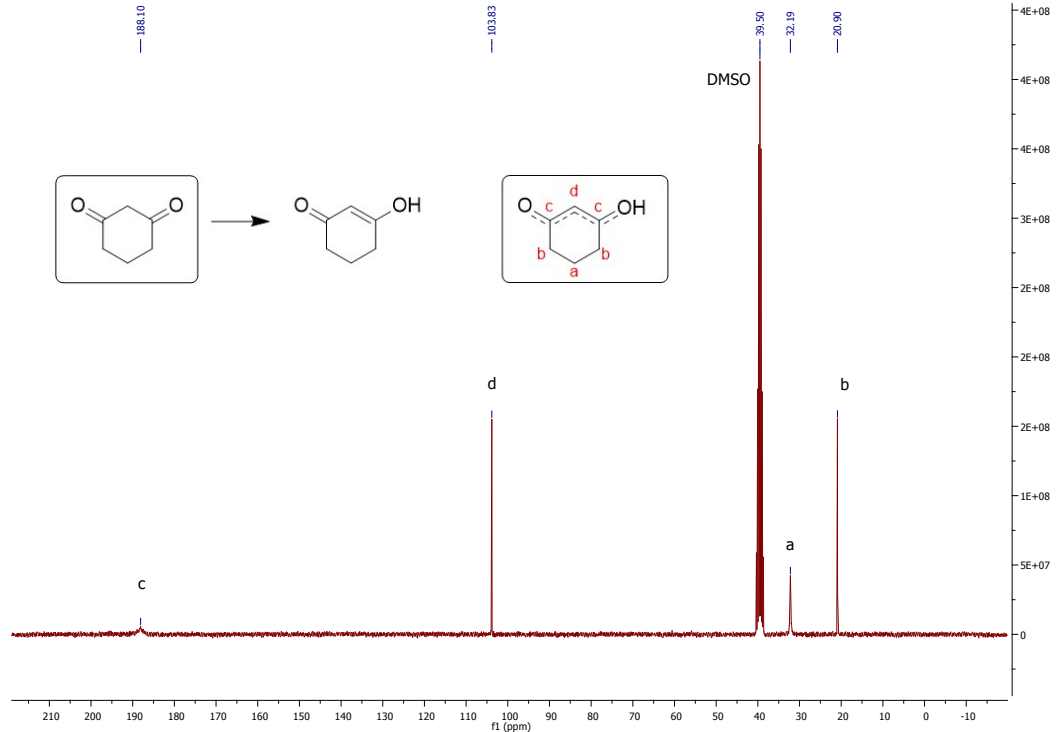


Figure S4.4.32:  $^{13}\text{C}$ -NMR spectrum of  $3\text{n}$  in  $\text{DMSO}-d_6$ .

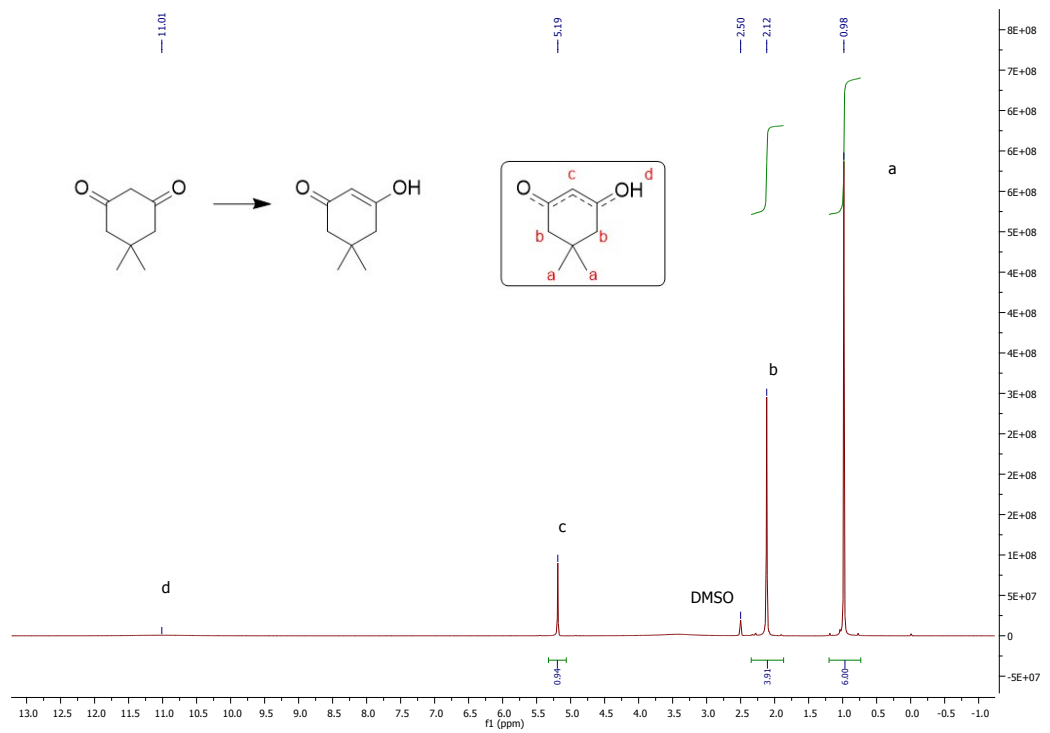


Figure S4.4.33: <sup>1</sup>H-NMR spectrum of 3o in DMSO-*d*<sub>6</sub>.

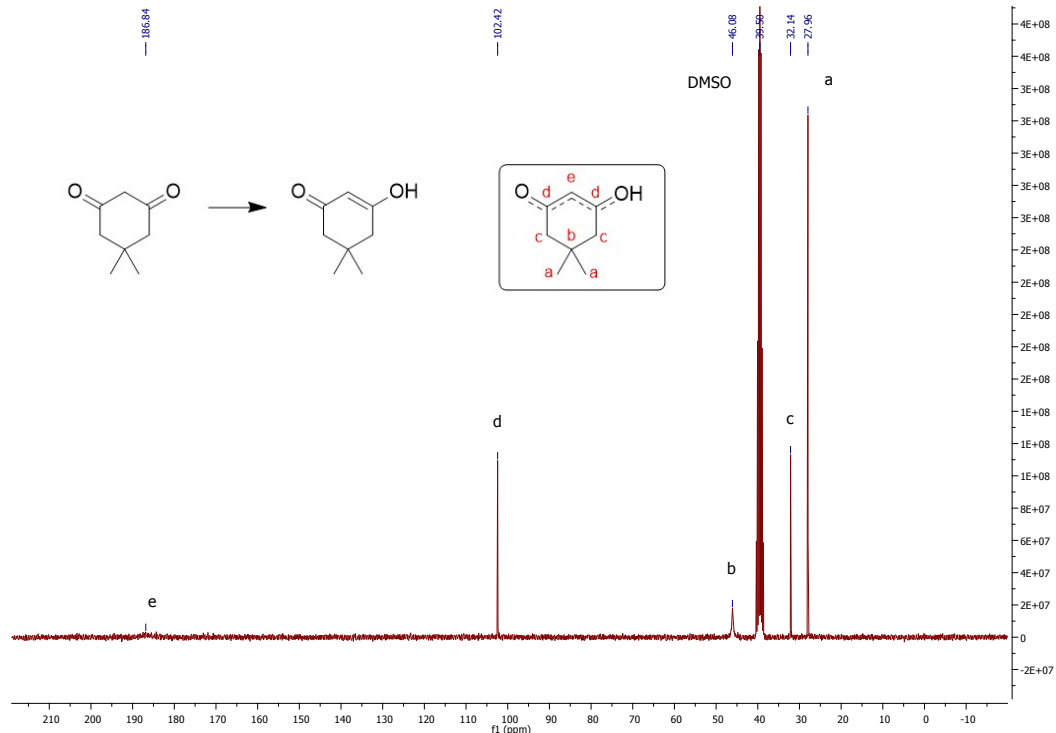


Figure S4.4.34: <sup>13</sup>C-NMR spectrum of 3o in DMSO-*d*<sub>6</sub>.

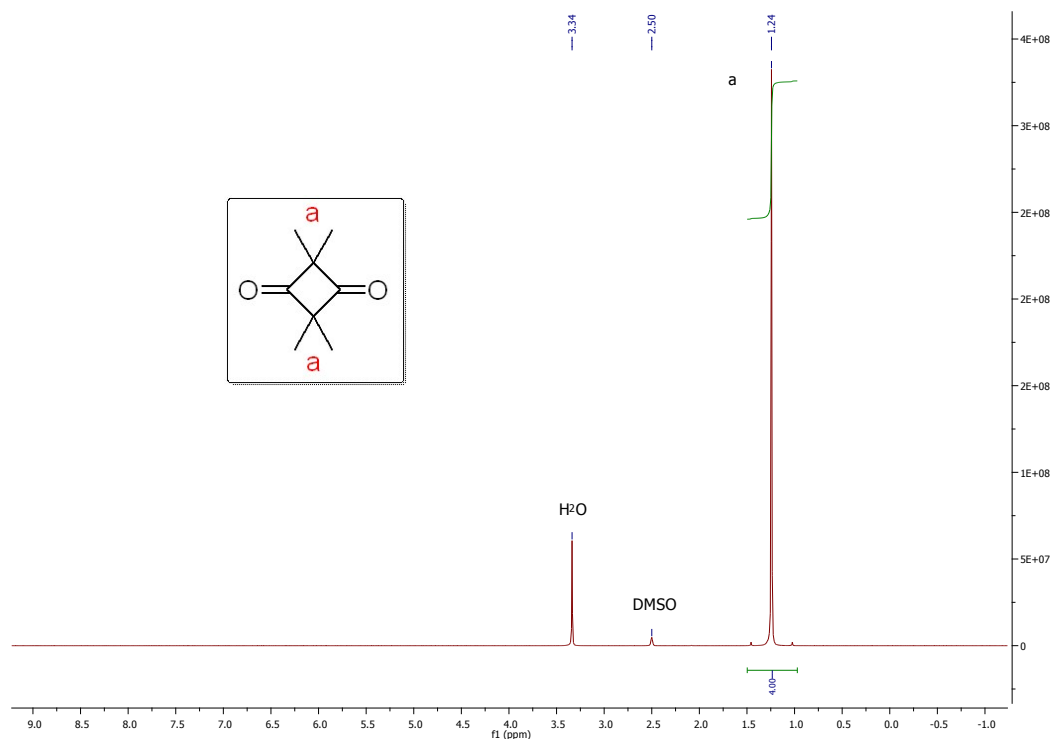


Figure S4.4.35:  $^1\text{H}$ -NMR spectrum of  $3\text{p}$  in  $\text{DMSO}-d_6$ .

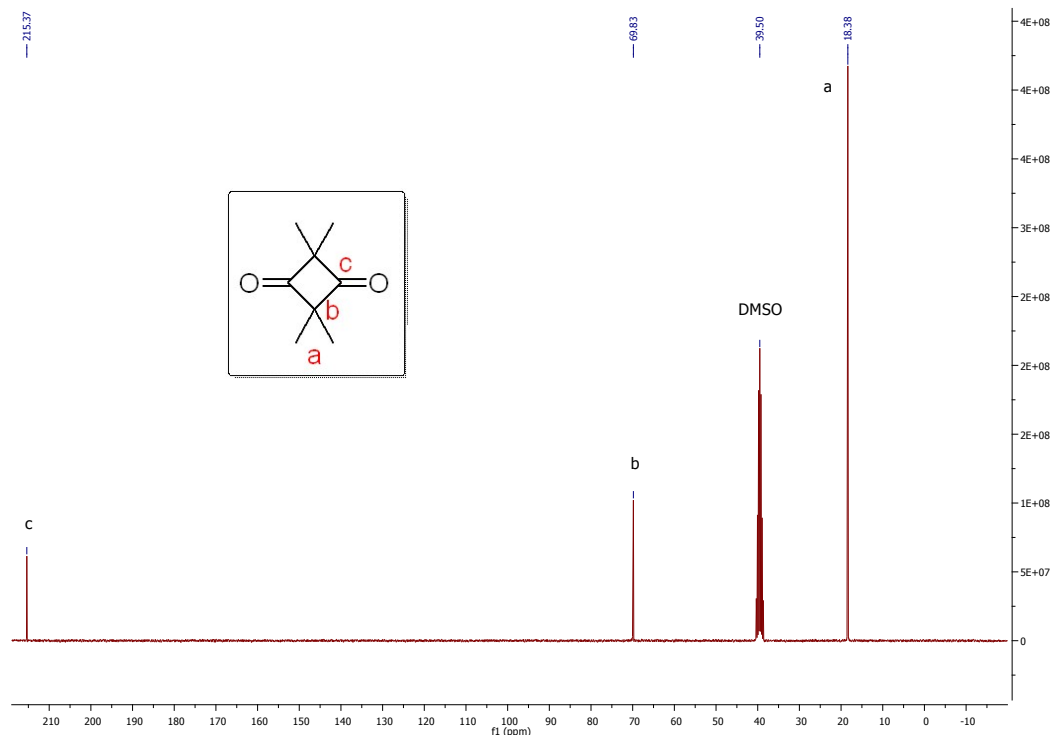


Figure S4.4.36:  $^{13}\text{C}$ -NMR spectrum of  $3\text{p}$  in  $\text{DMSO}-d_6$ .

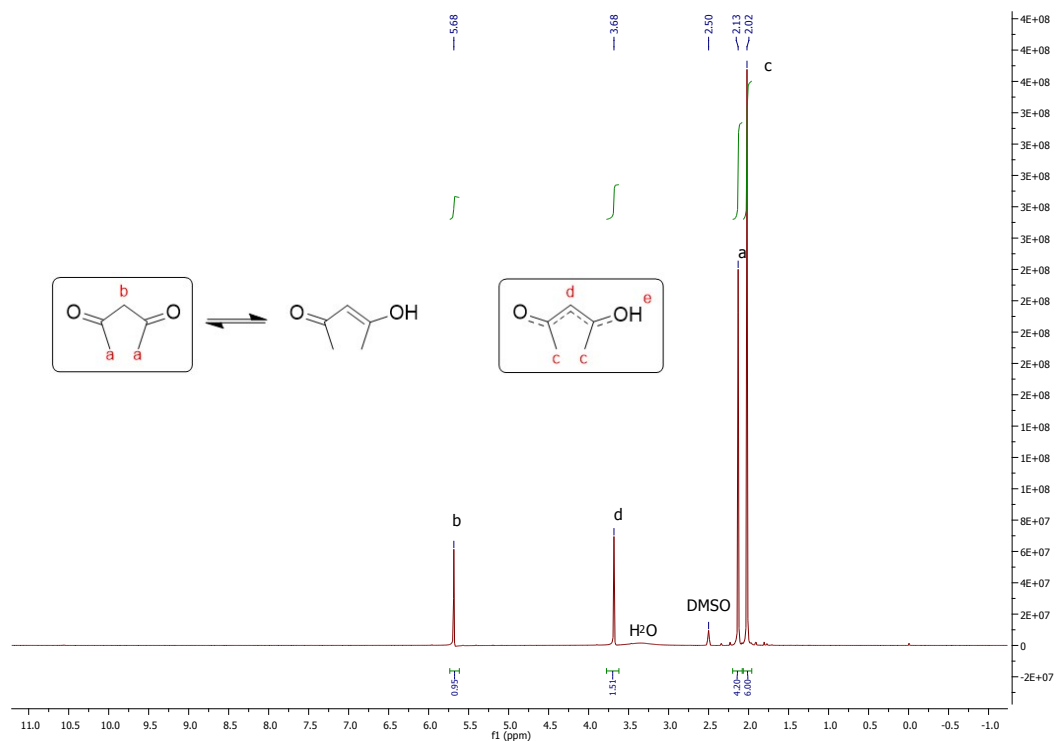


Figure S4.4.37:  $^1\text{H}$ -NMR spectrum of  $3q$  in  $\text{DMSO}-d_6$ .

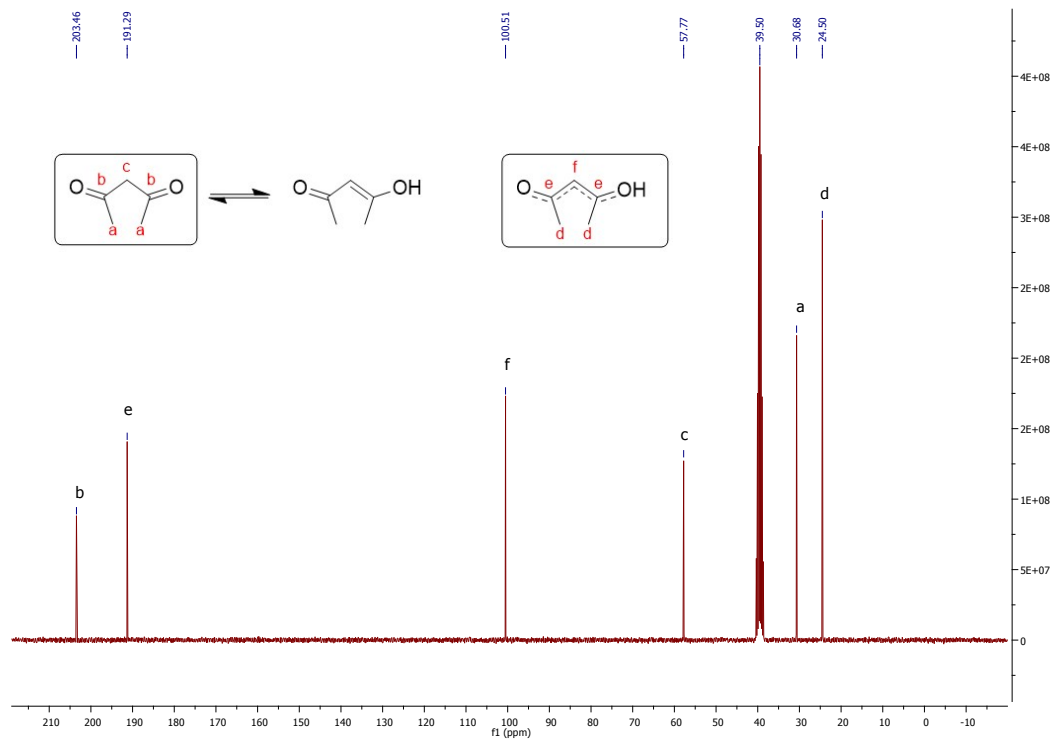


Figure S4.4.38:  $^{13}\text{C}$ -NMR spectrum of  $3q$  in  $\text{DMSO}-d_6$ .

S4.5 Hydrogenation products

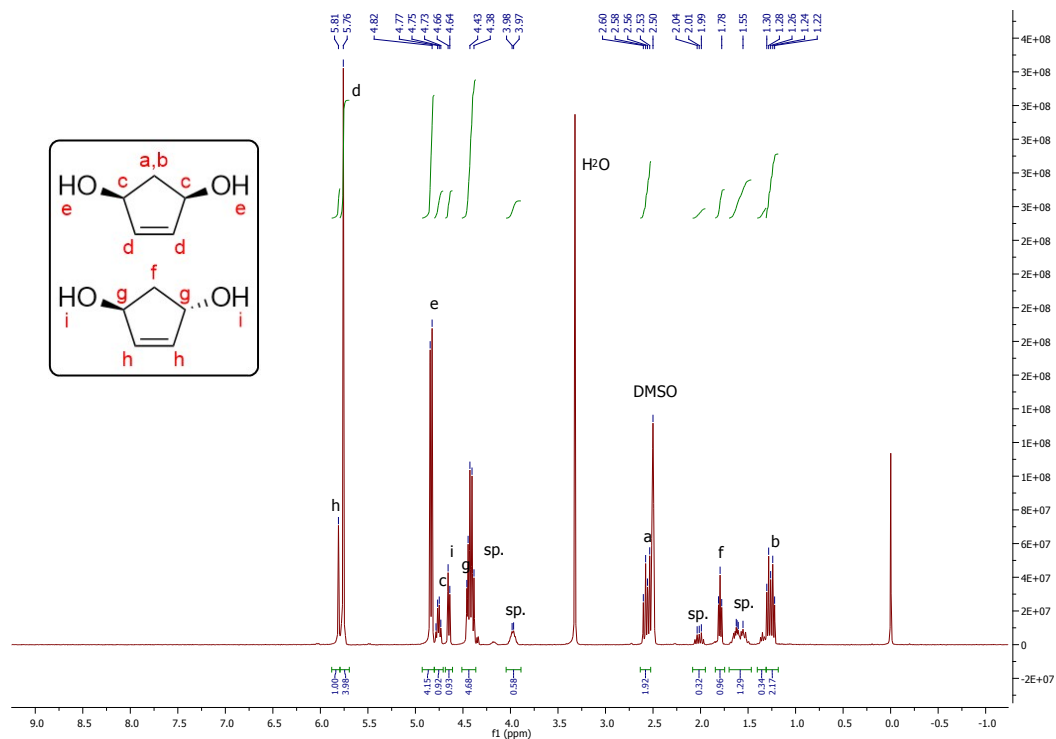


Figure S4.5.1:  $^1\text{H}$ -NMR spectrum of cpEdiol in  $\text{DMSO}-d_6$ . Traces of side products (sp.) were identified as cpAdiol.

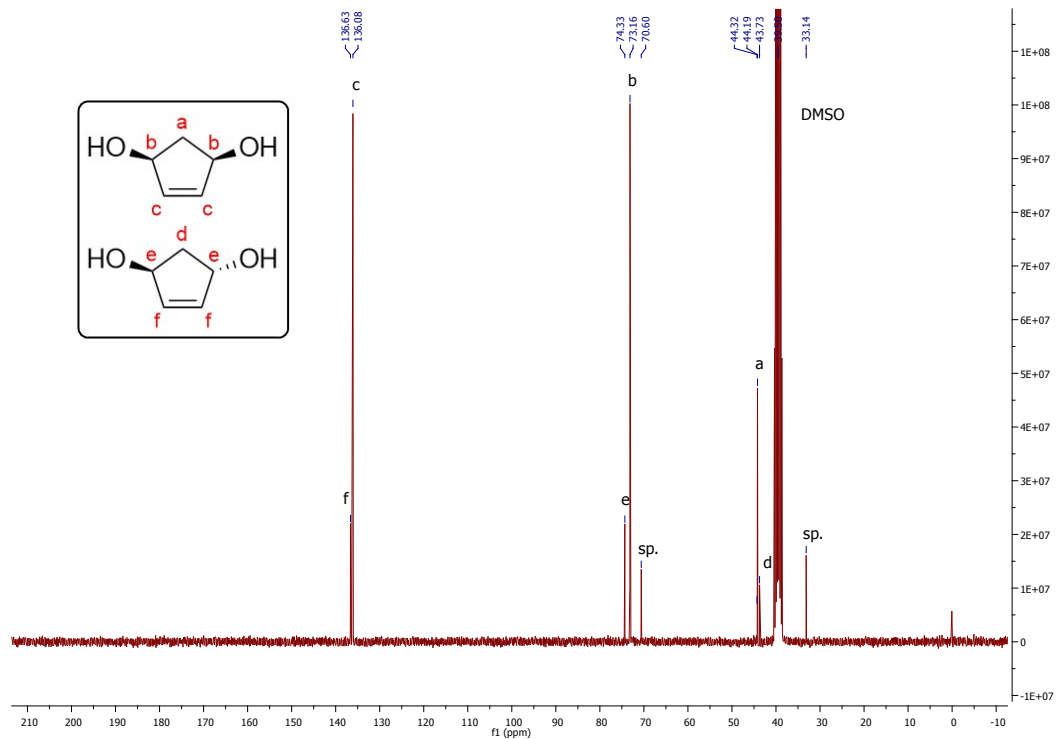


Figure S4.5.2:  $^{13}\text{C}$ -NMR spectrum of cpEdiol in  $\text{DMSO}-d_6$ . Traces of side products (sp.) were identified as cpAdiol.

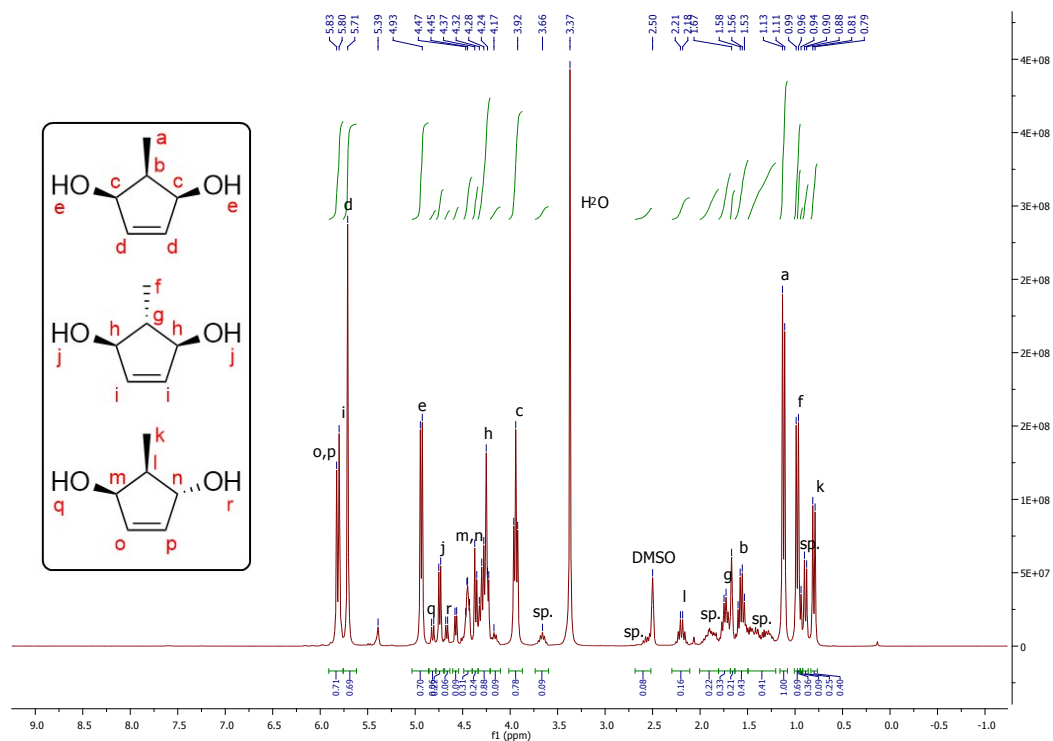


Figure S4.5.3:  $^1\text{H}$ -NMR spectrum of **2a** in  $\text{DMSO}-d_6$ . Traces of side products (sp.) were identified as alkene-hydrogenated derivatives of **2a**.

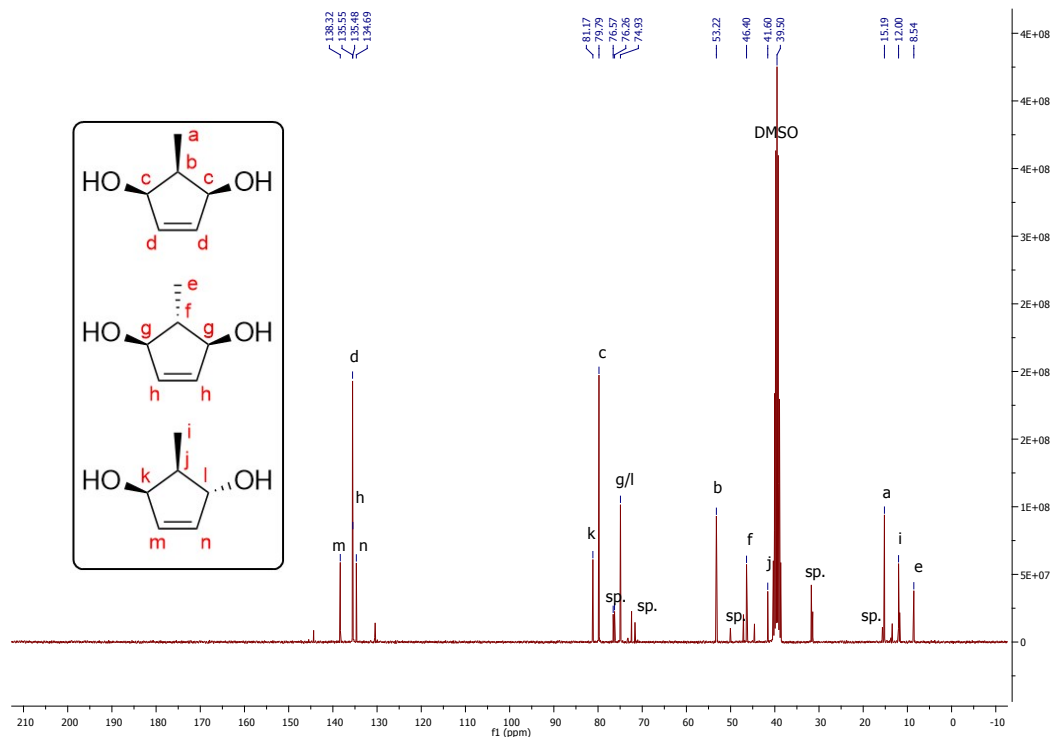


Figure S4.5.4:  $^{13}\text{C}$ -NMR spectrum of **2a** in  $\text{DMSO}-d_6$ . Traces of side products (sp.) were identified as alkene-hydrogenated derivatives of **2a**.

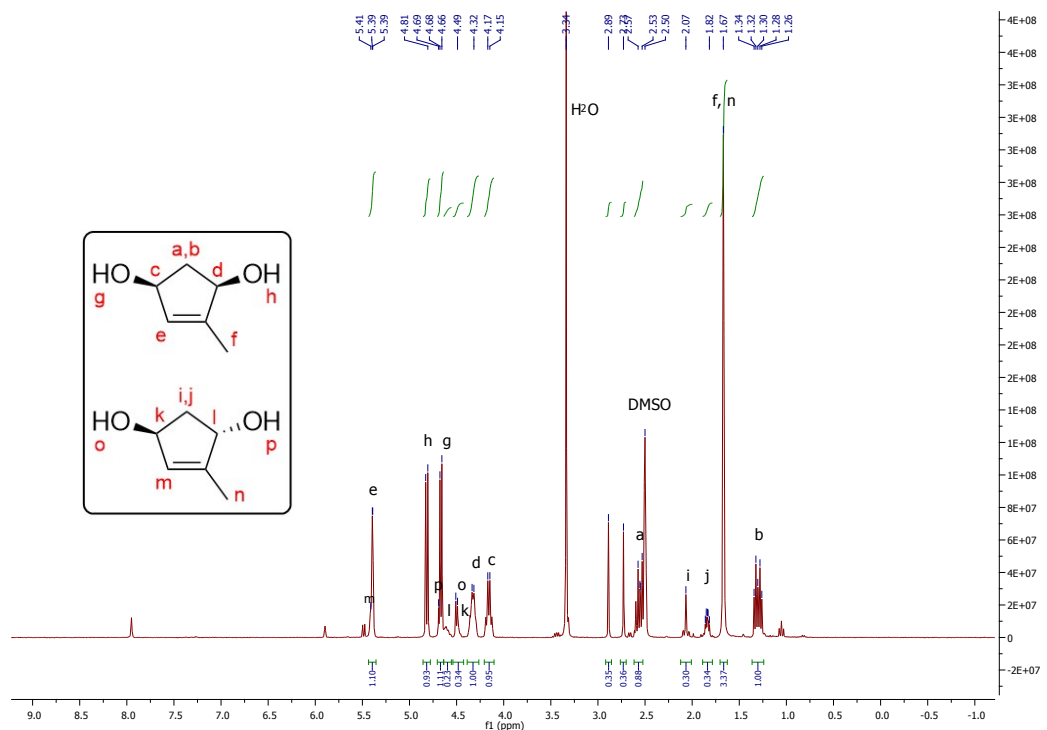


Figure S4.5.5:  $^1\text{H}$ -NMR spectrum of **2b** in  $\text{DMSO}-d_6$ .

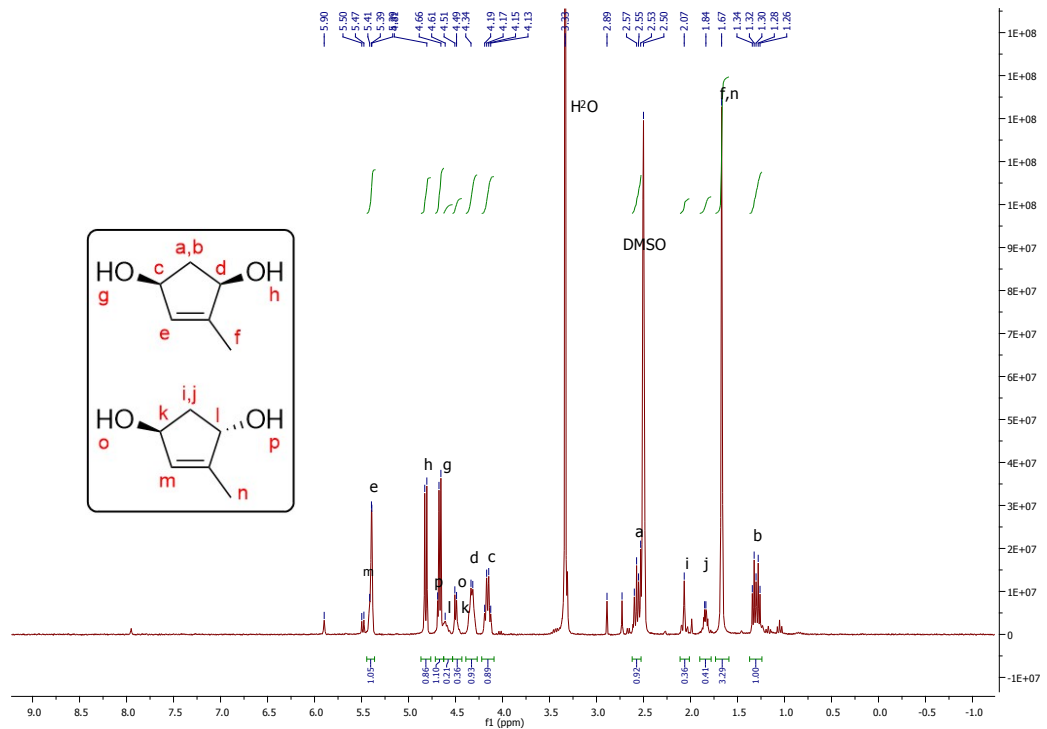


Figure S4.5.6:  $^1\text{H}$ -NMR spectrum of **2c**, in  $\text{DMSO}-d_6$ .

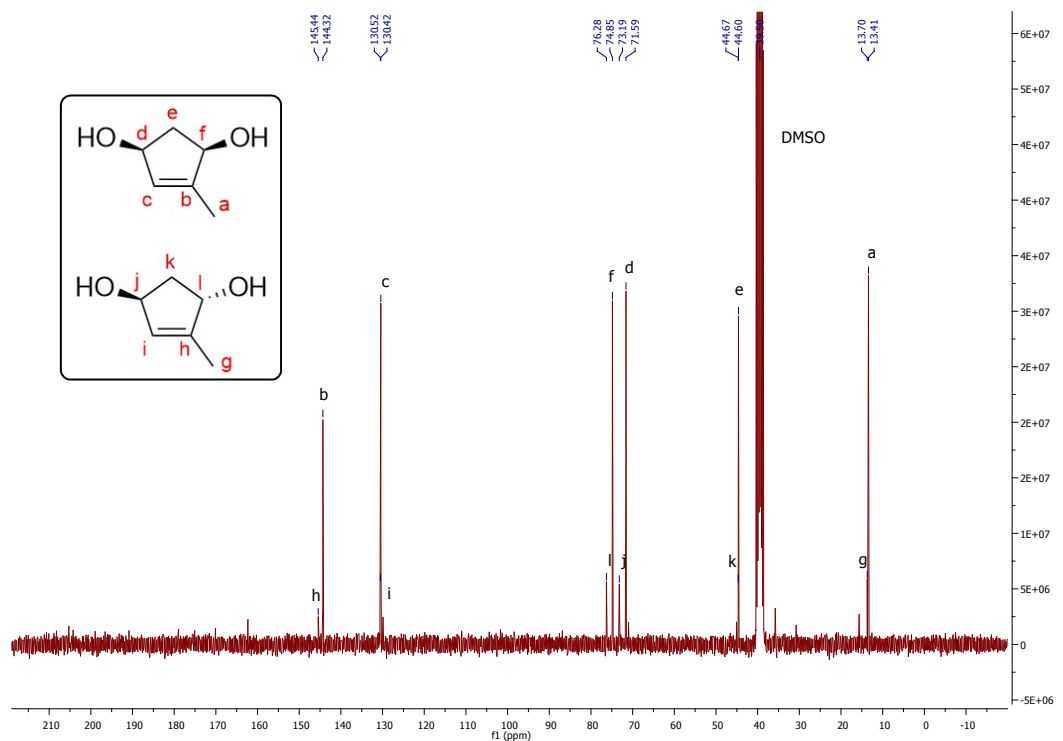


Figure S4.5.7:  $^{13}\text{C}$ -NMR spectrum of **2b** in  $\text{DMSO}-d_6$ .

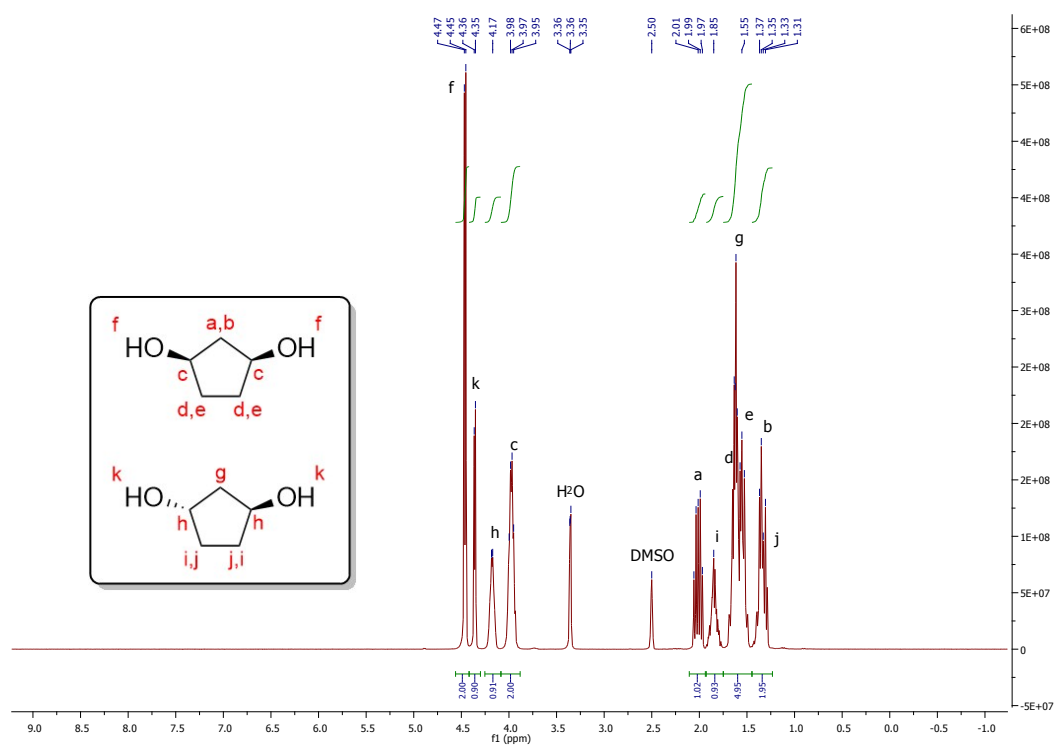


Figure S4.5.8:  $^1\text{H}$ -NMR spectrum of cpAdiol in  $\text{DMSO}-d_6$ .

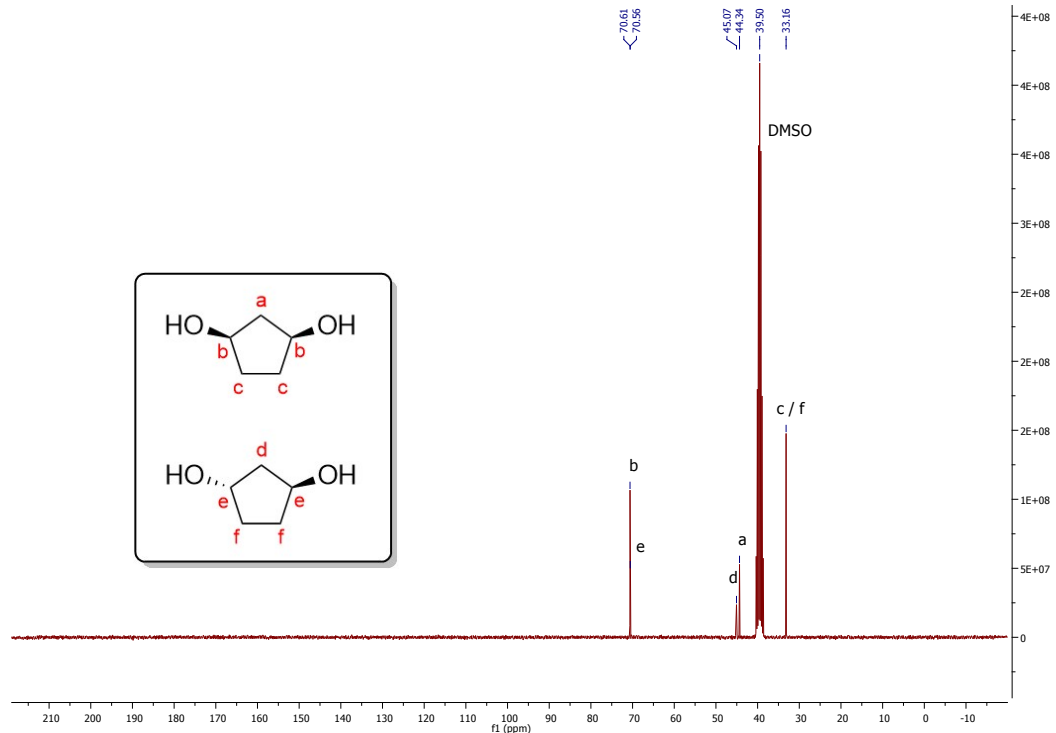


Figure S4.5.9:  $^{13}\text{C}$ -NMR spectrum of cpAdiol in  $\text{DMSO}-d_6$ .

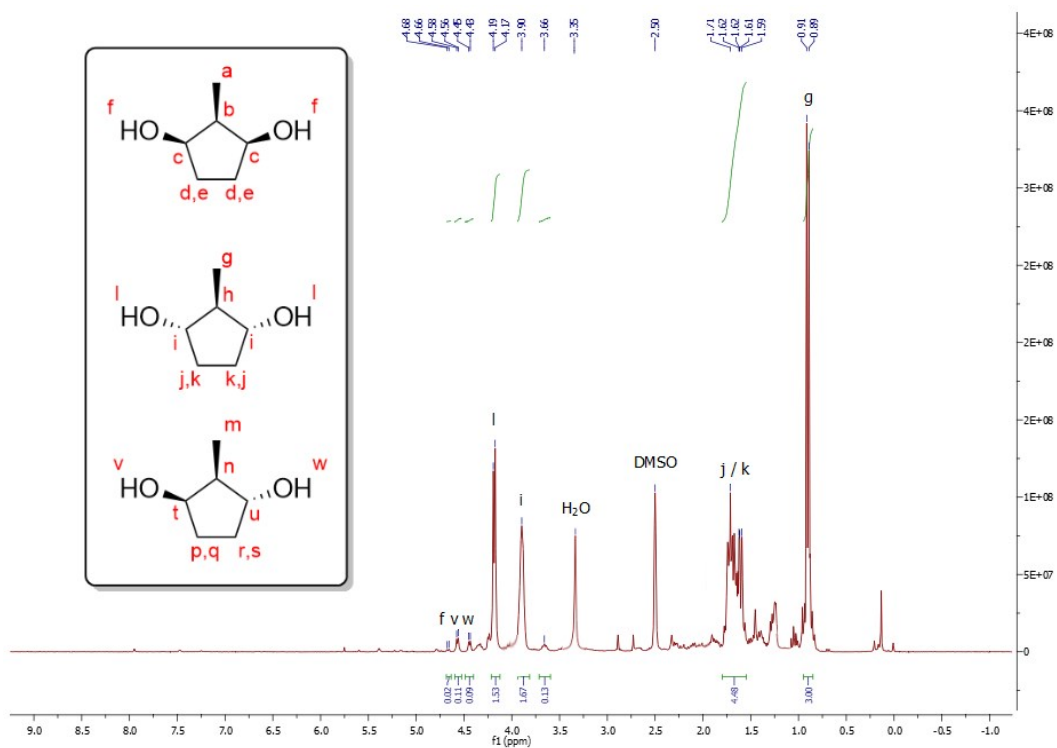


Figure S4.5.10:  $^1\text{H}$ -NMR spectrum of **5e** in  $\text{DMSO}-d_6$ .

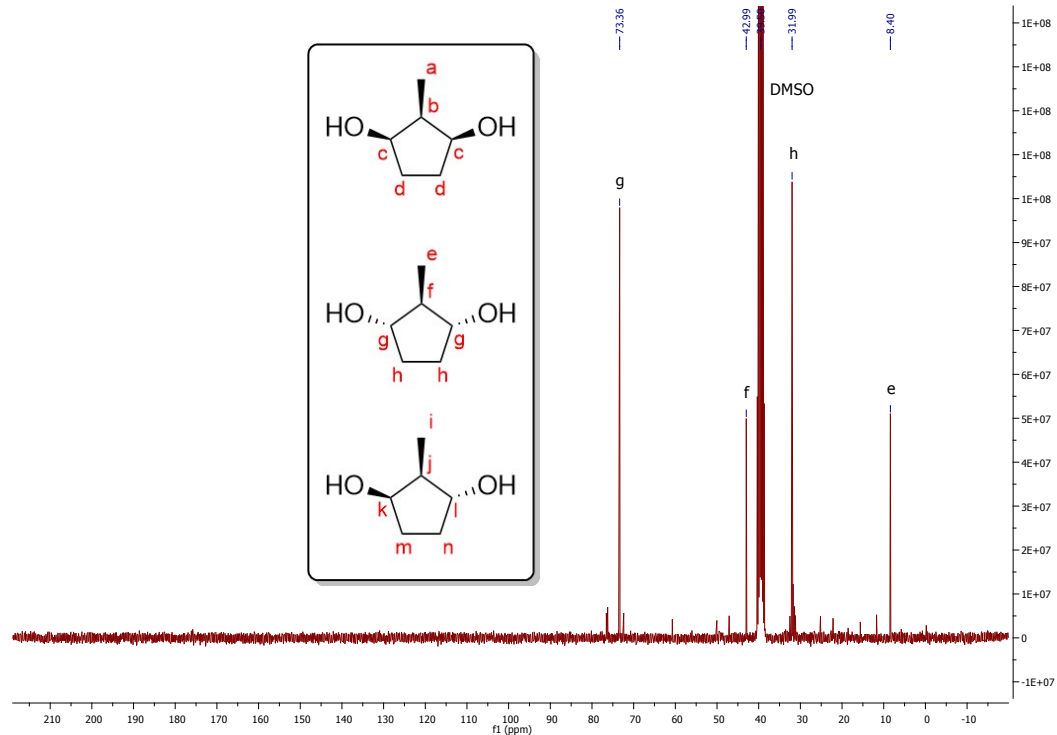


Figure S4.5.11:  $^{13}\text{C}$ -NMR spectrum of **5e** in  $\text{DMSO}-d_6$ .

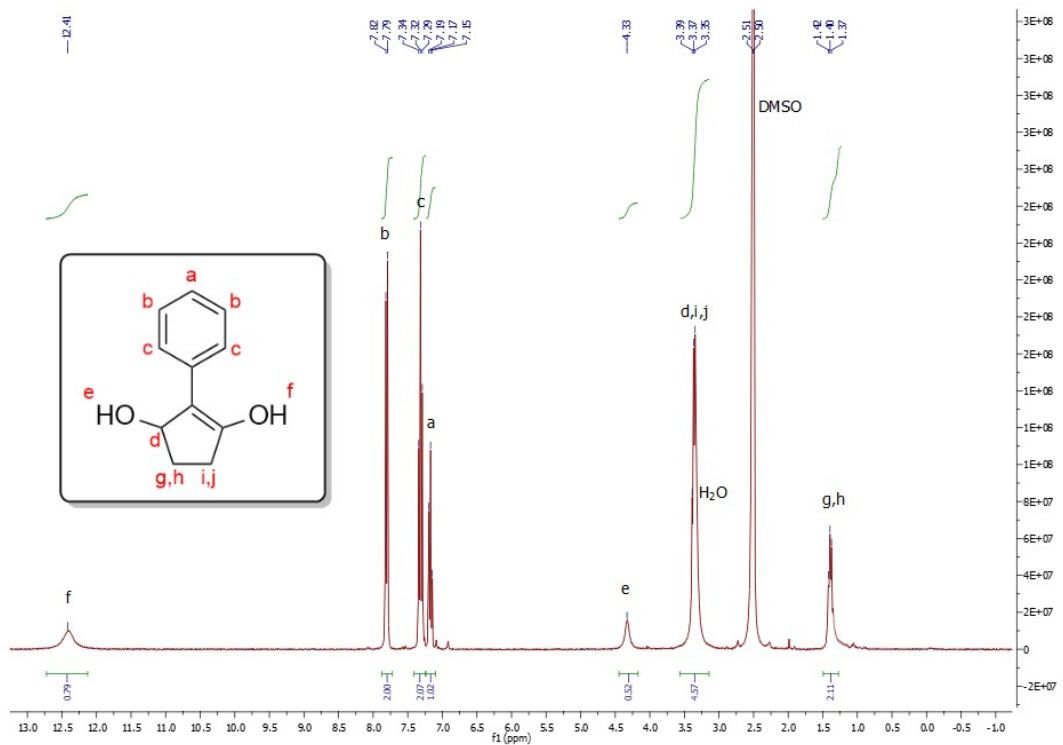


Figure S4.5.12: <sup>1</sup>H-NMR spectrum of **4f** in  $\text{DMSO}-d_6$ .

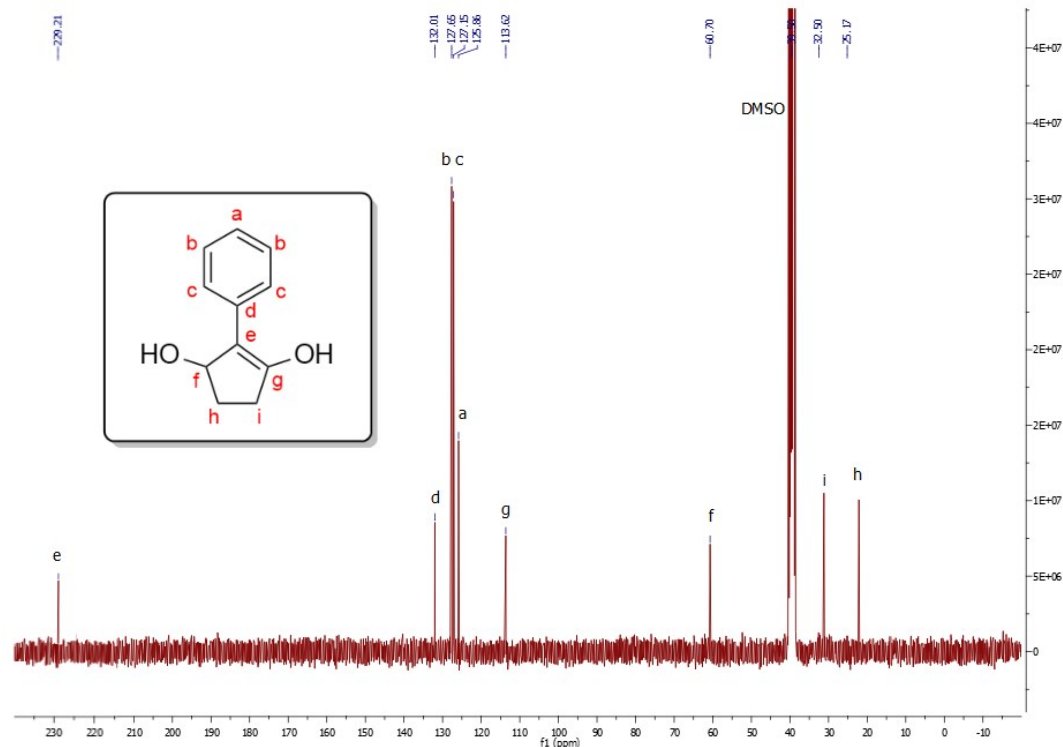


Figure S4.5.13: <sup>13</sup>C-NMR spectrum of **4f** in  $\text{DMSO}-d_6$ .

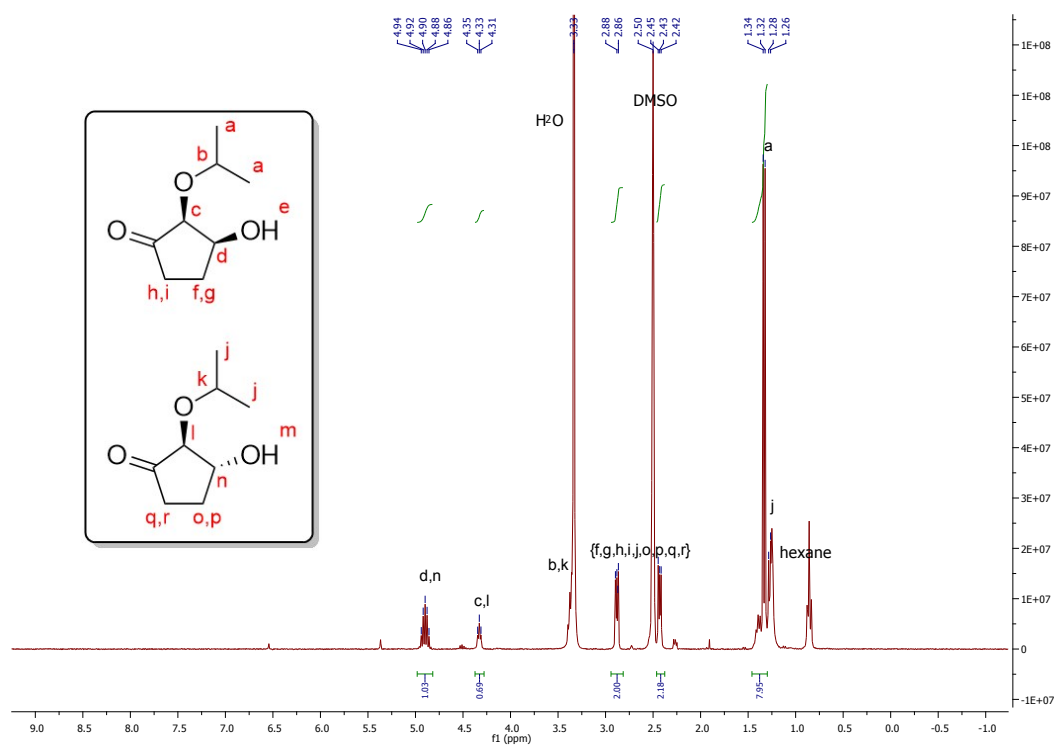


Figure S4.5.14:  $^1\text{H}$ -NMR spectrum of **4g** in  $\text{DMSO}-d_6$ .

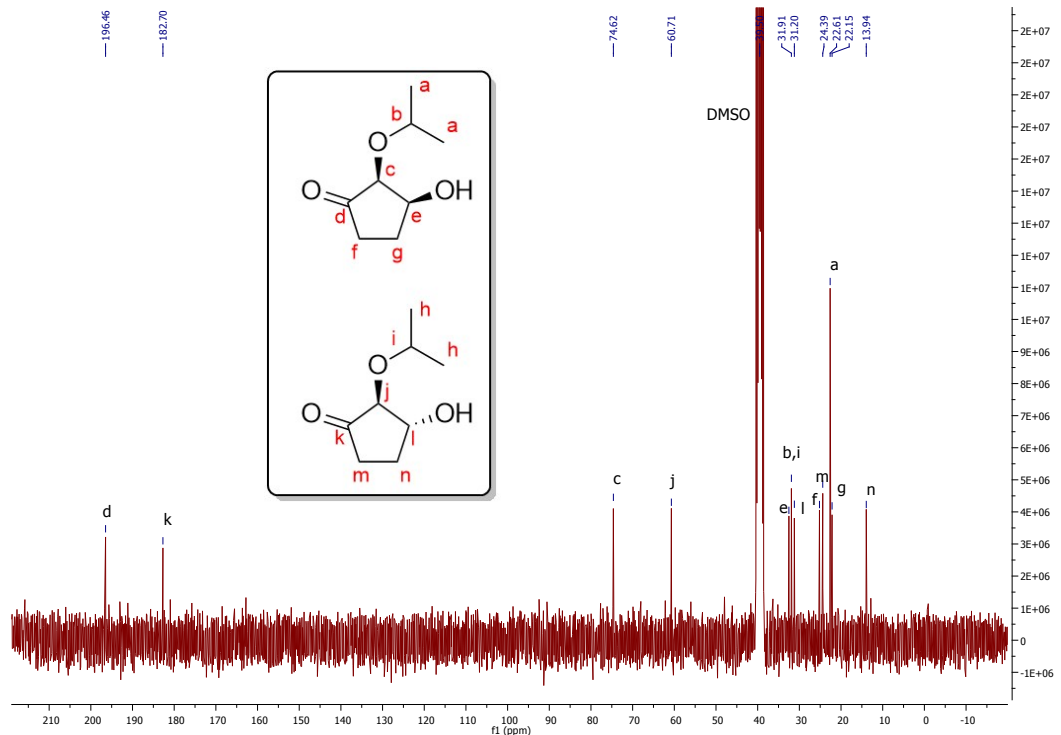


Figure S4.5.15:  $^{13}\text{C}$ -NMR spectrum of **4g** in  $\text{DMSO}-d_6$ .

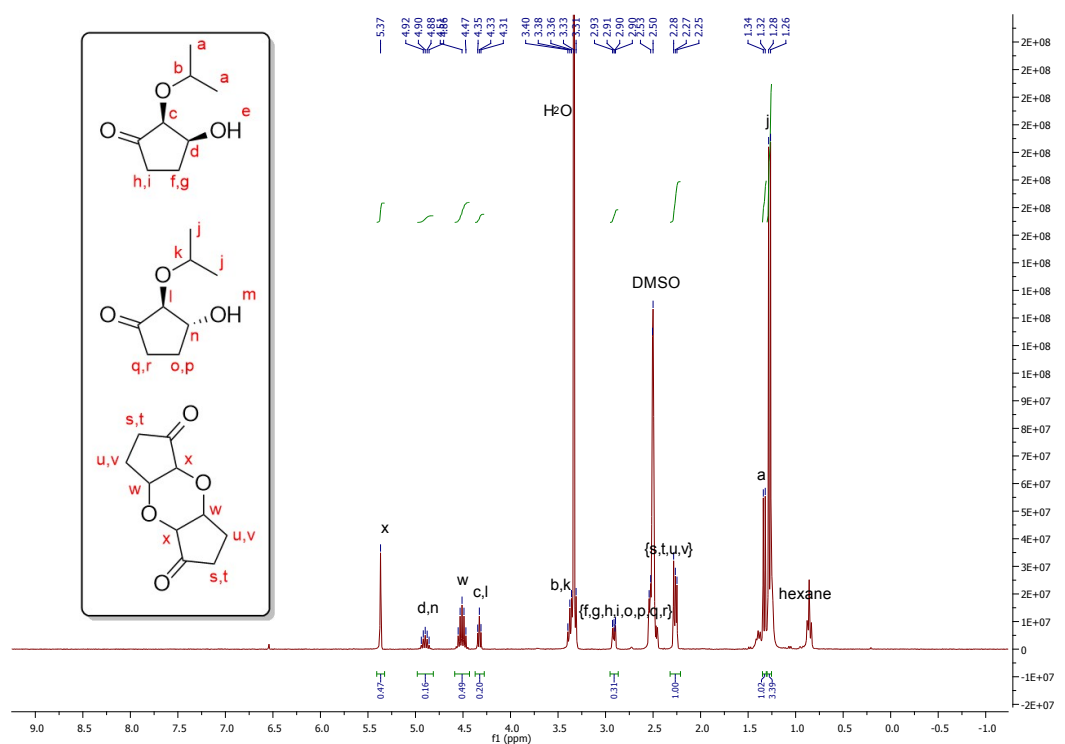


Figure S4.5.16: <sup>1</sup>H-NMR spectrum of **4h** and **5h** in  $\text{DMSO}-d_6$ .

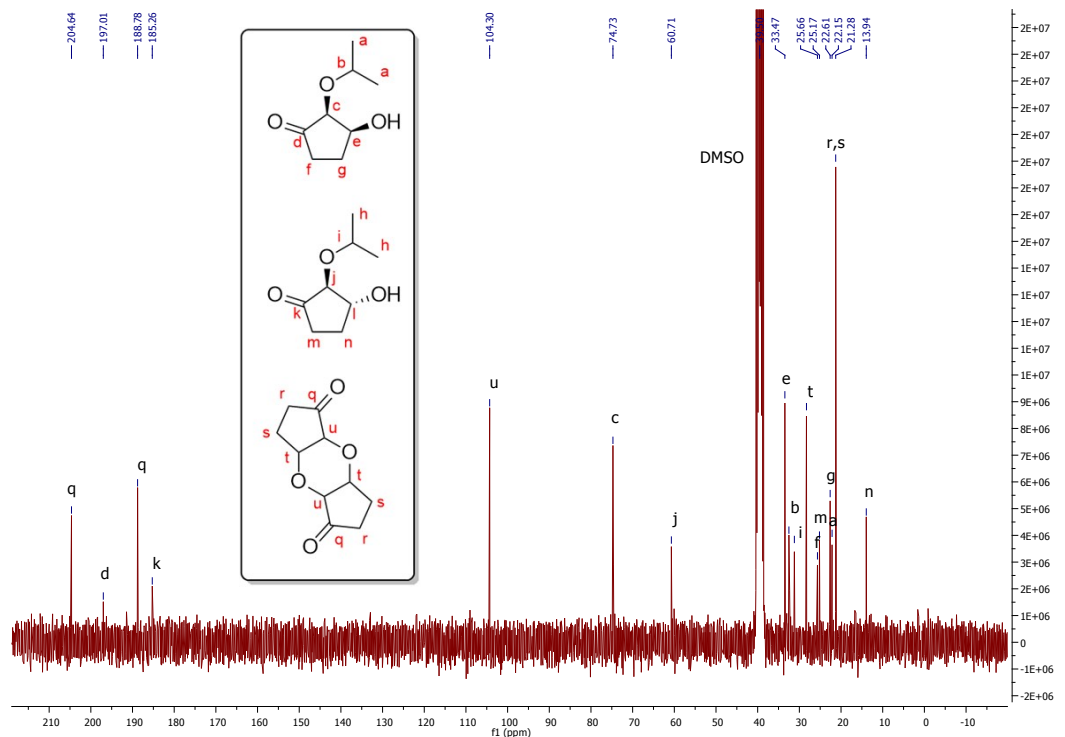


Figure S4.5.17: <sup>13</sup>C-NMR spectrum of **4h** and **5h** in  $\text{DMSO}-d_6$ .

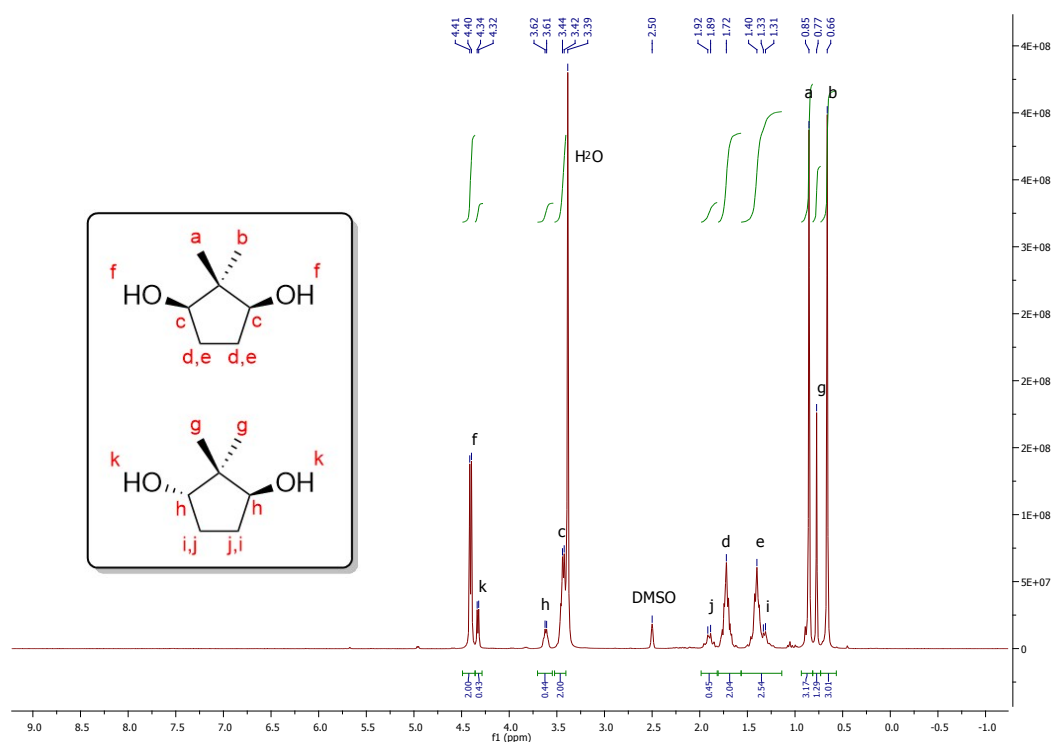


Figure S4.5.18: <sup>1</sup>H-NMR spectrum of **5i** in  $\text{DMSO}-d_6$ .

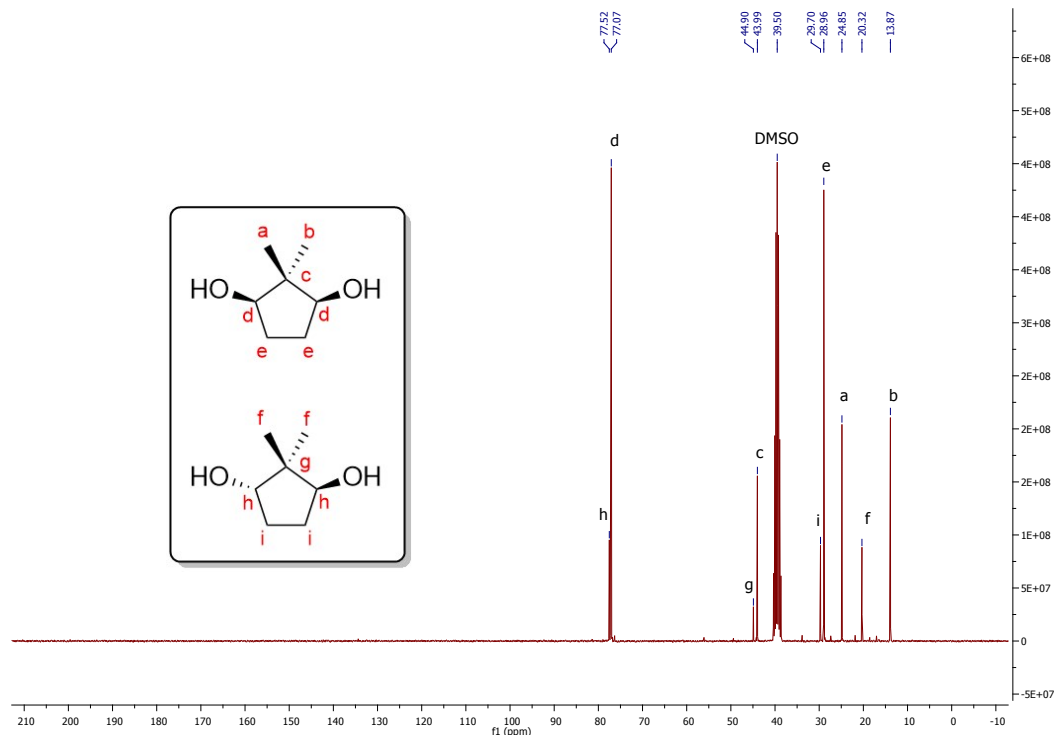


Figure S4.5.19: <sup>13</sup>C-NMR spectrum of **5i** in  $\text{DMSO}-d_6$ .

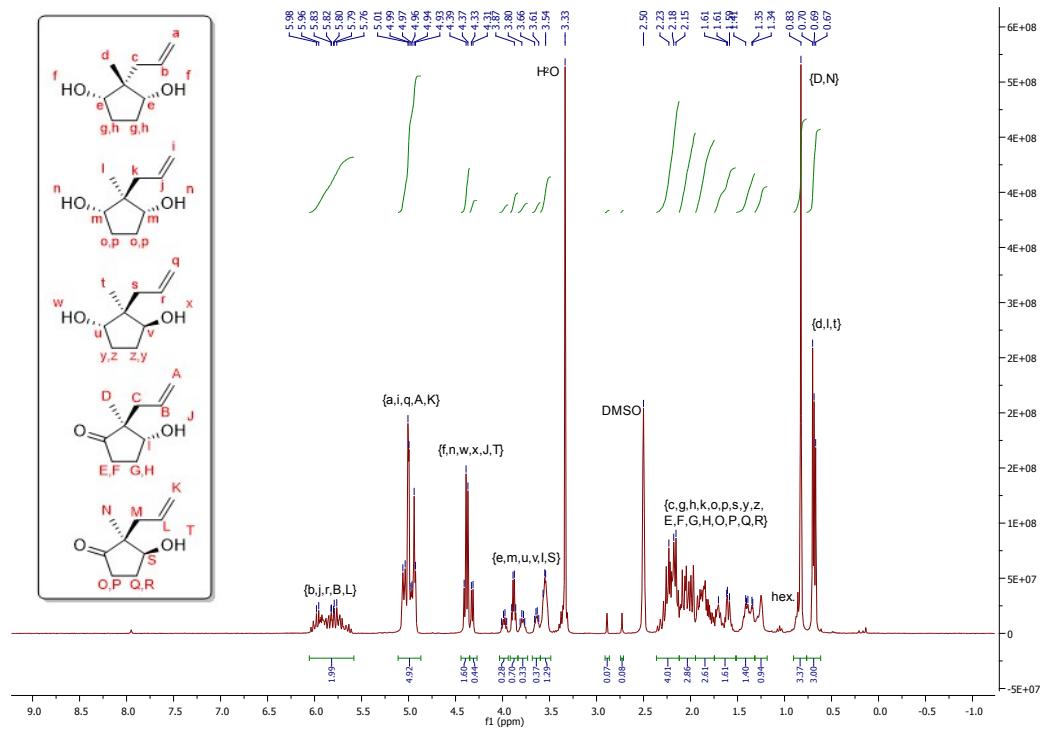


Figure S4.5.20: <sup>1</sup>H-NMR spectrum of a complex mixture of **4j** and **5j** in  $\text{DMSO}-d_6$ .

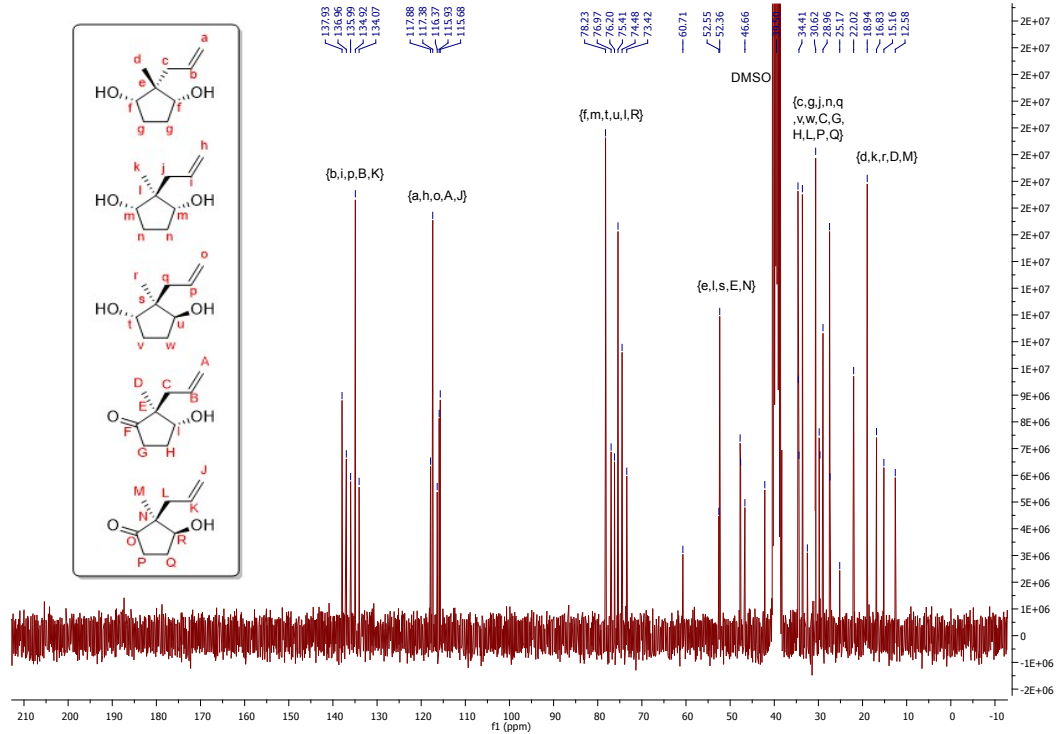


Figure S4.5.21: <sup>13</sup>C-NMR spectrum of a complex mixture of **4j** and **5j** in  $\text{DMSO}-d_6$ .

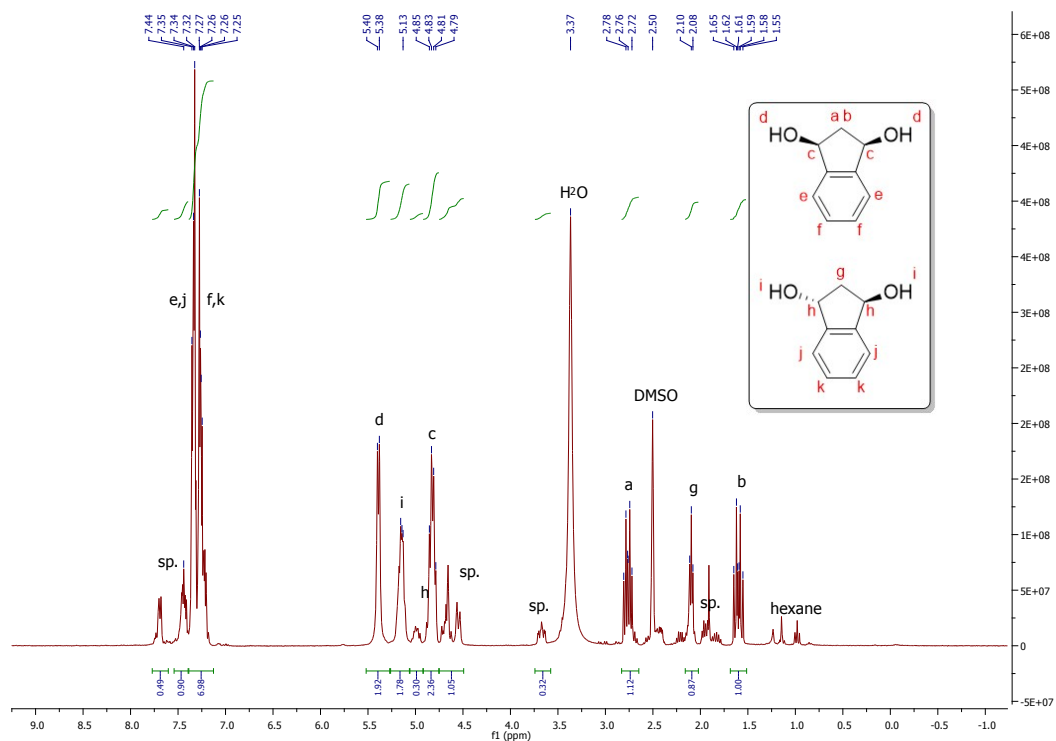


Figure S4.5.22:  $^1\text{H}$ -NMR spectrum of **5k** in  $\text{DMSO}-d_6$ . Traces of side products (sp.) were identified as **3k**-derived compounds.

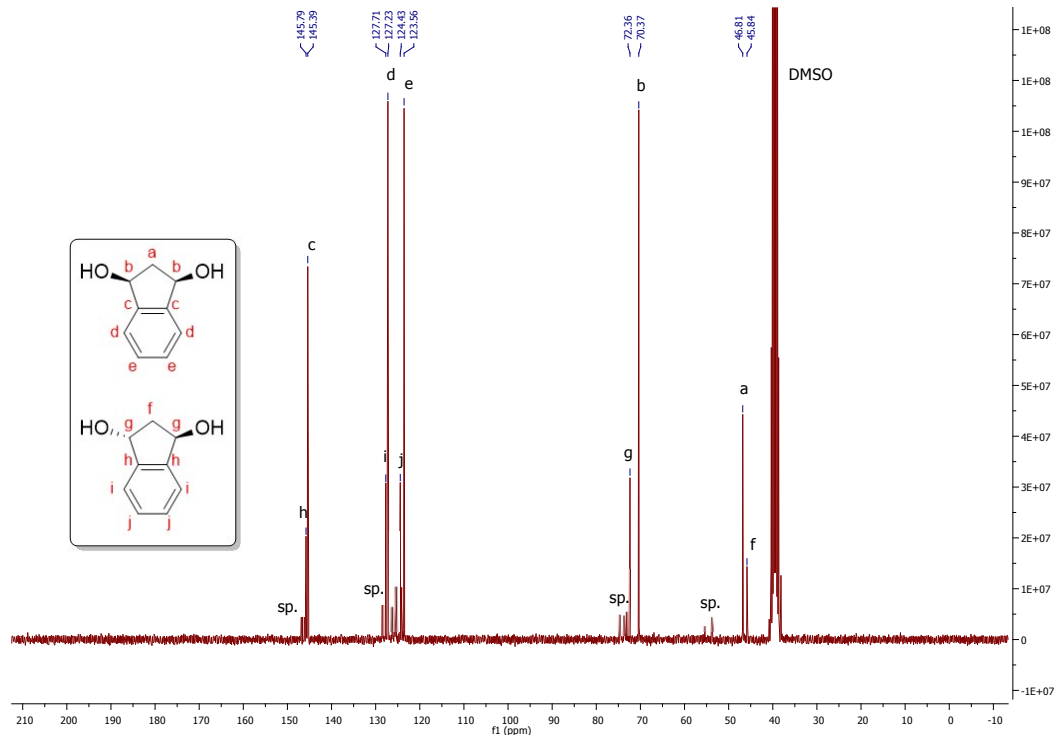


Figure S4.5.23:  $^{13}\text{C}$ -NMR spectrum of **5k** in  $\text{DMSO}-d_6$ . Traces of side products (sp.) were identified as **3k**-derived compounds.

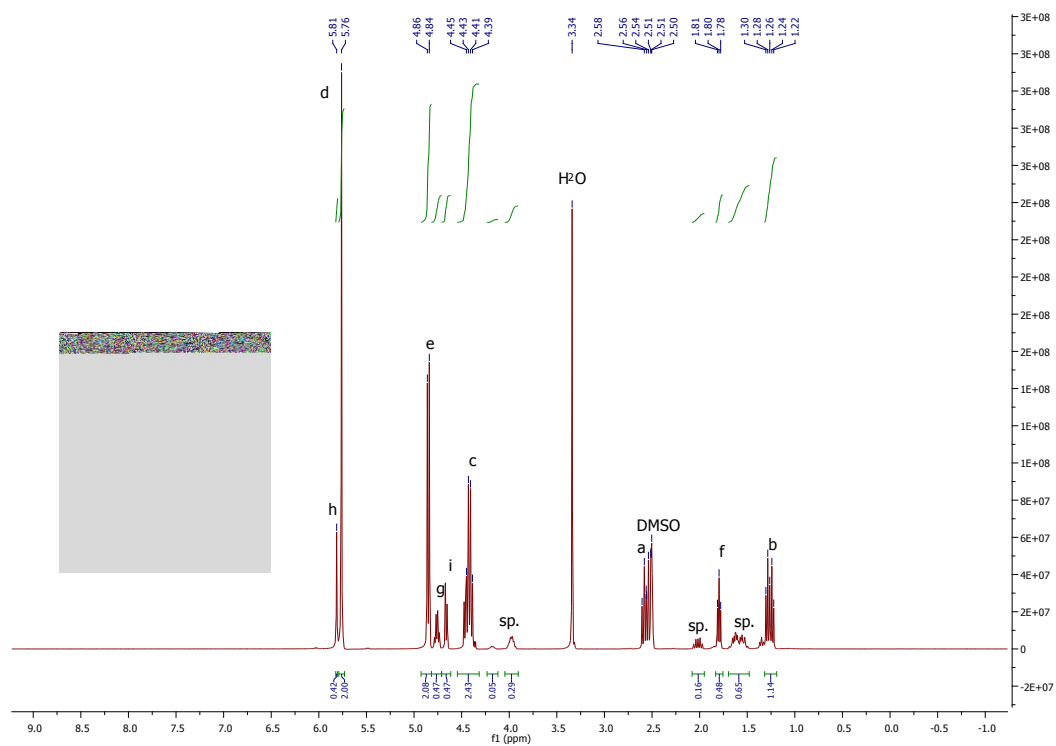


Figure S4.5.24:  $^1\text{H}$ -NMR spectrum of **5I** in  $\text{DMSO}-d_6$ . Traces of side products (sp.) were identified as cpAdiol.

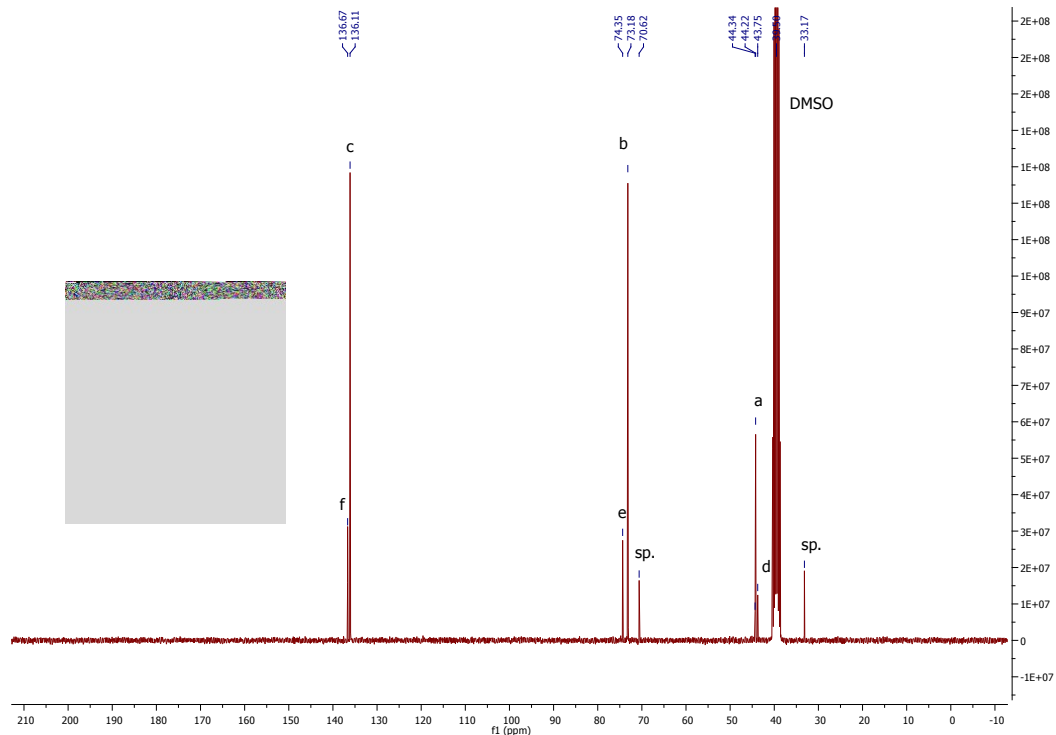


Figure S4.5.25:  $^{13}\text{C}$ -NMR spectrum of **5I** in  $\text{DMSO}-d_6$ . Traces of side products (sp.) were identified as cpAdiol.

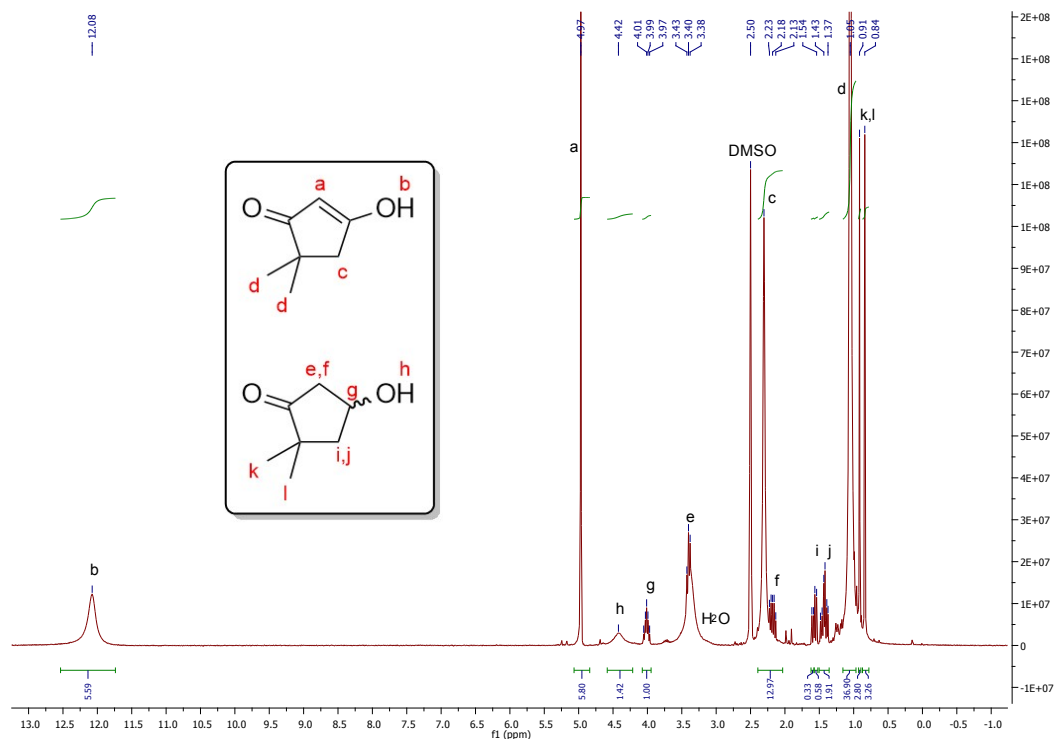


Figure S4.5.26: <sup>1</sup>H-NMR spectrum of 3m and 4m in DMSO-*d*<sub>6</sub>, the mixture could not be separated by column chromatography.

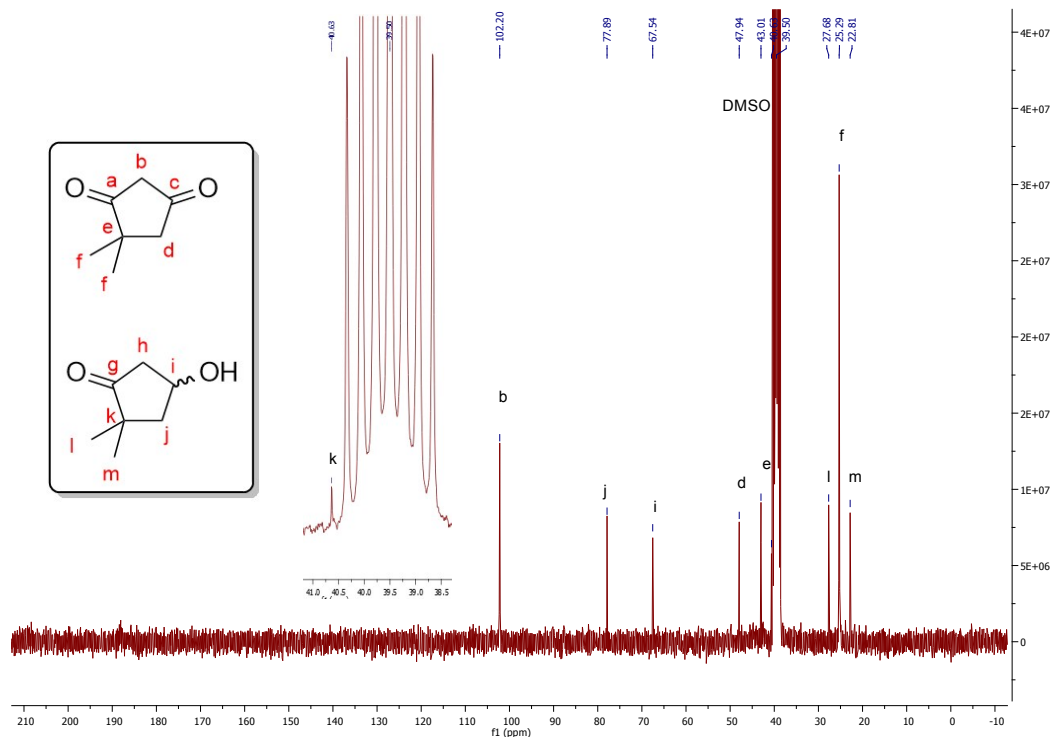


Figure S4.5.27: <sup>13</sup>C-NMR spectrum of 3m and 4m in DMSO-*d*<sub>6</sub>, the mixture could not be separated by column chromatography.

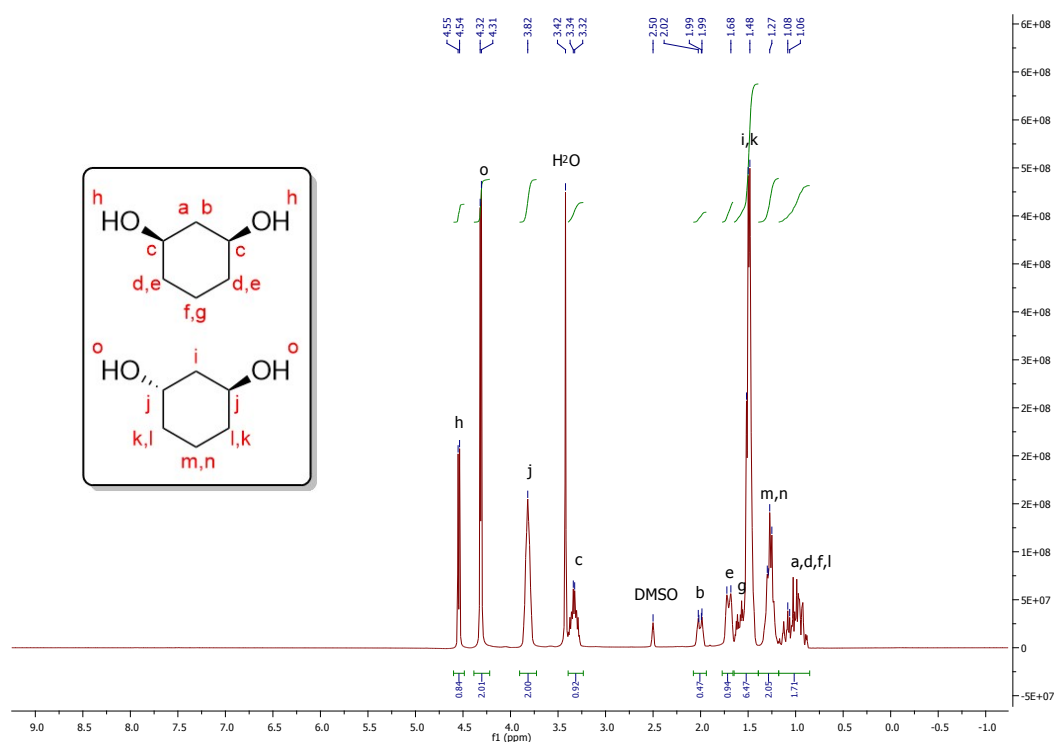


Figure S4.5.28:  $^1\text{H}$ -NMR spectrum of **5n** in  $\text{DMSO}-d_6$ .

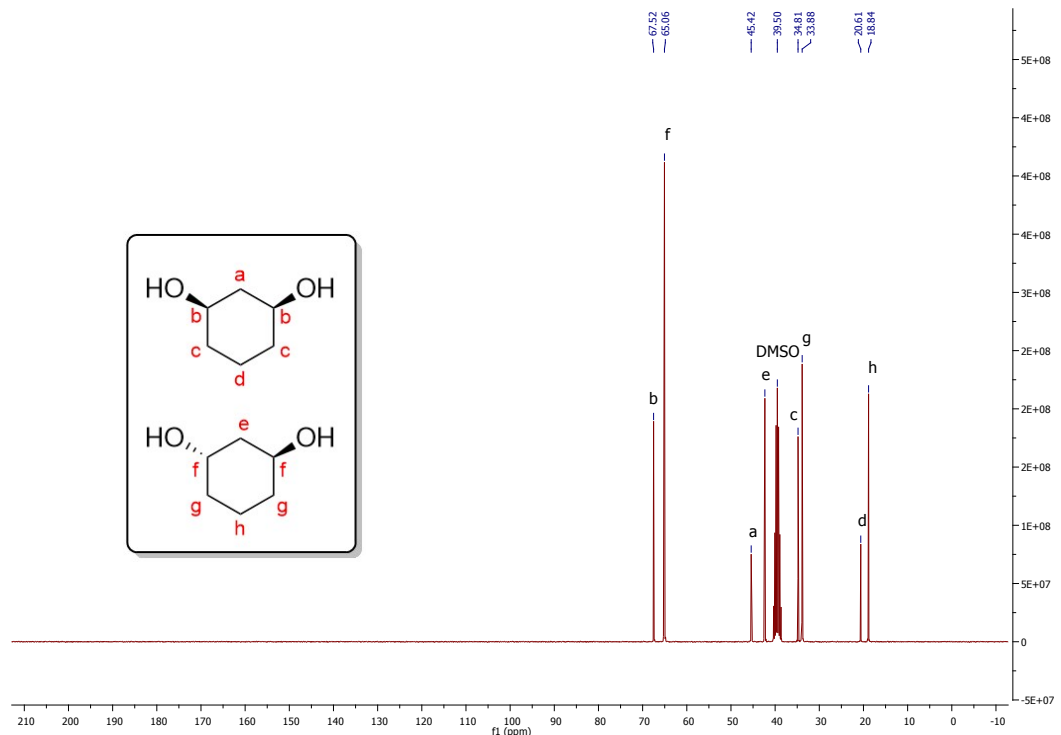


Figure S4.5.29:  $^{13}\text{C}$ -NMR spectrum of **5n** in  $\text{DMSO}-d_6$ .

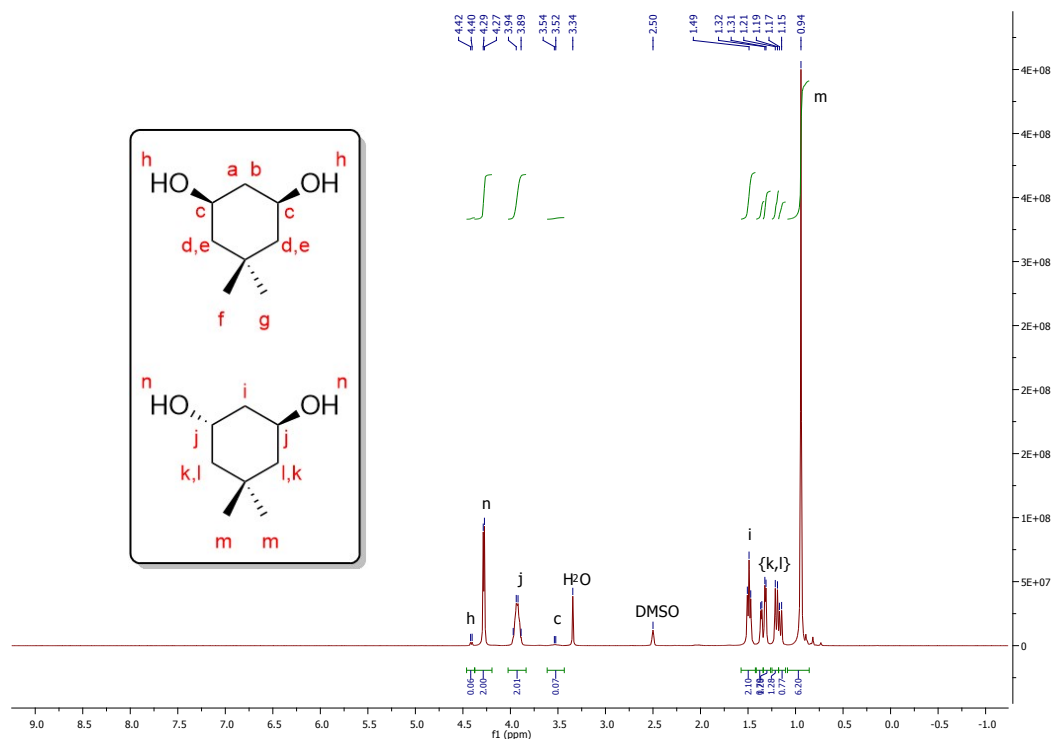


Figure S4.5.30: <sup>1</sup>H-NMR spectrum of **5o** in  $\text{DMSO}-d_6$ .

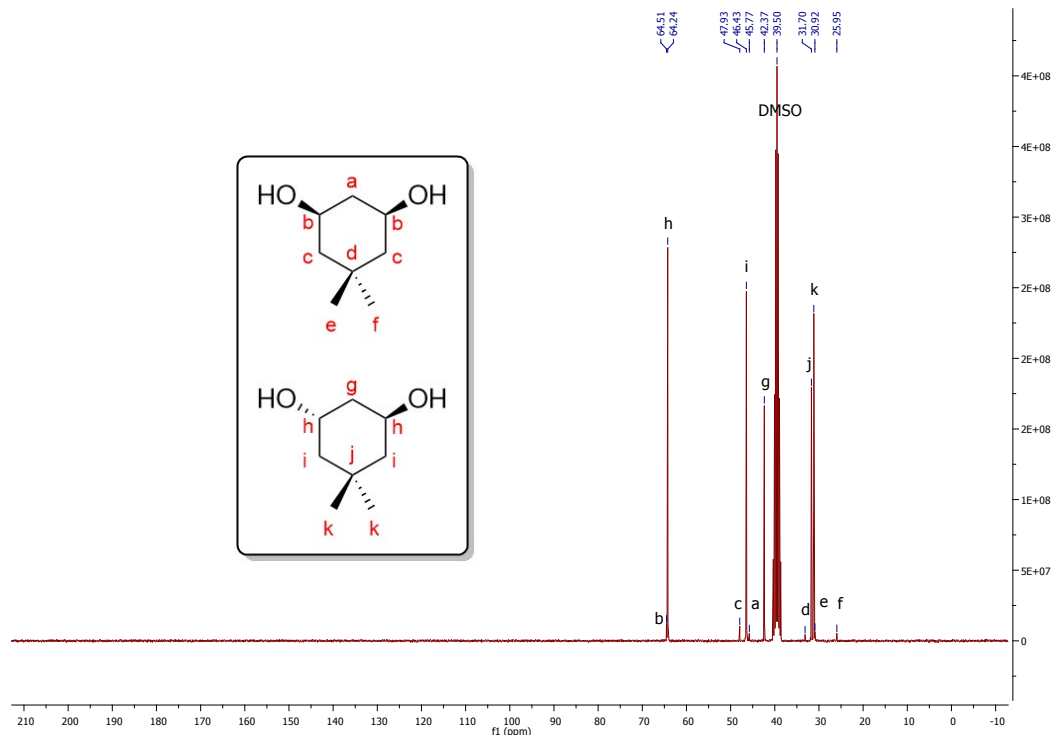


Figure S4.5.31: <sup>13</sup>C-NMR spectrum of **5o** in  $\text{DMSO}-d_6$ .

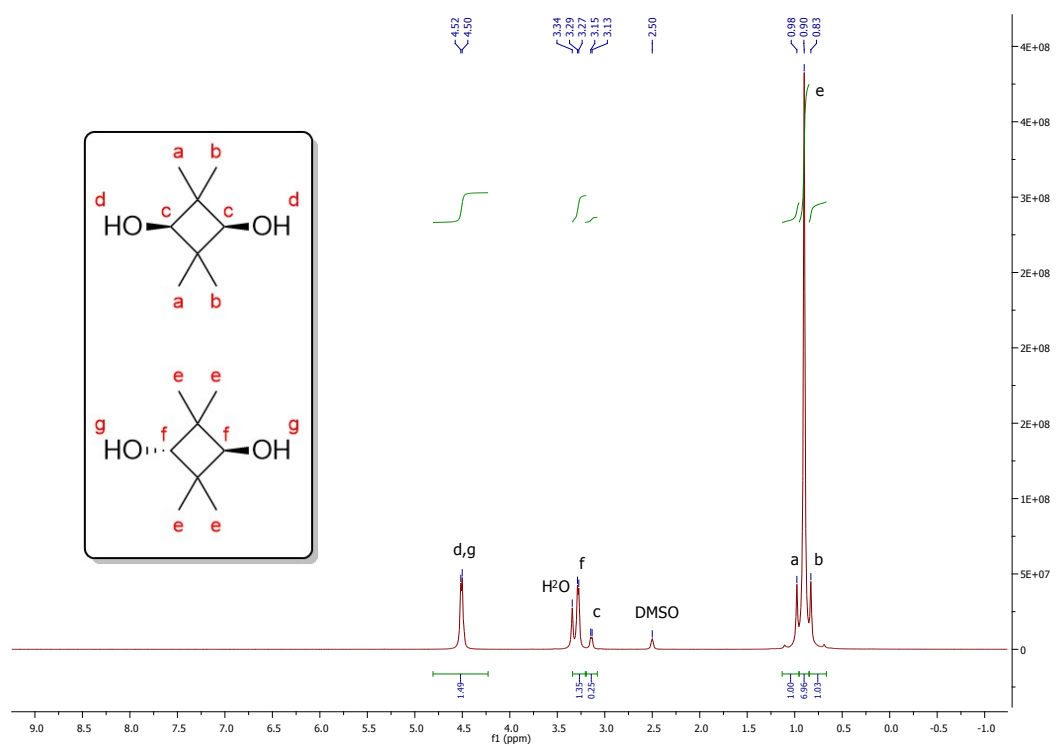


Figure S4.5.32:  $^1\text{H}$ -NMR spectrum of  $5\text{p}$  in  $\text{DMSO}-d_6$ .

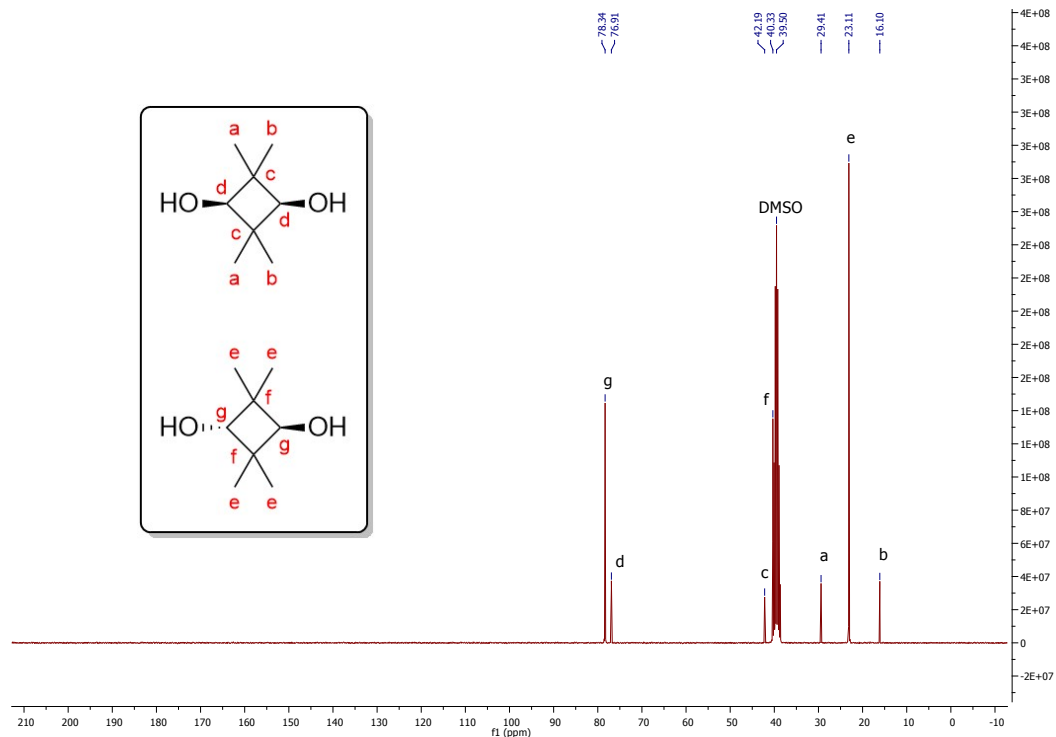


Figure S4.5.33:  $^{13}\text{C}$ -NMR spectrum of  $5\text{p}$  in  $\text{DMSO}-d_6$ .

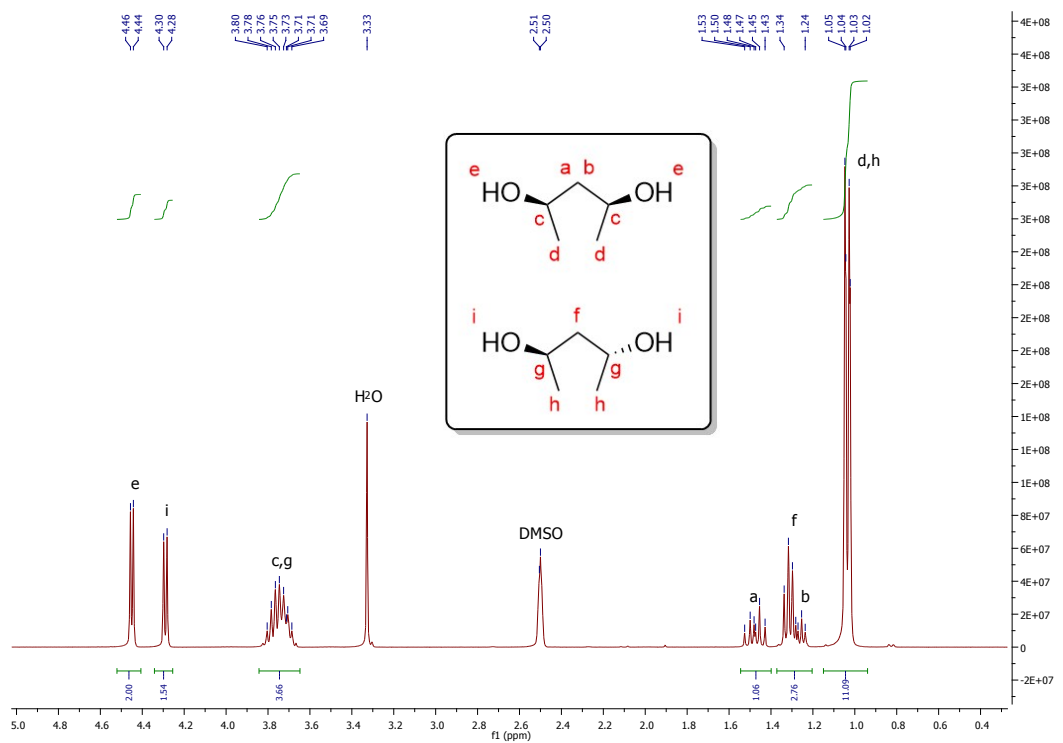


Figure S4.5.34:  $^1\text{H}$ -NMR spectrum of **5q** in  $\text{DMSO}-d_6$ .

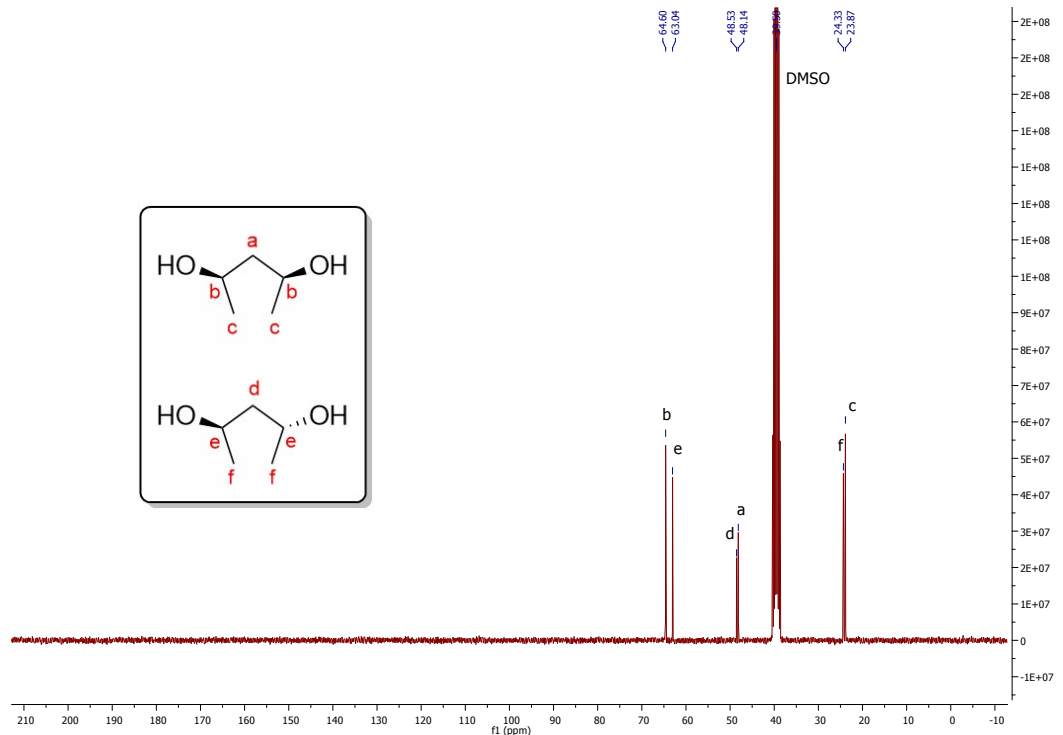


Figure S4.5.35:  $^{13}\text{C}$ -NMR spectrum of **5q** in  $\text{DMSO}-d_6$ .

## S5. FTIR analysis

S5.1 (*cyclopentadienone*)iron dicarbonyl mono-acetonitrile complexes:

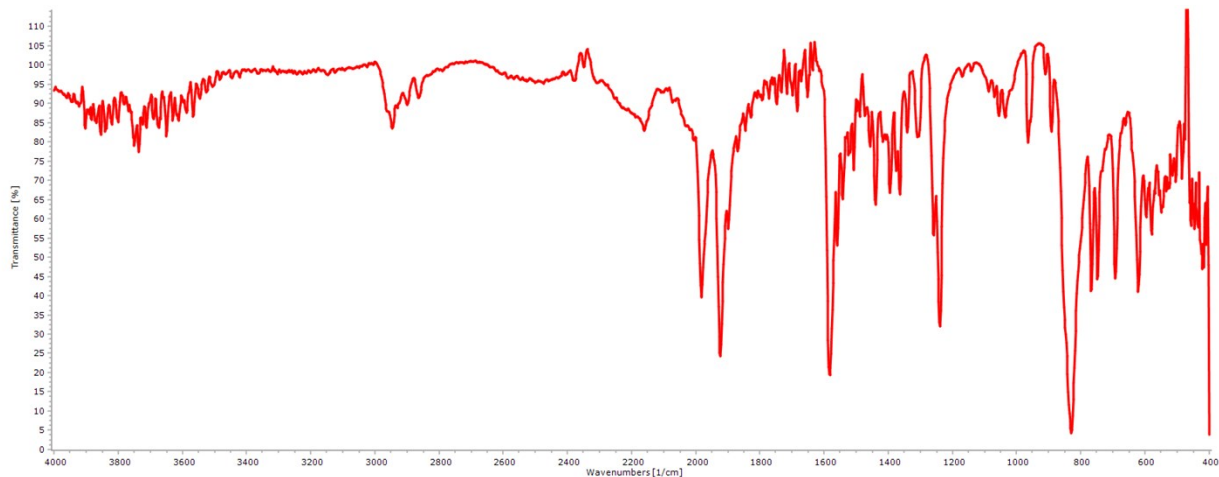


Figure 5.1.1: FTIR spectrum of catalyst **Fe-2a**.

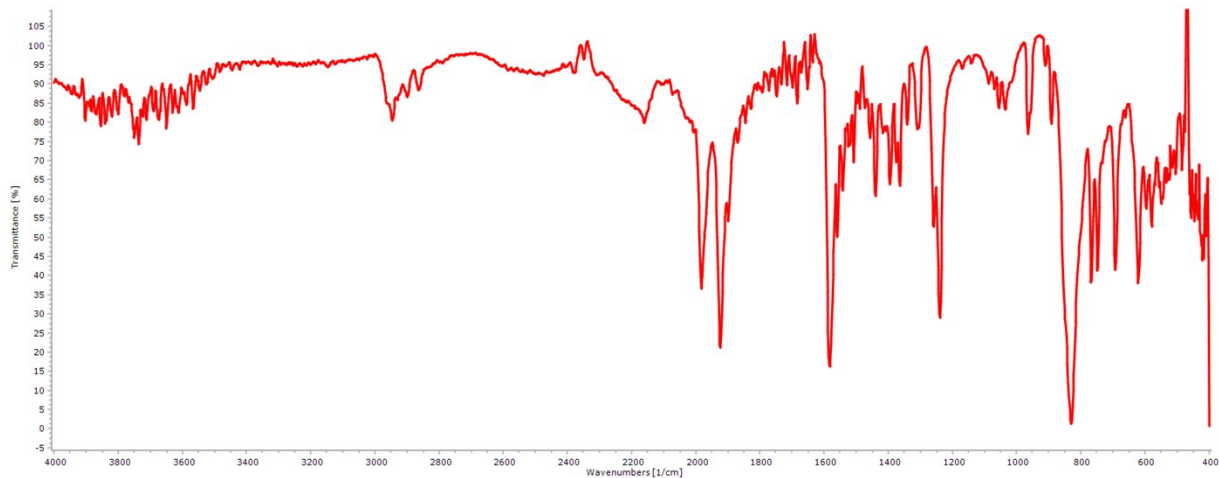


Figure 5.1.2: FTIR spectrum of catalyst **Fe-2b**.

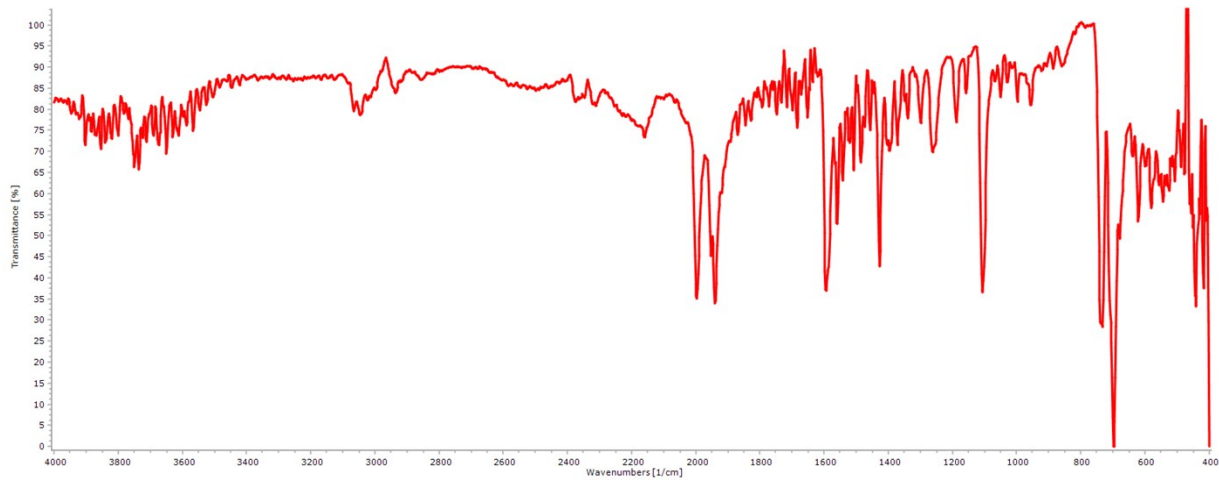


Figure 5.1.3: FTIR spectrum of catalyst **Fe-2c**.

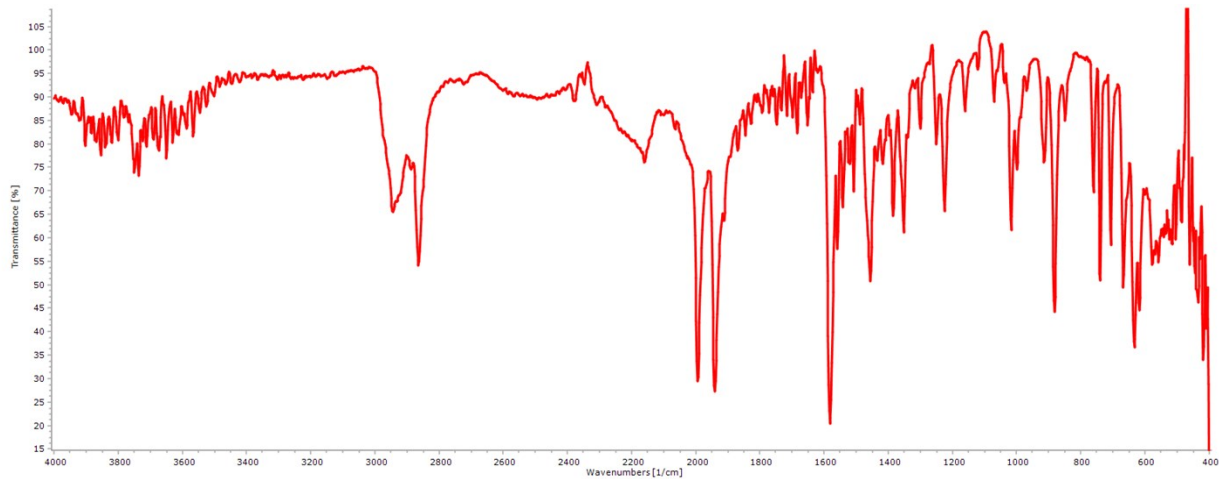


Figure 5.1.4: FTIR spectrum of catalyst **Fe-2d**.

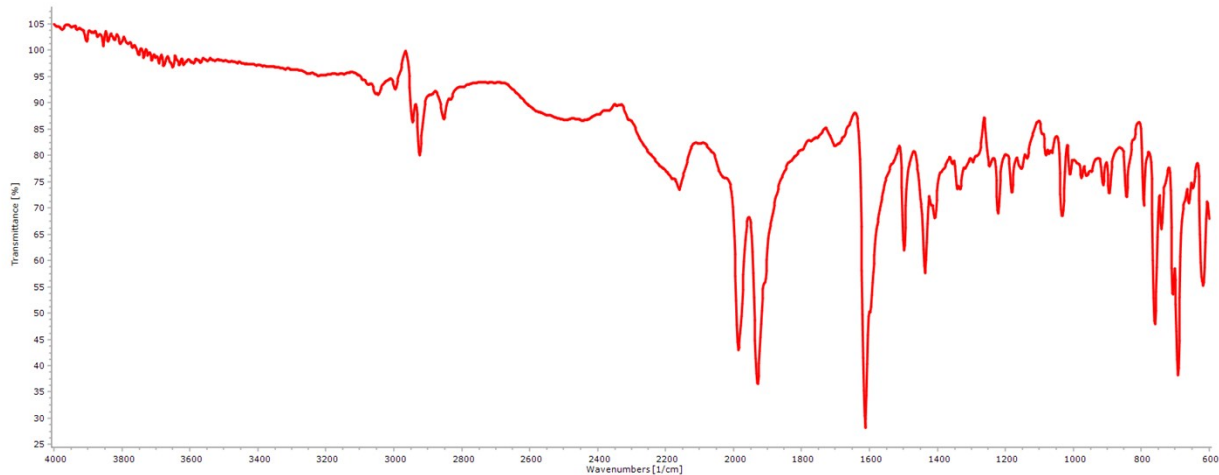


Figure 5.1.5: FTIR spectrum of catalyst **Fe-2e**.

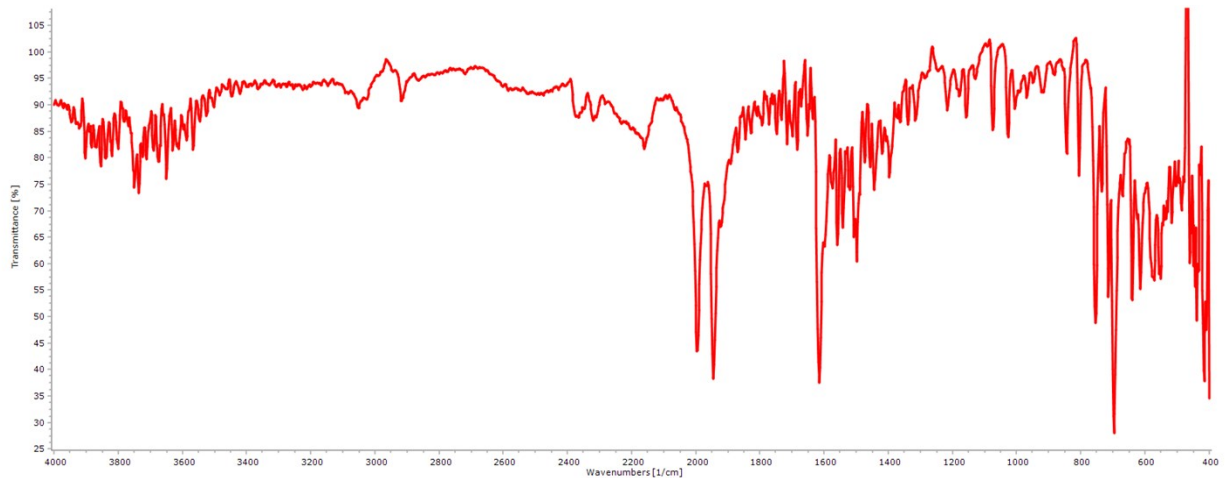


Figure 5.1.6: FTIR spectrum of catalyst **Fe-2f**.

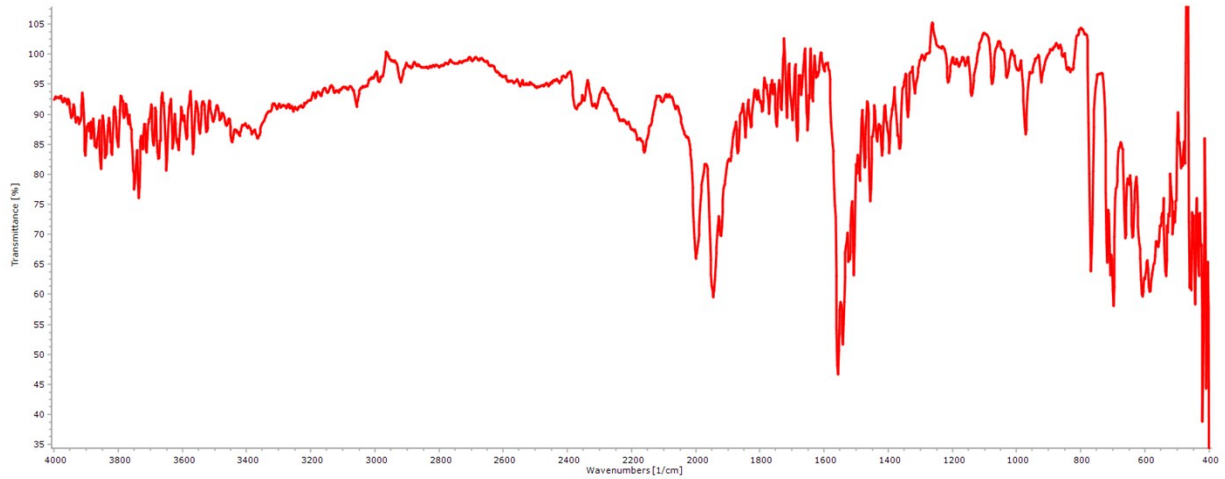
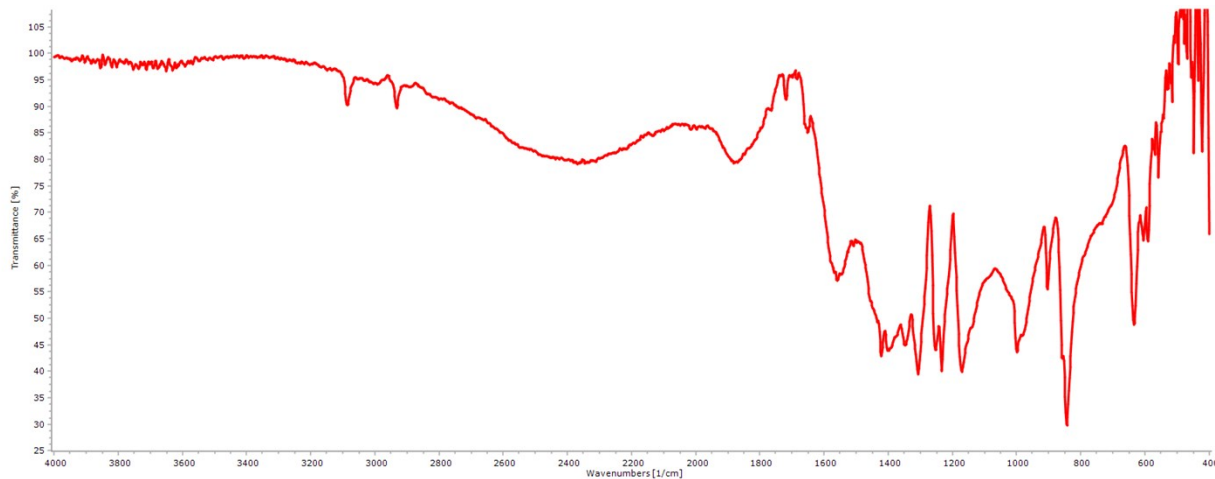
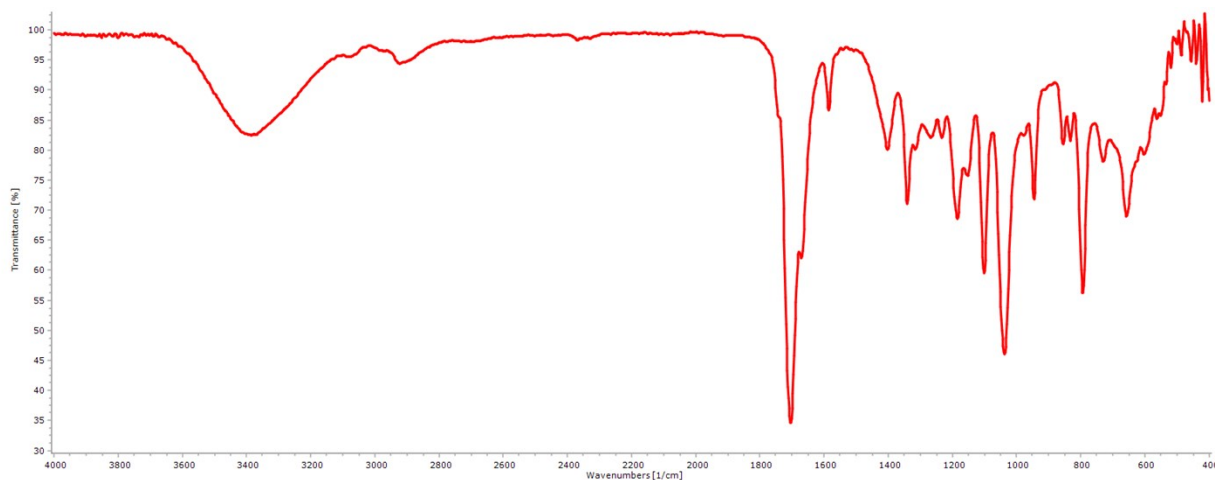


Figure 5.1.7: FTIR spectrum of catalyst **Fe-2g**.

*S5.2 Substrates:*



*Figure 5.2.1: FTIR spectrum of CPDO.*



*Figure 5.2.2: FTIR spectrum of 4-HCP.*

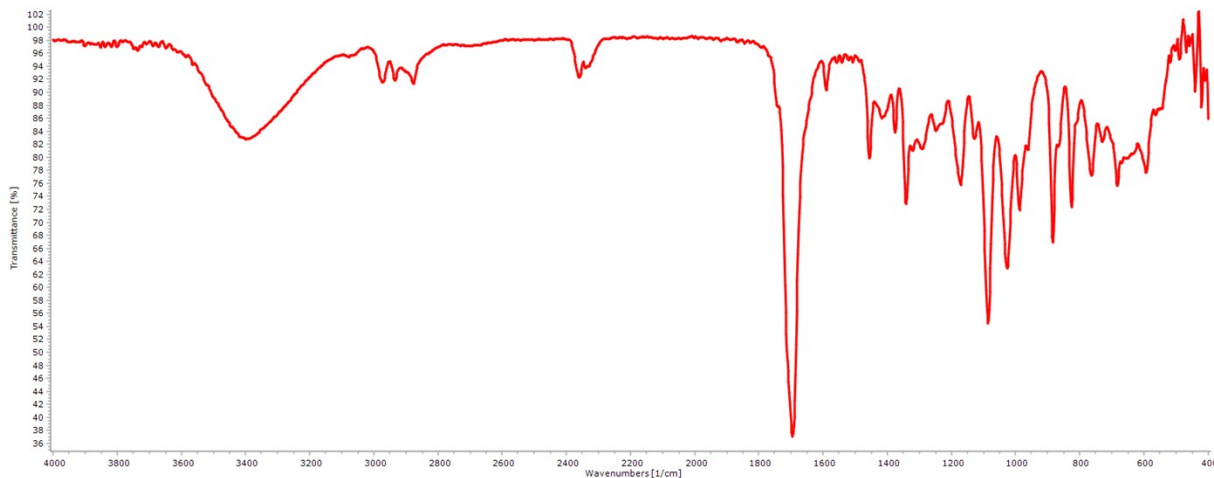


Figure 5.2.3: FTIR spectrum of **1a**.

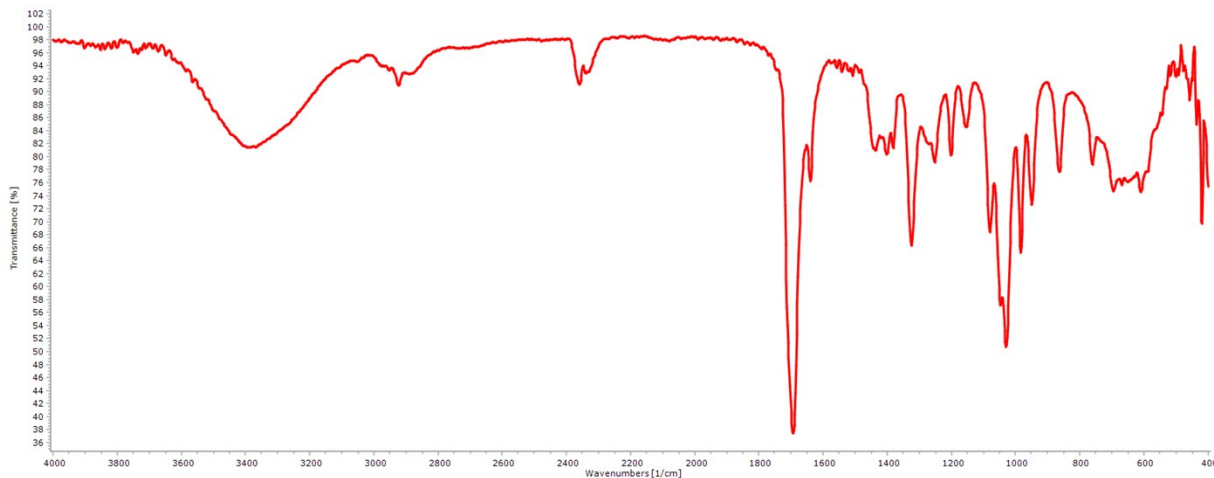


Figure 5.2.4: FTIR spectrum of **1b**.

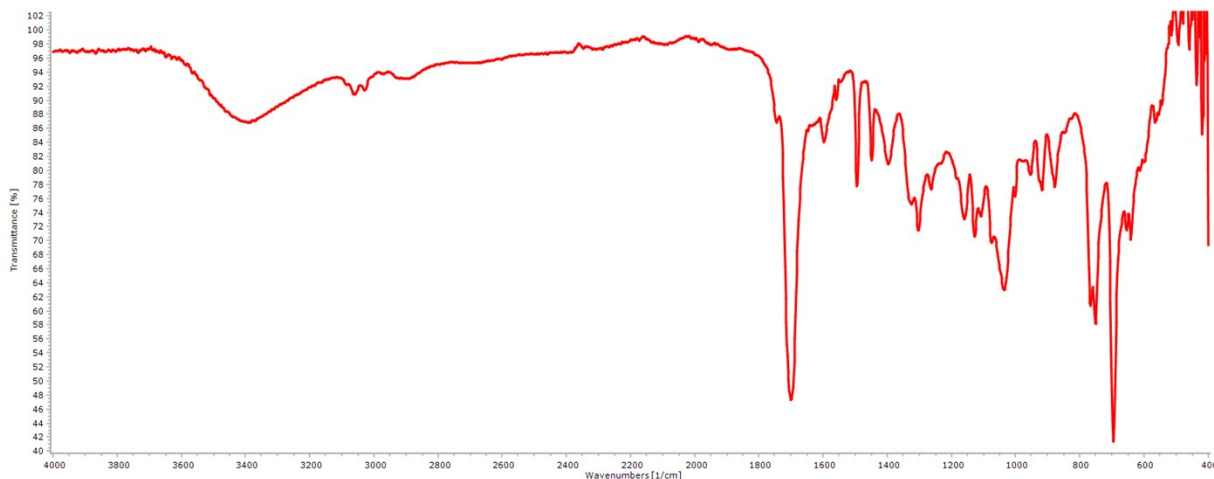


Figure 5.2.5: FTIR spectrum of **1d**.

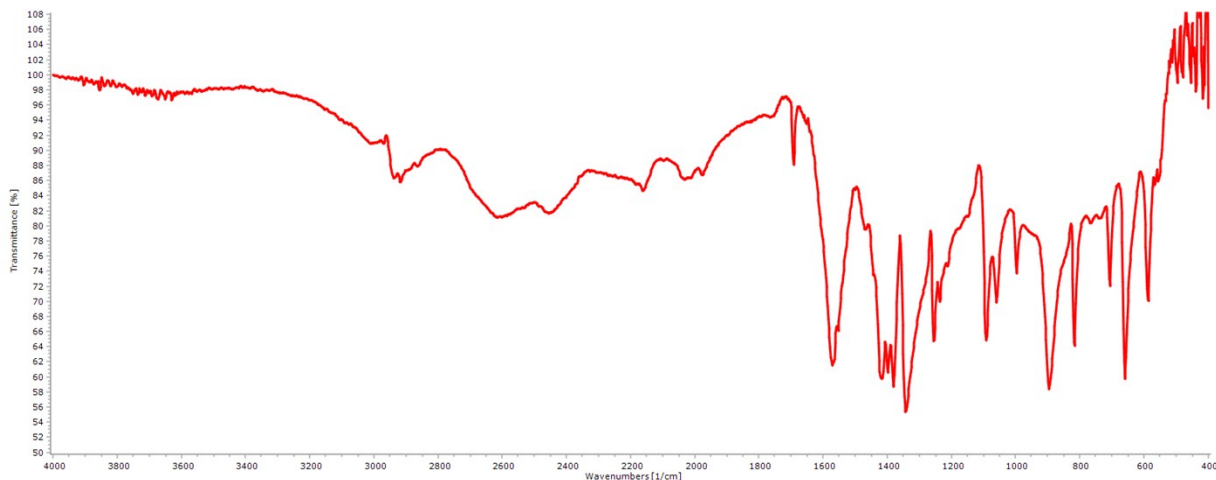


Figure 5.2.6: FTIR spectrum of 3e.

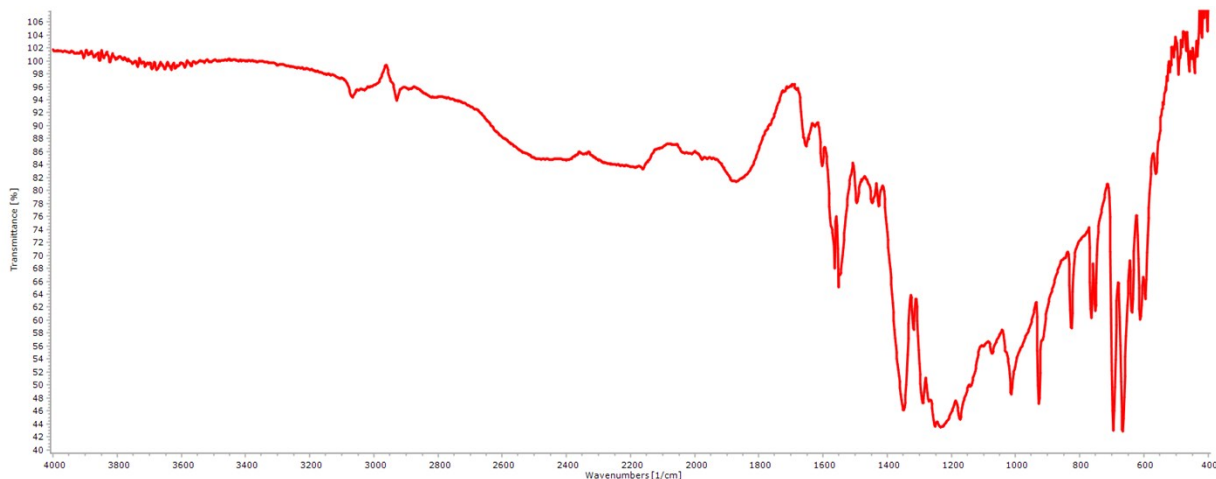


Figure 5.2.7: FTIR spectrum of 3f.

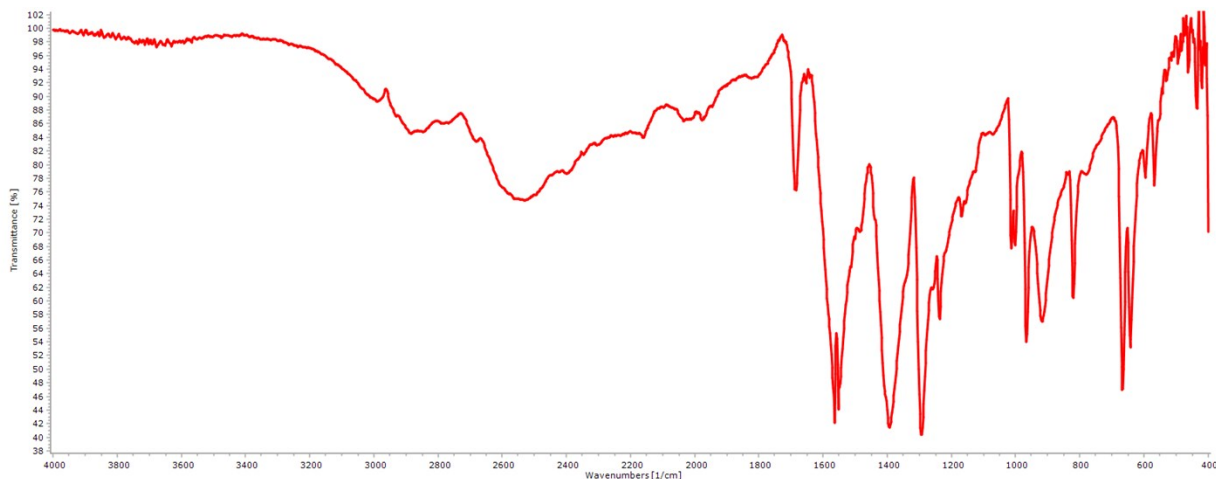


Figure 5.2.8: FTIR spectrum of 3g.

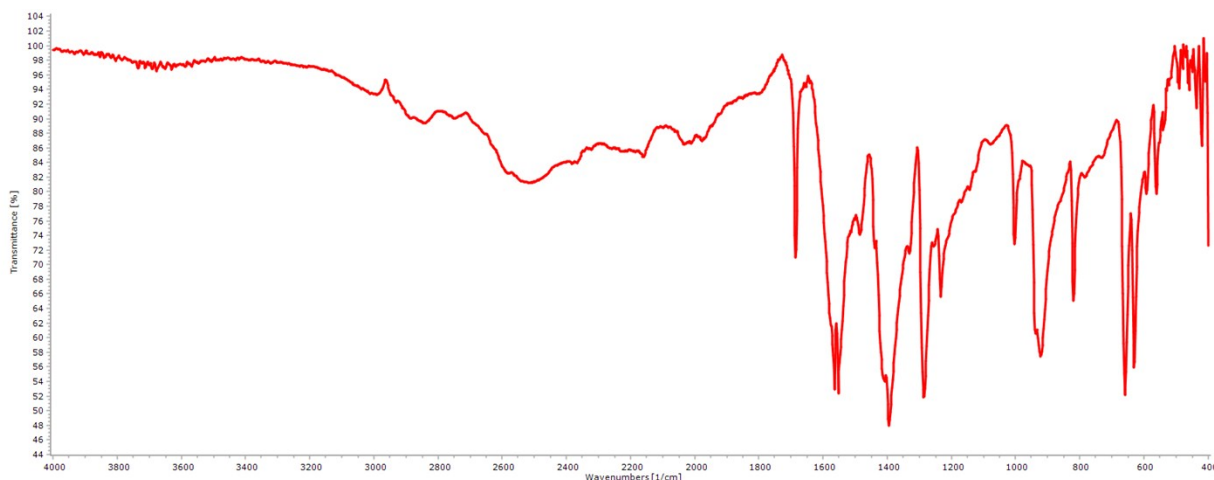


Figure 5.2.9: FTIR spectrum of **3h**.

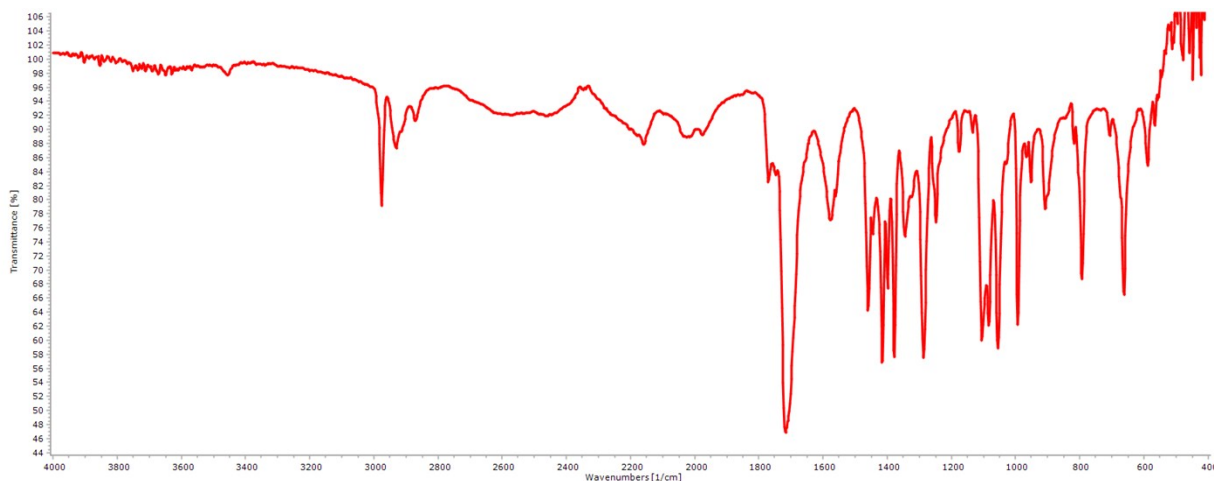


Figure 5.2.10: FTIR spectrum of **3i**.

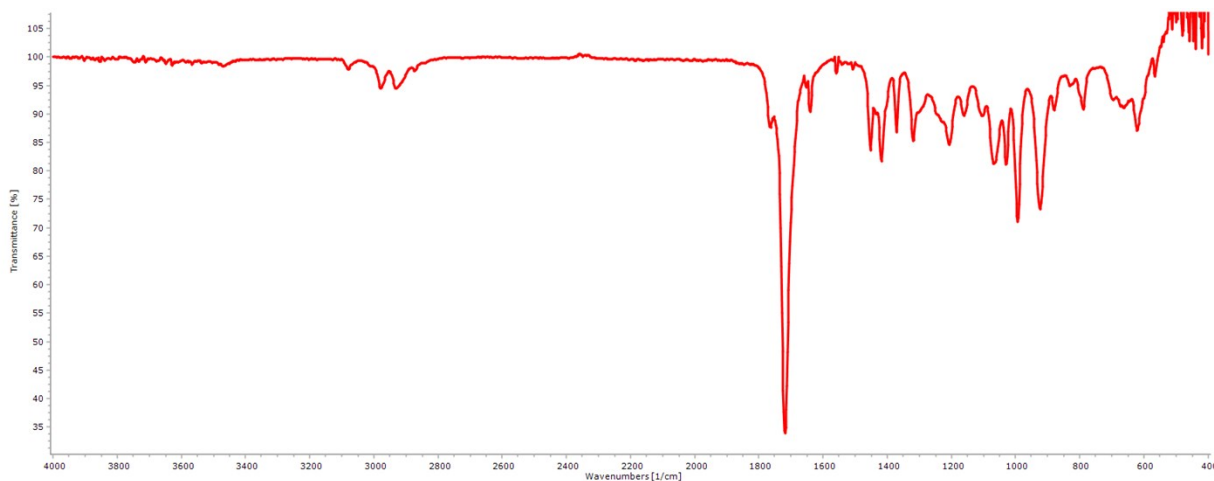


Figure 5.2.11: FTIR spectrum of **3j**.

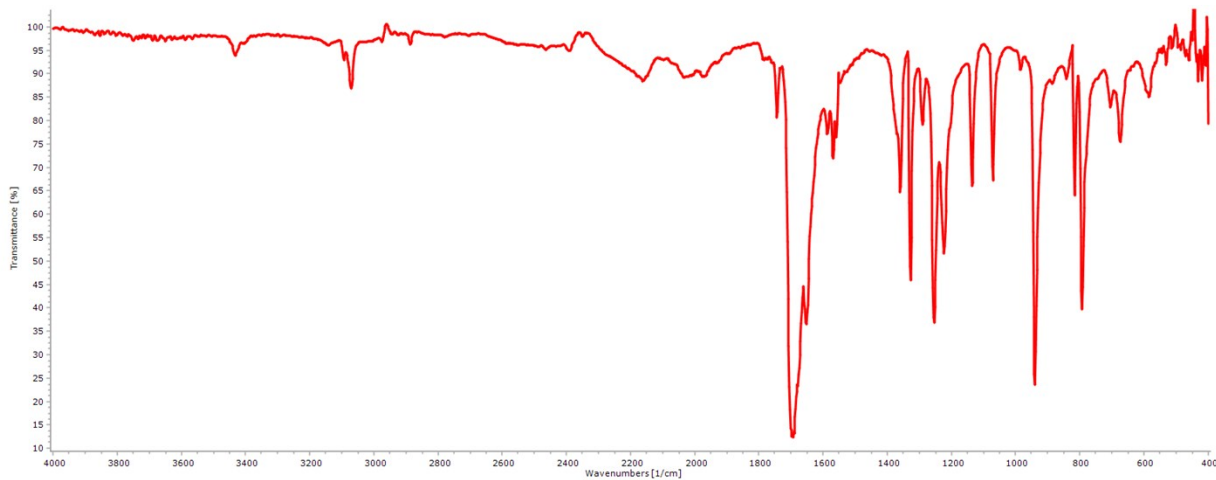


Figure 5.2.12: FTIR spectrum of **3k**.

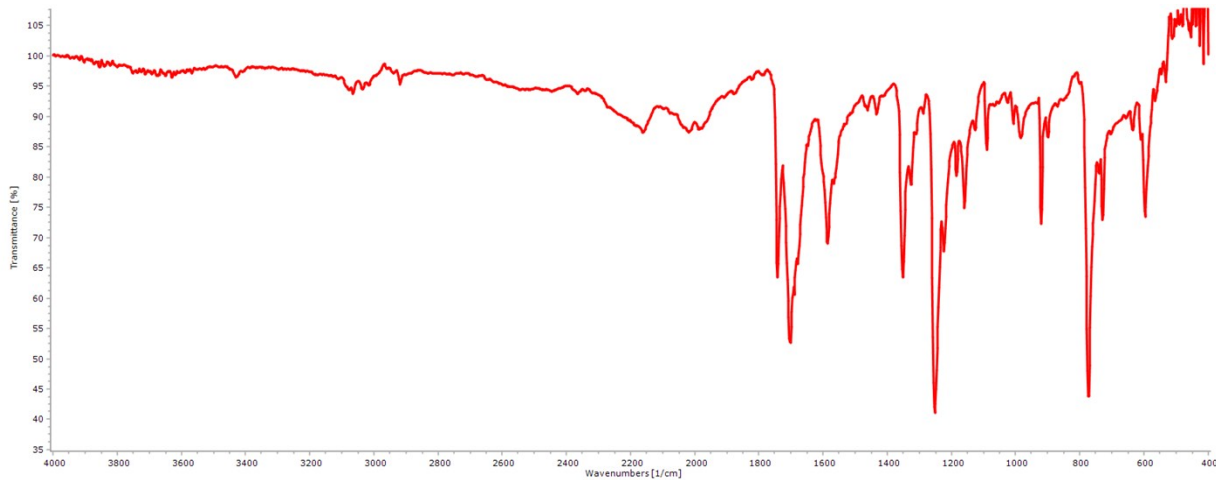


Figure 5.2.13: FTIR spectrum of **3l**.

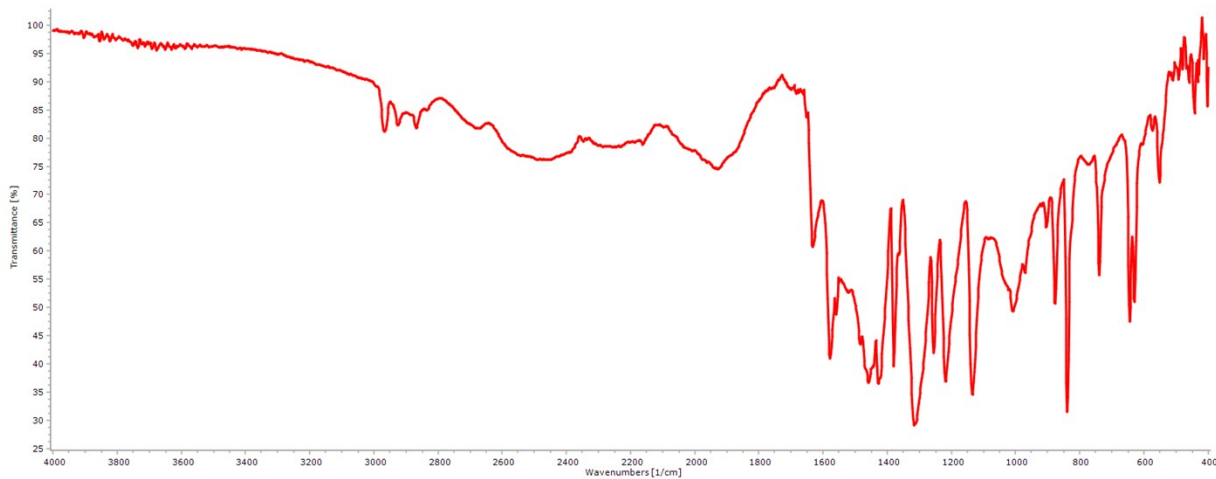


Figure 5.2.14: FTIR spectrum of **3m**.



Figure 5.2.15: FTIR spectrum of **3n**.

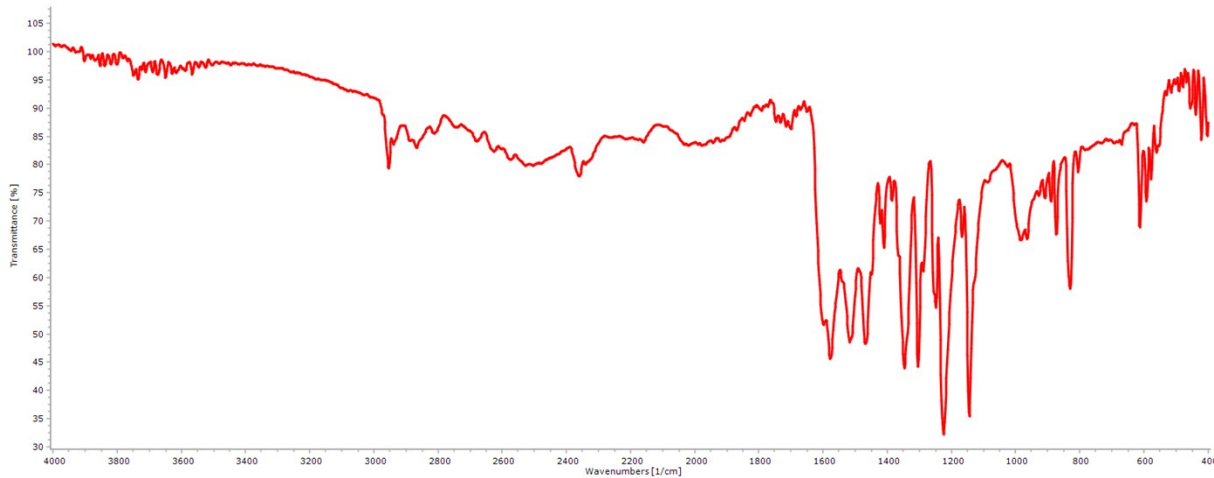


Figure 5.2.16: FTIR spectrum of **3o**.

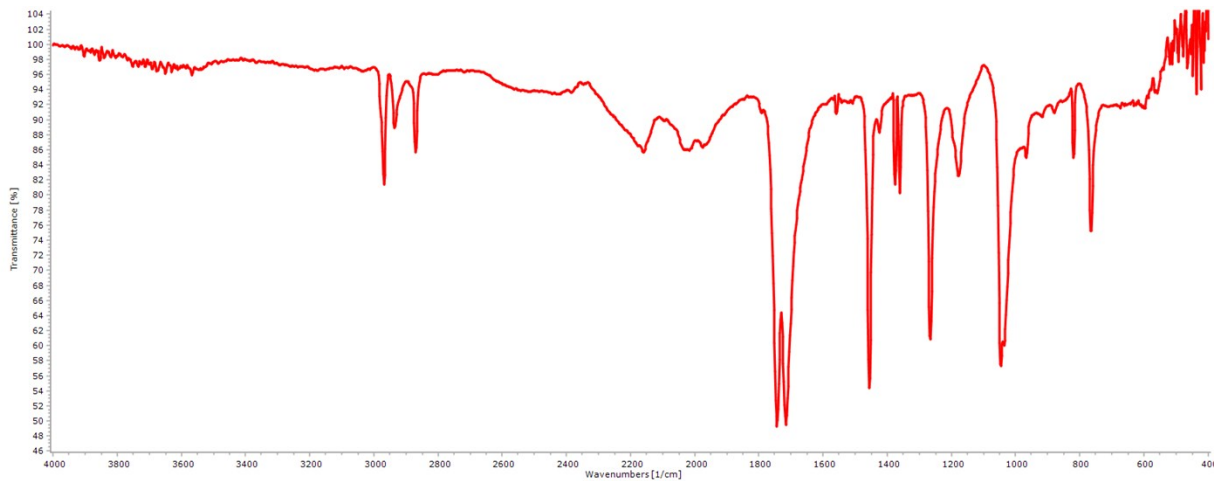


Figure 5.2.17: FTIR spectrum of **3p**.

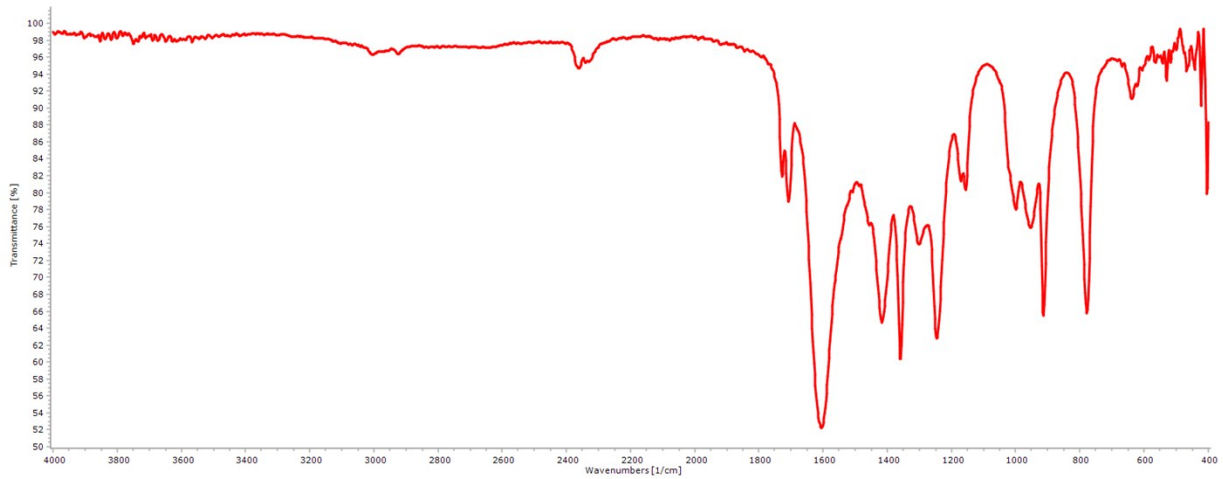


Figure 5.2.18: FTIR spectrum of 3q.

S5.3    *Hydrogenation products:*

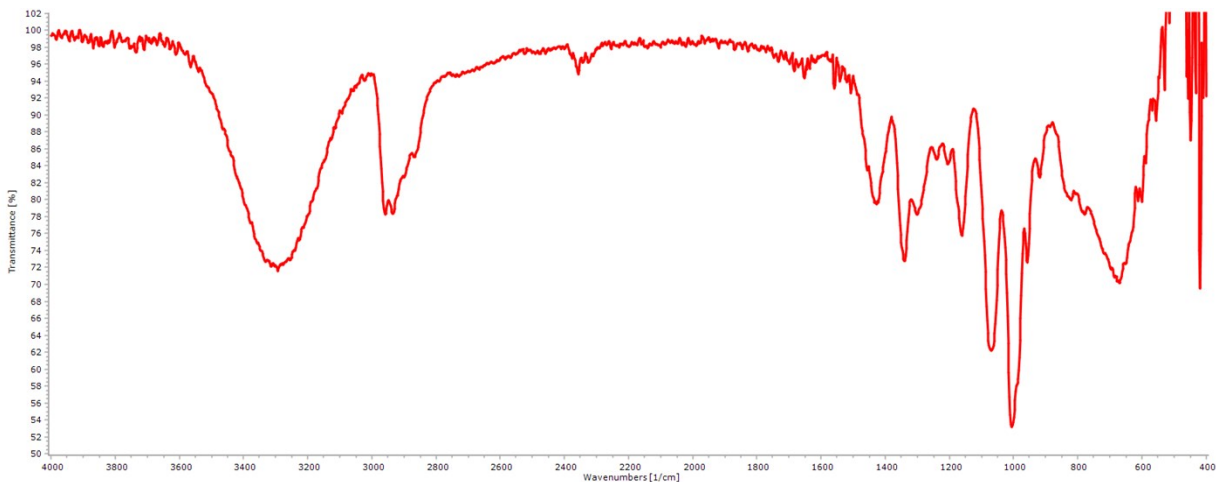


Figure 5.3.1: FTIR spectrum of *cpAdiol*.

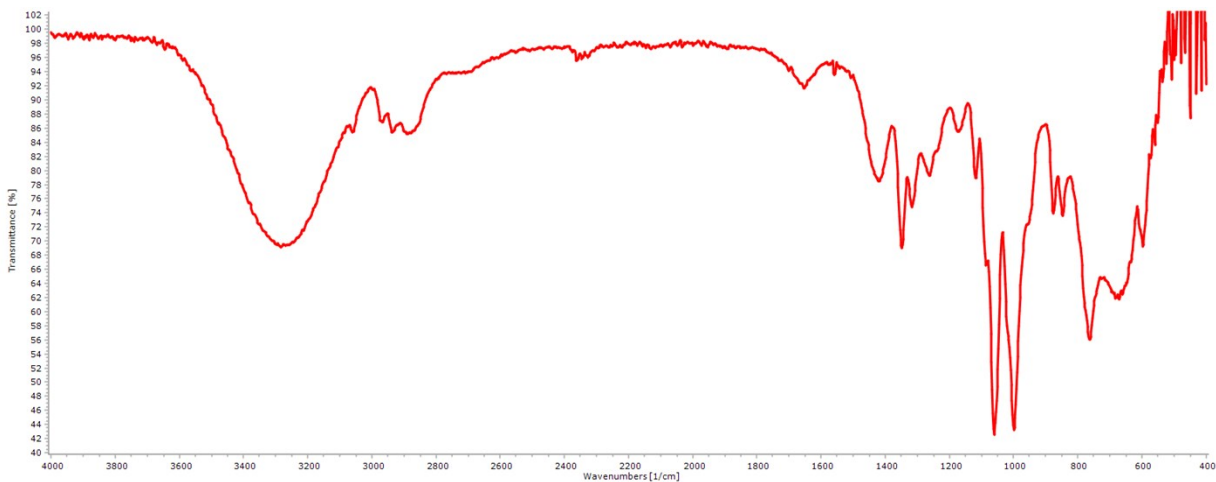


Figure 5.3.2: FTIR spectrum of *cpEdiol*.

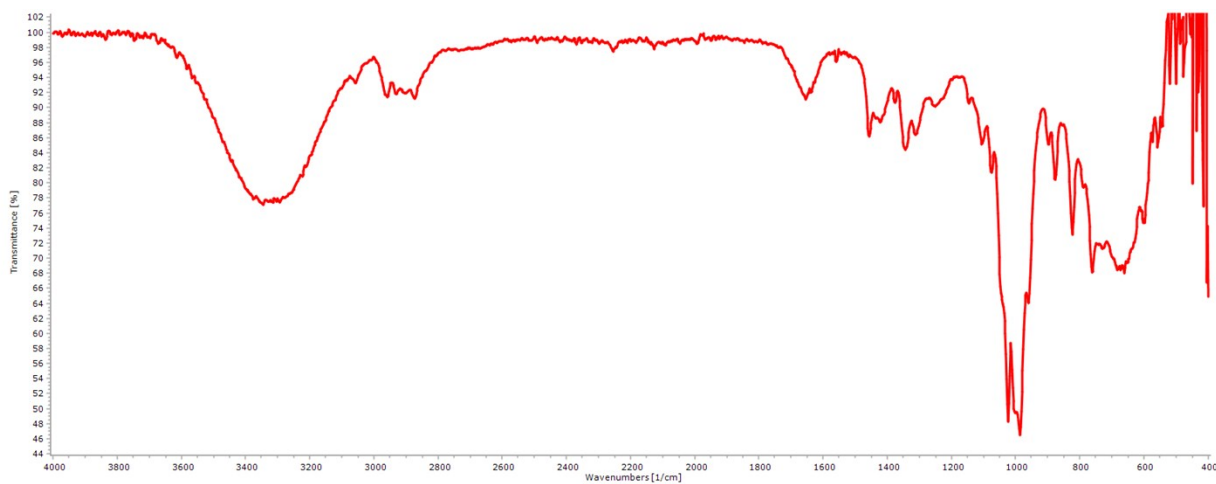


Figure 5.3.3: FTIR spectrum of 2a.

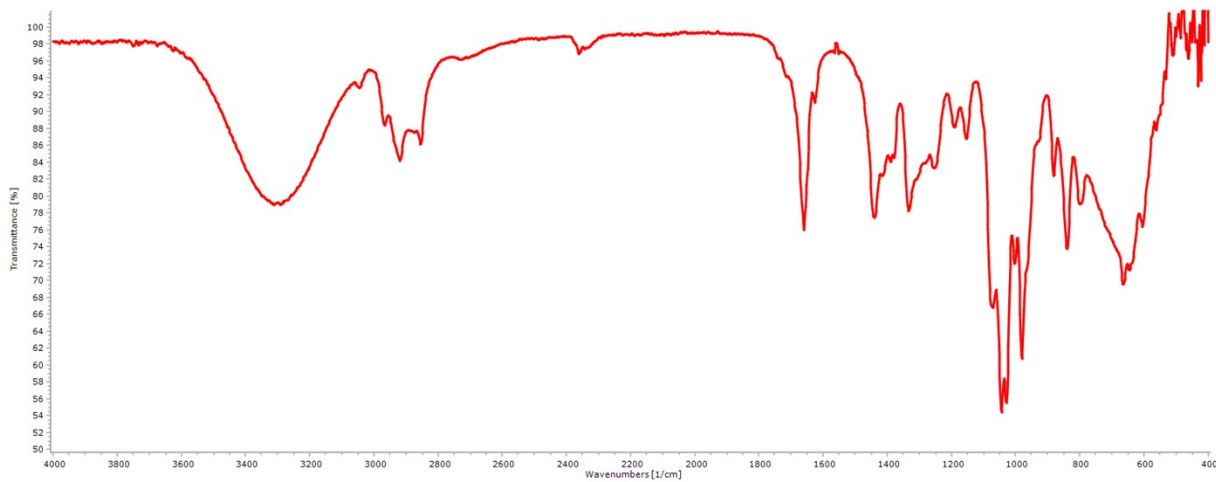


Figure 5.3.4: FTIR spectrum of 2b.

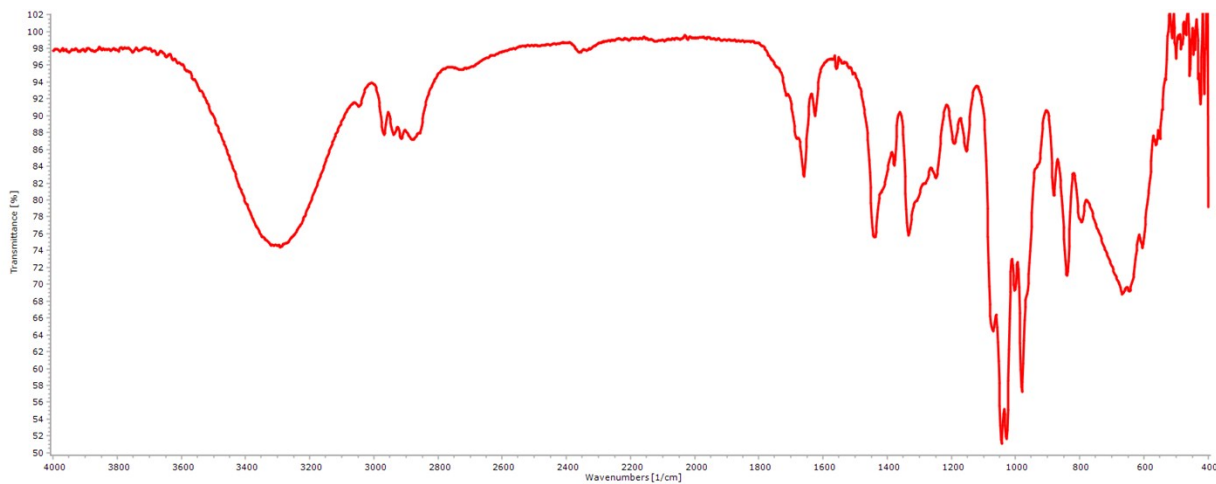


Figure 5.3.5: FTIR spectrum of 2c.

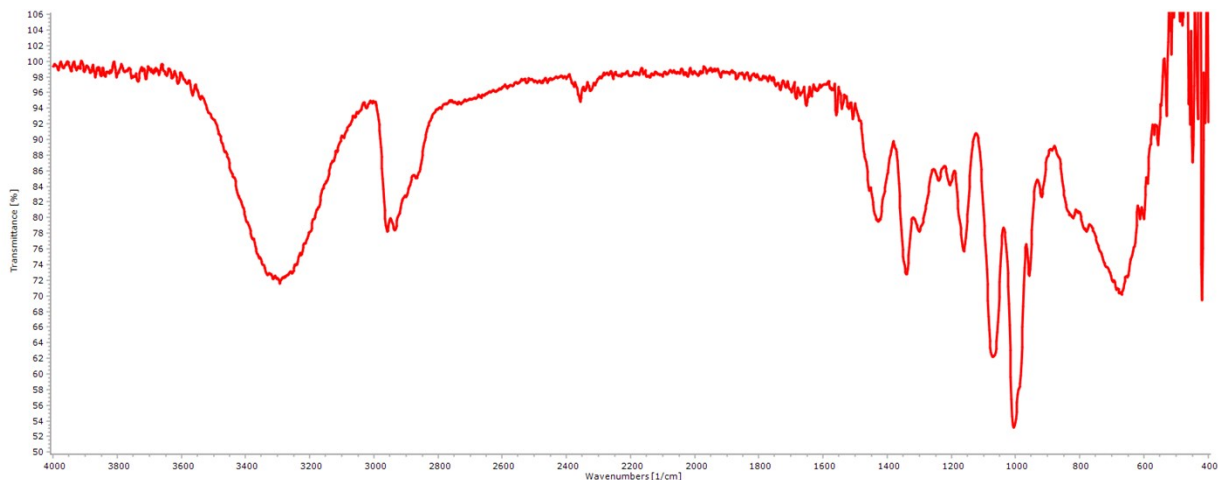


Figure 5.3.6: FTIR spectrum of **5e**

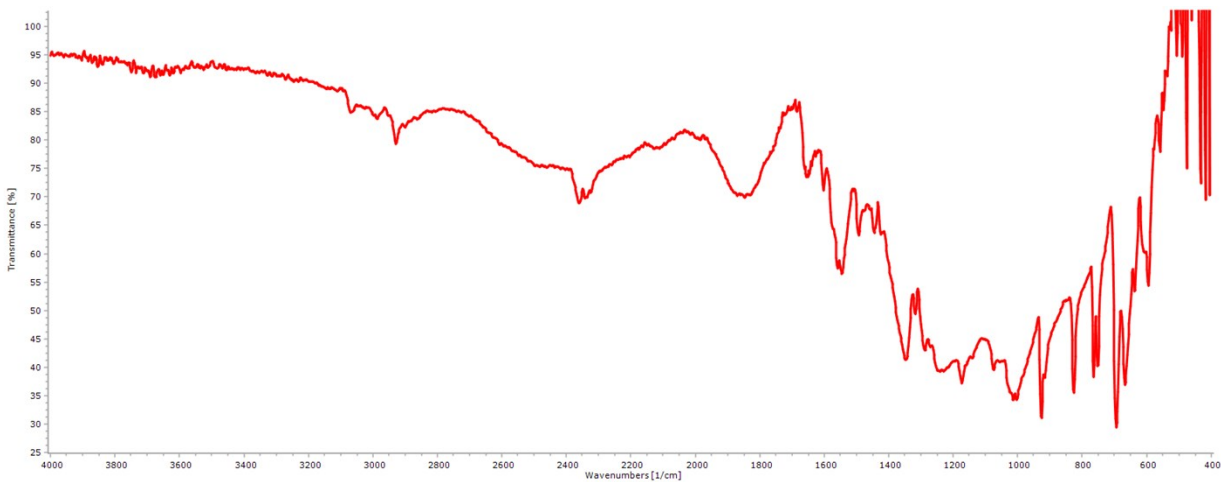


Figure 5.3.7: FTIR spectrum of **4f**.

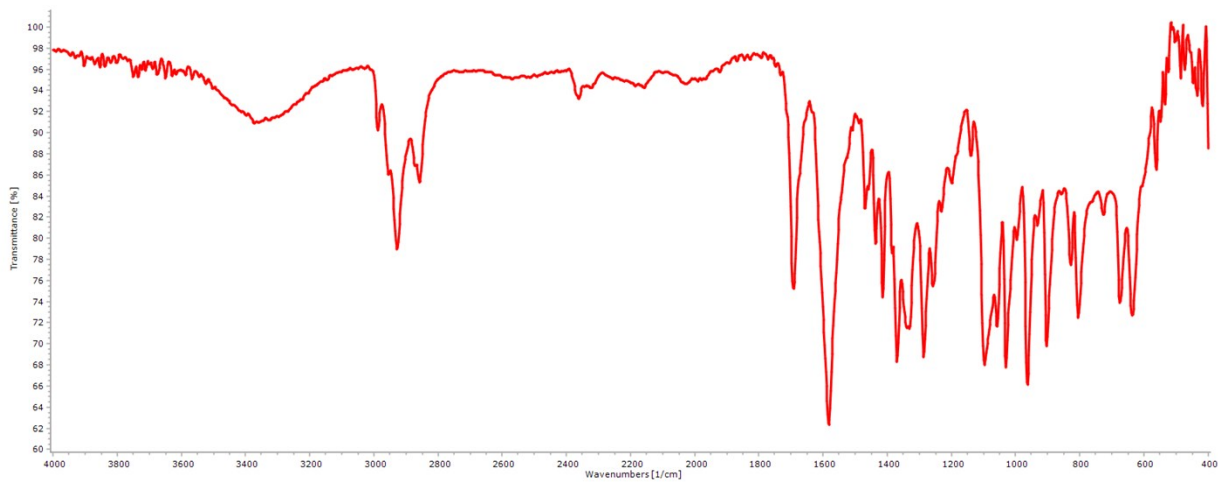


Figure 5.3.8: FTIR spectrum of **4g**.

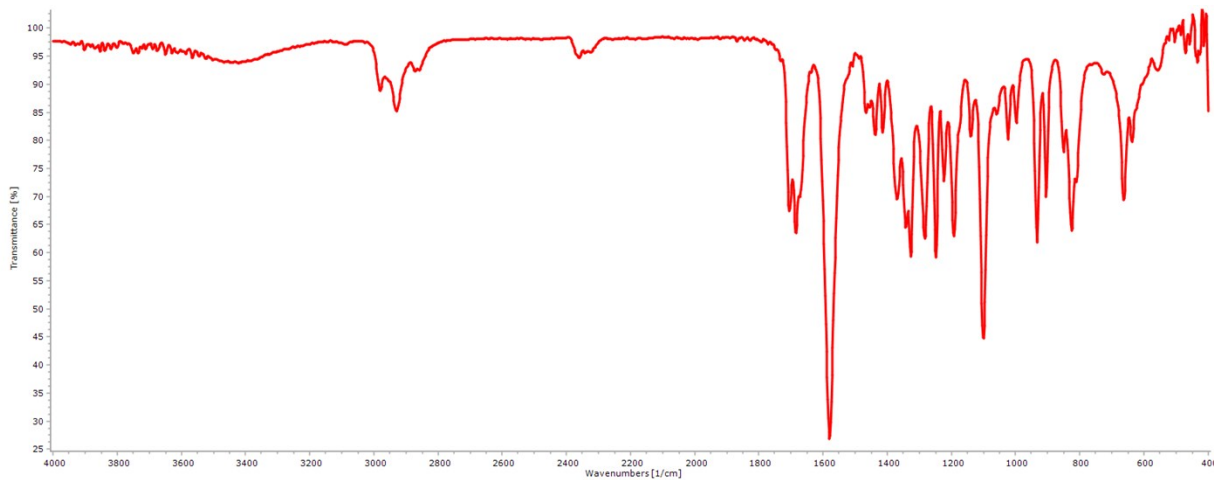


Figure 5.3.9: FTIR spectrum of a mixture of **4h** and **5h**.

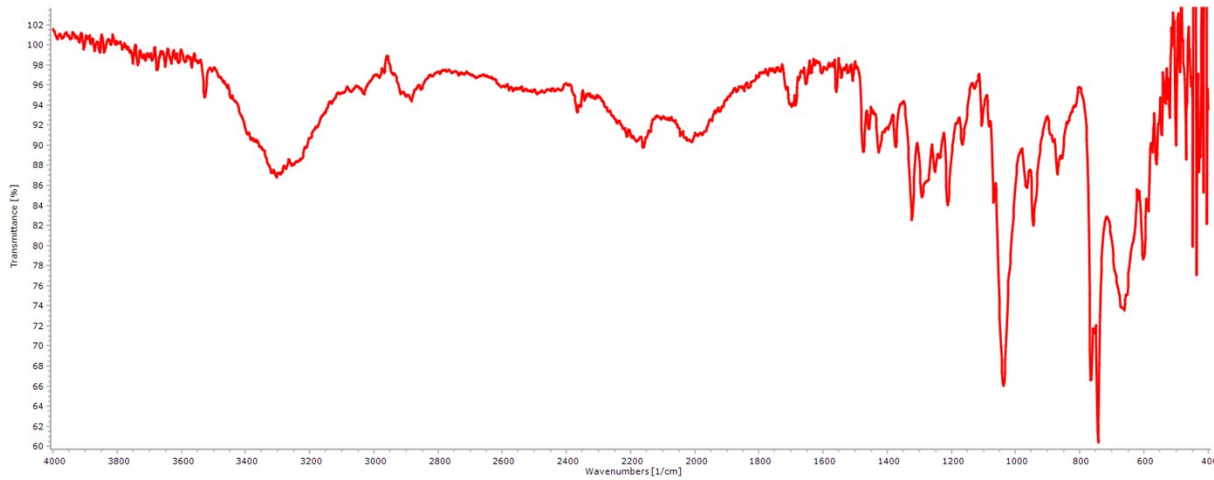


Figure 5.3.10: FTIR spectrum of **5i**.

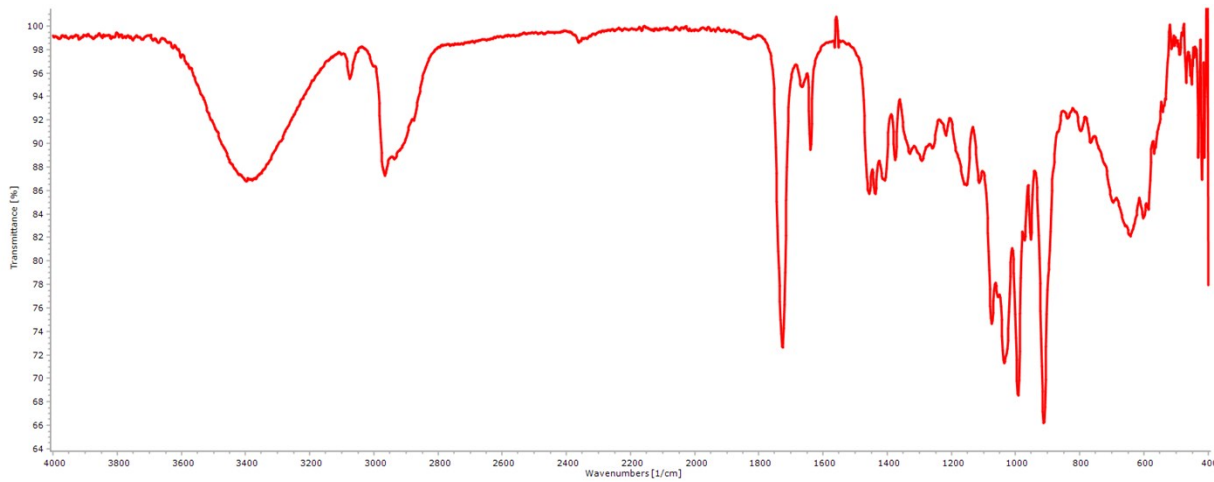


Figure 5.3.11: FTIR spectrum of a mixture of **4j** and **5j**.

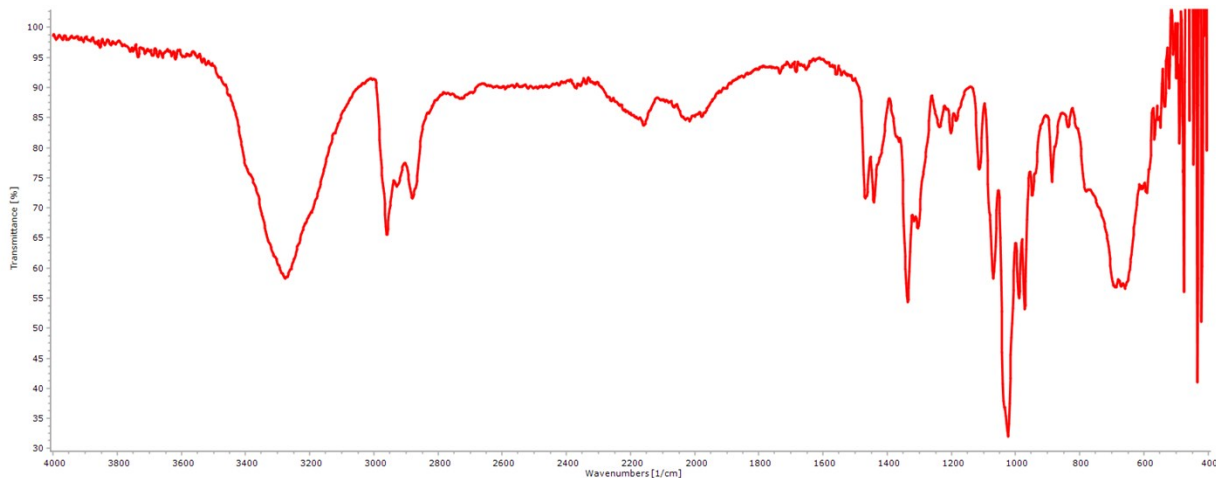


Figure 5.3.12: FTIR spectrum of **5l**.

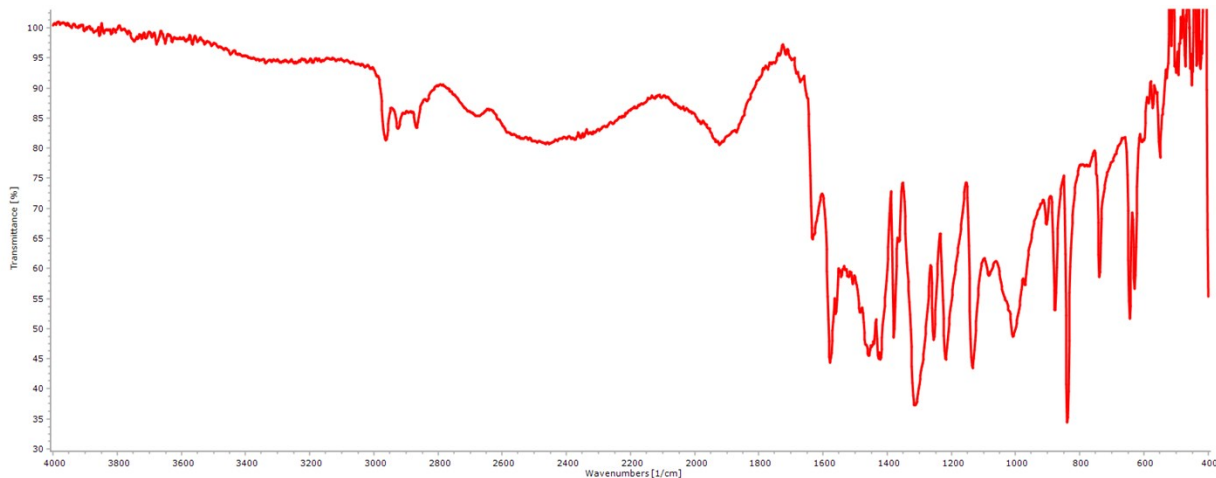


Figure 5.3.13: FTIR spectrum of a mixture of **3m** and **4m**.

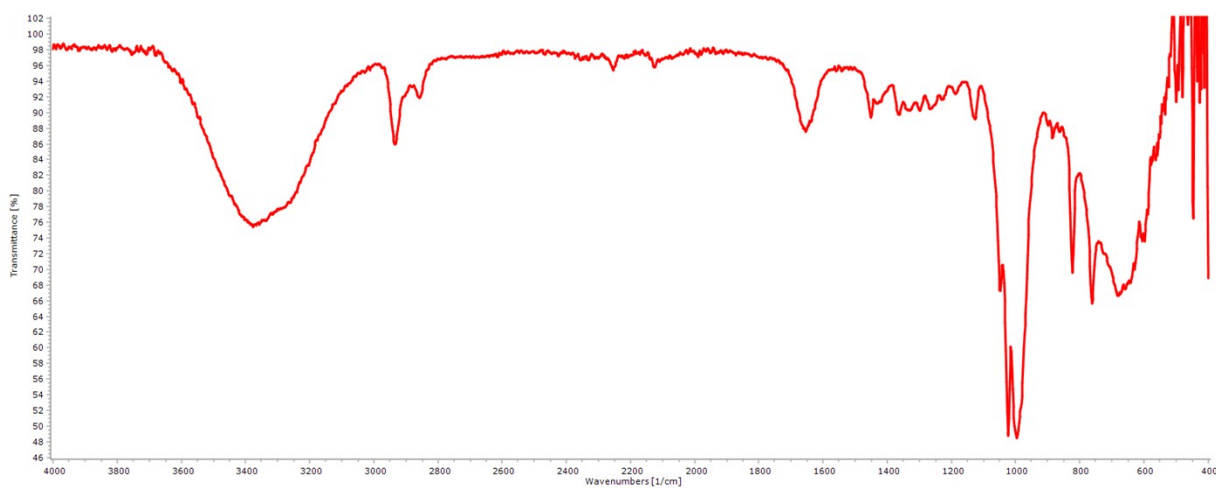


Figure 5.3.14: FTIR spectrum of **5n**.

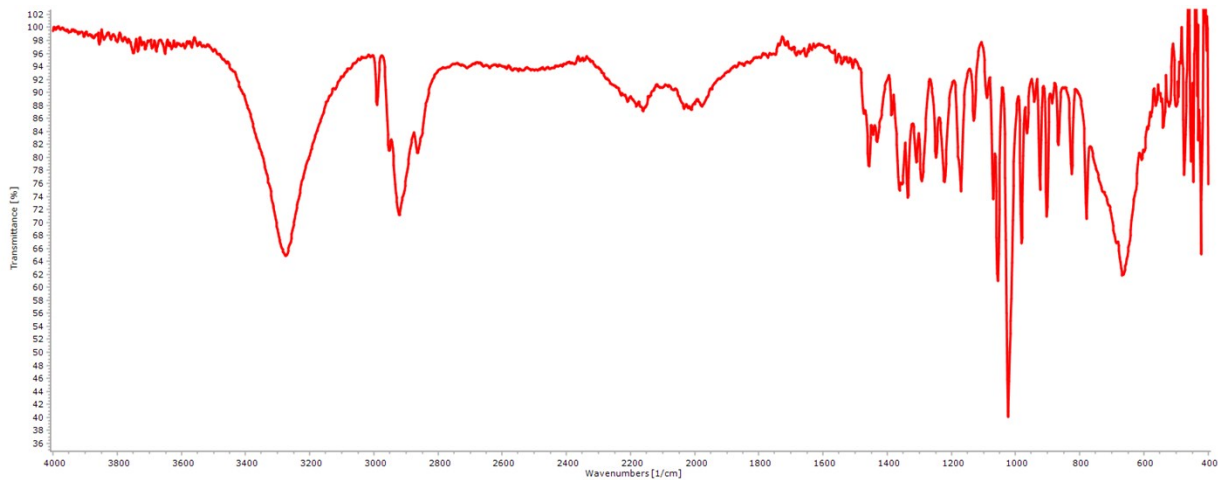


Figure 5.3.15: FTIR spectrum of **5o**.

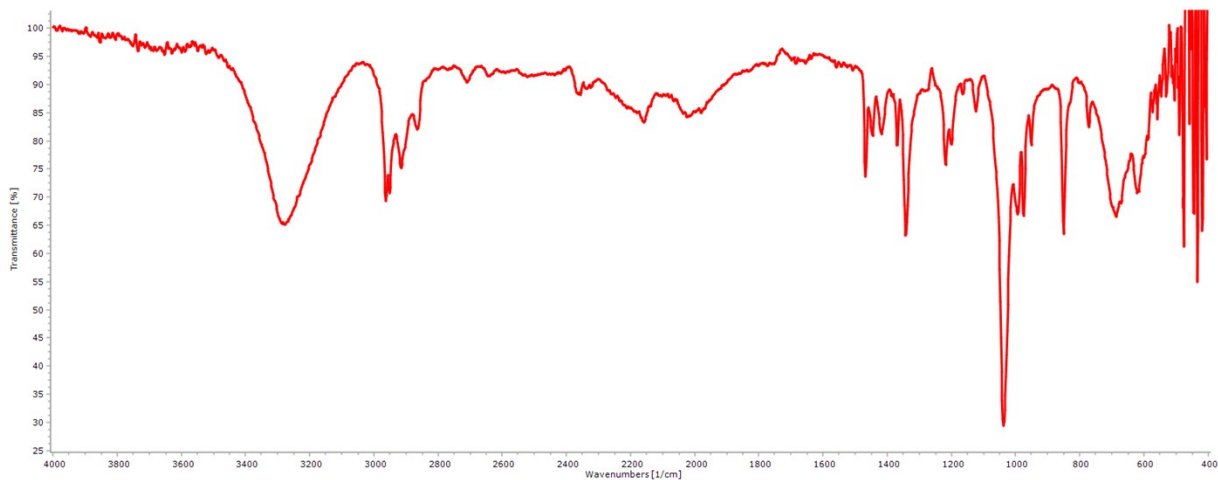


Figure 5.3.16: FTIR spectrum of **5p**.

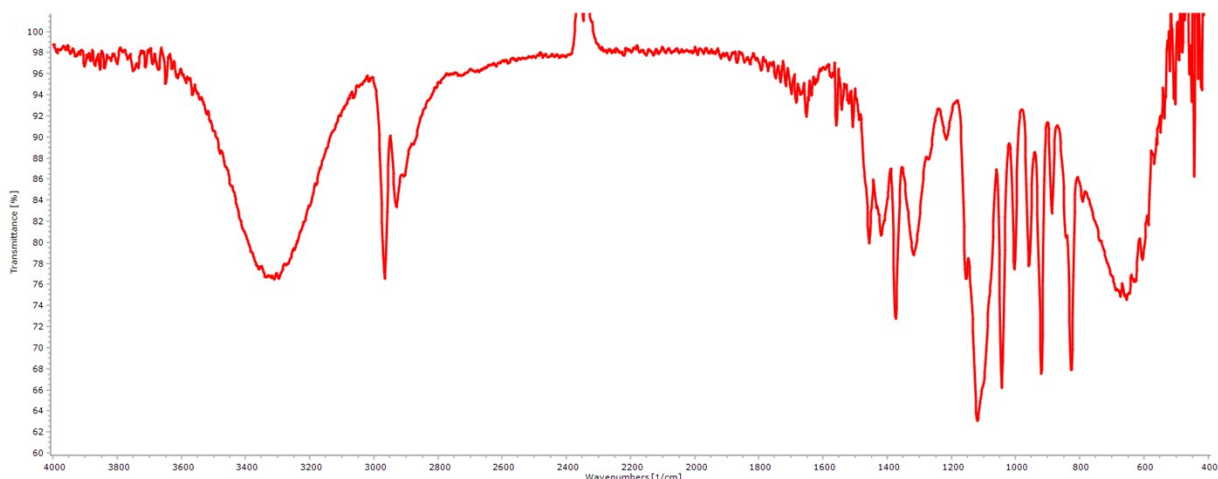


Figure 5.3.17: FTIR spectrum of **5q**.

## S6. HR-MS spectra of some hydrogenation products

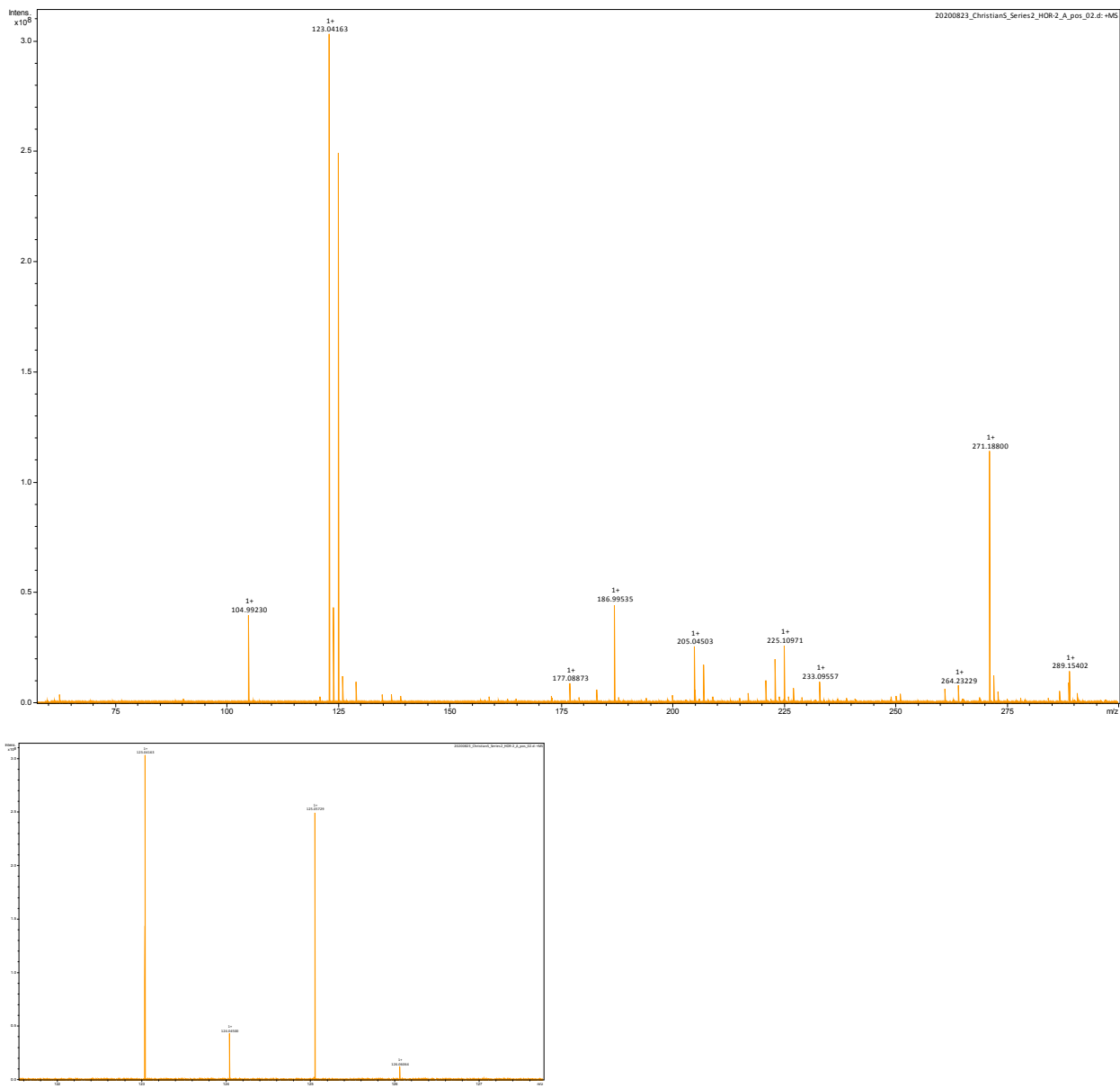
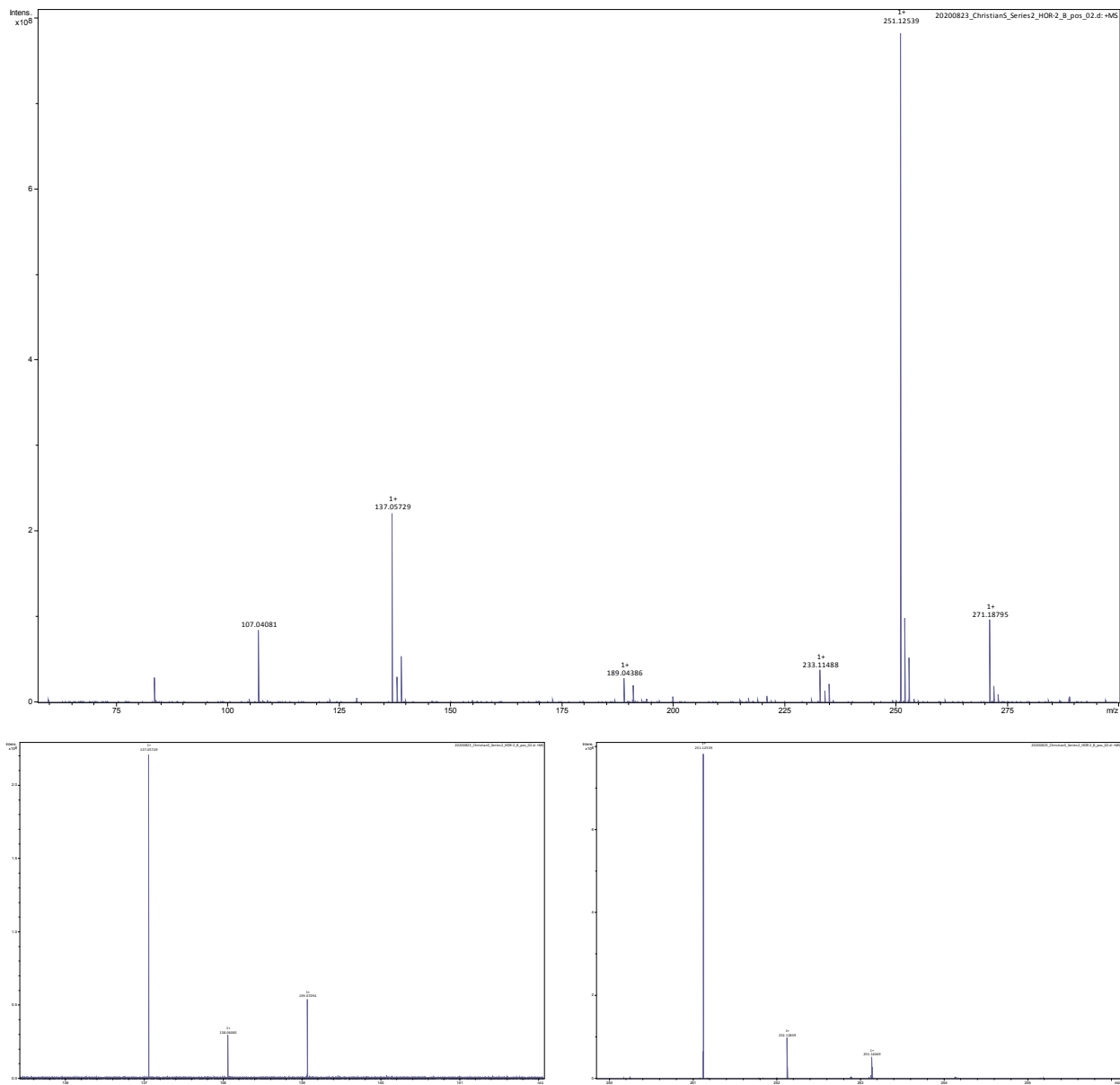
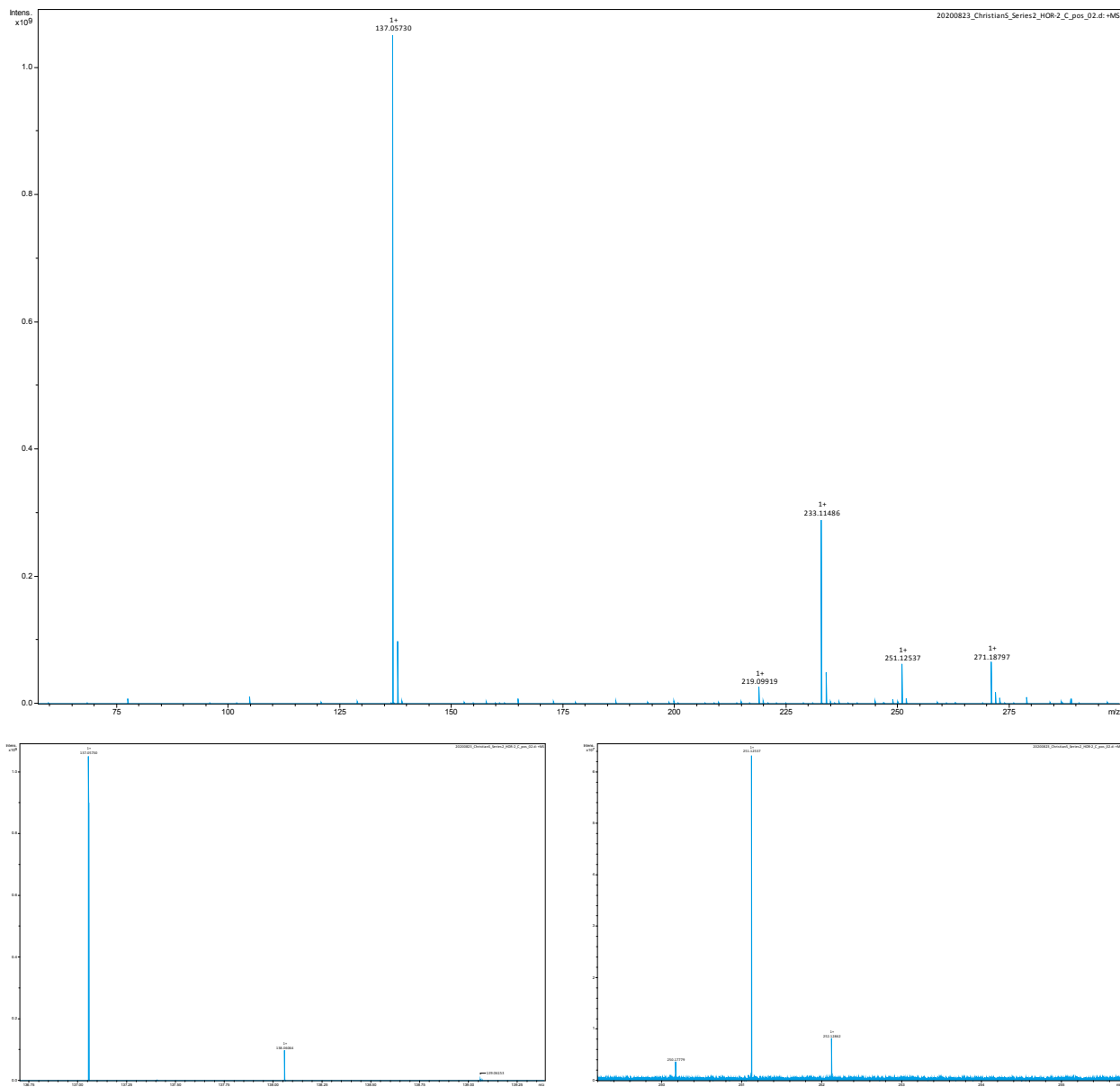


Figure S6.1: HR-MS analysis in ESI+ mode of compound *cpEdiol*; full spectrum (top) and zoom of [*cpEdiol* + Na]<sup>+</sup> (bottom).



*Figure S6.2:* HR-MS analysis in ESI<sup>+</sup> mode of compound **2a**; full spectrum (top), and zoom of  $[2\mathbf{a} + \text{Na}]^+$  (bottom-left), and zoom of  $[2(2\mathbf{a}) + \text{Na}]^+$  (bottom-right).



**Figure S6.3:** HR-MS analysis in ESI<sup>+</sup> mode of compound **2b**; full spectrum (top), and zoom of  $[2b + Na]^+$  (bottom-left), and zoom of  $[2(2b) + Na]^+$  (bottom-right).

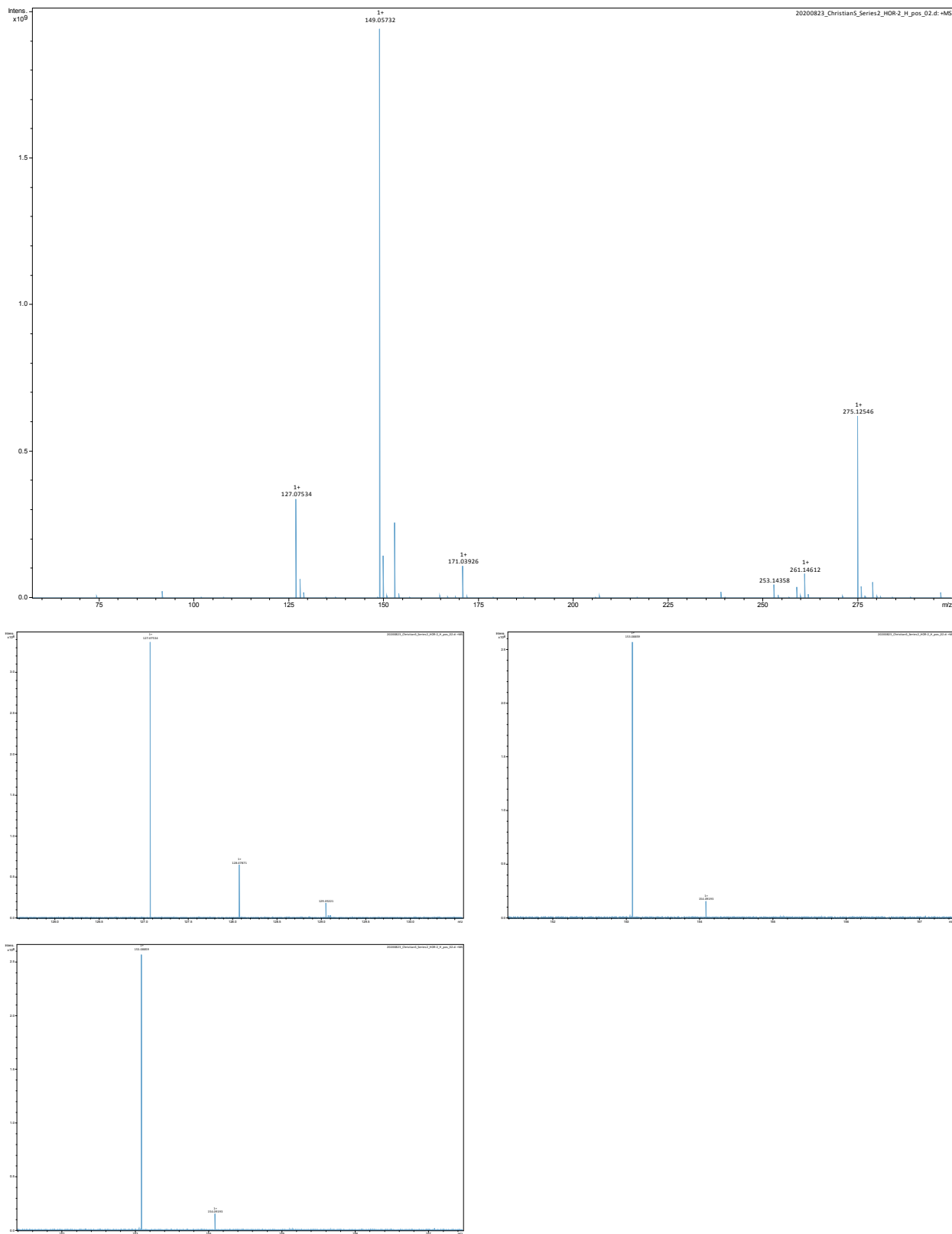


*Figure S6.4:* HR-MS analysis in ESI<sup>+</sup> mode of the mixture of compounds **3m** + **4m**; full spectrum (top), and zoom of  $[3\mathbf{m} + \mathbf{H}]^+$  (middle-left), and zoom of  $[3\mathbf{m} + \mathbf{Na}]^+$  (middle-right), and zoom of  $[4\mathbf{m} + \mathbf{Na}]^+$  (bottom).

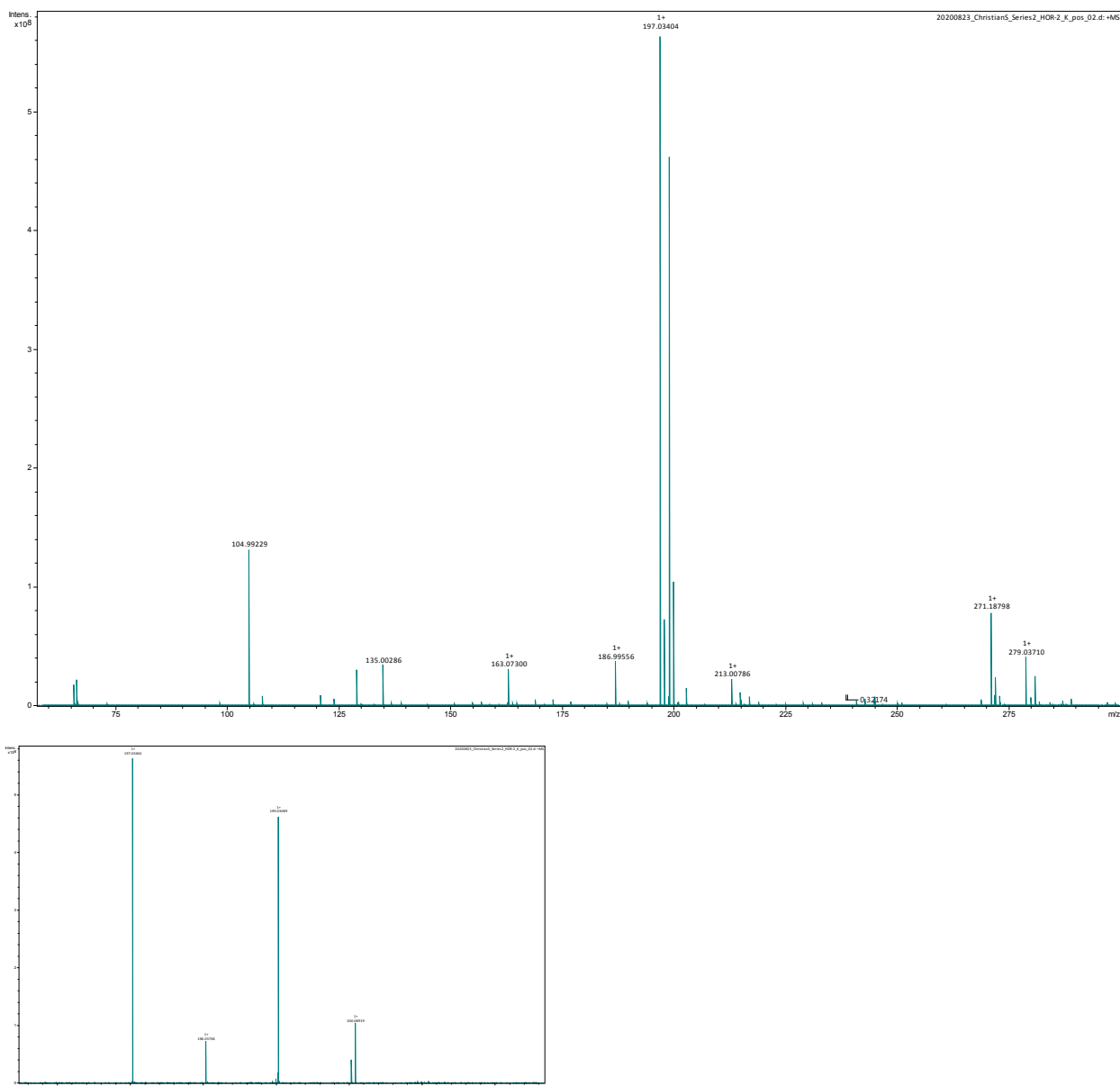
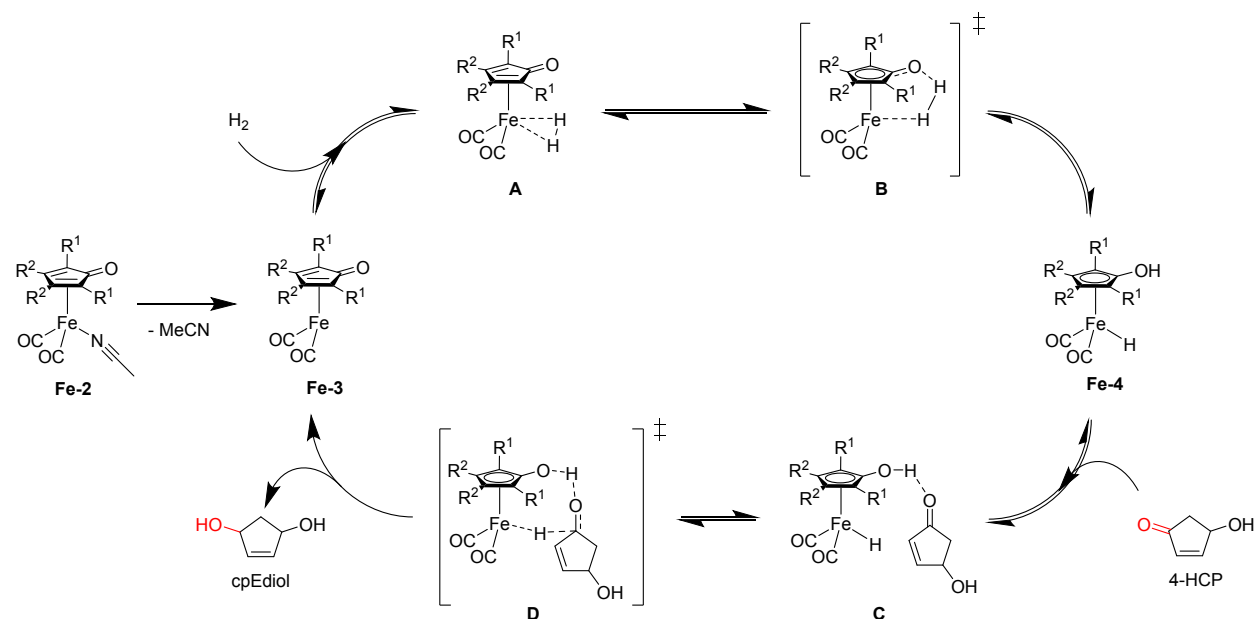


Figure S6.5: HR-MS analysis in ESI<sup>+</sup> mode of the mixture of compound **4h** and **5h**; full spectrum (top), and zoom of  $[4h + K]^{+}$  (bottom).

## S7. Miscellaneous

### S7.1 Mechanism for the Knölker-catalyzed hydrogenation of ketones



## S7.2 DFT calculations for the diastereomers of **5g/5h**

Computational calculations for all chemical geometries were performed using the ORCA software package (version 2.8.0). Optimizations were performed at the level of DFT by means of the hybrid B3LYP functional, and the basis set 6-31G was employed for all elements (*i.e.* C, H, O). All calculated structures were obtained without using redundant coordinates, and with an energy change precision of  $1.0 \cdot 10^{-14}$  au (*i.e.* ExtremeSCF convergence criteria, which is default for geometry optimizations). Vibrational frequency calculations were performed for all stationary points at the same level to identify the minimum energy states (zero imaginary frequencies), and to provide the Gibbs free energy values at 298.15 K and 1.0 atm.

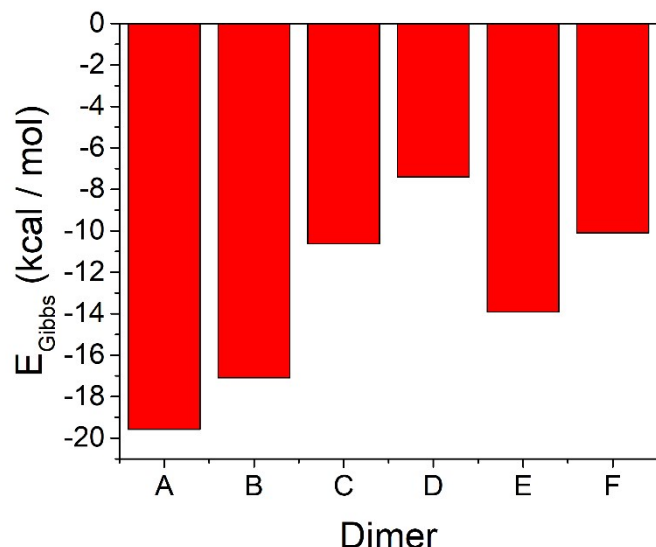


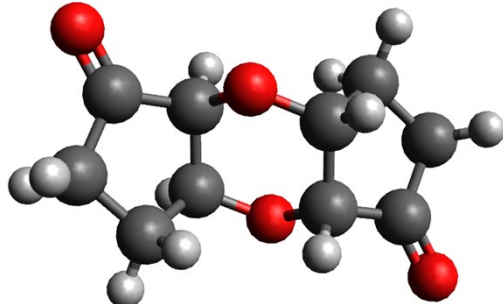
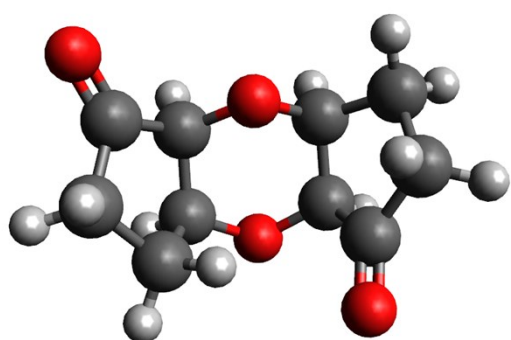
Figure S6.1: The Gibbs Free Energy values for the optimized molecular structures of all six isomers of **3h'**, calculated by DFT. All structures are normalized to the represented values, by subtracting 432050.00 kcal/mol from their calculated energy values.

Dimer A:  $E_{\text{Gibbs}} = -688.546548299 \text{ eH}$

C	-0.937090	-0.077549	0.779729
C	-1.665896	0.895095	-0.145807
C	-0.950017	2.252783	0.038396
H	-2.720952	0.937263	0.162307
H	-1.655976	0.523156	-1.175664
C	-0.348740	2.166846	1.464447
H	-1.615176	3.113755	-0.061196
H	-0.152148	2.370317	-0.698156
C	0.084575	0.701019	1.623559
O	0.704912	3.134429	1.760652
H	-1.121103	2.397878	2.205957
O	1.381189	0.482756	0.966658
H	0.131073	0.347959	2.660035
O	-1.128298	-1.291876	0.859129
C	2.050614	2.787953	1.356941
C	2.440707	1.317900	1.553764
C	2.408667	3.054567	-0.121822
H	2.693631	3.432538	1.971890
C	3.451804	2.028235	-0.560463
C	3.684646	1.122785	0.674330
H	4.357598	2.527202	-0.921193
H	3.040321	1.463541	-1.405852
H	4.575504	1.436767	1.232235
H	3.802260	0.067707	0.417027
H	2.583273	1.039211	2.604489
O	1.925493	3.943864	-0.825351

Dimer B:  $E_{\text{Gibbs}} = -688.542585695 \text{ eH}$

C	-1.044470	-0.046313	1.386764
C	-2.107264	0.746573	0.624284
C	-1.382485	2.006637	0.096022
H	-2.917693	0.996637	1.322928
H	-2.550845	0.128558	-0.163234
C	-0.181481	2.181208	1.059012
H	-2.015039	2.897496	0.076090
H	-1.019927	1.830868	-0.921999
C	0.268235	0.750196	1.388008
O	0.898303	3.029313	0.563792
H	-0.501259	2.686259	1.976458
O	1.037063	0.183026	0.269678
H	0.820197	0.648091	2.326411
O	-1.206035	-1.139563	1.930081
C	1.667131	2.462143	-0.554538
C	2.116847	1.031130	-0.225542
C	2.979835	3.258652	-0.553295
H	1.115168	2.564247	-1.492941
C	4.042630	2.465767	0.209186
C	3.317850	1.205703	0.737449
H	4.486210	3.083782	0.996704
H	4.853059	2.215702	-0.489458
H	2.955291	1.381473	1.755469
H	3.950405	0.314845	0.757382
H	2.436625	0.526079	-1.142987
O	3.141400	4.351901	-1.096613

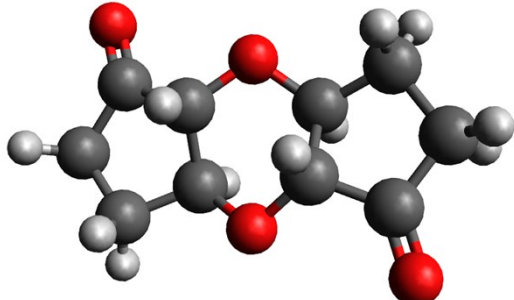
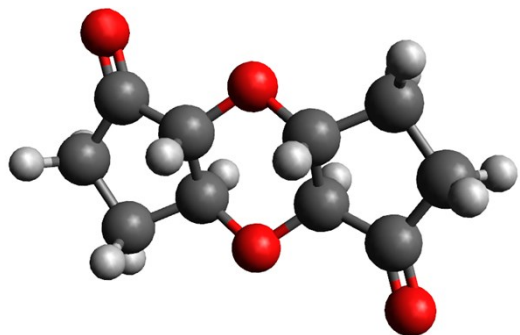


Dimer C:  $E_{\text{Gibbs}} = -688.532276330 \text{ eH}$

C	-1.209972	-0.224613	0.338084
C	-2.406522	0.747590	0.289691
C	-1.809779	2.150048	-0.052693
H	-2.893151	0.739268	1.273322
H	-3.153127	0.403325	-0.434129
C	-0.357568	1.996682	0.402931
H	-2.328303	2.969888	0.448129
H	-1.836192	2.341170	-1.131312
C	0.005868	0.583464	-0.082726
O	0.589581	2.985836	-0.111063
H	-0.304298	2.009653	1.504508
O	1.311266	0.143777	0.367032
H	-0.002203	0.613501	-1.190225
O	-1.250297	-1.411349	0.660646
C	1.895037	2.546172	0.338802
C	2.258409	1.132952	-0.146915
C	3.110810	3.354036	-0.082798
H	1.903021	2.516437	1.446257
C	4.307436	2.381989	-0.033320
C	3.710647	0.979425	0.308593
H	5.053320	2.726338	0.691223
H	4.795123	2.390455	-1.016429
H	3.737025	0.787743	1.387109
H	4.229090	0.159788	-0.192646
H	2.205090	1.120003	-1.248484
O	3.150697	4.540182	-0.407495

Dimer D:  $E_{\text{Gibbs}} = -688.527148485 \text{ eH}$

C	-1.705150	0.100873	0.587428
C	-2.817495	1.065163	0.134471
C	-2.088488	2.266449	-0.540563
H	-3.384826	1.373571	1.021853
H	-3.525309	0.555042	-0.528235
C	-0.689446	2.198667	0.081857
H	-2.583133	3.224152	-0.363200
H	-2.005183	2.124989	-1.624279
C	-0.389791	0.689731	0.089561
O	0.341972	2.955819	-0.629607
H	-0.733870	2.557239	1.121100
O	0.812537	0.328751	0.820955
H	-0.284663	0.366317	-0.962820
O	-1.860489	-0.937167	1.229118
C	1.624516	2.291376	-0.475118
C	1.746716	1.456250	0.811351
C	2.859711	3.181898	-0.401087
H	1.785166	1.609513	-1.330852
C	3.927451	2.388651	0.375790
C	3.230053	1.070300	0.828913
H	4.251762	2.997807	1.229104
H	4.813750	2.222498	-0.245839
H	3.563139	0.722328	1.808723
H	3.398774	0.262495	0.107820
H	1.526507	2.101430	1.674786
O	2.989589	4.314787	-0.862532

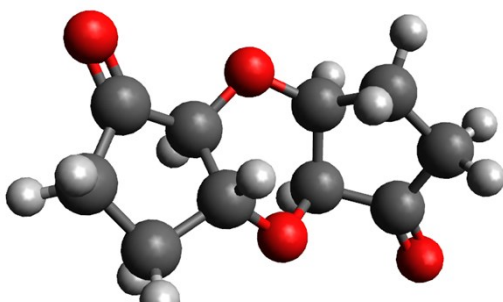
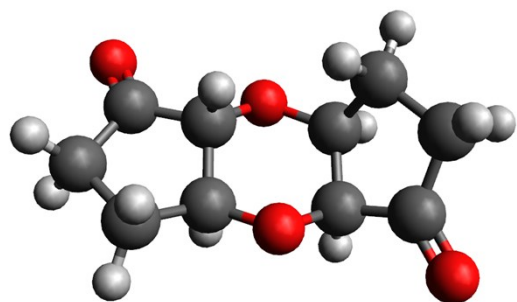


Dimer E:  $E_{\text{Gibbs}} = -688.537539935 \text{ eH}$

C	-1.657522	0.205612	0.767749
C	-2.635886	0.943152	-0.170024
C	-1.831581	2.131824	-0.785141
H	-3.487607	1.290553	0.428151
H	-3.039203	0.254356	-0.920338
C	-0.707583	2.319650	0.236823
H	-2.435134	3.031255	-0.924879
H	-1.399816	1.860778	-1.755335
C	-0.312197	0.892168	0.594003
O	0.465151	3.034635	-0.238337
H	-1.088701	2.820921	1.141886
O	0.600471	0.850130	1.704921
H	0.153324	0.448721	-0.305975
O	-1.931859	-0.742748	1.501894
C	1.457566	3.100378	0.857515
C	1.770661	1.706259	1.461993
C	2.779903	3.509072	0.190498
H	1.121726	3.835443	1.597899
C	3.684637	2.284868	0.056876
C	2.827891	1.084215	0.514718
H	4.562530	2.433614	0.701543
H	4.060656	2.200678	-0.967775
H	3.402970	0.304446	1.019761
H	2.333542	0.625061	-0.348058
H	2.197995	1.846339	2.460137
O	3.054464	4.654548	-0.168516

Dimer F:  $E_{\text{Gibbs}} = -688.531453980 \text{ eH}$

C	-1.976602	0.521049	1.131031
C	-2.638556	1.034108	-0.148559
C	-1.734152	2.183204	-0.647025
H	-3.650447	1.380135	0.104157
H	-2.758478	0.219102	-0.870180
C	-0.992703	2.666285	0.622285
H	-2.284955	2.998402	-1.122821
H	-1.000547	1.814715	-1.372014
C	-0.738916	1.382126	1.448079
O	0.192984	3.476816	0.296476
H	-1.650474	3.319533	1.209662
O	0.417356	0.576290	0.983031
H	-0.630310	1.554322	2.521784
O	-2.358755	-0.428312	1.815350
C	1.410816	2.802289	0.653302
C	1.410322	1.335252	0.239633
C	2.692230	3.324710	0.013812
H	1.565830	2.846363	1.748921
C	3.666672	2.132916	-0.044364
C	2.863768	0.901809	0.476118
H	4.567989	2.344768	0.540748
H	3.990372	2.005067	-1.084644
H	3.022022	0.746673	1.549197
H	3.117856	-0.026473	-0.039715
H	1.176951	1.274459	-0.834393
O	2.914278	4.466318	-0.386582



S7.3 Schematic representations of substrates aligning to Knölker's catalyst.

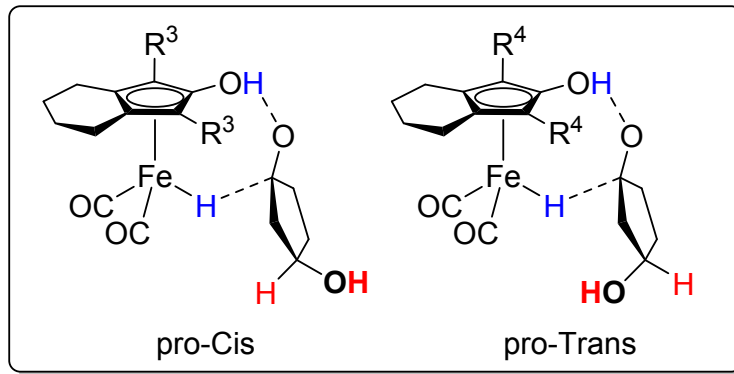


Figure S7.3.1: Binding modes of 3-HCP to Fe-4a.

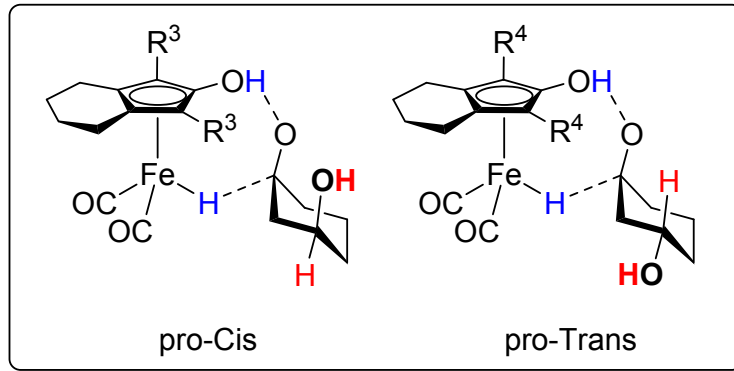


Figure S7.3.2: Binding modes of 4n to Fe-4a.

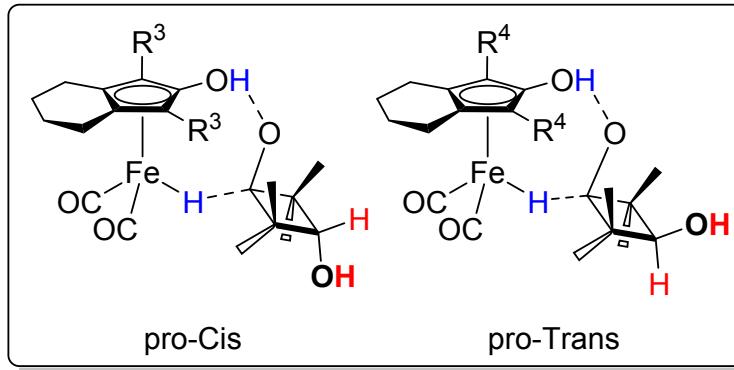


Figure S7.3.3: Binding modes of 4p to Fe-4a.

## S8. References

- [1] C. A. M. R. van Slagmaat, G. K. M. Verzijl, P. J. M. L. Quaedflieg, P. L. Alsters, S. M. A. De Wildeman, Hydrogenation of Cyclic 1,3-Diones to their 1,3-Diols using Heterogeneous Catalysts: Toward a Facile, Robust, Scalable, and Potentially Bio-based Route. *ACS Omega*, 2021, **6**, 4313 – 4328.
- [2] K. Ulbrich, P. Kreitmeier, O. Reiser, Microwave- or Microreactor-Assisted Conversion of Furfuryl Alcohols into 4-Hydroxy-2-cyclopentenones. *Synlett.*, 2010, **28**, 4719 – 4722.
- [3] C. Verrier, S. Moebs-Sanchez, Y. Queneau, F. Popowycz, The Piancatelli reaction and its variants: recent applications to high added-value chemicals and biomass valorization. *Org. Biomol. Chem.* 2018, **16**, 676 – 687.
- [4] S. Moulin, H. Dentel, A. Pagnoux-Ozherelyeva, S. Gaillard, A. Poater, L. Cavallo, J-F. Lohier, J-L. Renaud, Bifunctional (Cyclopentadienone)Iron-Tricarbonyl Complexes: Synthesis, Computational Studies and Application in Reductive Amination. *Chem. Eur. J.*, 2013, **19**, 17881 – 17890.
- [5] N. Dai, R. Shang, M. Fu, Y. Fu, Transfer Hydrogenation of Ethyl Levulinate to  $\gamma$ -Valerolactone Catalyzed by Iron Complexes. *Chin. J. Chem.*, 2015, **33**, 405 – 408.
- [6] C. A. M. R. van Slagmaat, S. M. A. De Wildeman, A Comparative Study of Structurally Related Homogeneous Ruthenium and Iron Catalysts for the Hydrogenation of Levulinic Acid to  $\gamma$ -Valerolactone. *Eur. J. Inorg. Chem.*, 2017, **6**, 694 – 702.
- [7] M. Kamitani, Y. Nishiguchi, R. Tada, M. Itazaki, H. Nakazawa, Synthesis of Fe-H/Si-H and Fe-H/Ge-H Bifunctional Complexes and Their Catalytic Hydrogenation Reactions toward Nonpolar Unsaturated Organic Molecules. *Organometallics*, 2014, **33**, 1532 – 1535.
- [8] T. J. Brown, M. Cumbes, L. J. Diorazio, G. J. Clarkson, M. Wills, Use of (Cyclopentadienone)iron Tricarbonyl Complexes for C-N Bond Formation Reactions between Amines and Alcohols. *J. Org. Chem.*, 2017, **82**, 10489 – 10503.
- [9] S. Fleischer, S. Zhou, K. Junge, M. Beller, General and Highly Efficient Iron-Catalyzed Hydrogenation of Aldehydes, Ketones, and  $\alpha,\beta$ -Unsaturated Aldehydes. *Angew. Chem. Int. Ed.* 2013, **52**, 5120 – 5124.
- [10] A. Chakraborty, R. G. Kinney, J. A. Krause, H. Guan, Cooperative Iron-Oxygen-Copper Catalysis in the Reductions of Benzaldehyde under Water-Gas Shift Reaction Conditions. *ACS Catal.*, 2016, **6**, 7855 – 7864.
- [11] S. A. Moyer, T. W. Funk, *Tetrahedron Lett.*, Air-stable iron catalysts for the Oppenauer-type oxidation of alcohols. **2010**, **51**, 5430–5433
- [12] T. W. Funk, A. R. Mahoney, R. A. Sponenburg, K. P. Zimmerman, D. K. Kim, E. E. Harrison, Synthesis and Catalytic Activity of (3,4-Diphenylcyclopentadienone)Iron Tricarbonyl Compounds in Transfer Hydrogenations and Dehydrogenations. *Organometallics*, 2018, **37**, 1133 – 1140.
- [13] Y. Tang, R. I. L. Meador, C. T. Malinchak, E. E. Harrison K. A. McCaskey, M. C. Hempel, T. W. Funk, (Cyclopentadienone)iron-Catalyzed Transfer Dehydrogenation of Symmetrical and Unsymmetrical Diols to Lactones. *J. Org. Chem.*, 2020, **85**, 1823 – 1834.
- [14] T. N. Plank, J. L. Drake, D. K. Kim, T. W. Funk, Air-Stable, Nitrile-Ligated (Cyclopentadienone)iron Dicarbonyl Compounds as Transfer Reduction and Oxidation Catalysts. *Adv. Synth. Catal.*, 2012, **354**, 597 – 601.
- [15] A. Cingolani, C. Cesari, S. Zacchini, V. Zanotti, M. C. Cassani, R. Mazzoni, Straightforward synthesis of iron cyclopentadienone N-heterocyclic carbene complexes, *Dalton Trans.*, 2015, **44**, 19063–19067.